BIOLOGY AND APPLICATIONS OF INDUSTRIAL MICROORGANISMS

Stefany Castaldi

Dottorato in biotecnologie
XXXIV ciclo

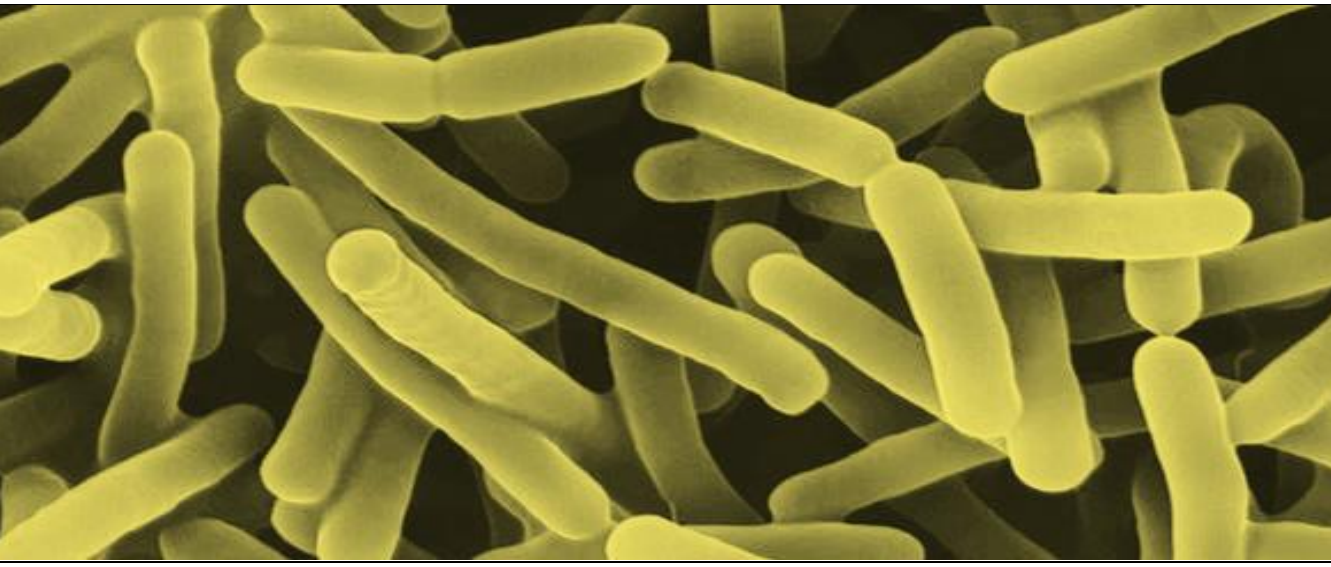

Università di Napoli Federico II

Dottorato in Biotecnologie – XXXIV ciclo

Università di Napoli Federico II

BIOLOGY AND APPLICATIONS OF INDUSTRIAL MICROORGANISMS

Stefany Castaldi

Dottorando:	Stefany Castaldi
Relatore:	Rachele Isticato
Coordinatore:	Prof. Marco Moracci

Settore Scientifico Disciplinare BIO/19

Alla mia famiglia

INDEX

RIASSUNTO

Il settore agricolo svolge un ruolo importante nel processo di sviluppo economico di un Paese. Tuttavia, negli ultimi anni ha dovuto affrontare diverse sfide che hanno messo a dura prova il suo sostentamento. Con oltre 7 miliardi di persone che vivono oggi sul pianeta e stime che raggiungono tra 8 e 11 miliardi entro il 2050, l'umanità sta affrontando la più grande sfida della sua storia cercando di mantenere un tipo di alimentazione sana e produttiva.
Per far fronte a questo continuo fabbisogno di nutrienti, è stata adottata una strategia basata sull'agricoltura intensiva. Si tratta di un sistema di intensificazione e meccanizzazione agricola che mira a massimizzare i rendimenti dei terreni disponibili attraverso vari mezzi, come l'uso consistente di pesticidi e fertilizzanti chimici. Le pratiche agricole intensive producono cibo più economico in rapporto alle dimensioni del terreno, il che contribuisce a nutrire una popolazione umana in costante espansione. Oggi però, l'agricoltura intensiva si è rilevata la più grande minaccia per l'ambiente determinando la comparsa di nuovi parassiti e la ricomparsa di parassiti precedentemente considerati "sotto controllo", senza dimenticarci che è responsabile di gran parte della deforestazione mondiale e dell'aumento di metalli pesanti nei suoli agricoli.
In aggiunta all'uso eccessivo di fertilizzanti e pesticidi chimici, anche metodi di irrigazione scadenti e vari stress abiotici come forti venti, temperature estreme, salinità del suolo, siccità e alluvioni hanno influenzato la produzione e le rese delle colture agricole. Tra questi, la salinità del suolo è uno degli stress ambientali più devastanti, in quanto provoca importanti riduzioni della superficie coltivabile, della produttività e della qualità delle colture. È stato stimato che a livello mondiale il 33% dei terreni agricoli irrigui sono afflitti da elevata salinità. Inoltre, le aree salinizzate stanno aumentando ad un tasso del 10% annuo a causa delle scarse precipitazioni, elevata evaporazione superficiale, alterazione delle rocce autoctone, irrigazione con acqua salata e scarse pratiche colturali. Si stima che oltre il 50% della terra arabile sarà salinizzato entro l'anno 2050.
Sebbene le piante abbiano evoluto diverse strategie di difesa per far fronte ai molteplici stress ambientali, biotici e abiotici, questi da soli

non bastano. Nasce quindi l'esigenza di trovare strategie biotecnologiche adeguate volte non solo a migliorare la produttività delle colture, ma anche la salute del suolo, attraverso interazioni che vengono ad instaurarsi tra le radici delle piante e i microrganismi che colonizzano la rizosfera. Negli anni si sono sempre di più sviluppate ricerche alternative definite "*eco-friendly*", volte a mitigare gli effetti nocivi dei prodotti agrochimici tossici, portando alla scoperta e al successivo utilizzo di prodotti biofertilizzanti utilizzando batteri benefici per il suolo.
Questo gruppo eterogeneo di batteri, definito *Plant Growth Promoting Rhizobacteria* (PGPR), non soltanto svolge un ruolo importante nell'aumentare la fertilità del suolo, ma migliora anche la crescita e il vigore delle piante. I PGPR colonizzando le radici, possono secernere diverse sostanze chimiche regolatorie, attive nella promozione della crescita delle piante, o nell'aumentare l'assorbimento dei nutrienti da parte della pianta, mediante la fissazione dell'azoto, solubilizzazione del P, o accelerando la mineralizzazione della materia organica (Figura1). Diversi lavori hanno dimostrato che i PGPR sono anche in grado di aumentare nella pianta la tolleranza agli stress abiotici. Inoltre, i PGPR possono essere utilizzati anche come agenti di biocontrollo (BCA) volti a proteggere le piante dagli agenti biotici dannosi, attraverso diversi meccanismi antagonisti o con l'induzione della resistenza sistemica delle piante.

Figura1: Rappresentazione schematica dell'attività diretta e indiretta svolta dai batteri che promuovono la crescita delle piante (PGPB).

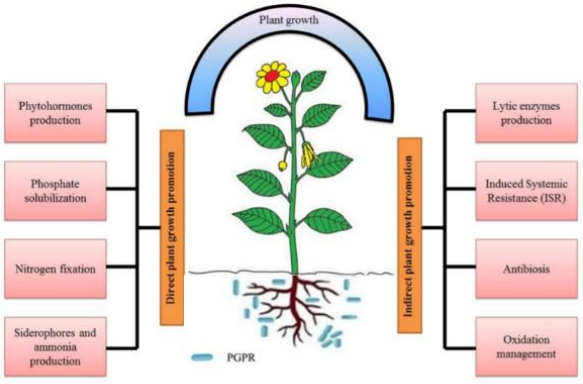

Pertanto, l'utilizzo di PGPR rappresenta una soluzione promettente per la sicurezza dell'ambiente e per l'aumento della resa agricola, con un impatto economico potenziale.
In questo contesto nasce il mio progetto di dottorato intitolato "*Biology and applications of industrial microorganisms*" che può essere suddiviso in due parti.
Nella prima parte del progetto, l'obiettivo è stato quello di purificare e caratterizzare metaboliti secreti da microrganismi con attività contro fitopatogeni fungini da utilizzare come alternativa eco-sostenibile ai pesticidi.
In particolare, lo studio è iniziato con l'identificazione di due nuove fitotossine (phaseocyclopentenones A and B) rilasciate dal fungo fitopatogeno *Macrophomina phaseolina* che infetta più di 500 specie di piante coltivate e selvatiche in tutto il mondo, come la soia, apportando gravi perdite economiche e alimentari. (**Capitolo II**).
Successivamente, mi sono occupata dell'isolamento di metaboliti secondari rilasciati dal batterio *Pseudomonas fluorescens* 9, ceppo isolato dal suolo in Argentina. Studi precedenti hanno identificato questo ceppo batterico come un promettente PGPR con notevoli attività biofertilizzanti e di biocontrollo. I miei studi si sono focalizzati nell'individuare le molecole responsabili dell'attività antifungina, individuando la fenazina come principale metabolita in grado di inibire la crescita di *M. phaseolina* e di altri due funghi (*Cercospora nicotianae* e *Colletotrichum truncatum*) che infettano piante di soia (**Capitolo III**). *L*a soia è una delle colture più importanti nel mondo, con un valore di mercato stimato di circa 146,23 miliardi di dollari nel 2017 i cui semi sono utilizzati a livello globale come fonte di proteine vegetali, mangimi per gli animali, combustibili e altri prodotti industriali. Nel 2021, il prezzo della soia ha raggiunto livelli record ripercuotendosi direttamente su vari settori, come quello dei mangimi destinati al settore zootecnico. Identificare metaboliti in grado di proteggere la pianta di soia dall'attacco di fitopatogeni ha quindi un elevato interesse economico.
Al fine di trovare ulteriori molecole in grado di proteggere la soia dall'attacco del fungo *M. phaseolina*, ho studiato la possibile attività antifungina del lipopolisaccaride grezzo (LPS), purificato e il corrispondete antigene-O (OPS) isolato da *Pseudomonas donghuensis* SVBP6. I risultati hanno imputato la principale attività all' OPS con una riduzione della crescita fungina pari al 75% (**Capitolo IV**).

In fine, durante lo studio volto all'identificazione delle fitotossine prodotte dal fungo *Truncatella angustata*, fitopatogeno che infetta il tronco della vite in Iran, sono stati identificati due metaboliti: isocumumarina(+)-6-idrossiramulosina già noto in letteratura e sorprendentemente l'acido fenazina-1-carbossilico (PCA). Il PCA è un noto metabolita batterico con attività antimicrobica e per la prima volta è stato identificato nei filtrati culturali del fungo *T. angustata*. Il PCA è stato quindi saggiato contro altri quattro diversi funghi responsabili della malattia del tronco della vite (*Phaeoacremonium minimum, Phaeoacremonium italicum, Fomitiporia mediterranea* e *Neofusicoccum parvum*). La forte capacità di inibizione del PCA contro questi quattro fungi fitopatogeni, suggerisce che *T. angustata* utilizzi questo metabolita per competere con altri antagonisti che attaccano la vite, per questo motivo il PCA potrebbe essere proposto come biofungicida (**Capitolo V**).

Nella seconda parte del mio progetto di dottorato mi sono occupata dell'isolamento, identificazione e caratterizzazione di una nuova collezione di batteri alofili, isolati da ambienti salini, appartenenti al genere *Bacillus* con potenziali applicazioni come biofertilizzanti o agenti di biocontrollo.

La scelta di selezionare soltanto batteri sporigeni deriva dal fatto che il genere *Bacillus* include già diverse specie di batteri eso ed endofiti con caratteristiche di promozione della crescita delle piante. Oltre ai benefici condivisi con altri PGPR, come la solubilizzazione del P nel suolo, la capacità di fissazione dell'azoto e la produzione di siderofori, *Bacillus* spp. sono adatti come biofertilizzanti perché: (i) essendo loro stessi membri comuni della microflora radicale delle piante, la loro applicazione ha un effetto scarso o nullo sulla composizione di altre comunità microbiche presenti nel suolo; (ii) questi batteri possono formare endospore e sopravvivere a condizioni ambientali avverse; (iii) le spore sono più stabili delle cellule vegetative durante la lavorazione e la conservazione dei preparati commerciali; (iv) batteri che crescono in ambienti estremi, come le saline, sviluppano strategie complesse per sopravvivere, che includono la produzione di una serie di diversi composti, come pigmenti antiossidanti, enzimi litici e composti antimicrobici, rendendoli a loro volta interessanti obiettivi biotecnologici.

Inizialmente ho ottenuto una raccolta di 22 Bacilli isolati dalla rizosfera della pianta nutrice *Juniperus sabina*. Recenti studi, attribuiscono alle piante nutrici la capacità di alterare la comunità

microbica del suolo, selezionando il microbiota più efficace in termini di mineralizzazione dei nutrienti e attività tipiche dei PGPR.
I batteri sono stati caratterizzati per le loro attività PGPR ed in particolare il ceppo *Bacillus* spp. RHFS10 è risultato essere il miglior PGPR con attività di biocontrollo contro *M. phaseolina*.
Studi di purificazione ed identificazione dei metaboliti rilasciati dal batterio, imputano l'attività antifungina alle *subtilisin-like-proteases* e alla *glucuronoxylanase*. Un ulteriore importante risultato ottenuto in questo studio, è stata la maggiore efficienza dei metaboliti antimicotici purificati rispetto al fungicida commerciale pentacloronitrobenzene PCNB, utilizzato come controllo positivo nei saggi di antagonismo, in termini di efficacia e durata nel tempo (**Capitolo VI**).
Successivamente sempre da ambiente salino ma questa volta dalla sabbia, ho isolato 20 batteri alofili appartenenti al genere *Bacillus*.
Anche in questo caso, i batteri sono stati caratterizzati per i tratti PGP ed infine sono stati selezionati sette promettenti ceppi da entrambe le collezioni (rizosfera e sabbia) per uno studio più approfondito riguardo l'attività di biocontrollo unendo esperimenti *in vitro* con lo studio dell'intero genoma, al fine di ricercare nuovi cluster di geni coinvolti nella biosintesi dei metaboliti secondari. I risultati ottenuti dimostrano che l'unione di entrambe le tecniche consente di avere un'indagine più approfondita della capacità biosintetica dei batteri PGPB (**Capitolo VII**).
I sette ceppi precedentemente selezionati, sono stati analizzati per le loro attività biofertilizzanti durante stress da salinità, con il fine di osservare se l'elevata concentrazione salina inibisse alcune attività enzimatiche importati nel ruolo di PGPB.
Due ceppi sono stati selezionati come PGPR più efficienti in condizioni di stress salino e analizzati per la loro capacità di migliorare la crescita delle piante di *Lotus japonicus* cresciute in 200 mM NaCl in esperimenti *in vitro.* (**Capitolo VIII**).
Infine i sette ceppi selezionati sono stati ulteriormente analizzati per il loro possibile utilizzo come fitodepurazione di suoli contaminati da metalli pesanti. Tre ceppi batterici, singolarmente o inconsorzio, sono stati selezionati per esperimenti *in vivo* ed inoculati in piante di grano cresciute in terreno contaminato da rame.
Soltanto due ceppi, *B. spp*. RHFS10 e *Bacillus gibsonii* RHF15, sono risultati promettenti, aumentando significativamente la lunghezza e il peso delle radici e dei germogli rispetto al ceppo *Bacillus amyloliquefaciens* RHFS18 e al consorzio. Certamente,

sono necessarie ulteriori indagini per confermare i dati ma, questi risultati preliminari, suggeriscono che i due PGPBs possono alterare la tossicità dei metalli sulla pianta di grano, rendendoli ottimi candidati per il ripristino potenziato di terreni contaminati.
Quest'ultima ricerca è stata svolta durante i 3 mesi trascorsi nel Centro Helmholtz per la ricerca ambientale - UFZ (Germania) sotto la diretta supervisione del Dr. Thomas Reitz (**Capitolo IX**).
I risultati sperimentali ottenuti durante questo percorso di dottorato, hanno permesso di ampliare la conoscenza di metaboliti secondari secreti da batteri PGPB con attività antifungina da poter utilizzare in futuro come bio-fungicidi. Inoltre, l'isolamento di nuovi batteri PGPB resistenti a condizioni avverse come l'elevata salinità o presenza di metalli pesanti, li rende ottimi candidati da poter utilizzare come bio-inoculanti.

SUMMARY

The possibility to improve agricultural crop yield by the beneficial bacteria inoculation has been an emerging area for the last decade. In a historic moment in which the increasing population coupled with land degradation aggravates challenges of crop production, the potential of the use of soil microorganisms to ensure agricultural productivity has a huge global impact on our society.

In this context, Plant Growth-Promoting (PGP) bacteria are receiving increasing attention as biofertilizers able to sustain the fertility of soils and replace agrochemical compounds with negative impacts on the environment.

Moreover, these beneficial bacteria represent the cheaper and easily available strategy for the mitigation of different biotic and abiotic stresses, reducing the phytopathogens infection, or alleviating environmental stresses respectively.

Consequently, PGPBs or their metabolites are exhibiting a gradual increase in demand on the world market as sustainable and eco-friendly tools.

In this Ph.D. thesis, the biotechnological potential of secondary metabolites secreted by bacteria and fungi as new natural fungicides is reported (**Chapter II-V**).

Moreover, the isolation and characterization of new plant growth-promoting bacteria, able to improve the plant growth under different stress conditions and with biocontrol activities, are also presented herein (**Chapter VI-IX**).

CHAPTER I: INTRODUCTION

1.1 Intensive farming and the impact on the environment

In the last century, the increase in the world population was three times greater than during the whole history of humanity. To deal with the consequently increased requirement of nutrients, crop production has been necessarily augmented mainly in wheat, rice, and maize yields. In turn, to guarantee high crop yield, several strategies have been developed, such as using pesticides and chemical fertilizers, increasing land acreage, or using agricultural intensification methods.
Nevertheless, agricultural intensification over the past decades, together with global climate change, has negatively impacted agricultural lands with a decrease in crop productivity and likely increasing levels of poverty and accumulation of pollutants in the environment. In fact, the most common pollutants present in the soil are the derivates of pesticides and fertilizers used in excess over the years (Mirsal et al., 2008).

1.2 Synthetic pesticides and chemicals fertilizers

The reduction of crop losses caused by pests and pathogens is a major challenge to agricultural production. Synthetic pesticides are chemical agents used to eliminate pests and can be divided into several groups, namely insecticides, herbicides, rodenticides, bactericides, fungicides, and larvicides, based on the types of targeted pests.
From 1990 to 2018, the amounts of used pesticides by all countries, especially in Asia and America, have been registered. As shown in Figure 1A, the average world quantity has increased from 1.55 $kg \cdot ha^{-1}$ in 1990 to 2.63 $kg \cdot ha^{-1}$ in 2018. Mainly, fungicides and bactericides are used more than the others (Figure 1B) (FAOSTAT, 2021).

Figure 1. Worldwide pesticide usage: (A) pesticides use per area of cropland; (B) pesticides use from 1990 to 2016 (FAOSTAT, 2021).

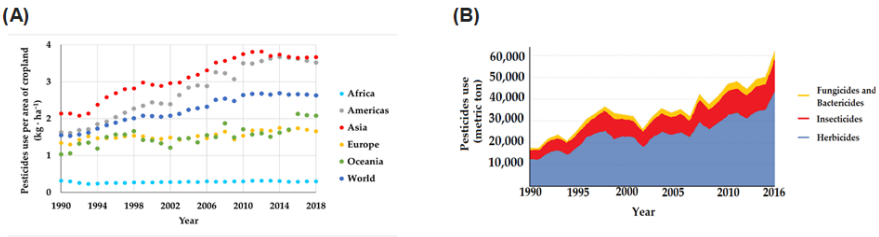

The number of synthetic pesticides used worldwide is increasing over the year, and by the year 2025, global pesticide usage has been estimated to increase up to 3.5 million tonnes (Sharma et al., 2019). In addition to more efficient control of biotic stress by pesticides, an increase in crop yield and quality is possible by improving plant nutrition. In the permanent agricultural land, the soil is very poor in nutrients and so inefficient. To make more efficient the soil, the use of chemical fertilizers containing phosphate, nitrate, ammonium, and potassium salts was increased (Table 1).

Table 1. World demand for nitrogen, phosphorus (phosphoric acid based) and potassium for other uses (thousand tonnes). (FAO, 2019.)

Year	2015	2016	2016	2017	2018	2019	2020
Nitrogen, N	36 930	37 663	38 320	38 965	39 569	40 127	40 660
Phosphorus (phos. acid based), as P_2O_5	6 444	6 677	7 036	7 170	7 291	7 482	7 734
Potassium, as K_2O	5 572	5 752	5 876	5 993	6 112	6 237	6 363
Total ($N+P_2O_5+K_2O$)	**48 946**	**50 092**	**51 232**	**52 128**	**52 972**	**53 846**	**54 757**

However, the uncontrolled use of pesticides and fertilizers has a negative impact on both agriculture and the environment.
The extensive use of pesticides is contaminating soil and water, causing damage to its microflora and microfauna and hindering the absorption of important mineral nutrients by plants (Abhilas et al., 2009). Furthermore, the excessive use of pesticides on different crop species leads to harmful effects on beneficial biota, including honey bees, predators, birds, plants, small mammals, and humans, creating an imbalance in the biodiversity of the entire ecological system (Damalas et al., 2011; Paoli et al., 2015; WHO, 2017).

Chemical fertilizers misuse has led to water bodies pollution, nitrate and heavy metal accumulation, and water eutrophication. Moreover, chemicals can get stored in crop plants, enter the food chain, and pose a threat to human health (FAOSTAT, 2021).

1.3 *eco-friendly* strategy: plant growth-promoting rhizobacteria

An eco-friendly and safe strategy that ensures agricultural productivity is to use beneficial soil bacteria (Oleńska, et al., 2020). This heterogeneous group of bacteria, namely plant growth-promoting rhizobacteria (PGPR), not only plays an essential role in increasing soil fertility but also enhance the growth and vigor of plants: PGPRs, colonizing the roots, may secrete several regulatory chemicals, which are active in plant growth promotion, in improving nutrient uptake by nitrogen fixation or P solubilization, in accelerating the mineralization of organic matter (Oleńska et al., 2020), and reducing abiotic stresses (Bhat et al., 2020) (Figure 3). Besides, PGPRs can be used as biocontrol agents (BCAs) to moderate plant disease through several antagonistic mechanisms or the induction of plants' systemic resistance (Meena et al., 2020). Therefore, the application of PGPR as biofertilizers has a relevant economic and environmental impact in terms of benefits, determining a significant increase of crop yields, and a reduction of conventional chemical fertilizer and pesticide.

Figure 3. Mechanisms used by PGPR for enhancing plant growth.

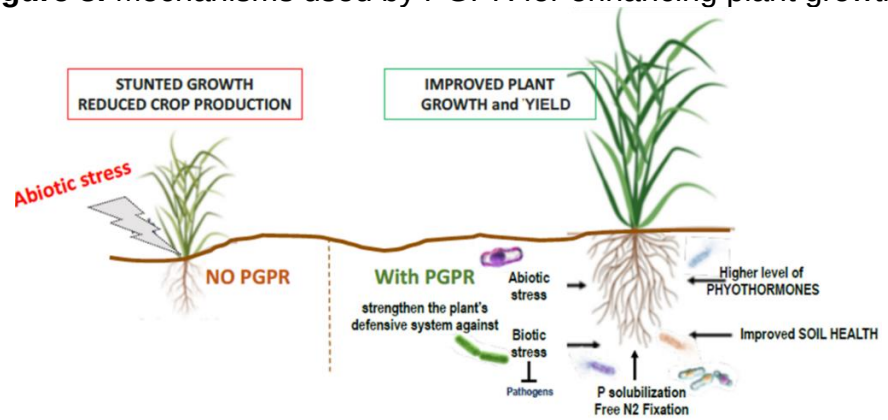

Many beneficial bacteria have been identified and developed into commercially available products for promoting plant growth (Crow et

al., 2014; Junaid et al., 2013) and currently, there are many ongoing studies focusing on evaluating new bacterial strains or improving the existing ones. The bacterial genera most commonly researched and reported as PGPR include *Agrobacterium, Arthrobacter, Azotobacter, Azospirillum, Bacillus, Burkholderia, Caulobacter, Chromobacterium, Erwinia, Flavobacterium, Micrococcus, Pseudomonas,* and *Serratia* (Bhattacharyya and Jha et al., 2012). *Pseudomonas* and *Bacillus* species are the predominant plant growth-promoting bacteria though the current research is largely focused on endospore-forming, Gram-positive bacteria in the genera *Bacillus* (Radhakrishnan et al., 2017).
The ability of the *Bacillus* spp. of producing endospores, a quiescent cell-forms able to resist harsh environmental conditions and several stresses, makes them more suitable candidates for PGPR-based commercial products since i) the resistance features of the spores can ensure the persistence of the bacteria in the environment for a long-period; ii) spores are more stable than vegetative cells during processing and storage of commercial preparations (Ricca et al., 2021).

A further advantage in the PGPR application is to utilize these beneficial microorganisms to increase plant tolerance to salt and heavy metals stress.
Soil salinity is one of the most devastating environmental stresses, which causes major reductions in cultivated land area, crop productivity and quality (Yamaguch and Blumwald et al., 2005; Shahbaz, and Ashraf et al., 2013). It has been estimated that worldwide 20% of total cultivated and 33% of irrigated agricultural lands are afflicted by high salinity. Furthermore, the salinized areas are increasing at a rate of 10% annually for various reasons, including low precipitation, high surface evaporation, weathering of native rocks, irrigation with saline water, and poor cultural practices. It has been estimated that more than 50% of the arable land would be salinized by the year 2050 (Jamil et al., 2011).
Although the plants have evolved proper defense strategies to cope with the different environmental stress, these alone are not enough. PGPR can mitigate the damage of salt stress and reduce the metals harmful effects via several direct and indirect mechanisms such as biofilm formation, siderophores, exopolysaccharide, and phytohormones production (Tiwari et al., 2016). Among PGPR, bacteria belonging to the Bacillus genus are excellent candidates to

use as an eco-friendly approach to sustainable agriculture in degraded soil, due to their ability to resist under different environmental stresses (salinity, pH, temperature) and the multiple plant growth-promoting characteristics (Figure 2) (Radhakrishnan et al., 2017).

Figure 2. Direct effect of *Bacillus*-secretions on plant protection from adverse environments.

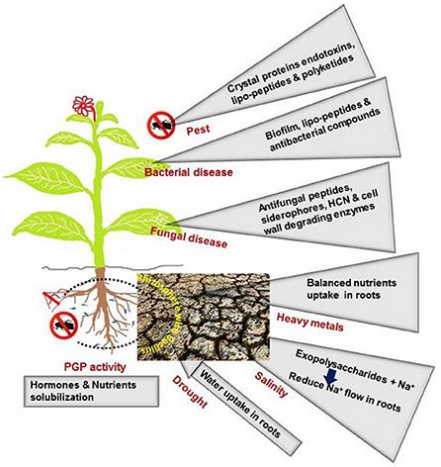

1.3.1 *Bacillus*-mediated plant growth promotion under abiotic and biotic stress conditions

Halo-tolerant plant growth-promoting rhizobacteria (HT-PGPR), when inoculated in salt soil, can enhance crop productivity in saline agriculture. In fact, these salt-tolerant bacteria increase the relative water content as well as the osmotic and turgor potential, improving the growth of salt-injured plants (Yang et al., 2016). In particular, it has been shown that Bacillus spp. can reduce the toxic effects of salinity in plants by i) inhibiting lipid peroxidation (Han, et al., 2014); ii) producing Exopolysaccharides (EPS) that binds Na+ and inhibits the transport into plant root cells (Ashraf al., 2004); iii) decreasing ROS formation and the programmed cell death enhancing the action of antioxidants enzymes such as Catalase or Peroxidase (Jha, and Subramanian, 2014); iv) producing plant hormones to enhance the concentrations of Indoleacetic acid (IAA) and Gibberellins (GAs)

reducing the synthesis of Abscisic acid (ABA) in plants grown under salt stress (Mohamed and Gomaa et al., 2012).

Moreover, the excessive use of fertilizers for a long time results in heavy metals accumulation in agricultural soils reduces soil fertility and decreases plant growth and productivity (Ai et al., 2020). The negative effect of heavy metals on plants starts in the rhizosphere through interaction with root exudates. A high concentration of Pb can cause different physiological and biochemical deficiencies (Shahid et al., 2011). In addition, the interaction between Cu and Zn affects the bioavailability of nutrients in the soil. Moreover, the heavy metals produce free radicals, increasing intracellular levels of reactive oxygen species (ROS), and in turn, damage to the biological molecules (e.g., proteins, nucleic acids, lipids, and enzymes), which may ultimately lead to the death of the entire plant (Wu et al., 2016).
Many PGPR are also able to heavy metal phytoremediation, solubilizing, or converting toxic metals to non-toxic forms (Kang et al., 2015c). *Bacillus* spp. alleviate this stress effect by: i) reducing lipid peroxidation and Superoxide dismutases (SOD) activity and increasing Amylase and Protease to promote plant growth in heavy metal-polluted soil (Pandey et al., 2013) and ii) increasing the balanced uptake of mineral nutrients and pigments synthesis in stressed plants (Malekzadeh et al., 2012).

1.3.2 Use of PGPR as BCA to disease prevention in plants

Plant disease-causing pathogenic bacteria, fungi, viruses and nematodes are major challenges in maintaining plant health and yield in agricultural lands (Narasimhan and Shivakumar et al., 2015). The application of PGPR microorganisms is an alternative to chemical fungicides, bactericides and nematicides and an effective environmentally friendly approach to improving plant growth and controlling many plant diseases (Radhakrishnan et al., 2013).
PGPR uses different strategies in order to reduce the densities of deleterious microbes by secreting different secondary metabolites that are deleterious to the growth or metabolic activities of plant pathogens (Beneduzi et al., 2012). These bacteria are able to biofilm formation around the root surface and secretion different toxins (surfactin, iturin, macrolactin, bacillomycin, and fengycin) destroying

the phytopathogenic populations and reducing disease incidence in plants (Elshakh et al., 2016; Hinarejos et al., 2016).
PGPR as biocontrol agents have the following advantages: i) these bacteria are isolated from the rhizosphere or plants therefore they are environmentally friendly and nontoxic (Beneduzi et al., 2012), ii) PGPR utilize root exudates leading to their rapid growth and mass production (Lugtenberg and Kamilova et al., 2009), iii) they adapt to the environment by colonizing and multiplying in the rhizosphere and interior of the plant (Compant et al., 2010), and iv) they undertake a defined range of functions including antibiosis, growth promotion, and induced systemic resistance (Compant et al., 2005).
Several commercial PGPR products are currently available for use on vegetables and new products are constantly being studied and commercialized in the market (Kumar et al., 2011).
Bacteria from both *Bacillus* and *Pseudomonas* genera are known to be appropriate candidates to be used in a bio-control approach due to their predominance in various environments, resilience and survival ability, but also for the number of bio-active molecules they are potentially able to produce (Raaijmakers et al., 2010).

For these reasons, intensive research on this group of microorganisms has been taken over to develop new biofertilizers and biocontrol agents.

1.3.3 *Bacillus* spp. and *Pseudomonas* spp. with bio-control activity

Bacteria belonging to the genus *Bacillus* are among most studied because they produce several secondary metabolites, divided into ribosomally synthesized peptides (e.g., bacteriocins), non-ribosomally synthesized peptides (e.g., lipopeptides, siderophores), polyketides (macrolides, polyenes), and volatile in-/organic compounds (VIC and VOC). Moreover, these compounds are accompanied by various spectra of action. Lipopeptides and VOCs, for instance, have direct antifungal activities as it is the case for the lipopeptide iturin A on *Rhizoctonia solani* (Yu et al., 2002) or volatiles pyrazine (2,5-dimethyl), benzothiazole, and phenol-(4-chloro-3-methyl) against *Alternaria solani* and *Botrytis cinerea* on tomato plants (Gao et al., 2017). But other VOCs (2,3-butanediol, methyl jasmonate, or methyl salicylate), as well as other lipopeptides

(surfactin, fengycin) are also able to induce systemic resistance in plants through an ethylene dependent pathway (Ongena et al., 2007; Jourdan et al., 2009).

Similarly, *Pseudomonas spp.* are also known to produce a broad range of bioactive metabolites such as lipopeptides, siderophores, polyketides, and volatile compounds with interesting activities against different phytopathogens. It has been shown that these metabolites enable pseudomonads to directly compete with plant pathogens, promote plant growth or induce systemic plant resistance. The best example among these *Pseudomonas spp.* metabolites are the phenazine-1-carboxylic acid (PCA) and 2,4-diacetylphloroglucinol (DAPG). The antifungal activity of this latter polyketide has been extensively reviewed on damping-off or root rot diseases in various crops (Ahmadzadeh and Sharifi Tehrani et al., 2009). Lipopeptides are another example of the multiple antagonistic mechanisms used by Pseudomonads bacteria. Some are known to lyse zoospores of *Phytophthora infestans* (De Bruijn et al., 2007) and to induce resistance in tomato plants infected by this pathogen (Bakker et al., 2007).

Moreover, both bacterial genera are able to produce microbial enzymes such as chitinases, cellulases, β-1, 3 glucanases, proteases, and lipases useful to lyse a portion of cell walls of many plant pathogenic fungi (Glick et al., 2012).

Currently, several studies are still in progress to identify new antifungal metabolites produced by PGPRs especially for the genera *Bacillus* spp. and *Pseudomonas* spp. in order to use them as bio-pesticides and clarify their modes of action to achieve optimum disease control.

References

Mirsal, I. A. Soil Pollution Origin, Monitoring & Remediation, 2nd ed.; Springer-Verlag: Berlin/Heidelberg, Germany. 2008, ISBN 9783540707752.

FAOSTAT. Available online: http://www.fao.org/faostat/en/?#data/EP/visualize (accessed on 8 April 2021).

Sharma, A., Kumar, V., Shahzad, B. *et al.* Worldwide pesticide usage and its impacts on ecosystem. SN Appl. Sci. 2019, 1, 1446.

FAO. 2019. World fertilizer trends and outlook to 2022. Rome.

Abhilash, P.C., Singh, N. Pesticide use and application: an Indian scenario. J Hazard Mater. 2009, 165, 1–12.

Damalas, C.A., Eleftherohorinos, I.G. Pesticide Exposure, Safety Issues, and Risk Assessment Indicators.Int. J. Environ. Res.Public Health. 2011, 8, 1402–141.

Paoli, D., Giannandrea, F., Gallo, M., Turci, R., Cattaruzza, M.S., Lombardo, F., Lenzi, A., Gandini, L. Exposure to polychlorinatedbiphenyls and hexachlorobenzene, semen quality and testicular cancer risk. J. Endocrinol. Invest. 2015, 38, 745–752.

World Health Organization (WHO) Agrochemicals, Health and Environment: Directory of Resources. 2017. Available online:https://www.who.int/heli/risks/toxics/chemicalsdirectory/en/ (accessed on 24 October 2020).

Oleńska, E., Małek, W., Wojcik, M., Swiecick, I., Thijs, S., Vangronsveld, J. Beneficial features of plant growth-promoting rhizobacteria for improving plant growth and health in challenging conditions: A methodical review. Sci Total Environ. 2020, 743, 140682.

Bhat, M.A., Kumar, V., Bhat ,M.A., Wani, I.A., Dar FL, Farooq I, Bhatti F, Koser R, Rahman S, Jan AT. Mechanistic Insights of the Interaction of Plant Growth-Promoting Rhizobacteria (PGPR) With Plant Roots Toward Enhancing Plant Productivity by Alleviating Salinity Stress. Front Microbiol. 2020, 20, 1952.

Meena, M., Swapnil, P., Divyanshu, K., Kumar, S., Harish, Tripathi, Y.N., Zehra, A., Marwal, A., Upadhyay RS. PGPR-mediated induction of systemic resistance and physiochemical alterations in plants against the pathogens: Current perspectives. J Basic Microbiol. 2020, 60, 828-861.

Crow, W. T. Effects of a commercial formulation of *Bacillus firmus* I1582 on golf course Bermuda grass infested with Belonolaimus longicaudatus. J of Nem. 2014, 46, 331.

Junaid, J. M., Dar, N. A., Bhat, T. A., Bhat, A. H., & Bhat, M. A. Commercial biocontrol agents and their mechanism of action in the management of plant pathogens. I J of Modern Plant & Animal Sci. 2013, 1, 39-57.

Bhattacharyya, P.N., Jha, D.K. Plant growth-promoting rhizobacteria (PGPR): emergence in agriculture. *World J Microbiol Biotechnol.* 2012, 28, 1327–1350.

Radhakrishnan, R., Hashem, A., Abd Allah, E.F. *Bacillus*: A Biological Tool for Crop Improvement through Bio-Molecular Changes in Adverse Environments. Front Physiol. 2017, 6, 667.

Ricca, E., Baccigalupi, L., Isticato, R. Spore-adsorption: Mechanism and applications of a nonrecombinant display system. Biotechnol Adv. 2021, 47, 107693.

Yamaguchi, T., Blumwald, E. Developing salt-tolerant crop plants: challenges and opportunities. Trends Plant Sci. 2005, 10, 615–620.

Shahbaz, M., Ashraf, M. Improving salinity tolerance in cereals. Crit. Rev. Plant Sci. 2013, 32, 237–249.

Jamil, A., Riaz, S., Ashraf, M., Foolad, M.R. Gene expression profiling of plants under salt stress. Crit. Rev. Plant Sci., 2011, 30, 435–458.

Tiwari, S., Lata, C., Chauhan, P. S., and Nautiyal, C. S. *Pseudomonas putida* attunes morphophysiological, biochemical and molecular responses in Cicer arietinum L. during drought stress and recovery. Plant Physiol. Biochem. 2016, 99, 108–117.

Yang, A., Akhtar, S. S., Iqbal, S., Amjad, M., Naveed, M., Zahir, Z. A., et al. Enhancing salt tolerance in quinoa by halotolerant bacterial inoculation. Funct. Plant Biol. 2016, 43, 632–642.

Han, Q.Q., Lü, X.P., Bai, J.P., Qiao, Y., Paré, P.W., Wang, S.M., Zhang, J.L., Wu, Y.N., Pang, X.P., Xu, W.B., Wang, Z.L. Beneficial soil bacterium *Bacillus subtilis* (GB03) augments salt tolerance of white clover. Front. Plant Sci. 2014, 5, 525.

Ashraf, M., Hasnain, S., Berge, O., and Mahmood, T. Inoculating wheat seedlings with exopolysaccharide-producing bacteria restricts sodium uptake and stimulates plant growth under salt stress. Biol. Fertil. Soils. 2004, 40, 157–162.

Jha, Y., and Subramanian, R.B. PGPR regulate caspase-like activity, programmed cell death, and antioxidant enzyme activity in paddy under salinity. Physiol. Mol. Biol. Plants. 2014, 20, 1–7.

Mohamed, H. I., and Gomaa, E. Z. Effect of plant growth promoting Bacillus subtilis and *Pseudomonas fluorescens* on growth and pigment composition of radish plants (Raphanus sativus) under NaCl stress. Photosynthetica. 2012, 50, 263–272.

Ai, P., Jin, K., Alengebawy, A., Elsayed, M., Meng, L., Chen, M., Ran, Y. Effect of application of different biogas fertilizer on eggplant production: Analysis of fertilizer value and risk assessment. Environ. Technol. Innov. 2020, 19, 101019.

Shahid M. et al. Heavy Metal Stress and Crop Productivity. In: Hakeem K. (eds) Crop Production and Global Environmental Issues. Springer, Cham. 2015, 1, 25.
Wu, X., Cobbina, S.J., Mao, G., Xu, H., Zhang, Z., Yang, L. A review of toxicity and mechanisms of individual and mixtures ofheavy metals in the environment. Environ. Sci. Pollut. Res. 2016, 23, 8244–8259.
Kang, S. M., Radhakrishnan, R., You, Y. H., Khan, A. L., Lee, K. E., Lee, J. D., et al. Enterobacter asburiae KE17 association regulates physiological changes and mitigates the toxic effects of heavy metals in soybean. Plant Biol. 2015c, 17, 1013–1022.
Pandey, S., Ghosh, P. K., Ghosh, S., De, T. K., andMaiti, T. K. Role of heavy metal resistant *Ochrobactrum* sp. and *Bacillus* spp. strains in bioremediation of a rice cultivar and their PGPR like activities. J. Microbiol. 2013, 51, 11–17.
Malekzadeh, E., Alikhani, H. A., Savaghebi-Firoozabadi, G. R., and Zarei, M. Bioremediation of cadmium-contaminated soil through cultivation of maize inoculated with plant growth–promoting rhizobacteria. Bioremediat. J. 2012, 16, 204–211.
Narasimhan, A., and Shivakumar, S. Evaluation of *Bacillus subtilis* (JN032305) biofungicide to control chilli anthracnose in pot controlled conditions. Biocontrol Sci. Technol. 2015, 25, 543–559.
Beneduzi, A., Ambrosini, A., and Passaglia, L.M.P. Plant growth-promoting rhizobacteria (PGPR): Their potential as antagonists and biocontrol agents. Genetics and Molecular Biology. 2012, 35, 1044-1051.
Elshakh, A. S. A., Anjum, S. I., Qiu, W., Almoneafy, A. A., Li, W., Yang, Z., et al. Controlling and defence-related mechanisms of *Bacillus* strains against bacterial leaf blight of rice. J. Phytopathol. 2016, 164, 534–546.
Hinarejos, E., Castellano, M., Rodrigo, I., Belles, J. M., Conejero, V., Lopez-Gresa, M. P., et al. *Bacillus subtilis* IAB/BS03 as a potential biological control agent. Eur. J. Plant Pathol. 2016, 146, 597–608.
Lugtenberg, B., and Kamilova, F. Plant-Growth-Promoting Rhizobacteria. Annual Review of Microbiology. 2009, 541, 556.
Compant, S., Clement, C., and Sessitsch, A. Plant growth-promoting bacteria in the rhizo- and endosphere of plants: Their role, colonization, mechanisms involved and prospects for utilization. Soil Biology & Biochemistry. 2010, 42, 669-678.
Compant, S., Reiter, B., Sessitsch, A., Nowak, J., Clément, C., Barka, E.A. Endophytic colonization of Vitis vinifera L. by plant

growth-promoting bacterium Burkholderia sp. strain PsJN Appl. Environ. Microbiol. 2005, 71, 71, 1685-1693.
Kumar, A., Prakash, A., and Johri, B.N. 2011a. - Bacteria in Agrobiology: Crop Productivity. Springer Heidelberg New York Dordrecht London. 2013, 59, 37240-7.
Raaijmakers, J. M., De Bruijn, I., Nybroe, O., and Ongena, M. Natural functions of lipopeptides from *Bacillus* and *Pseudomonas*: more than surfactants and antibiotics. FEMS Microbiol. Rev. 2010, 34, 1037–1062.
Yu, G. Y., Sinclair, J. B., Hartman, G. L., and Bertagnolli, B. L. Production of iturin A by *Bacillus amyloliquefaciens* suppressing *Rhizoctonia solani*. Soil Biol. Biochem. 2002, 34, 955–963.
Gao, Z., Zhang, B., Liu, H., Han, J., and Zhang, Y. Identification of endophytic Bacillus velezensis ZSY-1 strain and antifungal activity of its volatile compounds against Alternaria solani and Botrytis cinerea. Biol. Control. 2017, 105, 27–39.
Ongena, M., Jourdan, E., Adam, A., Paquot, M., Brans, A., Joris, B., et al. Surfactin and fengycin lipopeptides of *Bacillus subtilis* as elicitors of induced systemic resistance in plants. Environ. Microbiol. 2007, 9, 1084–1090.
Jourdan, E., Henry, G, Duby, F., Dommes, J., Barthélemy, J.P., Thonart, P., Ongena, M. Insights into the defense-related events occurring in plant cells following perception of surfactin-type lipopeptide from *Bacillus subtilis*. Mol. Plant Microbe Interact. 2009, 22, 456–468.
Ahmadzadeh, M., and Sharifi Tehrani, A. Evaluation of fluorescent pseudomonads for plant growth promotion, antifungal activity against *Rhizoctonia solani* on common bean, and biocontrol potential. Biol. Control. 2009, 48, 101–107.
De Bruijn, I., de Kock, M. J. D., Yang, M., de Waard, P., van Beek, T. A., and Raaijmakers, J. M. Genome-based discovery, structure prediction and functional analysis of cyclic lipopeptide antibiotics in Pseudomonas species. Mol. Microbiol. 2007, 63, 417–428.
Bakker, P. A., Pieterse, C. M., and Van Loon, L. Induced systemic resistance by *fluorescent Pseudomonas* spp. Phytopathology. 2007, 97, 239–243.
Glick BR. Plant growth-promoting bacteria: mechanisms and applications. Scientifica (Cairo). 2012, 2012-963401.

AIMS OF THE THESIS

This Thesis is divided into two parts as follows:
In the first part, the aim has been to discover eco-friendly alternatives for the safe control of fungal phytopathogens. To obtain these results:

- Two new phytotoxins secreted by *Macrophomina phaseolina* were identified. This fungus infects more than 500 different plants with agroindustrial relevance, such as soya and wheat (**Chapter II**).
- New secondary metabolites secreted by the PGPR *Pseudomonas fluorescens* 9 were isolated, identified and used to inhibit the growth of *M. phaseolina* and two other phytopathogenic fungi (*Cercospora nicotianae* and *Colletotrichum truncatum*) (**Chapter III**).
- It was investigated the role of the O-specific polysaccharide (OPS) isolated from the lipopolysaccharide (LPS) of *Pseudomonas donghuensis* SVBP6 in the antifungal activity against *M. phaseolina* (**Chapter IV**).
- Lastly, a new secondary metabolite secreted by the phytopathogenic fungus *Truncatella angustata* was identified and used to control fungi-host plant interactions (**Chapter V**).

The second part aims to identify a new collection of halophilic *Bacilli* bacteria to use in the sustainable agriculture industry. To obtain these results:

- A collection of 22 Bacilli was isolated from the saltpan rhizosphere and characterized for PGPR traits. Also, secondary metabolites with antifungal activity against *M. phaseolina*, secreted by the best PGPR bacterium it was identified (**Chapter VI**).

- A collection of 20 halophilic *Bacilli* was isolated from the salt-pans sand and studied for PGPR traits. Seven selected strains from both groups (rhizosphere and sand) were further analyzed with *in vitro* experiments to biocontrol activity. Finally, the whole genome was studied to discover novel gene clusters involved in the biosynthesis of secondary metabolites (**Chapter VII**).
- Seven selected strains were studied to improve the growth of the *Lotus japonicus* plant under salt stress conditions *in vitro* experiments. One bacterial strain was selected as the best PGPR with biofertilizer activity (**Chapter VIII**).
- From seven PGPB, three bacterial species were selected and studied to improve the growth of the wheat plants grown in the soil contaminated with heavy metals in *in vivo* experiments. This task was developed at Helmholtz Center for Environmental Research - UFZ (Germany) under the direct supervision of Dr. Thomas Reitz (**Chapter IX**).

Overview of objectives of the thesis

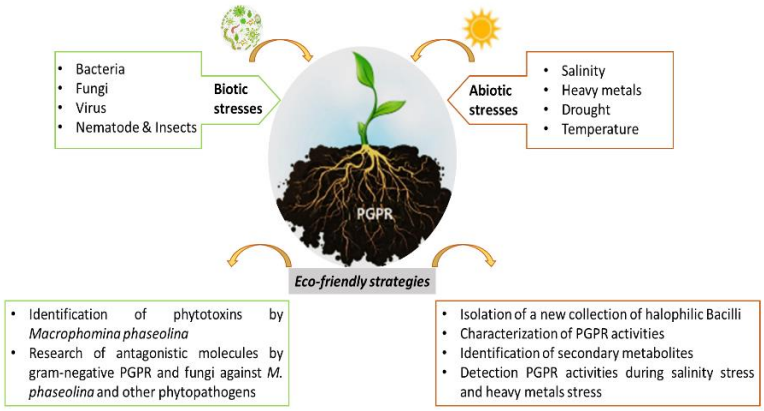

CHAPTER II: Phaseocyclopentenones A and B, Phytotoxic Penta- and Tetrasubstituted Cyclopentenones Produced by *Macrophomina phaseolina,* the Causal Agent of Charcoal Rot of Soybean in Argentina.

JOURNAL OF NATURAL PRODUCTS

pubs.acs.org/jnp

Article

Phaseocyclopentenones A and B, Phytotoxic Penta- and Tetrasubstituted Cyclopentenones Produced by *Macrophomina phaseolina*, the Causal Agent of Charcoal Rot of Soybean in Argentina

Marco Masi, Francisco Sautua, Roukia Zatout, Stefany Castaldi, Lorenzo Arrico, Rachele Isticato, Gennaro Pescitelli, Marcelo Anibal Carmona, and Antonio Evidente*

Cite This: https://dx.doi.org/10.1021/acs.jnatprod.0c01287

Read Online

ACCESS | Metrics & More | Article Recommendations | Supporting Information

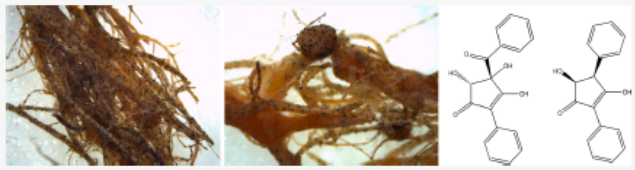

ABSTRACT: Two new penta- and tetrasubstituted cyclopentenones, named phaseocyclopentenones A and B (**1** and **2**), together with guignardone A (**3**), were isolated from *Macrophomina phaseolina* cultures. The phytopathogenic fungus was isolated from infected soybean tissues showing charcoal rot symptoms in Argentina. Charcoal rot is a devastating disease considering that soybean is one of the main legumes cultivated in the world. Phaseocyclopentenones A and B were characterized by 1D and 2D ^{1}H and ^{13}C NMR spectroscopic and HRESIMS spectrometric data and chemical methods as 4-benzoyl-3,4,5-trihydroxy-2-phenylcyclopent-2-enone and 3,5-dihydroxy-2,4-diphenylcyclopent-2-enone, respectively. The relative configuration of phaseocyclopentenones A and B was assigned by ^{1}H and NOESY NMR methods, while their absolute configurations were assigned by electronic circular dichroism methods. When assayed on a nonhost plant (*Solanum lycopersicum* L.) by the leaf puncture assay, phaseocyclopentenones A and B and guignardone A showed phytotoxic activity, while only **1** and **2** were toxic when tested on cuttings of the same plant. No phytotoxicity or antifungal activity was detected for the three compounds on the host plant soybean (*Glycine max* L.) and against some of its fungal pathogens, namely, *Cercospora nicotianae* and *Colletotrichum truncatum*, also isolated from infected soybean plants in Argentina.

Charcoal rot (CR) is one of the most common and severe dry root rot diseases that limits the productivity of many crops around the world. Economically significant losses caused by this disease have been reported in many important arable, vegetable, and fruit crops.[1,2] CR is caused by *Macrophomina phaseolina* (Tassi) Goidanish, a phytopathogenic fungus with a wide host range of about 500 cultivated and wild plant species in more than 100 families.[3] The serious negative impact of *M. phaseolina* has prompted research on the identification and characterization of genetic variability within its natural populations in order to better understand its complex biology.[4−8] Among the most economically important crops that *M. phaseolina* can infect, there is soybean (*Glycine max* L.), a Fabaceae or Leguminosae that was genetically modified. Currently, soybean is one of the most important crops in the world, with an estimated total market value of about 146.23 billion USD in 2017.[9] Soybean grains are utilized globally as a critical substrate for foods, feeds, fuels, and biobased materials. It is used not only for human consumption but also to produce low-cost, high protein produced in bulk as ingredients for remanufacture and formulated for several different foods.[10−12] Soybean is cultivated mainly in South America (Brazil, Argentina, Paraguay, and Bolivia), North America (United States and Canada), Asia (China and India), Eastern Europe, and Northern Asia (Russia and Ukraine).[13,14]

A recent review by Evidente et al. (2019)[15] describes some studies carried out to investigate the phytotoxins produced by

Received: November 30, 2020

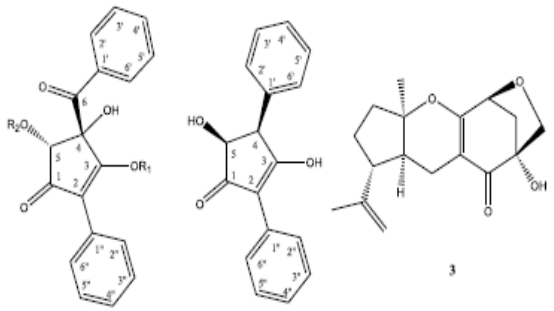

Figure 1. Structures of phaseocyclopentenones A and B (**1** and **2**), guignardone A (**3**), and the 3,5-di-*O*-acetyl derivative of phaseocyclopentenone A (**4**).

M. phaseolina that potentially are involved in the CR disease. Phaseolinone, an eremophilane sesquiterpenoid, which inhibits seed germination of black gram (*Phaseolus mungo* L.), was first isolated from culture filtrates of *M. phaseolina*, and its structure was determined by spectroscopic and chemical methods.[16] Its absolute configuration was assigned by comparison of its electronic circular dichroism (ECD) and ^{1}H NMR data with those of phomenone, another eremophilane sesquiterpenoid isolated from *Phoma exigua* and other *Phoma* sp. such as *Phoma destructiva* Plowr, responsible for wilt in tomato (*Solanum lycopersicum* L.).[17] Subsequently, phaseolinone was isolated in India from the culture filtrates of *M. phaseolina* together with asperlin, isoasperlin, phaseolinic acid, and acetylphomalactone. All the metabolites caused nonspecific leaf necrosis on several plants, but only phaseolinone induced disease symptoms in plants similar to those caused by the pathogen.[18]

Phaseolinone was not produced when *M. phaseolina* was isolated from infected soybean plants in Mississippi, while (−)-botryodiplodin appeared to be the main phytotoxin.[19] The latter is a mycotoxin previously isolated from *Botryodiplodia theobromae*, a fungus that causes rot in tropical fruits[20] and was synthesized as racemic mixture and as a pure enantiomer,[21−34] and its availability permitted a study of its role in plant disease.[3]

Recently, the metabolites produced by a strain of *M. phaseolina* isolated from *Eucalyptus globulus* were investigated and identified as the well-known fungal metabolites (3*R*,4*S*)-botryodiplodin, succinic acid, tyrosol, (*R*)-mellein, (3*R*,4*R*)-*cis*-4-hydroxymellein, and azelaic acid. However, no biological activities were reported for these metabolites.[25]

Soybean is the most important crop in Argentina, with an average cropping area of 18 million hectares in the last five years.[26] However, the growing conditions under monoculture and no-tillage systems have favored the occurrence and the severity of a large number of diseases, which constitute a serious constraint to production and the quality of the legume. Thus, many studies were carried out to develop biocontrol methods based on seed inoculation with biological control agents. Some bacteria were evaluated in dual in vitro tests for their antifungal activity combined with manganese phosphite. Two strains, *Pseudomonas fluorescens* 9 and *Bacillus subtilis* 54, were selected. Consequently, greenhouse experiments demonstrated that the greatest reductions in soybean disease severity induced by *M. phaseolina* were achieved when strain *P. fluorescens* 9 was applied singly or when strain *B. subtilis* 54 was combined with manganese phosphite, achieving 82% control in both cases.[27] Additionally, soybean seed treatments with two biological products (*Trichoderma viride* or *Bacillus subtilis*) proved to be useful in reducing the CR intensity at the field level.[28] Recently, *Pseudomonas donghuensis* strain SVBP6, isolated from an agricultural field plot in Argentina, showed a broad-spectrum and diffusible antifungal activity. From its culture filtrates the main antifungal metabolite was isolated and identified as 7-hydroxytropolone, which showed significant antifungal activity against *M. phaseolina*. This result is important for its potential practical application as a natural fungicide readily synthesized and bioformulated and as a precursor for novel bioactive tropolonoid compounds.[29]

On this basis it seemed essential to investigate the phytotoxins produced by a strain of *M. phaseolina* isolated from infected soybean tissues in Argentina. This article reports the isolation and chemical and biological characterization of two new penta- and tetrasubstituted cyclopentenones named phaseocyclopentenones A and B.

RESULTS AND DISCUSSION

The organic extract of the culture filtrates of *M. phaseolina*, obtained as described in the Experimental Section, was fractionated by a combination of column and TLC chromatography to afford two new metabolites, named phaseocyclopentenones A and B (**1** and **2**, Figure 1), and the known guignardone A (**3**, Figure 1). The meroterpenoid **3** showed the same physical (specific optical rotation), spectroscopic, and spectrometric (^{1}H, ^{13}C, COSY, HSQC, and HMBC NMR and ESIMS) data when compared to those reported after its first isolation from *Guignardia mangiferae*, an endophytic fungus isolated from *Ilex cornuta* leaves.[30] This is the first isolation of guigardone A (**3**) from *M. phaseolina*.

A preliminary investigation of the ^{1}H and ^{13}C NMR spectra of the two specialized metabolites (**1** and **2**) isolated from the Argentina strain of *M. phaseolina* showed that they shared two structural features, i.e., monosubstituted phenyl and cyclopentenone residues.

https://dx.doi.org/10.1021/acs.jnatprod.0c01287
J. Nat. Prod. XXXX, XXX, XXX−XXX

Table 1. ^{1}H and ^{13}C NMR and HSQC Data of Macrophenylcyclopentenones A and B (1 and 2)[a,b]

	1			2		
position	δ_C[c]	δ_H (J in Hz)	HMBC	δ_C[c]	δ_H (J in Hz)	HMBC
1	190.5, C		H-5	195.8, C		H-4, H-5
2	115.2, C		H-2″,6″	115.0, C		H-2″,6″, H-4
3	196.6, C		H-5	194.1, C		H-4, H-5
4	88.0, C		H-5	55.1, CH	4.14, d (5.9)	
5	79.7, CH	4.69, s		71.5, CH	4.79, d (5.9)	
6	200.3, C		H-2′,6′			
1′	136.7, C		H-3′,5′	136.4, C		H-3′,5′, H-4, H-5
2′, 6′	129.6, CH	8.05, d (8.0)	H-3′,5′, H-4′	129.7, CH	7.26, m[d]	H-3′,5′, H-4
3′, 5′	127.3, CH	7.43, t (8.0)	H-2′,6′	127.4, CH	7.40, t (7.7)	
4′	132.0, CH	7.53, t (8.0)	H-2′,6′, H-3′,5′	126.5, CH	7.29, t (7.7)	H-2′,6′
1″	130.8, C		H-3″,5″	131.5, C		H-3″,5″
2″, 6″	127.7, CH	7.83, d (8.0)	H-4″	127.8, CH	7.93, d (8.0)	H-4″
3″, 5″	127.4, CH	7.36, t (8.0)	H-2″,6″	127.4, CH	7.40, t (8.0)	
4″	126.4, CH	7.25, t (8.0)	H-2″,6″	126.0, CH	7.26 m[d]	H-2″,6″

[a]The chemical shifts are in δ values (ppm) from TMS. [b]2D $^{1}H,^{1}H$ (COSY) and $^{13}C,^{1}H$ (HSQC) NMR experiments delineated the correlations of all the protons and the corresponding carbons. [c]Multiplicities were assigned by DEPT spectrum. [d]These signals are overlapped.

Phaseocyclopentenone A (**1**) was determined to have a molecular formula of $C_{18}H_{14}O_5$ as deduced from its HRESIMS spectrum and consistent with 12 hydrogen deficiencies. The presence of the phenyl, benzoyl, and cyclopentenone residues was in agreement with the absorption bands for aromatic, olefinic, and carbonyl groups and the absorption maxima for conjugated aromatic systems observed in the IR[31] and UV[32] spectra, respectively. The IR spectra also showed the presence of bands typical of hydroxy groups.[31] Accordingly, its ^{1}H and COSY data[33] (Table 1) showed signals consistent with the aforementioned residues. In particular, a doublet (J = 8.0 Hz, H-2′,6′), a triplet (J = 8.0 Hz, H-3′,5′), and a triplet (J = 8.0 Hz, H-4′) resonating at δ 8.05, 7.43, and 7.53, respectively, accounted for the protons of the benzoyl group[32] supported by the C-6 carbonyl signal at δ 200.3 in the ^{13}C NMR spectrum (Table 1) which coupled in the HMBC spectrum[33] (Table 1) with H-2′,6′. In the same spectrum the quaternary sp^2 carbon (C-1′) of the same benzene ring at δ 136.7 coupled, as expected, with both H-3′,5′.[34]

Similar spin systems were observed for the other phenyl group. In fact, a doublet (J = 8.0 Hz, H-2″,6″), a triplet (J = 8.0 Hz, H-3″,5″), and a triplet (J = 8.0 Hz, H-4″) were observed at δ 7.83 7.36, and 7.25, respectively. H-3″,5″ in the HMBC spectrum coupled with the quaternary sp^2 carbon (C-1″) of the same ring resonating at δ 130.8. The two phenyl groups and the carbonyl group accounted for nine indices of hydrogen deficiency, and thus three other indices remained to be assigned. These were due to a pentasubstituted cyclopentenone ring. In fact, a quaternary olefinic carbon at δ 115.2 (C-2) coupled in the HMBC spectrum with H-2″,6″, while the proximal enolic carbon (C-3) appeared at δ 196.6, being also coupled in the HMBC spectrum with H-5 of a secondary hydroxylated carbon (C-5) resonating as a singlet at δ 4.69. H-5 coupled, in the same spectrum, with the carbonyl (C-1) of the cyclopentenone and the hydroxylated sp^3 tertiary carbon (C-4) present at δ 190.5 and 88.0, respectively.[32,34]

The correlations observed in the HSQC spectrum[35] (Table 1) permitted the assignment of the chemical shifts to the protonated carbons. In particular, the signals at δ 132.0, 129.6, 127.7, 127.4, 127.3, and 126.4 were attributed to C-4′, C-2′,6′, C-2″,6″, C-3″,5″, C-3′,5′, and C-4″. Thus, the chemical shifts were assigned to the protons and corresponding carbons as shown in Table 1, and phaseocyclopentenone A (**1**) was formulated as 4-benzoyl-3,4,5-trihydroxy-2-phenylcyclopent-2-enone. The relative configuration at C-4 and C-5 of **1** was assigned by the correlations observed in the NOESY spectrum.[35] In particular, a diagnostic correlation was observed between H-5 and H-2′,6′, indicating that H-5 and the benzoyl group are cofacial, suggesting the (4S*,5R*) relative configuration.

The structure assigned to **1** was supported by the other correlations observed in its HMBC spectrum (Table 1) and its HRESIMS spectrum. The latter, recorded in positive modality, showed the dimer protonated adduct $[2\ M + Na]^+$ and the protonated adduct $[M + H]^+$ ions at m/z 643 and 311.0927. A significant fragmentation peak produced from the protonated adduct by loss of water $[M + H - H_2O]^+$ was observed at m/z 293. When the same spectrum was recorded in negative modality, the dimer deprotonated adduct $[2\ M - H]^-$ and the deprotonated adduct $[M - H]^-$ ions were observed at m/z 619 and 309.0773, respectively.

The structure of **1** was also supported by preparing its 3,5-di-*O*-acetyl derivative (**4**). The ^{1}H NMR data of derivative **4** differed from that of **1** for the deshielding ($\Delta\delta$ 1.45) of H-5 appearing as a singlet at δ 6.14 and the presence of the singlets of the acetyl methyl groups of C-3 and C-5 at δ 2.09 and 1.92. The other acetyl group was located at C-3 for the absence of NOESY correlations between its methyl group and H-2′-6′. Thus, the hydroxy group at C-4 was not acetylated due to the well-documented difficulty to derivatize tertiary hydroxy groups. Its ESIMS data showed the protonated $[M + H]^+$ ion at m/z 395.

Phaseocyclopentenone B (**2**) had a molecular formula of $C_{17}H_{14}O_3$ as deduced from its HRESMS spectrum and consistent with 11 indices of hydrogen deficiency. As cited above, it contains the same phenyl and cyclopentenone residues as compound **1**. In fact, the absorption bands for aromatic, olefinic, and carbonyl groups and the absorption maxima for a conjugated aromatic system were observed in the IR[31] and UV[32] spectra, respectively. In addition, the IR spectrum also showed the presence of bands typical of hydroxy groups.[31] Thus, on the basis of these preliminary results, **2** should differ from **1** with respect to the nature of the moiety at C-4. In fact, **2** showed the presence of another monosub-

https://dx.doi.org/10.1021/acs.jnatprod.0c01287
J. Nat. Prod. XXXX, XXX, XXX−XXX

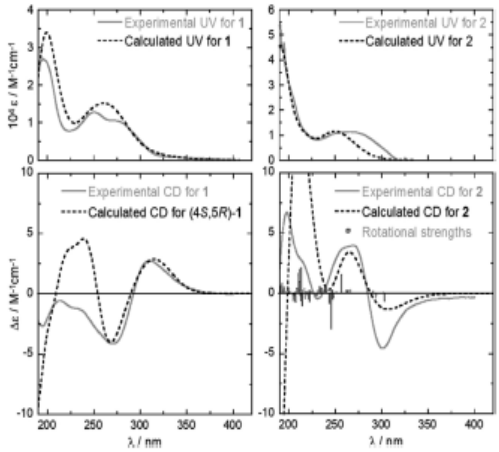

Figure 2. Experimental UV and ECD spectra of **1** and **2** measured in MeCN (solid gray lines) compared with the spectra calculated for (4*S*,5*R*)-**1** and (4*R*,5*S*)-**2** at the B3LYP/def2-TZVP//ωB97X-D/6-311+G(d,p) level. The vertical bars in the bottom right spectrum represent calculated rotational strengths (in arbitrary units). See Computational Section for details.

Table 2. Phytotoxic Activity of Compounds 1−3[a]

		1		2		3		
bioassay	plant	10^{-3}[c]	10^{-4}	10^{-3}	10^{-4}	10^{-3}	10^{-4}	control[b]
leaf puncture assay	*Solanum lycopersicum* L.	2	1	2	2	3	3	0
	Glycine max L.	0	0	0	0	0	0	0
cutting assay	*S. lycopersicum* L.	1	n.t.[d]	3	n.t.	n.t.	n.t.	0

[a]Observations were made 7 days after treatment. Intensity of necrosis on leaves in the leaf puncture assay: 3, severe necrosis; 2, intermediate necrosis; 1, slight necrosis; 0, no necrosis. Intensity of wilting symptoms in cutting assay: 3, complete wilting; 2, intermediate symptoms; 1, slight symptoms; 0, no symptoms. [b]4% MeOH in distilled water. [c]Molar concentration. [d]Not tested.

stituted phenyl group instead of the benzoyl and tertiary hydroxy groups present in **1**. As expected, the ^{1}H and ^{13}C NMR data of **2** confirmed by COSY, HSQC, and HMBC data (Table 1) supported the suggested structure. In particular the spectra differed from that of **1** in the presence of two coupled doublets (J = 5.9 Hz) observed at δ 4.79 and 4.14 (H-5 and H-4), which accounted for two adjacent methine groups, one of which was hydroxylated,[32] while their corresponding carbons resonated at δ 71.5 and 55.1 (C-5 and C-4), respectively.[34] Another difference was the absence of the benzoyl moiety, replaced by a phenyl group. The long-range HMBC couplings between C-1′ and C-2′,6′ at δ 136.4 and 129.7 with H-4 and between C-2 at δ 115.0 with H-2″,6″ permitted localization of the two phenyl group at C-4 and C-2, respectively. Thus, the chemical shifts were assigned to all the protons and corresponding carbons and reported in Table 1, and phaseocyclopentenone B was formulated as 3,5-dihydroxy-2,4-diphenylcyclopent-2-enone (**2**).

The structure assigned to **2** was supported by the other couplings observed in its HMBC spectrum (Table 1) and its HRESIMS data. The latter, acquired in positive modality, showed the dimer sodium $[2M + Na]^+$ and protonated $[2M + H]^+$ adducts and the protonated adduct $[M + H]+$ ions at m/z 555, 533, and 267.1023.

The relative configuration at carbons C-4 and C-5 was assigned by the correlations observed in the NOESY spectrum[33] between their geminal protons. Thus, H-4 and H-5 were *cis*-positioned and the relative configuration was (4*R**,5*S**).

Both metabolites **1** and **2** resisted crystallization, as well as the derivative **3**. Thus, the AC of phaseocyclopentenones A and B (**1** and **2**) was determined by means of ECD, using a standardized procedure.[35−37] ECD spectra of **1** and **2** were recorded in MeCN and simulated using an established approach, which is summarized in the Computational Section. Comparison between experimental and calculated spectra (Figure 2) permitted assignment of the absolute configurations as (4*S*,5*R*)-**1** and (4*R*,5*S*)-**2**.

It must be noticed that the agreement between experimental and calculated spectra is not completely satisfying in the short-wavelength region of the spectra. This fact may be ascribed to the presence of various chromophores with multiple transitions close in energy, which renders the wavelength region below 250 nm loaded with electronic excitations. This is shown in Figure 2 for compound **2**, for which a single strongly preferred conformer was obtained.

The phytotoxic activity was tested using two different bioassays. The culture filtrate, the organic extract (at a concentration of 1 mg/mL), and compounds **1** and **2** (at a

https://dx.doi.org/10.1021/acs.jnatprod.0c01287
J. Nat. Prod. XXXX, XXX, XXX−XXX

concentration of 10^{-3} M) were tested on tomato (*Solanum lycopersicum* L.) by a cutting assay. Strong phytotoxicity was observed testing the culture filtrate, the organic extract, and phaseocyclopentenone B (**2**), which caused strong wilting, while slight symptoms were detected for plants treated with compound **1**. Compounds **1** and **2** were also tested by the leaf puncture assay on tomato and soybean (*Glycine max* L.), together with guignardone A (**3**) (which was obtained in lower amount), at a concentration of 10^{-3} and 10^{-4} M. Compounds **1**–**3** showed phytotoxicity on tomato at both concentrations, while no activity was observed on the host plant (Table 2).

Compound **3** induced marked necrosis compared to compounds **1** and **2**, especially at the highest concentration (Figure 3).

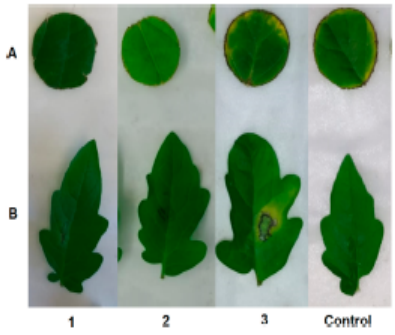

Figure 3. Phytotoxic activity induced by compounds **1**–**3** when tested at 10^{-3} M by the leaf-puncture assay on soybean (A: *Glycine max* L.) and on tomato (B: *Solanum lycopersicum* L.); control 4% MeOH in distilled water.

These results demonstrated the importance of the substituents present at C-4 and C-5 in compounds **1** and **2** to impart the phytotoxicity but also a different mechanism of action in the two bioassays. This is the first report on the phytotoxic activity of guignardone A also with respect to the other related meroterpenoids belonging to the same group of natural compounds. When assayed against *Colletotrichum truncatum* and *Cercospora nicotianae* (two fungi pathogenic to soybean), the metabolites **1**–**3** did not exhibit any antifungal activity.

In conclusion, two new phytotoxic specialized metabolites, named phaseocyclopentenones A and B, were isolated from a strain of *M. phaseolina* collected in Argentina from infected soybean plants together with the well-known fungal meroterpenoid guignardone A. The latter was isolated for the first time from *M. phaseolina*, which was previously shown to produce only the toxic sesquiterpene eremophilane phaseolinone[18] and the polyketide (-)-botryodiplodin, a toxin also produced by other phytopathogenic fungi.[19,20]

Fungal metabolites containing a dihydroxycyclopentenone core are known as naturally occurring compounds, such as kodaistatins A–D produced by *Aspergillus terreus* with antidiabetic activity, that are similar to phaseocyclopentenone A (**1**), but they differed in the position of the substituents attached to the core.[38] However, the closest compound to **1** is a synthetic compound prepared by a gold-catalyzed oxidative reaction of propargylic carbonates or acetates using 3,5-dichloropyridine.[39] Two fungal metabolites, named involutin and chamonixin, are the natural compounds closest to phaseocyclopentenone B (**2**), but they differ for the position and the nature of the substituents on the cyclopentenone core.[40]

EXPERIMENTAL SECTION

General Experimental Procedures. A P-1010 digital Jasco polarimeter was used to measure the optical rotations in MeOH; a PerkinElmer Spectrum 100 FT-IR spectrometer was employed to record IR spectra as a glassy film; a Jasco V-530 spectrophotometer was utilized to acquire UV spectra in MeCN solution; UV and ECD spectra were recorded at room temperature on a JASCO J815 spectropolarimeter, using 0.1 mm cells and concentrations of ca. 1.7×10^{-2} M in MeOH. ^{1}H and ^{13}C NMR spectra were recorded in $CDCl_3$, also used as internal standard, at 400/100 MHz on a Bruker spectrometer. COSY-45, HSQC, and HMBC experiments were performed using a Bruker microprogram. HRESI and ESI mass spectra and LC/MS analyses were carried out using the LC/MS TOF system Agilent 6230B, HPLC 1260 Infinity. A Phenomenex LUNA [C_{18} (2) 5u 150 × 4.6 mm column] was utilized to perform the HPLC separations. Preparative and analytical TLC were performed on silica gel (Merck, Kieselgel 60 F254, 0.50 and 0.25 mm, respectively) plates, while column chromatography (CC) was performed on silica gel (Merck, Kieselgel 60, 0.063–0.200 364 mm); the spots were visualized by exposure to UV light and/or by spraying with 10% H_2SO_4 in MeOH and with 5% phosphomolybdic acid in EtOH, followed by heating at 110 °C for 10 min. Sigma-Aldrich Co. (Milan, Italy) supplied all the reagents and the solvents.

Fungal Strain and Culture Conditions. The *M. phaseolina* 2013-1 strain was obtained from infected soybean roots growing in Pergamino, Buenos Aires, Argentina, and it was maintained on potato dextrose agar (PDA) in Petri dishes. The isolate was deposited in the fungal culture collection of the Plant Pathology Department of the University of Buenos Aires (FAUBA, Argentina). Later, the isolate was grown under stationary conditions in 2 L flasks containing 1 L of potato dextrose broth (PDB). Each flask was inoculated with 15 mycelial plugs and incubated at 25 °C in the dark for 15 days. Next, the mycelial mats were removed by centrifugation (7000 rpm for 30 min), and successive filtration of the supernatant was performed using 0.22 μm pore diameter membranes (Whatman, Maidstone, UK).

Extraction and Purification of Secondary Metabolites Produced by *M. phaseolina*. The culture filtrates of *M. phaseolina* (4 L), showing significative phytotoxic activity on tomato (*S. lycopersicum* L.), were combined and concentrated under vacuum at room temperature to 400 mL. Then, the culture was acidified to pH 2 with formic acid and extracted exhaustively with EtOAc (3 × 400 mL). The organic extracts were combined, dried (Na_2SO_4), and evaporated under reduced pressure. The corresponding residue (109.7 mg) was purified by silica gel column chromatography eluted with EtOAc–MeOH–H_2O, 85:10:5 (v/v/v), yielding eight groups of homogeneous fractions. The residue of the second fraction (8.3 mg) was purified on TLC eluted with CH_2Cl_2–MeOH, 1:1 (v/v), yielding guignardone A (**3**, 3.6 mg) as an amorphous solid. The residue of the seventh fraction (20.2 mg) was further purified on TLC eluted with $CHCl_3$–EtOAc–MeOH–H_2O, 2:2:1 (v/v/v), yielding phaseocyclopentenones A (**1**, 10.2 mg) and B (**2**, 7.5 mg) as two yellowish oils.

*Phaseocyclopentenone A (**1**)*: IR ν_{max} 3332 (OH), 1719 (C=O), 1676 (C=C) (1597, 1530, 1503 (Ar)); UV λ_{max} nm (log ε) 279 (4.54), 248 (4.45); ^{1}H and ^{13}C NMR data, see Table 1; HRESIMS (+) *m/z* 643 [2 M + Na]$^+$, 311.0927 [M + H]$^+$ (calcd for $C_{18}H_{15}O_5$, 311.0919), 293 [M + H − H_2O]$^+$; HRESIMS (−) *m/z* 619 [2 M − H]$^-$, 309.0773 [M − H]$^-$ (calcd for $C_{18}H_{13}O_5$, 309.0763).

*Phaseocyclopentenone B (**2**)*: $[\alpha]^{25}_D$ +33 (*c* 0.4); IR ν_{max} 3309 (OH), 1705 (C=O), 1627 (C=C), 1598, 1524, 1496 (Ar); UV λ_{max} nm (log ε) 277 (4.38); ^{1}H and ^{13}C NMR data, see Table 1; HRESIMS (+) *m/z* 555 [2 M + Na]$^+$, 533 [2 M + H]$^+$, 267.1023 [M + H]$^+$ (calcd for $C_{17}H_{14}O_5$, 267.1021).

https://dx.doi.org/10.1021/acs.jnatprod.6b01287
J. Nat. Prod. XXXX, XXX, XXX−XXX

Guignardone A (**3**): $[\alpha]^{25}_{D}$ +42 (*c* 0.3 acetone) [lit.:[30] $[\alpha]^{25}_{D}$ +42 (*c* 0.30 acetone)]; ^{1}H and ^{13}C COSY, HSQC, and HMBC NMR and ESIMS spectra (see SI) were similar to those previously reported.[30]

3,5-Di-*O*-acetyl Derivative of Phaseocyclopentenone A (4). Phaseocyclopentenone A (**1**, 1 mg) was acetylated with pyridine (20 μL) and Ac_2O (20 μL). The reaction was left at room temperature in the dark for 48 h and stopped by evaporation under a N_2 stream. The residue (1.2 mg) was purified by TLC, eluted with CH_2Cl_2−MeOH (9:1), to afford **4** as a homogeneous compound. ^{1}H NMR *δ* 8.04 (2H, d, *J* = 8.0 Hz, H-2′, H-6′), 7.95 (2H, d, *J* = 8.0 Hz, H-2″, H-6″), 7.52 (1H, t, *J* = 8.0 Hz, H-4′), 7.44 (2H, t, *J* = 8.0 Hz, H-3′, H-5′), 7.29 (2H, t, *J* = 8.0 Hz, H-3″, H-5″), 7.21 (1H, t, *J* = 8.0 Hz, H-4″), 6.14 (1H, s, H-5), 2.09 (3H, s, MeCO-C3), 1.92 (3H, s, MeCO-C5); ESIMS (+) *m*/*z* 395 $[M + H]^+$.

Computational Details. Molecular mechanics and preliminary density functional theory (DFT) calculations were run with Spartan'18 (Wavefunction, Inc., Irvine, CA, 2018),[41] with standard parameters and convergence criteria. Final DFT and time-dependent DFT (TDDFT) calculations were run with Gaussian'16[42] with default grids and convergence criteria. First, the conformational space of **1** and **2** was sampled with the Monte Carlo algorithm using the Merck molecular force field (MMFF). All conformers thus found were first optimized at the ωB97X-D/6-31G(d) level in vacuo, then at the ωB97X-D/6-311+G(d,p) level including the SMD solvent model for MeCN. The procedure led to four conformers for **1** and one conformer for **2** with sizable populations at 300 K. TDDFT calculations were run using B3LYP and CAM-B3LYP functionals (which led to consistent results) with the def2-TZVP basis set and including the IEF-PCM solvent model for MeCN. The calculations included 48 excited states (roots). ECD spectra were generated by applying a Gaussian band shape with a 0.4 eV exponential half-width, from dipole-length rotational strengths. The difference from dipole-velocity values was negligible. The calculated spectra in Figure 1 are plotted with SpecDis;[43] they are red-shifted by 10 nm (**1**) or 5 nm (**2**) and scaled by a factor 1.5 to compare with the experimental spectra.

Phytotoxicity Bioassay. *Tomato Cutting Assay.* The culture filtrate, the organic extract (at a concentration of 1 mg/mL), and phaseocyclopentenones A and B (**1** and **2**) were assayed on tomato (*S. lycopersicum* L.) cuttings. Tomato cuttings were taken from 21-day-old seedlings, and compounds **1** and **2** were assayed at a concentration of 10^{-3} M. Cuttings were placed in the test solutions (2 mL) for 72 h and then transferred to distilled water. MeOH in distilled water (4%) was used as a negative control. Three replications were performed for the organic extract and each metabolite. Symptoms were visually evaluated up to 7 days, and wilting symptoms were evaluated using a visual 0−3 scale (0 = no symptoms; 1 = slight symptoms; 2 = intermediate symptoms; 3 = complete wilting).

Leaf Puncture Assay. Compounds **1**−**3** were also tested on tomato and soybean (*Glycine max* L.) using the leaf puncture assay at concentrations of 10^{-3} and 10^{-4} M. Compounds **1**−**3** were first dissolved in MeOH (final concentration: 4%), and sterile distilled water was added to reach the required concentration. A droplet (20 μL) of the solutions was applied on the adaxial surface of the plant leaves, which were previously punctured with a sterile needle. The leaves were placed on the surface of a water-saturated filter paper in Petri dishes. A solution of 4% MeOH in distilled water was used as a negative control. The dishes were sealed with parafilm and incubated at 24 °C for 7 days in a temperature-regulated chamber. Three replications were performed for each metabolite and plant species. After 7 days of treatment, necrotic lesion development was evaluated by removing the Petri dish cover and using a visual 0−3 scale (0 = no symptoms; 1 = slight necrosis; 2 = intermediate necrosis; 3 = severe necrosis).

Antifungal Bioassay. The antagonistic potential of compounds **1**−**3** was tested against two strains of soybean pathogenic fungi, *Cercospora nicotianae*[44] and *Colletotrichum truncatum*,[45] isolated in Argentina, for inhibition of the mycelial radial growth. In brief, 6 mm diameter mycelial plugs from a 4-day-old culture of *C. nicotianae* or *C. truncatum* were placed in the center of PDA plates. For each compound, amounts of 50, 100, and 200 μg were dissolved in 20 μL of 4% MeOH and applied to the tops of different mycelial plugs. Pentachloronitrobenzene at a concentration of 25 μg/μL and 20 μL of 4% MeOH were used as positive and negative controls, respectively. The solvent was allowed to evaporate in a laminar flow cabinet, and the plates were incubated at 20 °C for 4−7 days or until the growth of the target fungi used as negative control covered the entire plate surface. Each treatment consisted of three replicates, and the experiment was repeated twice. The results were expressed as the presence or absence of growth (an indication of antifungal activity).

■ ASSOCIATED CONTENT

Supporting Information

The Supporting Information is available free of charge at https://pubs.acs.org/doi/10.1021/acs.jnatprod.0c01287.

1D and 2D ^{1}H and ^{13}C NMR and HRESIMS spectra of **1** and of **2** (PDF)

■ AUTHOR INFORMATION

Corresponding Author

Antonio Evidente − *Dipartimento di Scienze Chimiche, Università di Napoli Federico II, Complesso Universitario Monte S. Angelo, 80126 Napoli, Italy*; orcid.org/0000-0001-9110-1656; Phone: +39 081 2539178; Email: evidente@unina.it

Authors

Marco Masi − *Dipartimento di Scienze Chimiche, Università di Napoli Federico II, Complesso Universitario Monte S. Angelo, 80126 Napoli, Italy*; orcid.org/0000-0003-0609-8902

Francisco Sautua − *Facultad de Agronomía, Cátedra de Fitopatología, Universidad de Buenos Aires, C1053 CABA Buenos Aires, Argentina*

Roukia Zatout − *Dipartimento di Scienze Chimiche, Università di Napoli Federico II, Complesso Universitario Monte S. Angelo, 80126 Napoli, Italy; Laboratoire de Mycologie, de Biotechnologie et de l'Activité Microbienne (LaMyBAM), Département de Biologie Appliquée, Université des Frères Mentouri, Constantine 25017, Algeria*

Stefany Castaldi − *Dipartimento di Biologia, Università di Napoli Federico II, Complesso Universitario Monte S. Angelo, 80126 Napoli, Italy*

Lorenzo Arrico − *Dipartimento di Chimica e Chimica Industriale, Università di Pisa, 56124 Pisa, Italy*; orcid.org/0000-0002-3563-894X

Rachele Isticato − *Dipartimento di Biologia, Università di Napoli Federico II, Complesso Universitario Monte S. Angelo, 80126 Napoli, Italy*

Gennaro Pescitelli − *Dipartimento di Chimica e Chimica Industriale, Università di Pisa, 56124 Pisa, Italy*; orcid.org/0000-0002-0869-5076

Marcelo Aníbal Carmona − *Facultad de Agronomía, Cátedra de Fitopatología, Universidad de Buenos Aires, C1053 CABA Buenos Aires, Argentina*

Complete contact information is available at: https://pubs.acs.org/10.1021/acs.jnatprod.0c01287

Notes

The authors declare no competing financial interest.

■ ACKNOWLEDGMENTS

G.P. acknowledges the CINECA award under the ISCRA initiative for the availability of high-performance computing

CHAPTER III: *Pseudomonas fluorescens* Showing Antifungal Activity against *Macrophomina phaseolina*, a Severe Pathogenic Fungus of Soybean, Produce Phenazine as the Main Active Metabolite.

biomolecules

MDPI

Article

Pseudomonas fluorescens Showing Antifungal Activity against *Macrophomina phaseolina*, a Severe Pathogenic Fungus of Soybean, Produces Phenazine as the Main Active Metabolite

Stefany Castaldi [1,*], Marco Masi [2], Francisco Sautua [3], Alessio Cimmino [2], Rachele Isticato [1], Marcelo Carmona [3], Angela Tuzi [2] and Antonio Evidente [2]

[1] Dipartimento di Biologia, Università di Napoli Federico II, Complesso Universitario Monte S. Angelo, Via Cintia 4, 80126 Napoli, Italy; isticato@unina.it
[2] Dipartimento di Scienze Chimiche, Università di Napoli Federico II, Complesso Universitario Monte S. Angelo, Via Cintia 4, 80126 Napoli, Italy; marco.masi@unina.it (M.M.); alessio.cimmino@unina.it (A.C.); angela.tuzi@unina.it (A.T.); evidente@unina.it (A.E.)
[3] Cátedra de Fitopatología, Facultad de Agronomía, Universidad de Buenos Aires, Ciudad Autónoma de Buenos Aires C1417DSE, Argentina; sautua@agro.uba.ar (F.S.); carmonam@agro.uba.ar (M.C.)
* Correspondence: stefany.castaldi@unina.it

Citation: Castaldi, S.; Masi, M.; Sautua, F.; Cimmino, A.; Isticato, R.; Carmona, M.; Tuzi, A.; Evidente A. *Pseudomonas fluorescens* Showing Antifungal Activity against *Macrophomina phaseolina*, a Severe Pathogenic Fungus of Soybean, Produce Phenazine as the Main Active Metabolite. *Biomolecules* **2021**, *11*, 1728. https://doi.org/10.3390/biom11111728

Academic Editor: Pio Maria Furneri

Received: 26 October 2021
Accepted: 17 November 2021
Published: 19 November 2021

Publisher's Note: MDPI stays neutral with regard to jurisdictional claims in published maps and institutional affiliations.

Abstract: *Pseudomonas fluorescens* 9 and *Bacillus subtilis* 54, proposed as biofungicides to control *Macrophomina phaseolina*, a dangerous pathogen of soybean and other crops, were grown *in vitro* to evaluate their ability to produce metabolites with antifungal activity. The aim of the manuscript was to identify the natural compounds responsible for their antifungal activity. Only the culture filtrates of *P. fluorescens* 9 showed strong antifungal activity against *M. phaseolina*. Its organic extract contained phenazine and mesaconic acid (1 and 2), whose antifungal activity was tested against *M. phaseolina*, as well as *Cercospora nicotianae* and *Colletotrichum truncatum*, other pathogens of soybean; however, only compound 1 exhibited activity. The antifungal activity of compound 1 was compared to phenazine-1-carboxylic acid (PCA, 3), 2-hydroxyphenazine (2-OH P, 4), and various semisynthetic phenazine nitro derivatives in order to perform a structure–activity relationship (SAR) study. PCA and phenazine exhibited the same percentage of growth inhibition in *M. phaseolina* and *C. truncatum*, whereas PCA (3) showed lower activity against *C. nicotianae* than phenazine. 2-Hydroxyphenazine (4) showed no antifungal activity against *M. phaseolina*. The results of the SAR study showed that electron attractor (COOH and NO_2) or repulsor (OH) groups significantly affect the antifungal growth, as well as their α- or β-location on the phenazine ring. Both PCA and phenazine could be proposed as biopesticides to control the soybean pathogens *M. phaseolina*, *C. nicotianae*, and *C. truncatum*, and these results should prompt an investigation of their large-scale production and their suitable formulation for greenhouse and field applications.

Keywords: *Pseudomonas fluorescens*; *Macrophomina phaseolina*; phenazine; phenazine analogs and derivatives; soybean pathogens; antifungal activity; SAR

1. Introduction

Food demand has increased with the gradual growth of the world population, which is expected to reach almost 10 billion by 2050 [1,2]. Likewise, agricultural production has increased over time with the development of technology and biotechnology innovations. As a consequence, the environmental pollution of soil and water has negatively and significantly affected the quality and quantity of agricultural production [3,4]. Microbial pathogens, weeds, and animal pests among the biotic stresses are responsible for heavy

losses affecting crop yields. The use of chemical pesticides (herbicides, insecticides, fungicides, bactericides, etc.) has increased over time. Their massive use during the last 5–6 decades has become a threat to environmental preservation and a severe risk to human and animal health. Among the biotic stresses, fungal pathogens are the main causal agents of crop diseases. Their ability to produce phytotoxins plays an important role in inducing plant disease symptoms [5,6].

Macrophomina phaseolina (Tassi) Goid is one of the most virulent and yield-limiting phytopathogens [7,8]. This necrotrophic fungus can infect more than 500 plant species in more than 100 families causing dry root and stem rot, known as charcoal rot (CR) [9]. CR is an important disease of leguminous crops such as soybean, chickpea, peanut, alfalfa, bean, and pea, as well as of cereals such as maize, sorghum, and sugarcane. Recently, *M. phaseolina* was reported as responsible for grapevine decline in Iran [10]. The first studies on the phytotoxins produced by *M. phaseolina* reported the purification and the properties of the exotoxin produced by the pathogen isolated in India [11]. Subsequently, the main phytotoxin structure, an eremophilane sesquiterpenoid named phaseolinone, was determined [12]. Recently, from strain 2013-1 of *M. phaseolina*, obtained from infected soybean roots growing in Pergamino, Argentina, two new phytotoxic penta- and tetra-substituted cyclopentenones, named phaseocyclopentenones A and B, together with guignardone A, were isolated. [13].

Fungi belonging to other genera such as *Cercospora* and *Colletotrichum* are causal agents of several diseases of soybean in Argentina and Brazil, which have also developed resistance or changes in sensitivity to commonly used fungicides [14–18].

A collection of bacteria were isolated to soybean plants and screened for their antagonistic activity against *M. phaseolina* aiming to avoid the use of chemical fungicides. Two of them, identified as *Pseudomonas fluorescens* 9 and *Bacillus subtilis* 54 resulted most promising and were tested further using in vitro assays, as well as in the greenhouse. In particular, *P. fluorescens* 9 showed a greater reduction in disease than *B. subtilis* [19]. These results are not surprising, as the microbial antagonisms performed by beneficial bacteria and fungi against different phytopathogens are well known [20]. In fact, some bacterial metabolites have shown antifungal activity against pathogens of some important crops, such as phenazine-1-carboxylic acid and 2-hydroxyphenazine, which are produced by *Pseudomonas chlororaphis* subsp. *aureofaciens* strain M7. These metabolites, compared to some semisynthetic phenazine-1-carboxylic acid (PCA) derivatives, were assayed against a group of crop and forest plant-pathogenic fungi. Among the compounds tested, PCA was active against almost all tested pathogens. Instead, 2-hydroxyphenazine (2-OH P) weakly inhibited a few fungal species. The results of a structure–activity relationship (SAR) study, testing the four semisynthetic derivatives of PCA, showed that the carboxyl group is a structural feature important for the antifungal activity of PCA [21]. It is known that the PCA completely inhibited in vitro [22] and in vivo [23] the growth of *Seiridium cardinale*, a fungus that induces canker of common Italian cypress (*Cupressus sempervirens* L.). Another example is *Emericella* sp. SMA01, a marine symbiotic fungus that produced PCA as the main metabolite with antifungal activity against *Phytophthora capsici*, *Gibberella zeae*, and *Verticillium dahliae* with IC_{80} values of 23.26–53.89 μg/mL [24]. PCA was also produced by *Streptomyces kebangsaanensis* isolated from the stem of a Malaysian ethnomedicinal plant, *Portulaca oleracea* in 2013. PCA inhibited *Fusarium solani* isolates, UZ541/12, and UZ667/13 at a minimal inhibitory concentration of 18.00 μg/mL [25]. Phenazine derivatives also showed inhibitor activity toward clinical antibiotic-resistant bacteria such as *Mycobacterium tuberculosis* in the range 18.3 to 146.5 μM [26].

This study reports the isolation, chemical characterization, and antifungal activity of phenazine and mesaconic acid produced by *P. fluorescens* 9 against *M. phaseolina*, *C. nicotianae*, and *C. truncatum*, all isolated from soybean in Argentina. The antifungal activity of phenazine was compared to that of PCA and 2-OH P, as well as some other semisynthetic derivatives prepared by nitration of phenazine to evaluate their potential as natural fungicides. The results of a structure–activity relationship (SAR) study are also discussed.

2. Materials and Methods

2.1. General Experimental Procedures

A Bruker spectrometer (Karlsruhe, Germany) working at 400 MHz was used to record ^{1}H-NMR spectra in $CDCl_3$ which was used as an internal standard. The LC/MS TOF system Agilent 6230B, HPLC 1260 Infinity was used to record ESI mass spectra. The Phenomenex LUNA (C18 (2) 5 µm 150 × 4.6 mm column was used for HPLC separation. Analytical and preparative thin-layer chromatography (TLC) was performed on silica gel plates (Kieselgel 60, F_{254}, 0.25 and 0.5 mm respectively) or on reverse-phase (Whatman, KC18 F_{254}, 0.20 mm, plates (Merck, Darmstadt, Germany). UV light and/or iodine vapors were used to visualize the compounds (CC: silica gel, Merck, Kieselgel 60, 0.063–0.200 mm). The samples of standard phenazine and meseconic acid were purchased from Sigma Aldrich. The samples of PCA and 2OH P (**3** and **4**) were obtained from the culture filtrate of *P. chlororaphis* subsp. *aureofaciens* strain M71, as previously reported [21].

2.2. Bacterial and Fungal Strains

P. fluorescens 9 and *B. subtilis* 54 strains were isolated from soil samples and healthy soybean plants collected in the field from different locations in the Santa Fe Province, Argentina as previously reported [19]. The *M. phaseolina* 2013-1 strain was obtained from infected soybean roots grown in Pergamino, Buenos Aires, Argentina, as previously reported [13]. *Cercospora nicotianae* isolate Cn_2017_BOL34 was obtained from soybean leaves with Cercospora leaf blight symptoms sampled from commercial soybean fields in Santa Cruz, Bolivia in 2017 as previously reported [15]. The strain 17-5-1 of *Colletotrichum truncatum* was isolated from soybean leaves with anthracnose symptoms sampled from commercial soybean fields in Roldán, Santa Fe, Argentina in 2017. The strain identified was kept in the culture collection of the Department of Plant Pathology, FAUBA.

2.3. Cell-Free Supernatants

Bacteria were grown in minimal medium M9 (composition according to the Cold Spring Harb Protoc 2010 for 1 L: (1×) M9 salts mixture from Sigma-Aldrich (Saint-Louis, MO, USA) supplemented with 20% glucose, 1 M $MgSO_4$, and 1 M $CaCl_2$) at 28 ± 2 °C for 72 h with shaking at 150 rpm. Then, the cells were removed by centrifugation (7000× *g* for 30 min), and supernatants were filtered using 0.22 µm pore diameter membranes (Corning® New York, NY, USA) and concentrated 1:10.

2.4. Production, Extraction, and Purification of Metabolites from Pseudomonas Fluorescens 9 and Production of the Crude Extract of Bacillus subtilis 54

P. fluorescens 9 and *B. subtilis* 54 were grown separately in minimal medium M9 for 72 h with shaking at 150 rpm. Cells were removed by centrifugation (7000× *g* for 30 min), and supernatants were filtered using 0.22 µm pore diameter membranes (Corning®). The culture filtrate (1 L for each bacterium) was lyophilized, and the material obtained was dissolved in distilled water (100 mL). A 50 mL aliquot was alkalinized with ammonia (37%) up to pH 10 and extracted with ethyl acetate (3 × 50 mL). The organic extracts were combined, washed with distilled water, and dehydrated with Na_2SO_4. The filtrates were evaporated under reduced pressure, obtaining an amorphous yellow solid residue (15 mg for *P. fluorescens* 9) and white solid residue (8 mg for *B. subtilis* 54). Only the crude extract of *P. fluorescens* 9 was purified by TLC on silica gel eluted with chloroform–*iso*-propanol (97:3) yielding a pure homogenous solid that was identified, as reported below, as phenazine (**1**, 2.1 mg). The other 50 mL of the initial culture filtrate was acidified with formic acid up to pH 2 and extracted with ethyl acetate (3 × 50 mL). The organic extracts were treated as above reported to give a white crystal identified, as reported below, as mesaconic acid (**2**, 3.5 mg).

1. Phenazine (**1**): yellow amorphous solid, ^{1}H-NMR δ: 8.29 (4H, dd, J = 6.5 and 3.3 Hz), 7.88 (4H, dd, J = 6.5 and 3.3 Hz). ESI MS (+) m/z: 181 $[M + H]^+$.

2. Mesaconic acid (**2**): white crystals, ^{1}H-NMR (CD_3OD) δ: 6.76 (1H, q, *J* = 1.4 Hz), 2.23 (3H, d, *J* = 1.4 Hz). ESI MS (−): *m*/*z* 129 $[M - H]^-$.

2.5. Nitration of Phenazine

Phenazine (**1**, 200 mg) was added to a mixture of concentrated sulfuric acid (0.5 mL) and nitric acid (37%, 0.5 mL). The reaction was carried at 50 °C for 4 days. The solution was poured into ice water, and its pH was adjusted to 9–10 with concentrated NaOH (**12** N), before extraction with ethyl acetate (3 × 70 mL). The organic extracts were combined, dried (Na_2SO_4), filtered, and evaporated under reduced pressure, yielding a yellow solid residue (150 mg). This was purified on a silica gel column eluted with methylene chloride. Ten homogeneous fractions were obtained (F1–F10). F2 (3.2 mg) was isolated as a yellow amorphous solid and identified as 1,9-dinitrophenazine (**7**). F3 (10.9 mg) was further purified by TLC eluted with methylene chloride, yielding a yellow amorphous solid (2.5 mg) identified as 2,9-dinitrophenazine (**8**). F5 (28.4 mg) was further purified by TLC eluted with methylene chloride–*iso*-propanol 98:2, yielding a yellow amorphous solid (23.5 mg) identified as 1,3-dinitrophenazine (**6**). Lastly, F8 (14.4 mg) was further purified by TLC eluted with methylene chloride–*iso*-propanol 95:5, yielding a yellow amorphous solid (**5**, 3.0 mg) identified as 2-nitrophenazine.

1. 2-Nitrophenazine (**5**): yellow amorphous solid, ^{1}H-NMR δ: 9.24 (1H, d. *J* = 3.4 Hz, H-1), 8.60 (1H, dd, *J* = 9.5 and 3.4 Hz, H-3), 8.43 (1H, d, *J* = 9.5 Hz, H-4), 8.33 (2H, m, H-6 and H-9), 7.99 (2H, m, H-7 and H-8), Figure S1. ESI MS (+) *m*/*z*: 226 $[M + H]^+$.
2. 1,3-Dinitrophenazine (**6**): yellow amorphous solid, ^{1}H-NMR δ: 9.28 (1H, d, *J* = 2.2 Hz, H-4), 9.26 (1H, d, *J* = 2.2 Hz, H-2), 8.70 (2H, m, H-7 and H-8), 8.51 (2H, m, H-6 and H-9), Figure S2. ESI MS (+) *m*/*z*: 271 $[M + H]^+$, ESI MS (−) *m*/*z*: 269 $[M - H]^-$.
3. 1,9-Dinitrophenazine (**7**): yellow amorphous solid, ^{1}H-NMR δ: 8.60 (2H, br d, *J* = 8.6 Hz, H-4 and H-6), 8.30 (2H, dd, *J* = 7.7 and 1.2 Hz, H-2 and H-8), 8.04 (2H, m, H-3 and H-7), Figure S3. ESI MS (+) *m*/*z*: 271 $[M + H]^+$, ESI MS (−) *m*/*z*: 269 $[M - H]^-$.
4. 2,9-Dinitrophenazine (**8**): yellow amorphous solid, ^{1}H-NMR δ: 9.26 (1H, d, *J* = 2.5 Hz, H-1), 8.69 (1H, dd, *J* = 9.0 and 2.5 Hz, H-3), 8.59 (1H, br d, *J* = 8.9 Hz H-6), 8.53 (1H, d, *J* = 9.0 Hz, H-4), 8.39 (1H, br d, *J* = 8.9 Hz, H-8), 8.04 (1H, t, *J* = 8.9 Hz, H-7), Figure S4. ESI MS (+) *m*/*z*: 271 $[M + H]^+$, ESI MS (−) *m*/*z*: 269 $[M - H]^-$.

2.6. Crystal Structure Determination of Mesaconic Acid (2)

Single crystals of mesaconic acid (**2**) suitable for X-ray structure analysis were obtained by slow evaporation of a solution of **2** in ethyl acetate. One selected crystal was mounted in flowing N_2 at 173 K on a Bruker Nonius Kappa CCD diffractometer equipped with Oxford Cryostream apparatus (graphite monochromated MoKα radiation λ = 0.71073 Å, CCD rotation images, thick slices, φ and ω scans to fill asymmetric unit). The structure was solved by direct methods using the SIR97 program [27] and anisotropically refined by the full matrix least-squares method on F^2 against all independent measured reflections using the SHELXL-2018/3 program [28]. The hydroxy H atoms were located in difference Fourier maps and freely refined with Uiso (H) equal to 1.2 Ueq of the carrier atom. All the other hydrogen atoms were introduced in calculated positions and refined according to the riding model. Crystals were of poor quality, and the structure was refined as a two-component twin using HKLF5 procedure. Crystallographic data of **2**: empirical formula: $C_5H_6O_4$; formula weight: 130.10 g·mol^{-1}; monoclinic, P $2_1/c$; a: 7.079(2) Å; b: 11.8200(**7**) Å; c: 6.8680(**15**) Å; β: 97.92(2)°; V: 569.2(2) Å^3; Z: 4, Dx: 1.518 Mg/m^3; independent reflections: 4831; final R indices [I > 2sigma(I)]: R1 = 0.1347, wR2 = 0.3625; largest diffraction peak and hole: 0.665 and −0.697 e.A^{-3}. All crystallographic data for **2** were deposited in the Cambridge Crystallographic Data Center with deposition number CCDC 2121226. These data can be obtained free of charge from www.ccdc.cam.ac.uk/data_request/cif. The room-temperature crystal structure of mesaconic acid was previously reported by Gupta et al. [29].

2.7. Antifungal Assay

To test the cell-free supernatants (CSFs) of *P. fluorescens* 9 and *B. subtilis* 54, 100 µL aliquots were placed on the potato dextrose agar (PDA) plate at 1.5 cm from the fungal disc (6 × 6 mm diameter) of *M. phaseolina*. As a positive control, fungicidal pentachloronitrobenzene ≥94% (PCNB) (Sigma-Aldrich, Saint-Louis, MO, USA) dissolved in toluene was used. Toluene alone was used as a negative control. The experiment was performed in triplicate; the plates were incubated at 28 °C for 5 days and examined for zones of inhibition of grown colonies [30].

The crude extracts of both bacteria were dissolved in 4% methanol and tested against *M. phaseolina* at a final concentration of 10 mg/mL as described above. To detect the antifungal activity of compounds obtained by *P. fluorescens* 9 phenazine (**1**), of its natural analogs (**3** and **4**), and of semisynthetic derivatives (**5**–**8**), as well as that of mesaconic acid (**2**), against *M. phaseolina*, *C. nicotianae*, and *C. truncatum*, the dual-culture plate method was carried out as previously described by Puopolo et al. [21] with some modifications. The fungi were grown in Potato Dextrose Agar (PDA) separately at 28 ± 2 °C for 5–7 days. Fungal plugs of 6 × 6 mm diameter were placed at the center of PDA plates, and each compound at 25, 50, 100, 200, 300, 500, and 1000 µg/mL, with a final concentration of 4% methanol, was placed on the opposite four sides of the plates 1.5 cm away from the fungal disc. Plates containing the fungal plugs alone were used as a positive control. As a negative control, 4% MeOH was applied on the top of each fungal plug positioned in the center of the Petri dish. All plates were incubated at 28 ± 2 °C for 5–7 days, and the experiments were performed in triplicate. The percentage inhibition of fungal growth was calculated using the following formula:

$$\% = [(Rc - Ri)/Rc] \times 100 \quad (1)$$

where Rc is the radial growth of the test fungi in the control plates (mm), and Ri is the radial growth of the fungi in the presence of different compounds tested (mm). The results show the antifungal activity of different compounds analyzed by ANOVA using Tukey's test.

2.8. Minimal Inhibitory Concentration (MIC_{80})

The minimal inhibitory concentration (MIC_{80}) was determined using the broth microdilution method in 24-well microplates, as described by Mefteh et al. [31] with some modifications. Serial dilution of each compound (**3**, **1**, and **5**–**8**) was prepared to get final concentrations ranging from 1 to 100 µg/mL dissolved in 4 % of MeOH. Each well contained ultrapure Milli-Q water with different tested compounds dissolved and a fungal plug (4 × 4 mm) resuspended in 2× PD broth in a final volume of 500 µL. The wells containing the different fungal plugs with only PD broth were used as a positive control and with the added of 4% MeOH as a negative control. The experiment was performed in triplicate. The plates were incubated at 28 °C for 7 days. The MFC values of different tested compounds (**1**, **3**, and **5**–**8**) were interpreted as the concentrations able to inhibit 50% of fungal growth. Finally, the percentage inhibition of fungal growth was calculated using the formula described above.

2.9. Data Analysis

All statistical analyses were performed using GraphPad Prism (GraphPad 243 Software, San Diego, CA), and the data were expressed as the mean ± SEM. Differences among groups were compared by ANOVA or *t*-test as indicated in figure legends. Differences were considered statistically significant at $p < 0.05$.

3. Results and Discussion

Both the culture filtrates and their corresponding organic extracts obtained from the selected strains *P. fluorescens* 9 and *B. subtilis* 54 [19] were tested for their ability to inhibit

the growth of *M. phaseolina* in vitro. As shown in Figure 1, the CSFs of *P. fluorescens* 9 and *B. subtilis* 54 inhibited the fungus growth by 65% and 60%, respectively, in agreement with the results previously reported [19]. However, when the corresponding crude organic extracts were tested, only that of the first bacterium confirmed its strong antifungal activity, inhibiting the growth of *M. phaseolina* by about 75% (Figure 1).

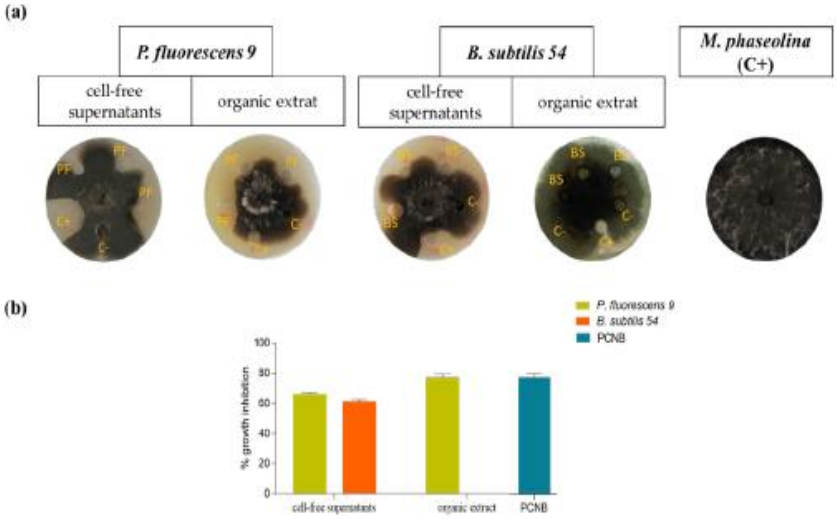

Figure 1. Antifungal activity of cell-free supernatants (CSFs) and respective organic extracts of *P. fluorescens* 9 and *B. subtilis* 54 against *M. phaseolina*. (a) CSFs of bacterial strains collected after 72 h of growth and the respective organic extracts were tested for their ability to inhibit the mycelial growth of *M. phaseolina*. C+: positive control, pentachloronitrobenzene (PNCB) 0.5 mg/mL; C−: negative control, toluene. All experiments were performed in triplicate with three independent trials. (b) The percentage inhibition of fungal growth was reported as the percentage reduction in the diameter of the fungal mycelia compared to the control plate. Data are presented as means ± standard deviation ($n = 3$). For comparative analysis of groups of data, one-way ANOVA was used; *p*-values were extremely significant ($p < 0.0001$).

Thus, the organic extract of *P. fluorescens* 9 culture filtrates was fractionated, as reported in detail Section 2, to yield phenazine and mesaconic acid (2-methyl-1,4-butenoic acid), as indicated by numbers **1** and **2**, respectively, in Figure 2. Both **1** and **2** were identified by ^{1}H-NMR (Figure 3a,b) and ^{13}C-NMR (Figure 4a,b), as well as ESI MS spectra, in comparison with those of commercially available standards recorded in the same conditions. The standards were also used in co-chromatography analyses developed in different solvent mixtures. Mesaconic acid was crystallized by slow evaporation of ethyl acetate solution, and X-ray analysis was carried out. The crystal data corresponding to that structure have already published [29].

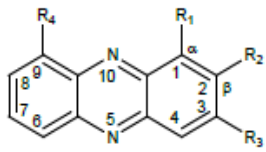

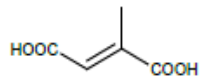

2

1, $R_1=R_2=R_3=R_4=H$
3, $R_1=COOH$, $R_2=R_3=R_4=H$
4, $R_1=R_3=R_4=H$, $R_2=OH$
5, $R_1=R_3=R_4=H$, $R_2=NO_2$,
6, $R_1=R_3=NO_2$, $R_2=R_4=H$
7, $R_1=R_4=NO_2$, $R_2=R_3=H$
8, $R_2=R_4=NO_2$, $R_1=R_3=H$

Figure 2. Structure of phenazine (1), its natural analogs 1-carboxy and 2-hydroxy-phenazine (3 and 4), and four mono- and dinitro derivatives (5–8) and mesaconic acid (2).

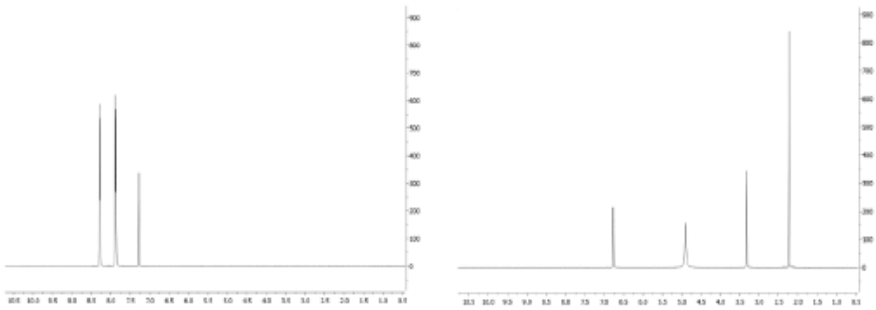

(a) **(b)**

Figure 3. (a) ^{1}H-NMR spectrum of phenazine (1) recorded in $CDCl_3$ at 400 MHz; (b) ^{1}H-NMR spectrum of mesaconic acid (2) recorded in CD_3OD at 400 MHz.

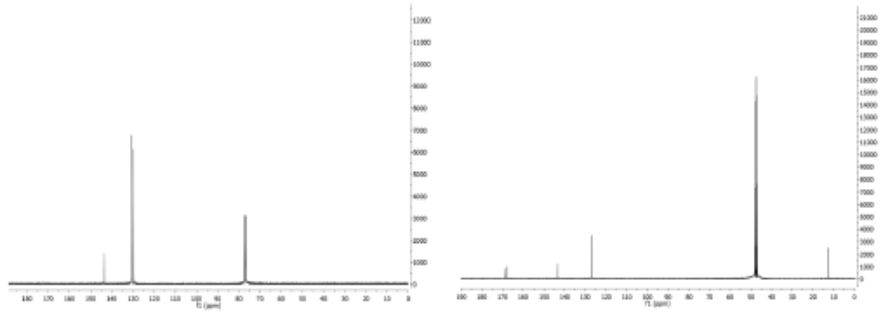

(a) **(b)**

Figure 4. (a) ^{13}C-NMR spectrum of phenazine (1) recorded in $CDCl_3$ at 125 MHz; (b) ^{13}C-NMR spectrum of mesaconic acid (2) recorded in CD_3OD at 125 MHz.

Mesaconic acid (2) was crystallized by slow evaporation of ethyl acetate solution. The compound was undoubtedly identified by the X-ray analysis as mesaconic acid, and the

molecular structure is reported in Figure 5. The crystal structure of mesaconic acid, previously reported at room temperature by Gupta et al. [29], was redetermined at 173 K.

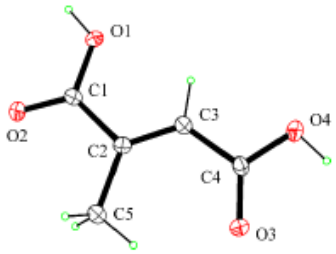

Figure 5. ORTEP view of the molecular structure of 2. Thermal ellipsoids were drawn at the 30% probability level.

Mesaconic acid and several other organic acids having a methyl or methylene side-chain have been reported, as well as their interconversion biological systems. Mesaconate hydration is also the key biosynthetic step to obtain D-citromalate in *P. fluorescens* [32]. The natural occurrence of mesaconic acid in a variety of plants and animals has also been reported [33].

Phenazines have primarily been isolated from *Pseudomonas*, *Streptomyces*, as well as from a few other soil or marine organisms. They show several biological activities including antimalaria, antibiotic, antitumor, and antiparasitic activities, which were reviewed together with their biosynthesis and the preparation of semisynthetic derivatives [34]. More than 100 different natural phenazine analogs and over 6000 synthetic compounds have been investigated as potential anticancer agents, and the results were critically reviewed [35].

The antifungal activity of phenazine and its natural analogs is of particular interest for their potential application in agriculture as biofungicides. In fact, the isolation of PCA (**3**) (Figure 2) from *P. chlororaphis* subsp. *aureofaciens* strain M7, as well as its ability to completely inhibit *S. cardinale* in vitro [22] and in vivo [23], was previously mentioned. 1-Hydroxyphenazine together with cereusitin was also produced, as the main metabolite, from a strain *P. aeruginosa* 2016NX1, isolated from the root of *Millettia specisoa*. 1-Hydroxyphenazine strongly inhibited the growth of several common plant-pathogenic fungi and bacteria such as *Cochliobolus miyabeanus*, *Diaporthe citri*, *Salmonella* sp., and *Klebsiella oxytoca*, and its potential as a biocontrol agent was evaluated [36]. Instead, 2-hydrophenazine (**4**) as reported above exhibited only slight antifungal activity. *P. aeruginosa* KU_BIO2, obtained from soil, was also able to produce a pyocyanin blue-green phenazine pigment which showed interesting ecofriendly medicine, agriculture, and environment applications. In fact, it showed remarkable dye properties and significant inhibition of *Magnaporthe grisea* and *Xanthomonas oryzae* growth, causal agents of two different severe rice diseases [37]. A mutation in the gltA gene of the *P. chlororaphis* subgroup from a native isolate from Argentina was recently reported as a determinant inductor of a phenotypic change associated with phenazine production, which is essential for the bacterial antifungal activity [38]. In addition, phenazine derivatives were also produced by fluorescent pseudomonads (FPs) proposed for the control of sheath blight of rice [39].

Thus, phenazine and mesaconic acid (**1** and **2**) isolated from *P. fluorescens* 9 (which are FPs) were spot-inoculated in PDA plates to test for their antifungal activity against some phytopathogenic fungi isolated from infected soybean, *M. phaseolina*, *C. nicotianae*, and *C. truncatum*, as described in Section 2. As shown in Figure 6, only phenazine exhibited a strong antifungal activity when spot-inoculated (25 µg/mL), inhibiting the growth of *M. phaseolina* by around 40%, *C. nicotianae* by 100%, and *C. truncatum* by around 50%.

Mesaconic acid tested up to 1 mg/mL used in the spot inoculation against the same pathogenic fungi did not show any antifungal activity. The variation in activity (75% against 40%) observed when testing the crude extract (Figure 1) and phenazine (Figure 6) on *M. phaseolina* is probably due to the other metabolites present in the crude organic extract obtained from CSFs of *P. fluorescens* 9. These compounds, although present in very low amounts, as shown by TLC analysis, could probably act synergically with phenazine, obtaining major inhibitory activity.

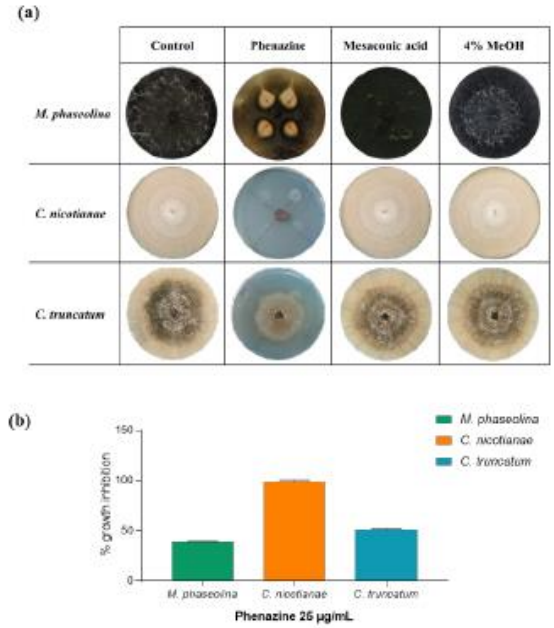

Figure 6. Effects of phenazine (1) and mesaconic acid (2) produced by *P. fluorescens* 9. The graphic shows the ability of phenazine to inhibit the fungal growth at a concentration of 25 µg/mL. (a) Representative photos of the antifungal assay for in vitro inhibition of mycelial growth of *M. phaseolina*, *C. nicotianae*, and *C. truncatum*: positive control (fungi alone), phenazine, mesaconic acid, and negative control (4% MeOH). (b) Inhibition of fungal growth by phenazine reported as the percentage reduction in the diameter of the fungal mycelia in the treated plate compared to that in the control plate. Data are presented as means ± standard deviation ($n = 3$) compared to control fungi grown alone. For comparative analysis of groups of data, one-way ANOVA was used; p-values were extremely significant ($p < 0.001$).

Considering these results, the activity of phenazine (1) was compared with that of PCA (3), 2-OH P (4) (for this analog, only against *M. phaseolina*), and some synthetic derivatives, which were prepared in order to study the effect of one or more electron attractor groups such as NO_2 linked to the phenazine carbon skeleton at the two different positions α (C-1,C-4, C-6, and C-9) and β (C-2, C-3, C7, and C-8).

In fact, nitration of phenazine, carried out with a classic sulfur–nitric acid mixture [40] at room temperature for a long time (4 days), yielded 2-nitro, 1,3-dinitro, 1,9-dinitro,

and 2,9-dinitro phenazine (5–8). These derivatives were characterized by their ^{1}H-NMR and ESI MS spectra (as detailed in Section 2).

The nitrophenazine derivatives (5–8), compared with phenazine and PCA, were assayed against the pathogenic fungi *M. phaseolina*, *C. nicotianae*, and *C. truncatum* (Figure 5). As shown in Figure 7, PCA (3) exhibited antifungal activity when spot-inoculated at 25 µg/mL (the same concentration used for phenazine). This represents the minimal concentration able to inhibit the fungal growth. PCA (3) and phenazine exhibited the same percentage of growth inhibition of *M. phaseolina* and *C. truncatum*. In contrast, when tested against *C. nicotianae* PCA (3) showed a lower inhibition percentage (78%) than phenazine (100%). When 2-hydroxyphenazine (4) was tested against *M. phaseolina* at a final concentration from 25 µg/mL to 1 mg in 10 µL of spot inoculation, it showed no antifungal activity (data not shown).

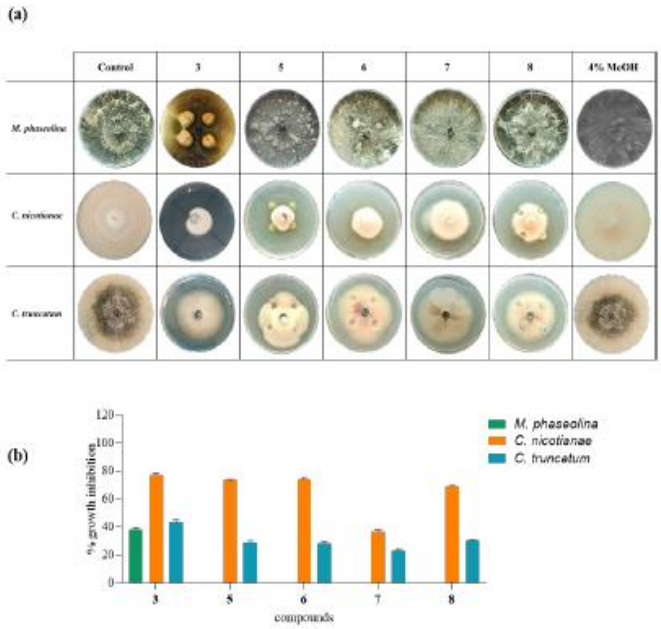

Figure 7. Effects of PCA (3) and phenazine derivates (5–8) against *M. phaseolina*, *C. nicotianae*, and *C. truncatum*. The graphic shows the fungal inhibition growth by tested compounds at a concentration of 25 µg/mL. (a) Representative photos of the biological assay for in vitro inhibition of mycelial growth of *M. phaseolina*, *C. nicotianae*, and *C. truncatum*. The positive controls were fungi grown on PDA plates, and the negative control was 4% MeOH. (b) Inhibition of fungal growth reported as the percentage reduction in the diameter of the fungal mycelia in the treated plate compared to that in the control plate. 3 = phenazine-1carboxylic acid (PCA); 5 = 2-nitrophenazine; 6 = 1,3-nitrophenazine; 7 = 1,9-dinitrophenazine; 8 = 2,9-dinitrophenazine. Data are presented as means ± standard deviation (n = 3) compared to control fungi grown alone. For comparative analysis of groups of data, one-way ANOVA was used; p-values were extremely significant ($p < 0.0001$).

Finally, all inactive nitrophenazine derivatives (5–8) were tested against *M. phaseolina* with spot-inoculation in PDA plates at concentrations from 25 µg/mL to 1 mg/mL of spot inoculation, but they did not show antifungal activity. In contrast, all derivates showed

antifungal activity against *C. nicotianae* and *C. truncatum*. In particular, the best activity was found against *C. nicotianae* with about 70% inhibition at a final concentration of 25 µg/mL.

In order to identify the minimal inhibitory concentration able to inhibit the fungal growth of 50%, the tested compounds were subjected to a microdilution plate assay against *M. phaseolina*, *C. nicotianae*, and *C. truncatum*. As shown in Table 1, for compounds **3** and **1**, 35 µg/mL was necessary to inhibit *M. phaseolina* by 50%, 15 µg/mL was necessary to inhibit *C. nicotianae*, and 25–30 µg/mL was necessary to inhibit *C. truncatum*. Regarding the phenazine derivatives, when tested on *C. nicotianae*, compounds **5**, **6**, and **8** showed an MIC_{50} of 20 µg/mL, while that of compound **7** was 40 µg/mL. Instead, all phenazine derivates (**5**–**8**) inhibited *C. truncatum* by 50% at 60 µg/mL.

Table 1. The MIC_{50} of PCA (**3**), phenazine (**1**), and phenazine derivates (**5**–**8**) against *M. phaseolina*, *C. nicotianae*, and *C. truncatum*.

	MIC_{50} (µg/mL)		
Compounds	***M. phaseolina***	***C. nicotianae***	***C. truncatum***
3	35 µg/mL	15 µg/mL	25 µg/mL
1	35 µg/mL	15 µg/mL	30 µg/mL
5	-	20 µg/mL	60 µg/mL
6	-	20 µg/mL	60 µg/mL
7	-	40 µg/mL	60 µg/mL
8	-	20 µg/mL	60 µg/mL

Phenazine and PCA could be proposed as natural antagonists for the control of not only *M. phaseolina* but also *C. nicotianae* and *C. truncatum*. According to the SAR study and considering the inhibition of *M. phaseolina*, the nature of the carboxylic and 2-hydroxy groups, which are electron attractor and electron repulsor groups, respectively, present in PCA and 2-OH P (**3** and **4**), significantly affects the inhibition of *M. phaseolina*, as **3** had the same strong inhibition as **1**, while **4** was inactive. Instead, the strong inhibition activity of 1-hydroxyphenazine reported on different pathogenic fungi and bacteria [32] indicates that only the position α or β to which the substituents are bonded play a role in imparting activity. Thus, 2-nitrophezine and 1,3-dinitro and 2,9 dinitro-phenazine should be inactive as at least one of the substituents is in the β-position. Lastly, 1,9-dinitro phenazine is probably inactive due to the well-known steric hindrance in this kind of phenazine derivative. Derivatives **5**–**8** affected the other two fungi differently from *M. phaseolina*. In particular, on *C. nicotianae*, all four derivatives **5**–**8** showed a slightly reduced activity with respect to **1** and **3**, whereas, on *C. truncatum*, the inhibition effect of these derivatives was significantly reduced; in particular, derivative **7** showed a markedly reduced inhibition of both fungi. Thus, the activity is probably also dependent on the sensitivity of fungal species.

Future studies will focus on the characterization of these compounds in order to test them at different temperatures and pH, as well as in other environmental conditions, to observe their resistance via in vitro and in vivo experiments in plants infected by phytopathogens. Other studies will focus on optimizing their large-scale production and finding the best formulation for their application in the field.

Supplementary Materials: The following are available online at www.mdpi.com/article/10.3390/biom11111728/s1: Figure S1: ^{1}H-NMR spectrum of 2-nitrophenazine (**5**), recorded in $CDCl_3$ at 400 MHz; Figure S2: ^{1}H-NMR spectrum of 1,3-dinitrophenazine (**6**), recorded in $CDCl_3$ at 400 MHz; Figure S3: ^{1}H-NMR spectrum of 1,9-dinitrophenazine (**7**), recorded in $CDCl_3$ at 400 MHz; Figure S4: ^{1}H-NMR spectrum of 2,9-dinitrophenazine (**8**), recorded in $CDCl_3$ at 400 MHz.

Author Contributions: Conceptualization, S.C., M.M., F.S., M.C., and A.E.; methodology, S.C. and M.M.; writing—original draft preparation, S.C., M.M., and A.E.; writing—review and editing, S.C., M.M., F.S., A.C., R.I., M.C., A.T. and A.E. All authors have read and agreed to the published version of the manuscript.

Funding: This research received no external funding.

Institutional Review Board Statement: Not applicable.

Informed Consent Statement: Not applicable.

Data Availability Statement: Not applicable.

Acknowledgments: A.E. is associated with the Istituto di Chimica Biomolecolare, CNR, Pozzuoli, Italy.

Conflicts of Interest: The authors declare no conflicts of interest.

References

1. Tilman, D.; Balzer, C.; Hill, J.; Befort, B.L. Global food demand and the sustainable intensification of agriculture. *Proc. Natl. Acad. Sci. USA* **2011**, *108*, 20260–20264. https://doi.org/10.1073/pnas.1116437108.
2. *The Future of Food and Agriculture-Trends and Challenges*; FAO: Rome, Italy, 2017.
3. Rosegrant, M.W.; Cline, S.A. Global food security: Challenges and policies. *Science* **2003**, *302*, 1917–1919. https://doi.org/10.1126/science.1092958.
4. Foley, J.A.; Ramankutty, N.; Brauman, K.A.; Cassidy, E.S.; Gerber, J.S.; Johnston, M.; Mueller, N.D.; O'Connell, C.; Ray, D.K.; West, P.C.; et al. Solutions for a cultivated planet. *Nature* **2001**, *478*, 337–342. https://doi.org/10.1038/nature10452.
5. Ballio, A.; Graniti, A. Phytotoxins and their involvement in plant disease. *Experientia* **1991**, *47*, 751–864. https://doi.org/10.3390/toxins3121569.
6. Evidente, A.; Cimmino, A.; Masi, M. Phytotoxins produced by pathogenic fungi of agrarian plants. *Phytochem. Rev.* **2019**, *18*, 843–870. https://doi.org/10.1007/s11101-019-09624-0.
7. Islam, M.S.; Haque, M.S.; Islam, M.M.; Emdad, E.M.; Halim, A.; Hossen, Q.M.M.; Hossain, M.Z.; Ahmed, B.; Rahim, S.; Rahman, M.S.; et al. Tools to kill: Genome of one of the most destructive plant pathogenic fungi *Macrophomina phaseolina*. *BMC Genom.* **2012**, *13*, 493. https://doi.org/10.1186/1471-2164-13-493.
8. Marquez, N.; Giachero, M.L.; Declerck, S.; Ducasse, D.A. *Macrophomina phaseolina*: General characteristics of pathogenicity and methods of control. *Front. Plant Sci.* **2021**, *12*, 634397. https://doi.org/10.3389/fpls.2021.634397.
9. Su, G.; Suh, S.O.; Schneider, R.W.; Russin, J.S. Host specialization in the charcoal rot fungus, *Macrophomina phaseolina*. *Phytopathology* **2001**, *91*, 120–126. https://doi.org/10.1094/PHYTO.2001.91.2.120.
10. Farnaz, A.A.; Narmani, A.; Arzanlou, M. *Macrophomina phaseolina* associated with grapevine decline in Iran. *Phytopat. Mediterr.* **2018**, *57*, 107–111. https://doi.org/10.14601/Phytopathol_Mediterr-20691.
11. Gupta, S.; Chandran, R.R.; Divekar, P.V. Botryodiplodin—A new antibiotic from *Botryodiplodia theobromae*. II. Production, isolation and biological properties. *Indian Exp. J. Biol.* **1966**, *4*, 152–153. https://doi.org/10.3390/toxins12010025.
12. Dhar, T.K.; Siddiqui, K.A.; Ali, E. Structure of phaseolinone, a novel phytotoxin from *Macrophomina phaseolina*. *Tetrahedron Lett.* **1982**, *23*, 5459–5462. https://doi.org/10.1016/0040-4039(82)80157-3.
13. Masi, M.; Sautua, F.; Zatout, R.; Castaldi, S.; Arrico, L.; Isticato, R.; Pescitelli, G.; Carmona, M.A.; Evidente, A. Phaseocyclopentenones A and B, phytotoxic penta- and tetra-substituted cyclopentenones produced by *Macrophomina phaseolina*, the causal agent of charcoal rot of soybean in Argentina. *J. Nat. Prod.* **2021**, *84*, 459–465. https://doi.org/10.1021/acs.jnatprod.0c01287.
14. Carmona, M.; Sautua, F.; Scandiani, M.; Bello, R.; Lopez, V.; Luque, A. In vitro sensitivity assessment of late season soybean pathogens to fungicide mixtures. *Australas. Plant Dis. Notes* **2017**, *12*, 1–4. https://doi.org/10.1007/s13314-017-0244-7.
15. Sautua, F.J.; Doyle, V.P.; Price, P.P.; Porfiri, A.; Fernandez, P.; Scandiani, M.M.; Carmona, M.A. Fungicide resistance in *Cercospora* species causing cercospora leaf blight and purple seed stain of soybean in Argentina. *Plant Pathol.* **2020**, *69*, 1678–1694. https://doi.org/10.1111/ppa.13261.
16. Dias, M.D.; Pinheiro, V.F.; Café-Filho, A.C. Impact of anthracnose on the yield of soybean subjected to chemical control in the north region of Brazil. *Summa Phytopathol.* **2016**, *42*, 18–23. https://doi.org/10.1590/0100-5405/2114.
17. Poti, T.; Mahawan, K.; Cheewangkoon, R.; Arunothayanan, H.; Akimitsu, K.; Nalumpang, S. Detection and molecular characterization of carbendazim-resistant *Colletotrichum truncatum* isolates causing anthracnose of soybean in Thailand. *J. Phytopathol.* **2020**, *168*, 267–278. https://doi.org/10.1111/jph.12888.
18. Guimarães, G.R. Morfologia, Patogenicidade e Sensibilidade à Fungicidas de Isolados de *Colletotrichum truncatum* (Schw.) Andrus & WD Moore. Ph.D. Thesis, Universidade Federal de Uberlândia, Uberlândia, Brazil, 2021; Volume 83, https://doi.org/10.14393/ufu.te.2021.148.
19. Simonetti, E.; Viso, N.P.; Montecchia, M.; Zilli, C.; Balestrasse, K.; Carmona, M. Evaluation of native bacteria and manganese phosphite for alternative control of charcoal root rot of soybean. *Microbiol. Res.* **2015**, *180*, 40–48. https://doi.org/10.1016/j.micres.2015.07.004.
20. Castaldi, S.; Petrillo, C.; Donadio, G.; Piaz, F.D.; Cimmino, A.; Masi, M.; Evidente, A.; Isticato, R. Plant growth promotion function of *Bacillus sp.* strains isolated from salt-pan rhizosphere and their biocontrol potential against *Macrophomina phaseolina*. *Int. J. Mol. Sci.* **2021**, *24*, 22–3324. https://doi.org/10.3390/ijms22073324.
21. Puopolo, G.; Masi, M.; Raio, A.; Andolfi, A.; Zoina, A.; Cimmino, A.; Evidente, A. Insights on the susceptibility of plant pathogenic fungi to phenazine-1-carboxylic acid and its chemical derivatives. *Nat. Prod Res.* **2013**, *27*, 956–966. https://doi.org/10.1080/14786419.2012.696257.

22. Raio, A.; Puopolo, G.; Cimmino, A.; Danti, R.; Della Rocca, G.; Evidente, A. Biocontrol of cypress canker by the phenazine producer *Pseudomonas chlororaphis* subsp. *aureofaciens* strain M71. *Biol. Control* **2011**, *58*, 133–138. https://doi.org/10.1016/j.biocontrol.2011.04.012.
23. Raio, A.; Reveglia, P.; Puopolo, G.; Cimmino, A.; Danti, R.; Evidente, A. Involvement of phenazine-1-carboxylic acid in the interaction between *Pseudomonas chlororaphis* subsp. *aureofaciens* strain M71 and *Seiridium cardinale* in vivo. *Microbiol. Res.* **2017**, *199*, 49–56. https://doi.org/10.1016/j.micres.2017.03.003.
24. Yue, Y.; Yu, H.; Li, R.; Hu, L.; Liu, S.;Li, P. Isolation and identification of antimicrobial metabolites from sea anemone-derived fungus *Emericella* sp. SMA01. *J. Oceanol. Limnol.* **2021**, *39*, 1010–1019.
25. Mazlan, N.A.; Santhanam, J.; Zin, N.M.; Santiago, C. Effects of combination of phenazine-1-carboxylic acid from *Streptomyces kebangsaanensis* with amphotericin B on clinical *Fusarium solani* species. *Malays. J. Microbiol.* **2020**, *16*, 432–437.
26. Halicki, P.C.B.; Nunes da Silva Júnior, E.; de Melo Jardim, G.A.; de Almeida, R.G.; de Menezes Vicenti, J.R.; Gonçalves, B.L.; Almeida da Silva, P.E.; Fernandes Ramos, D. Benzo [a] phenazine derivatives: Promising scaffolds to combat resistant *Mycobacterium tuberculosis*. *Chem. Biol. Drug Des.* **2021**, *98*, 352-362. https://doi.org/10.1111/cbdd.13853.
27. Altomare, A.; Burla, M.C.; Camalli, M.; Cascarano, G.L.; Giacovazzo, C.; Guagliardi, A.; Moliterni, A.G.G.; Polidori, G.; Spagna, R. SIR97: A new tool for crystal structure determination and refinement. *J. Appl. Crystallogr.* **1999**, *32*, 115–119.
28. Sheldrick, G.M. Crystal structure refinement with SHELXL. *Acta Crystallogr. Sect. C Struct. Chem.* **2015**, *71*, 3–8.
29. Gupta, M.P.; Yadav, S.R.P. The crystal structure of mesaconic acid, C5H6O4. *Acta Crystallogr. Sect. B Struct. Sci. Cryst.* **1972**, *28*, 2682–2686. https://doi.org/10.1107/S0567740872006776.
30. Rahman, M.M.; Hossain, D.M.; Suzuki, K.; Shiiya, A.; Suzuki, K.; Dey, T.K.; Nonaka, M.; Harada, N. Suppressive effects of *Bacillus spp.* on mycelia, apothecia and sclerotia formation of *Sclerotinia sclerotiorum* and potential as biological control of white mold on mustard. *Australas. Plant Pathol.* **2016**, *45*, 103–117. https://doi.org/10.1007/s13313-016-0397-4.
31. Mefteh, F.B.; Daoud, A.; Chenari Bouket, A.; Alenezi, F.N.; Luptakova, L.; Rateb, M.E.; Kadri, A.; Gharsallah, N.; Belbahri, L. Fungal root microbiome from healthy and brittle leaf diseased date palm trees (*Phoenix dactylifera* L.) reveals a hidden untapped arsenal of antibacterial and broad spectrum antifungal secondary metabolites. *Front. Microbiol.* **2017**, *28*, 8–307. https://doi.org/10.3389/fmicb.2017.00307.
32. Katsuki, H.; Ariga, N.; Katsuki, F.; Nagai, J.; Egashira, S.; Tanaka, S. Enzymic hydration of mesaconate by *Pseudomonas fluorescens*. *Biochim. Biophys. Acta* **1962**, *56*, 545–551. https://doi.org/10.1016/0006-3002(62)90606-6.
33. Lardy, H.A. The metabolism of itaconic acid by liver mitochondria. *J. Biol. Chem.* **1957**, *229*, 865–879. https://doi.org/10.1016/s0021-9258(19)63691-4.
34. Laursen, J.B.; Nielsen, J. Phenazine natural products: Biosynthesis, synthetic analogues, and biological activity. *Chem. Rev.* **2004**, *104*, 1663–1686. https://doi.org/10.1021/cr020473j.
35. Cimmino, A.; Evidente, A.; Mathieu, V.; Andolfi, A.; Lefranc, F.; Kornienko, A.; Kiss, R. Phenazines and cancer. *Nat. Prod. Rep.* **2012**, *29*, 487–501. https://doi.org/10.1039/c2np00079b.
36. Liu, T.T.; Ye, F.C.; Pang, C.P.; Yong, T.Q.; Tang, W.D.; Xiao, J.; Lu, Z.J. Isolation and identification of bioactive substance 1-hydroxyphenazine from *Pseudomonas aeruginosa* and its antimicrobial activity. *Lett. Appl. Microbiol.* **2020**, *71*, 303–310. https://doi.org/10.1111/lam.13332.
37. De Britto, S.; Gajbar, T.D.; Satapute, P.; Sundaram, L.; Lakshmikantha, R.Y.; Jogaiah, S.; Ito, S.I. Isolation and characterization of nutrient dependent pyocyanin from *Pseudomonas aeruginosa* and its dye and agrochemical properties. *Sci. Rep.* **2020**, *10*, 1–12. https://doi.org/10.1038/s41598-020-58335-6.
38. Agaras, B.C.; Valverde, C.F. A mutation in the glta gene from a native isolate of the *Pseudomonas chlororaphis* subgroup induces a phenotypic change associated with phenazine production. *Arch. Phytopatol. Plant Protect.* **2019**, *52*, 601–624. https://doi.org/10.1080/03235408.2018.1549649.
39. Karmegham, N.; Vellasamy, S.; Natesan, B.; Sharma, M.P.; Al Farraj, D.A.; Elshikh, M.S. Characterization of antifungal metabolite phenazine from rice rhizosphere fluorescent pseudomonads (FPs) and their effect on sheath blight of rice. *Saudi J. Biol. Sci.* **2020**, *27*, 3313–3326.
40. Carey, F.A.; Sundberg, R.J. *Advanced Organic Chemistry: Part B: Reactions and Synthesis*, 4th ed.; Kluwer Academic/Plenum: New York, NY, USA, 2003; Volume 80, pp. 880–883. https://doi.org/10.1021/ed080p883.2.

CHAPTER IV: Structural studies on the *O*-specific polysaccharide of the lipopolysaccharide from *Pseudomonas donghuensis* strain SVBP6, with antifungal activity against the phytopathogenic fungus *Macrophomina phaseolina*.

International Journal of Biological Macromolecules 182 (2021) 2019–2023

Contents lists available at ScienceDirect

International Journal of Biological Macromolecules

journal homepage: www.elsevier.com/locate/ijbiomac

Structural studies on the *O*-specific polysaccharide of the lipopolysaccharide from *Pseudomonas donghuensis* strain SVBP6, with antifungal activity against the phytopathogenic fungus *Macrophomina phaseolina*

Evelina L. Zdorovenko [a], Andrey S. Dmitrenok [a], Marco Masi [b], Stefany Castaldi [c], Federico M. Muzio [d], Rachele Isticato [c], Claudio Valverde [d], Yuriy A. Knirel [a], Antonio Evidente [b,*]

[a] N. D. Zelinsky Institute of Organic Chemistry, Russian Academy of Sciences, Leninsky Prospekt 47, 119991 Moscow, Russia
[b] Department of Chemical Sciences, University of Naples Federico II, Complesso Universitario Monte S. Angelo, Via Cintia 4, 80126 Naples, Italy
[c] Department of Biology, University of Naples Federico II, Complesso Universitario Monte S. Angelo, Via Cintia 4, 80126 Naples, Italy
[d] Laboratorio de Fisiología y Genética de Bacterias Beneficiosas para Plantas—Centro de Bioquímica y Microbiología del Suelo, Departamento de Ciencia y Tecnología, Universidad Nacional de Quilmes—CONICET, Buenos Aires, Argentina

ARTICLE INFO

Keywords:
Pseudomonas donghuensis
Macrophomina phaseolina
Lipopolysaccharide
O-specific polysaccharide structure
NMR spectroscopy
Antifungal activity

ABSTRACT

An *O*-specific polysaccharide (OPS) was isolated from the lipopolysaccharide (LPS) of *Pseudomonas donghuensis* SVBP6, a bacterium with a broad-spectrum antifungal activity *in vitro*, particularly that against *Macrophomina phaseolina*. This latter is one of the most virulent and dangerous pathogens of plants, including soybean which is an economically important crop in Argentina today. The OPS was studied by sugar analysis and spectroscopy (1D and 2D ^{1}H and ^{13}C NMR) showing the following trisaccharide repeating unit:

→6)-α-D-ManpNAc-(1 → 3)-β-L-Rhap-(1 → 4)-β-D-Glcp-(1→.

The crude LPS, the purified LPS and the *O*-chain were assayed for their antifungal activity against *M. phaseolina* at 25, 50, 100, and 200 μg plug^{-1}. The results showed that the crude LPS best inhibition was at 200 μg plug^{-1}, able to inhibit the fungus growth by about 45%, while purified LPS and the corresponding OPS, in the same condition, reduced fungus growth by 65%, and 75%, respectively. Furthermore, the purified LPS and OPS significantly reduced the growth of *M. phaseolina* already at 100 μg plug^{-1} compared to the crude LPS. The structure of the *O*-chain is unique among the bacterial LPS and this is the first time that both the antifungal activity of a bacterial LPS and its corresponding *O*-chain were described.

1. Introduction

Pseudomonas donghuensis strain SVBP6 is a bacterium isolated from agrarian soil in Argentina, which showed a significant and broad-spectrum antifungal activity *in vitro* [1,2] due to the secondary metabolites it synthesizes [3]. The microbial antagonisms exhibited by bacterial metabolites is well known and representative example is the phenazine-1-carboxylic acid, produced by *Pseudomonas chlororaphis* subsp. *aureofaciens* strain M7, which was able to completely inhibit *in vitro* [4] and *in vivo* [5] the growth of *Seiridium cardinale*, the fungus responsible for bark canker of common cypress (*Cupressus sempervirens* L.). Another example is maculosin, the cyclo-L-Pro-L-Tyr dipeptide belonging to the family of 2,5-diketopiperazines, produced by *Lysobacter capsici* AZ78, that completely inhibits *in vitro* and *in vivo* the growth of *Phytophthora infestans* and *Plasmopara viticola*. These latter fungi are the causal agents of potato late blight and grapevine downy mildew, respectively [6].

P. donghuensis showed significant antifungal activity *in vitro* against *Macrophomina phaseolina*, one of the most virulent and dangerous plant pathogens [7]. This fungus causes the charcoal rot disease of about 500 [8] agrarian crops including ground nut, beans and tobacco and was also reported to be responsible for grapevine decline in Iran [9]. In

* Corresponding author.
E-mail address: evidente@unina.it (A. Evidente).

https://doi.org/10.1016/j.ijbiomac.2021.05.187
Received 4 February 2021; Received in revised form 30 April 2021; Accepted 26 May 2021
Available online 31 May 2021

Argentina, *M. phaseolina* is responsible for charcoal rot disease of soybean [*Glycine* max (L.) Merr], which is an economically important crop today [10]. Thus, to avoid the use of chemical fungicides many efforts were focused to find bacterial metabolites with an antagonistic activity against *M. phaseolina*, such as those produced by *Pseudomonas fluorescens* 9 and *Bacillus subtilis* 54 [11]. Recently, 7-hydroxytropolone was identified as the main antifungal metabolite produced by *P. donghuensis* strain SVBP6, which displayed a broad spectrum and diffusible antifungal activity against *M. phaseolina*, *Fusarium graminearum* and *Fusarium semitectum* [3].

Isolation and structure determination of lipopolysaccharides (LPSs) from these bacteria could be important for the elucidation of their role in microbial antagonisms. In fact, LPS has a dramatic neutralizing propensity and a potent membrane-disruptive activity against microbial cells [12]. Structural studies of LPS components, including the *O*-specific polysaccharide (OPS), may have a chemotaxonomic value for characterizing strains and species within a genus.

In this paper, we report the isolation and structure determination of the OPS component of the LPS from *P. donghuensis* strain SVBP6. Results of studies on the antifungal activity of both LPS and OPS against *M. phaseolina* are also presented and discussed.

2. Experimental

2.1. Cultivation of bacteria

Strain SVBP6 of *P. donghuensis* was isolated from agricultural soil in Argentina and grown as recently reported by Muzio et al. [3].

2.2. Isolation of the LPS and OPS

Crude LPS (350 mg) was isolated by extraction of liophylized cells (4.8 g) with phenol-water [13] followed by removal of nucleic acids and proteins by precipitation with aq 50% OCl_3CO_2H. The LPS obtained (50 mg) was hydrolyzed with aq 2% HOAc at 100 °C for 2 h, a lipid precipitate was removed by centrifugation (13,000*g*, 20 min), and the carbohydrate portion was fractionated by GPC on a column (56 × 2.6 cm) of Sephadex G-50 (S) in 0.05 M pyridinium acetate buffer pH 4.5 monitored with a differential refractometer (Knauer, Germany) to afford OPS preparation (9 mg) and a low-molecular mass fraction (Fig. S1).

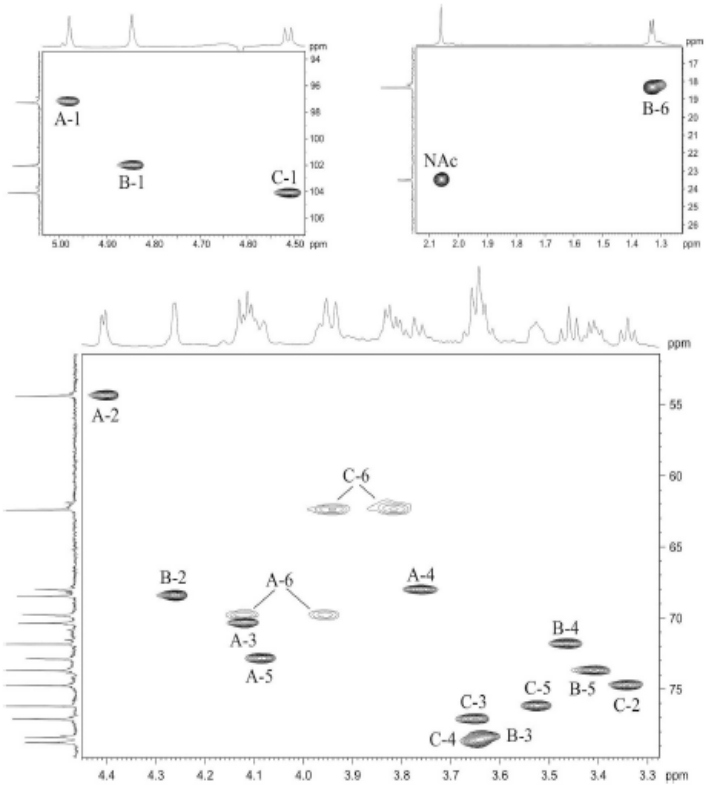

Fig. 1. Tracing connectivities in the 2D $^{1}H,^{13}C$ HSQC of the *O*-chain (OPS) from *P. donghuensis* strain SVBP6.

2.3. Molecular mass determination of OPS

The molecular mass of the OPS was established by HPLC on a TSK G3000PW$_{XL}$ column (0.78 × 30 cm) using an Agilent 1260 Infinity 2 chromatograph (Agilent, USA) with a refractometer detector in 0.2 M PBS pH 9.0 (Fig. S2). The Shodex P10 (Shodex, Japan) MW 11800D and Shodex P5 (Shodex, Japan) MW 5900 Da dextrans were used as references.

2.4. Sugar analyses

An OPS sample (0.5 mg) was hydrolyzed with 2 M CF_3CO_2H (120 °C, 2 h). Monosaccharides were analyzed as the alditol acetates by GLC on a HP-5 capillary column using a Maestro (Agilent 7820) chromatograph (Interlab, Russia) and a temperature gradient of 160 °C (1 min) to 290 °C at 7 °C min^{-1} [14]. The absolute configuration of Rha and Glc was determined by GLC of the acetylated (*S*)-2-octyl glycosides as described [15].

2.5. NMR spectroscopy

An OPS sample was deuterium-exchanged by freeze-drying twice from D_2O and then examined as a solution in 99.9% D_2O. ^1H and ^{13}C NMR spectra were recorded using a Bruker Avance II 600 MHz spectrometer (Germany) at 50 °C using internal sodium 3-trimethylsilylpropanoate-2,2,3,3-d4 (δ_H 0.0 ppm, δ_C −1.6 ppm) as references. 2D NMR experiments were performed using standard Bruker software, and Bruker TopSpin 2.1 program was used to acquire and process the NMR data. A spin-lock time of 60 ms and a mixing time of 200 ms was used in TOCSY and ROESY experiments, respectively. The HSQC spectrum was recorded with multiplicity editing during selection step. The HMBC spectrum was recorded with a 60-ms delay for evolution of long-range couplings.

2.6. Antifungal activity of LPS and OPS against M. phaseolina

The polysaccharides, isolated from *P. donghuensis* SVBP6 was tested against the phytopathogenic fungus *M. phaseolina*. The strain 2013-1 of *M. phseaolina* used in this study was obtained from infected soybean roots growing in Pergamino, Buenos Aires, Argentina, and it was maintained on potato dextrose agar (PDA) in Petri dishes. The isolate was deposited in the fungal culture collection of the Plant Pathology Department of the University of Buenos Aires (PAUBA, Argentina). The sensitivity of the fungus to this compound was evaluated on Potato dextrose agar (PDA) as the inhibition of the mycelial radial growth. In brief, mycelial plugs (6 × 6 mm diameter) were cut from the margin of actively growing 4-day-old colonies and one plug was placed in the center of a 9 cm diameter Petri dish with the mycelia in contact with the medium. Then, different amounts (25, 50, 100, and 200 μg/plug) of compound dissolved in Milli-Q ultrapure water, were applied separately on the top of each plug. Similarly, the crude and purified LPS and OPS were tested separately against *M. phaseolina*. The negative control was obtained by applying 20 μL of Milli-Q ultrapure water. The plates were incubated at 28 °C for 5 days. The percentage of inhibition of the fungal growth was calculated using the following formula:

$$\% = [(Rc - Ri)Rc \times 100]$$

where Rc is the radial growth of the test pathogen in the control plates (mm), and Ri is the radial growth of the test pathogen in the test plates (mm). The experiment was repeated in triplicate.

2.7. Statistical analysis

All the statistical analyses were performed using GraphPad Prism 8 software. Data were expressed as mean ± SEM. Differences among groups were compared by ANOVA or *t*-test as indicated in the figure legends. Differences were considered statistically significant at $p < 0.05$.

3. Results and discussion

3.1. Structure determination of OPS

A LPS preparation was obtained from the bacterial cell mass by the hot phenol/water method [13] and purified by removal of nucleic acids and proteins by precipitation with aq 50% CCl_3CO_2H. An OPS sample was isolated by GPC on Sephadex G-50 (Fig. S1). Since the OPS eluted on the G-50 column with a rather wide peak, we carried out an additional experiment and determined the range of the molecular mass of the *O*-polysaccharide by HPLC. It was found that the molecular mass of fraction Ib >5900 Da and fraction Ia >11,800 Da (Fig. S2).

Sugar analysis by GLC of the alditol acetates obtained after acid hydrolysis of the OPS revealed Rha and Glc in the ratio ~1:1 and small peak corresponded to the ManNAc (Fig. S3). Determination of the absolute configurations by GLC of the acetylated glycosides with (*S*)-2-octanol indicated that rhamnose has the L configuration and Glc the D configuration. Further studies showed that the OPS also includes ManNAc, and its D configuration was established based on the ^{13}C NMR chemical shifts using the known regularities in the glycosylation effects [16] as summarized and calculated by GODDESS NMR simulation service [17].

The ^1H NMR spectrum of the OPS (Fig. S4) contained signals for three anomeric protons at δ 4.51–4.98, other sugar ring protons at δ 3.34–4.41, CH_3 group (H-6) of Rha at δ 1.33, and *N*-acetyl group at δ 2.06. The ^{13}C NMR spectrum of the OPS showed signals for three anomeric carbons at δ 97.3–104.1, one nitrogen-bearing carbon at δ 54.4, one CH_3 group (C-6) of Rha at δ 18.4, two CH_2OH groups (C-6 of hexoses) at δ 62.4 and 69.3, other sugar ring carbons at δ 68.0–78.8, and *N*-acetyl group at δ 23.1 (CH_3) and 176.3 (CO). Therefore, the OPS is

Table 1
^1H and ^{13}C NMR chemical shifts (δ, ppm) of the *O*-specific polysaccharide of *P. donghuensis* SVBP6[a].

Sugar residue	H-1 *C-1*	H-2 *C-2*	H-3 *C-3*	H-4 *C-4*	H-5 *C-5*	H-6 (a,b) *C-6*
→6)-α-D-ManpNAc-(1 → A	4.98 *97.3*	4.41 *54.4*	4.12 *70.4*	3.76 *68.0*	4.09 *72.9*	3.96, 4.12 *69.3*
→3)-β-L-Rhap-(1 → B	4.85 *102.0*	4.26 *68.4*	3.65 *78.8*	3.46 *71.9*	3.41 *73.7*	1.33 *18.4*
→4)-β-D-Glcp-(1 → C	4.51 *104.1*	3.34 *74.7*	3.65 *77.7*	3.63 *78.3*	3.53 *76.1*	3.82, 3.94 *62.4*

[a] ^{13}C NMR chemical shifts are italicized. Chemical shifts for the *N*-acetyl group are δ_H 2.06, δ_C 23.1 (Me) and 176.3 (CO).

Table 2
Correlations for H-1 and C-1 in the 2D $^1H,^1H$ ROESY and $^1H,^{13}C$ HMBC spectra of the *O*-specific polysaccharide of *P. donghuensis* SVBP6.

Anomeric atom in sugar residue (δ, ppm)	Correlation(s) to atoms in sugar residue(s) (δ, ppm)	
	$^1H,^1H$ ROESY	$^1H,^{13}C$ HMBC
A H-1 (4.98)	A H-2 (4.41), B H-2 (4.26), H-3 (3.65)	A C-2 (54.4), C-3 (70.4), C-5 (72.9), B C-3 (78.8)
A C-1 (97.3)		A H-2 (4.41), C H-3 (3.65)
B H-1 (4.85)	B H-2 (4.26), H-3 (3.65), H-5 (3.41), C H-4 (3.63), H-5 (3.53)	B C-2 (68.4), C-5 (73.7), C C-4 (78.3)
B C-1 (102.0)		B H-2 (4.26), H-5 (3.41), C H-4 (3.63)
C H-1 (5.20)	A H-6a,b (3.96, 4.12), C H-2 (3.34), H-3 (3.65), H-5 (3.53)	A C-6 (69.3), C C-2 (74.7), C-5 (76.1)
C C-1 (104.1)		A H-6a,b (3.96, 4.12), C H-2 (3.34), H-5 (3.53)

composed of trisaccharide repeating units containing one residue each of Glc, Rha, and an *N*-acetylhexosamine (HexNAc).

Tracing connectivities in the 2D $^{1}H,^{1}H$ COSY, $^{1}H,^{1}H$ TOCSY, and $^{1}H,^{13}C$ HSQC (Figs. 1, S5–S8) spectra enabled assignment of the ^{1}H and ^{13}C NMR signals of the OPS (Table 1). As a result, spin systems were identified for the residues of HexNAc (**A**), Rha (**B**), and Glc (**C**). The assignment was based on correlations between H-1 to H-5 for Glc, H-1 to H-2 and H-2 to H-6 for Rha and HexNAc in the TOCSY spectrum, as well as between H-2 and C-2 of HexNAc in the HSQC spectrum. The assignment of the proton signals within each spin system was performed using the COSY and TOCSY spectra (Figs. S5 and S6).

The relative configurations and the pyranose form of the monosaccharides were determined based on $^{3}J_{H,H}$ coupling constants estimated from the 1D and 2D NMR spectra. Particularly, a relatively small $^{3}J_{H\text{-}2,H\text{-}3}$ value of < 4 Hz and large $^{3}J_{H\text{-}3,H\text{-}4}$ and $^{3}J_{H\text{-}4,H\text{-}5}$ values of > 8 Hz indicated that HexNAc has the *manno* configuration and is thus ManNAc.

C-5 chemical shifts of δ 72.9, 73.7 and 76.1 of ManNAc (**A**), Rha (**B**) and Glc (**C**), respectively, in the ^{13}C NMR spectrum of the OPS, as compared with the published data for the corresponding monosaccharides [18] (δ 73.3 and 77.6 for α- and β-ManNAc, respectively, δ 69.5 and 73.2 for α- and β-Rha, δ 72.4 and 77.2 for α- and β-Glc, respectively), as reported by GODDESS NMR simulation service [17] showed that ManNAc (**A**) was α-linked, whereas Rha (**B**) and Glc (**C**) had the β configuration.

Relatively low-field positions at δ 69.3, 78.8, and 78.3 of the signals for C-6 of ManNAc (**A**), C-3 of Rha (**B**) and C-4 of Glc (**C**), as compared with their positions in the corresponding non-substituted monosaccharides [16], defined the substitution pattern of the monosaccharide

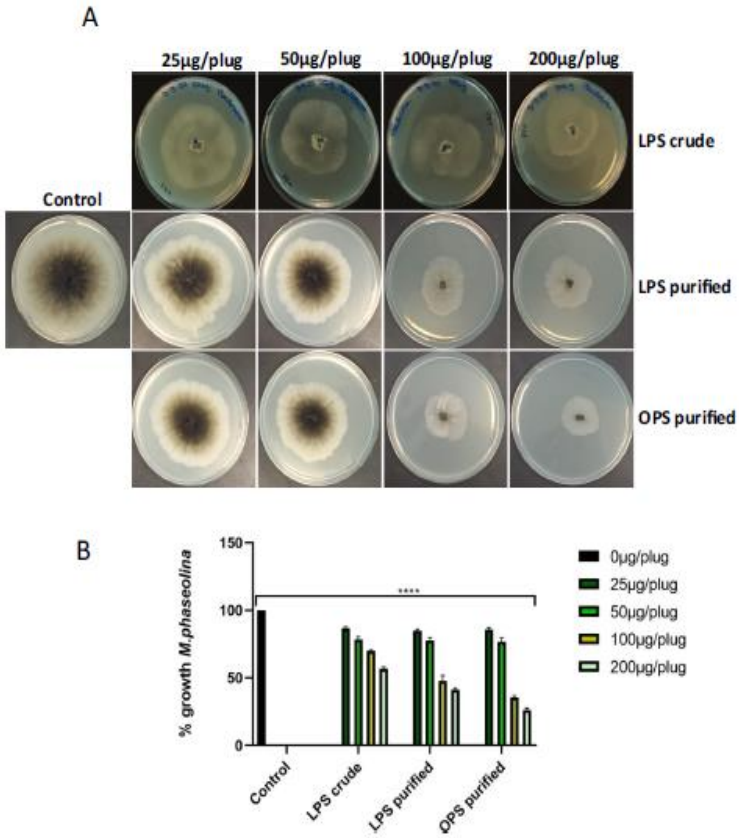

Fig. 2. Antifungal assay.
A) The crude extract of LPS, pure LPS, and pure OPS from *P. donghuensis* strain SVBP6 tested at 25, 50, 100, and 200 µg/plug against *M. phaseolina* for 5 days at 28 °C. The negative control was Milli-Q ultrapure water.
B) Graphical representation of the inhibition of the fungal growth of *M. phaseolina* by the crude LPS, and the purified LPS and OPS compounds from *P. donghuensis*. Data are presented as means ± standard deviation (n = 3 replication for the three compounds) compared to control *M. phaseolina* grown without compounds. ANOVA statistical differences are highly significant as indicated ****$p < 0.0001$.

residues in the OPS. The sequence of the monosaccharides in the repeating unit was determined by correlations between the anomeric and linkage atoms in the $^{1}H,^{1}H$ ROESY and $^{1}H,^{13}C$ HMBC spectra of the OPS (Table 2, Figs. S7, S8).

Therefore, the OPS of *P. donghuensis* SVBP6 is linear and has the following structure:

$$\underset{\mathbf{A}}{\rightarrow 6)\text{-}\alpha\text{-}D\text{-}ManpNAc\text{-}(1\rightarrow 3)\text{-}\beta\text{-}L\text{-}Rhap\text{-}(1\rightarrow 4)\text{-}\beta\text{-}D\text{-}Glcp\text{-}(1\rightarrow}$$
$$\mathbf{A} \qquad \mathbf{B} \qquad \mathbf{C}$$

According to a systematic search in the Carbohydrate Structure Database, this structure is unique among the known bacterial polysaccharide structures [19].

3.2. Biological activity of LPS and OPS

In order to identify if the crude LPS isolated from *P. donghuensis* had antifungal activity, different amounts (25, 50, 100, and 200 μg plug^{-1}) of the sample, were tested against the phytopathogenic fungus *M. phaseolina* (Fig. 2A). The graphical representation (Fig. 2B) showed that the best inhibition was at 200 μg plug^{-1}, able to inhibit the fungus growth by about 45%. To confirm the role of LPS in microbial antagonism, the purified LPS and the corresponding OPS were separately assayed against *M. phaseolina* using the same test. Also in this case (Fig. 2A), the best inhibition was observed at 200 μg plug^{-1} for both samples but with a stronger activity for the OPS. In fact, in this case, the purified LPS decreases the fungus growth by 65%, and the OPS by 75% (Fig. 2B). Another important difference shown in Fig. 2, is that the purified LPS and OPS reduced significantly more the growth of *M. phaseolina* already at 100 μg plug^{-1} compared to the crude LPS. The best performance showed by purified OPS alone suggests that the antifungal activity can be also attributed to this component. Furthermore, this is the first time that both the antifungal activity of a bacterial LPS and its corresponding *O*-chain were described. However, polysaccharides from different natural sources were also reported for their antifungal activity as those produced by brown seaweed [20], by plants [21] and by mushrooms [22,23].

In conclusion, LPS and/or OPS isolated from *P. donghuensis* SVBP6 could be used together with the already reported secondary metabolite 7-hydroxytropolone, produced by the bacterium as an extracellular antifungal compound [3], to develop an integrated and more efficient management of *M. phaseolina* biocontrol.

CRediT authorship contribution statement

Evelina L. Zdorovenko: Formal analysis, Writing - Original Draft Investigation, Visualization; **Andrey S. Dmitrenok:** Formal analysis; Investigation; **Marco Masi:** Investigation; **Stefany Castaldi:** Investigation; **Federico M. Muzio:** Investigation; **Rachele Isticato:** Writing - Review & Editing; **Claudio Valverde:** Writing - Review & Editing; **Yuriy A. Knirel:** Supervision, Writing - Review & Editing; **Antonio Evidente:** Project administration, Writing - Original Draft, Supervision

Acknowledgements

Prof. A. Evidente is associate to Istituto di Chimica Biomolecolare del CNR, Pozzuoli, Italy. F.M. Muzio was supported by a Ph.D. fellowship from CONICET C. Valverde is member of CONICET. We thank Marcelo Aníbal Carmona (Facultad de Agronomía, Cátedra de Fitopatología, Universidad de Buenos Aires, Buenos Aires, Argentina) to supply the strain of *Macrophomina phaseolina* used in this study. Database-assisted NMR structure elucidation was funded by Russian Science Foundation grant 18-14-00098P.

Appendix A. Supplementary data

Supplementary data to this article can be found online at https://doi.org/10.1016/j.ijbiomac.2021.05.187.

References

[1] B.C. Agaras, M. Scandiani, A. Luque, L. Fernández, F. Farina, M. Carmona, M. Gally, A. Romero, L. Wall, C. Valverde, Quantification of the potential biocontrol and direct plant growth promotion abilities based on multiple biological traits distinguish different groups of *Pseudomonas* spp. isolates, Biolog. Control 90 (2015) 173–186.
[2] B.C. Agaras, A. Iriarte, C. Valverde, Genomic insights into the broad antifungal activity, plant-probiotic properties, and their regulation, in *Pseudomonas donghuensis* strain SVBP6, PLoS One 13 (2018), e0194088.
[3] F.M. Muzio, B.C. Agaras, M. Masi, A. Tuzi, A. Evidente, C. Valverde, 7-Hydroxytropolone is the main metabolite responsible for the fungal antagonism of *Pseudomonas donghuensis* strain SVBP6, Environ. Microbiol. 22 (2020) 2550–2653.
[4] A. Raio, G. Puopolo, A. Cimmino, R. Danti, G. Della Rocca, A. Evidente, Biocontrol of cypress canker by the phenazine producer *Pseudomonas chlororaphis* subsp. *aureofaciens* strain M71, Biol. Control 58 (2011) 133–138.
[5] A. Raio, P. Reveglia, G. Puopolo, A. Cimmino, R. Danti, A. Evidente, Involvement of phenazine-1-carboxylic acid in the interaction between *Pseudomonas chlororaphis* subsp. *aureofaciens* strain M71 and *Seiridium cardinale* in vivo, Microbiol. Res. 199 (2017) 49–56.
[6] A. Cimmino, G. Puopolo, M. Perazzolli, A. Andolfi, D. Melck, I. Pertot, A. Evidente, Cyclo (L-PRO-L-TYR), the fungicide isolated from *Lysobacter capsici* AZ78: a structure–activity relationship study, Chem. Heterocycl. Com. 50 (2014) 290–295.
[7] H.K. Abbas, N. Bellaloui, C. Accinelli, J.R. Smith, W.T. Shier, Toxin production in soybean (*Glycine max* L.) plants with charcoal rot disease and by *Macrophomina phaseolina*, the fungus that causes the disease, Toxins 11 (2019) 645.
[8] G. Su, S.O. Suh, R.W. Schneider, J.S. Russin, Host specialization in the charcoal rot fungus *Macrophomina phaseolina*, Phytopathology 91 (2001) 120–126.
[9] A.A. Farnaz, A. Narmani, M. Arzanlou, *Macrophomina phaseolina* associated with grapevine decline in Iran, Phytopathol. Mediterr. 57 (2018) 107–111.
[10] C.G. Zilli, M.A. Carmona, E. Simonetti, D.M. Santa-Cruz, G.G. Yannarelli, K. B. Balestrasse, Biocontrol of *Macrophomina phaseolina* (Tassi) Goid: differential production of H_2O_2 and in the relationship pathogen–PGPR in soybean seedling, Biocontrol Sci. Technol. 28 (2018) 416–422.
[11] E. Simonetti, N.P. Viso, M. Montecchia, C. Zilli, K. Balestrasse, M. Carmona, Evaluation of native bacteria and manganese phosphite for alternative control of charcoal root rot of soybean, Microbiol. Res. 180 (2015) 40–48.
[12] J. Wang, S. Chou, Z. Yang, Y. Yang, Z. Wang, J. Song, X. Dou, A. Shan, Combating drug-resistant fungi with novel imperfectly amphipathic palindromic peptides, J. Med. Chem. 61 (2018) 3889–3907.
[13] O. Westphal, K. Jann, Bacterial lipopolysaccharide extraction with phenol, Methods Carbohydr. Chem. 5 (1965) 83–91.
[14] J.S. Sawardeker, J.H. Sloneker, A quantitative determination of monosaccharides as their alditol acetates by gas liquid chromatography, Analyt. Chem. 37 (5) (1965) 1602–1603.
[15] K. Leontein, J. Lönngren, Determination of the absolute configuration of sugars by gas-liquid chromatography of their acetylated 2-octyl glycosides, Methods Carbohydr. Chem. 9 (1993) 87–89.
[16] A.S. Shashkov, G.M. Lipkind, Y.A. Knirel, N.K. Kochetkov, Stereochemical factors determining the effects of glycosylation on the ^{13}C chemical shifts in carbohydrates, Magn. Reson. Chem. 26 (1988) 735–747.
[17] R.R. Kapaev, Ph.V. Toukach, Improved carbohydrate structure generalization scheme for ^{1}H and ^{13}C NMR simulations, Analyt. Chem. 87 (2015) 7006–7010.
[18] G.M. Lipkind, A.S. Shashkov, Y.A. Knirel, E.V. Vinogradov, N.K. Kochetkov, A computer-assisted structural analysis of regular polysaccharides on the basis of 13C-n.m.r. data, Carbohydr. Res. 175 (1988) 59–75.
[19] P.V. Toukach, K.S. Egorova, Carbohydrate structure database merged from bacterial, archaeal, plant and fungal parts, Nucl. Acids Res. 44 (2016) D1229–D1236.
[20] A. Citkowska, M. Szekalska, K. Winnicka, Possibilities of fucoidan utilization in the development of pharmaceutical dosage forms, Mar. Drugs 17 (2019) 458.
[21] D. Salarbashi, J. Bazeli, E. Fahmideh-Rad, Fenugreek seed gum: biological properties, chemical modifications, and structural analysis–a review, Intern. J. Biol. Macromol. 138 (2019) 386–393.
[22] M. Öztürk, G. Tel-Çayan, A. Muhammad, P. Terzioglu, M.E. Duru, Mushrooms: a source of exciting bioactive compounds, in: Atta-ur-Rahman (Ed.), Studies in Natural Products Chemistry, Vol. 45, Elsevier, Amsterdam. Netherlands, 2015, pp. 363–456.
[23] J.M.F. Wan, Polysaccharide Krestin (PSK) and polysaccharopeptide (PSP), in: Abba Kastin (Ed.), Handbook of Biologically Active Peptides: Fungal Peptides, Elsevier Inc., USA, 2013, pp. 180–184.

CHAPTER V: Phenazine-1-Carboxylic Acid (PCA), Produced for the First Time as an Antifungal Metabolite by *Truncatella angustata* a Causal Agent of Grapevine Trunk Disease (GTDs) in Iran.

JOURNAL OF AGRICULTURAL AND FOOD CHEMISTRY

pubs.acs.org/JAFC

Article

Phenazine-1-Carboxylic Acid (PCA), Produced for the First Time as an Antifungal Metabolite by *Truncatella angustata*, a Causal Agent of Grapevine Trunk Diseases (GTDs) in Iran

Alessio Cimmino,[‖] Zeinab Bahmani, Stefany Castaldi,[‖] Marco Masi, Rachele Isticato, Jafar Abdollahzadeh,* Jahanshir Amini, and Antonio Evidente*

Cite This: https://doi.org/10.1021/acs.jafc.1c03877

Read Online

ACCESS | Metrics & More | Article Recommendations

ABSTRACT: The phytopathogenic fungus *Truncatella angustata*, associated with grapevine trunk diseases (GTDs) in Iran, produces the well-known secondary metabolite isocoumumarin (+)-6-hyroxyramulosin and surprisingly also phenazine-1-carboxylic acid (PCA). PCA, identified by spectroscopic (essentially ^{1}H NMR and ESI MS) spectra, is a bacterial metabolite well known for its antifungal activity and was found for the first time in *T. angustata* culture filtrates. The antifungal activity of PCA was assayed against four different fungi responsible for GTDs, *Phaeoacremonium minimum*, *Phaeoacremonium italicum*, *Fomitiporia mediterranea*, involved in grapevine esca disease, and *Neofusicoccum parvum*, responsible for Botryosphaeria dieback. The activity was compared with that of the known commercial fungicide, pentachloronitrobenzene, and the close phenazine. PCA and phenazine exhibited strong antifungal activity against all phytopathogenic fungi, inhibiting the fungal growth by about 90−100% and 80−100%, respectively. These results suggested that *T. angustata* could use PCA to compete with other phytopathogenic fungi that attack grapevine and thus PCA could be proposed as a biofungicide against the fungi responsible for grapevine esca and Botryosphaeria dieback diseases.

KEYWORDS: *Truncatella angustata, phenazine-1-carboxylic acid (PCA), phenazine, antifungal activity, biological control*

INTRODUCTION

The economic importance of grapevine (*Vitis vinifera* L.) has grown exponentially in recent years and many efforts have been made to increase its production yield and the organoleptic qualities of wine.[1,2] Unfortunately, grapevine can be affected by several biotic stress agents that are considered a major threat to the economic sustainability of viticulture.[2,3] Among these, pathogenic fungi cause significant losses by inducing severe diseases in different plant organs. They are able to produce toxic metabolites belonging to several classes of naturally occurring compounds whose role in the plant−pathogen interaction is under study.[3] However, the most important grapevine diseases are related to the woody tissues, i.e., trunk and cordons, and are called grapevine trunk diseases (GTDs). There are no effective methods for the control of GTDs and the prevention of infections is mainly based on the application of chemical pesticides.[4] For these reasons, environmentally friendly alternatives for controlling GTDs are urgently needed and could be based on the use of natural fungicides.

Truncatella angustata was recently reported as one of the causal agents of GTDs in Iran and was shown to produce (+)-6-hydroxyramulosin, a well-known phytotoxin.[5] Surprisingly, *T. angustata* also produced a yellow compound, which showed antifungal activity against some fungi involved in GTDs, suggesting a potential role in the microbial interaction in the diseased grapevine.

Thus, the aims of this manuscript were the isolation and chemical and biological characterization of this metabolite. This was identified as phenazine-1-carboxylic acid (PCA), a compound frequently isolated from *Pseudomonas* spp. and well known for its antifungal activity and potential application in agriculture as a potential fungicide to control phytopathogens that infect the agricultural plants with high world market value.[6,7]

Thus, this manuscript reports the isolation of phenazine-1-carboxylic acid for the first time from the culture filtrates of the phytopathogenic fungus *T. angustata* and its involvement in GTDs in Iran. Its role in completely inhibiting the growth of other fungi competing in the same environment has also been discussed.

MATERIALS AND METHODS

General Experimental Procedures. ^{1}H NMR spectra were recorded at 400 MHz, respectively, in $CDCl_3$ on a Bruker spectrometer (Karleshrue, Germany). The same solvent was used as an internal standard. Electrospray ionization (ESI) mass spectra and liquid chromatography LC/MS analyses were performed using the

Received: June 28, 2021
Revised: September 15, 2021
Accepted: September 28, 2021

LC/MS time-of-flight (TOF) system Agilent 6230B (Agilent Technologies, Milan, Italy) and high-performance liquid chromatography (HPLC) 1260 Infinity. The HPLC separations were performed with a Phenomenex (Bologna, Italy) LUNA (C_{18} (2) 5 μm 150 × 4.6 mm). Analytical and preparative thin-layer chromatography (TLC) was performed on silica gel plates (Merck, Kieselgel 60, F_{254}, 0.25 and 0.5 mm, respectively) or on reverse phase (Whatman, C_{18} F_{254}, 0.20 mm) plates (Merck, Darmstadt, Germany), and the compounds were visualized by exposure to UV light and/or iodine vapors CC: silica gel (Merck, Kieselgel 60, 0.063−0.200 mm). The sample of standard phenazine was purchased from Sigma-Aldrich (Milan, Italy).

Fungal Strains. The strain of *T. angustata* (CJAZBSRK1) used in this study was obtained from a vineyard showing symptoms of grapevine trunk diseases including decline and vascular discoloration and necrosis, located in Dinavar district, Sahneh, Kermanshah Province, Iran. The fungus was purified using a single-spore technique. DNA extraction, PCR, and maximum parsimony analysis were carried out as described by Abdollahzadeh et al. (2009).[8] For the identification of *T. angustata* ITS region of ribosomal DNA was amplified. To confirm its pathogenicity under greenhouse conditions (22−28 °C), Koch's postulates were followed. *T. angustata* strain (CJAZBSRK1) was stored on potato dextrose agar (PDA) at 4−8 °C in the fungal collection of the Department of Plant Protection, University of Kurdistan, Iran. The fungal strains of *Phaeoacremonium minimum*, *Fomitiporia mediterranea*, and *Neofusicoccum parvum* were supplied by Prof. Laura Mugnai of the Department of Science and Technology Agriculture, Food, Environmental and Forestry (DAGRI), Sec. Pathology and Entomology, University of Florence, Florence, Italy. The strain of *Phaeoacremonium italicum* was supplied by Prof. Antonia Carlucci of the Department of Agricultural Sciences, Food, Natural Resources and Engineering, University of Foggia, Foggia, Italy.

Production, Extraction, and Purification of PCA. For metabolite production, *T. angustata* was inoculated and grown in a stationary culture (final volume 5 L) of the Potato Dextrose Broth (PDB) as previously reported.[5] The lyophilized culture filtrates (5 L) of *T. angustata* were dissolved in 1/10 of the initial volume (pH 6) and extracted with EtOAc as recently reported.[5] The organic extracts were combined, dried (Na_2SO_4), and evaporated under reduced pressure, giving a corresponding residue of 330 mg. This latter was purified by silica gel column chromatography and eluted with $CHCl_3$/*i*-PrOH (9/1, v/v) to (7/3, v/v) yielding seven homogeneous fraction groups. The residue of fraction 2 (10.0 mg) was further purified by TLC on the reverse phase eluted with CH_3CN/H_2O (7:3, v/v), yielding a yellow amorphous solid identified as phenazine-1-carboxylic acid (PCA) (**1**, Rf 0.48, 6.0 mg).

Antifungal Assays. The phytopathogenic fungi *P. minimum* (PV.FLA.188), *P. italicum* (Pm 45), *F. mediterranea* (PV.FLA.132), and *N. parvum* (PV.FLA.41) were grown separately on PDA in Petri dishes at 25 °C ± 1 for 7/8 days in darkness. The *in vitro* antifungal bioassays were carried out according to the method previously described by Pucpolo et al. (2013)[9] with some modifications. PCA and phenazine dissolved in MeOH and pentachloronitrobenzene (PCNB) (Sigma-Aldrich, Saint Louis, MO) dissolved in toluene were placed on the opposite four sides of the plates 1.5 cm away from the fungal disk at a final concentration of 25 μg/μL. MeOH and toluene were used in the same conditions as negative controls. The plates were incubated at 25 °C ± 1 for 7/8 days and examined for zones of inhibition of grown colonies. Plates containing the fungal plugs alone were used as control. The experiments were performed in triplicate. The percentage of inhibition of the fungal growth was calculated using the following formula

$$\% = [(R_c - R_i)/R_c] \times 100$$

where R_c is the radial growth of the test pathogen in the control plates (mm) and R_i is the radial growth of the test pathogen in the test plates (mm). The results were analyzed by analysis of variance (ANOVA) using Tukey's test.

RESULTS AND DISCUSSION

PCA (**1**, Figure 1) was isolated from the organic extract of *T. angustata* culture filtrates and identified by comparing its ^{1}H NMR and ESI MS with those previously reported[10] and those of an authentic sample previously isolated from *Pseudomonas chlorophasis* subsp. *aureofaciens* strain M71.[10]

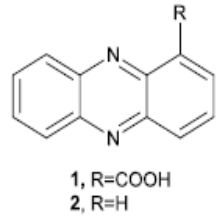

Figure 1. Structure of phenazine-1-carboxylic acid and phenazine (**1** and **2**).

This *Pseudomonas* strain produced compound **1** together with 2-hydroxyphenazine and was proposed as a potential agent for the biocontrol of *Seiridium cardinale*, the fungus responsible for the bark canker of Italian cypress (*Cupressus sempervirens* L.).[10] When **1** was applied *in vitro* against *S. cardinale*, the canker size was reduced, indicating that it is directly involved in the control of the pathogen by *P. chlororaphis* subsp. *aureofaciens* strain M71.[10] This result was also confirmed by field experiments.[11] Studies were also carried out to estimate the spectrum of the activity of PCA, 2-hydroxyphenazine, and four semisynthetic PCA derivatives against a group of pathogenic fungi of agricultural and forest plants by an agar plate bioassay. PCA was active against most of the plant pathogens tested, showing that the carboxyl group is a structural feature important for the antifungal activity.[9]

PCA belongs to the well-known synthetic and natural phenazine group, which includes more than 100 different compounds of natural origin and over 6000 synthetic compounds. Many of them were studied for their potential application in different fields such as in medicine as anticancer agents[12] and against cystic fibrosis.[13,14] It could also be used in other biotechnological applications as fluorescent material for the advancement of modern science and technology.[15]

Rarely, PCA was isolated from fungi. In fact, **1** and its amide were previously isolated from *Nigrospora oryzae* obtained from the medicinal plant *Cocinia grandis*, and the carboxyamide showed antifungal activity against the plant pathogen *Cladosporium cladosporioides*.[16]

Recently, **1** was reported as an antimicrobial metabolite isolated from the sea anemone-derived fungus *Emericella* sp., showing antifungal activity against *Phytophthora capsici*, *Gibberella zeae*, and *Verticillium dahliae*.[17]

In addition, some of the authors isolated phenazine from *Pseudomonas fluorescens* 9,[18] a strain isolated in Argentina and proposed for the control of *Macrophomina phaseolina*, which infects soybean and more than 500 plant species belonging to more than 100 families, causing dry root and stem rot, known as charcoal rot (CR).[19] Thus, PCA (**1**), phenazine (**2**, Figure 1), 2-hydroxyphenazine, and some mono and dinitrophenazine derivatives, prepared by nitration of **2**, were assayed against *M. phaseolina* and also against two other destructive fungi

https://doi.org/10.1021/acs.jafc.1c03877
J. Agric. Food Chem. XXXX, XXX, XXX−XXX

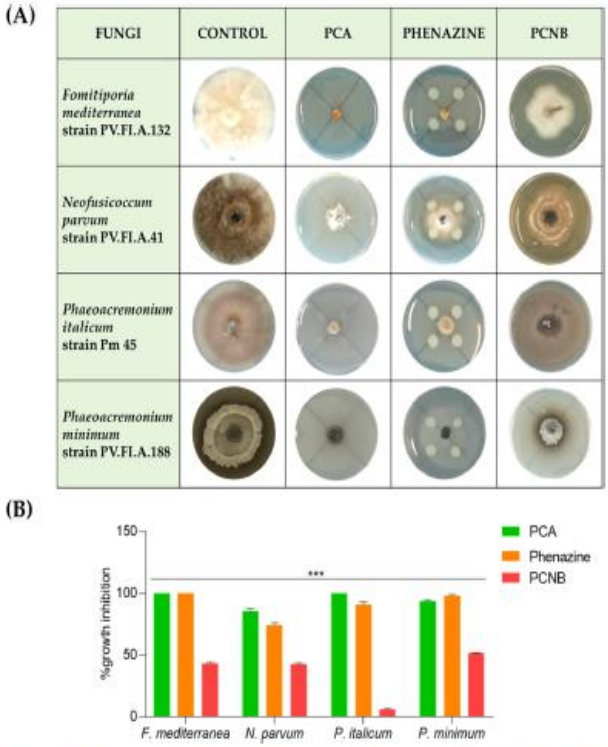

Figure 2. *In vitro* antifungal activity of PCA: phenazine-1-carboxylic acid; phenazine and PCNB: pentachloronitrobenze tested at 25 μg/μL. (A) Representative photographs of the antifungal assay for *in vitro* inhibition of mycelial growth of *P. minimum*, *P. italicum*, *F. mediterranea*, and *N. parvum*. (B) Inhibition of fungal growth by PCA, phenazine, and PCNB reported as the percentage reduction in the diameter of the fungal mycelia in the treated plate compared to that in the control plate. Data are presented as mean ± standard deviation (n = 3) compared to control fungi grown alone. For comparative analysis of groups of data, one-way ANOVA was used and p values are presented in the figure: ***: extremely significant <0.001.

infecting soybeans such as *Cercospora nicotianae* and *Colletotrichum truncatum*. Phenazine and PCA showed the same strong antifungal activity against the three pathogens while 2-hydroxyphenazine, assayed only against *M. phaseolina*, was inactive. Finally, all nitrophenazine derivatives not showed antifungal activity against *M. phaseolina* while exhibited antifungal activity against *C. nicotianae* and *C. truncatum*. In particular, in *C. nicotianae*, they showed a slightly reduced activity than in **1** and **2**, while on *C. truncatum*, the inhibition effect of these derivatives appeared to be significantly reduced. Thus, probably the activity is also dependent on the sensitivity of the fungal species.[18]

Consequently, PCA and phenazine can be evaluated for their potential antifungal activity against the fungi involved in GTDs.

PCA (**1**) compared to phenazine (**2**) and the commercial fungicide pentachloronitrobenzene (PCNB) were assayed against some fungi involved in GTDs as *P. minimum*, *P. italicum*, *F. mediterranea* involved in esca disease[3,20] and *Na. parvum*, one of the causal agents of Botryosphaeria dieback.[3] As shown in Figure 2, the PCA exhibited strong antifungal activity against all phytopathogenic fungi, inhibiting the fungal growth by about 90−100% when spot-inoculated at a final concentration of 25 μg/μL. Similarly, phenazine has shown strong growth-inhibiting activity in all fungi, respectively, by 80−100% when tested at the same concentration of PCA. A different result was obtained with the commercial fungicide PCNB. At the same concentration (25 μg/μL) used for PCA and phenazine, the PCNB showed a lower fungal growth inhibition activity by about 10−48%.

In conclusion, this manuscript reports for the first time the isolation of phenazine-1-carboxylic acid from a phytopathogenic fungus as *T. angustata*, a causal agent of GTDs in Iran. Its isolation as a fungal metabolite is very rare considering that only three other fungi, two of which were isolated from marine organisms, have been reported as PCA producers. The production of PCA by *T. angustata* is probably due to inhibit the growth of other pathogenic fungi that could attack

https://doi.org/10.1021/acs.jafc.1c03877
J. Agric. Food Chem. XXXX, XXX, XXX−XXX

grapevine. This hypothesis has been confirmed by the results of the bioassays carried out against some fungi responsible for GTDs. In fact, the PCA has shown strong antifungal activity inhibiting the fungal growth of *P. minimum*, *P. italicum*, *F. mediterranea*, and *N. parvum* of about 90−100%. Thus, PCA could be proposed as a biofungicide against the fungi responsible for grapevine esca and Botryosphaeria dieback diseases.

AUTHOR INFORMATION

Corresponding Authors

Jafar Abdollahzadeh − *Department of Plant Protection, Agriculture Faculty, University of Kurdistan, 416 Sanandaj, Iran*; Email: j.abdollahzadeh@uok.ac.ir

Antonio Evidente − *Department of Chemical Sciences, University of Naples Federico II, Complesso Universitario Monte S. Angelo, 80126 Napoli, Italy*; orcid.org/0000-0001-9110-1656; Email: evidente@unina.it

Authors

Alessio Cimmino − *Department of Chemical Sciences, University of Naples Federico II, Complesso Universitario Monte S. Angelo, 80126 Napoli, Italy*; orcid.org/0000-0002-1551-4237

Zeinab Bahmani − *Department of Plant Protection, Agriculture Faculty, University of Kurdistan, 416 Sanandaj, Iran*

Stefany Castaldi − *Department of Biology, University of Naples Federico II, Complesso Universitario Monte S. Angelo, 80126 Napoli, Italy*

Marco Masi − *Department of Chemical Sciences, University of Naples Federico II, Complesso Universitario Monte S. Angelo, 80126 Napoli, Italy*; orcid.org/0000-0003-0609-8902

Rachele Isticato − *Department of Biology, University of Naples Federico II, Complesso Universitario Monte S. Angelo, 80126 Napoli, Italy*

Jahanshir Amini − *Department of Plant Protection, Agriculture Faculty, University of Kurdistan, 416 Sanandaj, Iran*; orcid.org/0000-0003-4777-4073

Complete contact information is available at: https://pubs.acs.org/10.1021/acs.jafc.1c03877

Author Contributions

‖A.C. and S.C. contributed equally to this work.

Notes

The authors declare no competing financial interest.

ACKNOWLEDGMENTS

The authors thank Prof. Laura Mugnai, Department of Science and Technology Agriculture, Food, Environmental and Forestry (DAGRI), Sec. Pathology and Entomology, University of Florence, Florence, Italy, for supplying strains of *Phaeoacremonium minimum*, *Fomitiporia mediterranea*, and *Neofusicoccum parvum*, and Prof. Antonia Carlucci, Department of Agricultural Sciences, Food, Natural Resources and Engineering, University of Foggia, Foggia, Italy, for supplying the strain *Phaeoacremonium italicum*. Zeinab Bahmani was supported by University of Kurdistan, Sanandaj and received a grant from Ministry of Science, Research and Technology, Tehran, Iran.

REFERENCES

(1) Gramaje, D.; Urbez-Torres, J. R.; Sosnowski, M. R. Managing grapevine trunk diseases with respect to etiology and epidemiology: current strategies and future prospects. *Plant Dis.* **2018**, *102*, 12−39.

(2) Fontaine, F.; Pinto, C.; Vallet, J.; Clément, C.; Gomes, A. C.; Spagnolo, A. The effects of grapevine trunk diseases (GTDs) on vinephysiology. *Eur. J. Plant Pathol.* **2016**, *144*, 707−721.

(3) Masi, M.; Cimmino, A.; Reveglia, P.; Mugnai, L.; Surico, G.; Evidente, A. Advances on fungal phytotoxins and their role in grapevine trunk diseases. *J. Agric. Food Chem.* **2018**, *66*, 5948−5958.

(4) Mondello, V.; Songy, A.; Battiston, E.; Pinto, C.; Coppin, C.; Trotel-Aziz, P.; Clement, C.; Mugnai, L.; Fontaine, F. Grapevine trunk diseases: a review of fifteen years of trials for their control with chemicals and biocontrol agents. *Plant Dis.* **2018**, *102*, 1189−1217.

(5) Cimmino, A.; Bahmani, Z.; Masi, M.; Abdollahzadeh, J.; Evidente, A. Phytotoxins produced by *Didymella glomerata* and *Truncatella angustata*, associated with grapevine trunk diseases (GTDs) in Iran *Nat. Prod. Res.* 2021, DOI: 10.1080/14786419.2021.1979544.

(6) Verma, C.; Jandaik, S.; Gupta, B. K.; Kashyap, N.; Suryaprakash, V. S.; Kashyap, S.; Kerketta, A. Microbial metabolites in plant disease management: Review on biological approach. *Int. J. Chem. Stud.* **2020**, *8*, 2570−2581.

(7) Wang, S. Y.; Shi, X. C.; Chen, X.; Laborda, P.; Zhao, Y. Y.; Liu, F. Q.; Laborda, P. Biocontrol ability of phenazine-producing strains for the management of fungal plant pathogens: A review. *Biol. Control* **2021**, *155*, No. 104548.

(8) Abdollahzadeh, J.; Goltapeh, E. M.; Javadi, A.; Shams-Bakhsh, M.; Zare, R.; Phillips, A. J. L. *Barriopsis iraniana* and *Phaeobotryon cupressi*: two new species of the Botryosphaeriaceae from trees in Iran. *Persoonia* **2009**, *23*, 1−8.

(9) Puopolo, G.; Masi, M.; Raio, A.; Andolfi, A.; Zoina, A.; Cimmino, A.; Evidente, A. Insights on the susceptibility of plant pathogenic fungi to phenazine-1-carboxylic acid and its chemical derivatives. *Nat. Prod. Res.* **2013**, *27*, 956−966.

(10) Raio, A.; Puopolo, G.; Cimmino, A.; Danti, R.; Della Rocca, G.; Evidente, A. Biocontrol of cypress canker by the phenazine producer *Pseudomonas chlororaphis* subsp. *aureofaciens* strain M71. *Biol. Control* **2011**, *58*, 133−138.

(11) Raio, A.; Reveglia, P.; Puopolo, G.; Cimmino, A.; Danti, R.; Evidente, A. Involvement of phenazine-1-carboxylic acid in the interaction between *Pseudomonas chlororaphis* subsp. *aureofaciens* strain M71 and *Seiridium cardinale* in vivo. *Microbiol. Res.* **2017**, *199*, 49−56.

(12) Cimmino, A.; Evidente, A.; Mathieu, V.; Andolfi, A.; Lefranc, F.; Kornienko, A.; Kiss, R. Phenazines and cancer. *Nat. Prod. Rep.* **2012**, *29*, 487−501.

(13) Hunter, R. C.; Klepac-Ceraj, V.; Lorenzi, M. M.; Grotzinger, H.; Martin, T. R.; Newman, D. K. Phenazine content in the cystic fibrosis respiratory tract negatively correlates with lung function and microbial complexity. *Am. J. Respir. Cell Mol. Biol.* **2012**, *47*, 738−745.

(14) Zhao, J.; Yu, W. Interaction between *Pseudomonas aeruginosa* and *Aspergillus fumigatus* in cystic fibrosis. *PeerJ* **2018**, *6*, No. e5931.

(15) Dou, W.; He, X. Recent progress in the development and applications of molecular materials based on vibration-induced emission (VIE). *J. East China Univ. Sci. Technol.* **2019**, *45*, 685−696.

(16) Thanabalasingam, D.; Kumar, N. S.; Jayasinghe, L.; Fujimoto, Y. Endophytic fungus *Nigrospora oryzae* from a medicinal plant *Coccinia grandis*, a high yielding new source of phenazine-1-carboxamide. *Nat. Prod. Commun.* **2015**, *10*, 1659−1660.

(17) Yue, Y.; Yu, H.; Li, R.; Hu, L.; Liu, S.; Li, P. Isolation and identification of antimicrobial metabolites from sea anemone-derived fungus *Emericella* sp. SMA01. *J. Oceanol. Limnol.* **2021**, *39*, 1010−1019.

(18) Castaldi, S.; Masi, M.; Sautua, F.; Cimmino, A.; Isticato, R.; Carmona, M.; Evidente, A. Phenazine, a metabolite isolated from *Pseudomonas fluorescences* with antifungal activity against three severe pathogenic fungi of soybean. Natural analogs and semisynthetic derivatives: structure-activity relationships. *Toxins*, 2021 submitted.

(19) Su, G.; Suh, S. O.; Schneider, R. W.; Russin, J. S. Host specialization in the charcoal rot fungus, *Macrophomina phaseolina*. *Phytopathology* **2001**, *91*, 120−126.
(20) Raimondo, M. L.; Lops, F.; Carlucci, A. *Phaeoacremonium italicum* sp. nov., associated with esca of grapevine in southern Italy. *Mycologia* **2014**, *106*, 1119−1126.

https://doi.org/10.1021/acs.jafc.1c03877
J. Agric. Food Chem. XXXX, XXX, XXX−XXX

CHAPTER VI: Plant Growth Promotion Function of *Bacillus* sp. Strains Isolated from Salt-Pan Rhizosphere and Their Biocontrol Potential against *Macrophomina phaseolina*.

International Journal of *Molecular Sciences*

MDPI

Article

Plant Growth Promotion Function of *Bacillus* sp. Strains Isolated from Salt-Pan Rhizosphere and Their Biocontrol Potential against *Macrophomina phaseolina*

Stefany Castaldi [1], Claudia Petrillo [1], Giuliana Donadio [2], Fabrizio Dal Piaz [3], Alessio Cimmino [4], Marco Masi [4], Antonio Evidente [4] and Rachele Isticato [1,*]

[1] Department of Biology, University of Naples Federico II, Complesso Universitario Monte S. Angelo, Via Cinthia 4, 80126 Naples, Italy; stefany.castaldi@unina.it (S.C.); claudia.petrillo@unina.it (C.P.)
[2] Department of Pharmacy, University of Salerno, 84084 Fisciano, Italy; gdonadio@unisa.it
[3] Department of Medicine, Surgery and Dentistry, University of Salerno, Via Giovanni Paolo II, 84084 Fisciano, Italy; fdalpiaz@unisa.it
[4] Department of Chemical Sciences, University of Naples Federico II, Complesso Universitario Monte S. Angelo, Via Cinthia 4, 80126 Naples, Italy; alessio.cimmino@unina.it (A.C.); marco.masi@unina.it (M.M.); evidente@unina.it (A.E.)
* Correspondence: isticato@unina.it; Tel.: +39-08-167-9038

Abstract: In recent decades, intensive crop management has involved excessive use of pesticides or fertilizers, compromising environmental integrity and public health. Accordingly, there has been worldwide pressure to find an eco-friendly and safe strategy to ensure agricultural productivity. Among alternative approaches, Plant Growth-Promoting (PGP) rhizobacteria are receiving increasing attention as suitable biocontrol agents against agricultural pests. In the present study, 22 spore-forming bacteria were selected among a salt-pan rhizobacteria collection for their PGP traits and their antagonistic activity against the plant pathogen fungus *Macrophomina phaseolina*. Based on the higher antifungal activity, strain RHFS10, identified as *Bacillus vallismortis*, was further examined and cell-free supernatant assays, column purification, and tandem mass spectrometry were employed to purify and preliminarily identify the antifungal metabolites. Interestingly, the minimum inhibitory concentration assessed for the fractions active against *M. phaseolina* was 10 times lower and more stable than the one estimated for the commercial fungicide pentachloronitrobenzene. These results suggest the use of *B. vallismortis* strain RHFS10 as a potential plant growth-promoting rhizobacteria as an alternative to chemical pesticides to efficiently control the phytopathogenic fungus *M. phaseolina*.

Keywords: plant growth-promoting bacteria; spore-forming bacteria; *Bacillus vallismortis*; *Macrophomina phaseolina*; phenotypic and genotypic characterization; biocontrol agents

check for updates

Citation: Castaldi, S.; Petrillo, C.; Donadio, G.; Piaz, F.D.; Cimmino, A.; Masi, M.; Evidente, A.; Isticato, R. Plant Growth Promotion Function of *Bacillus* sp. Strains Isolated from Salt-Pan Rhizosphere and Their Biocontrol Potential against *Macrophomina phaseolina*. *Int. J. Mol. Sci.* **2021**, *22*, 3324. https://doi.org/10.3390/ijms22073324

Academic Editor: Hans-Peter Mock

Received: 8 February 2021
Accepted: 18 March 2021
Published: 24 March 2021

Publisher's Note: MDPI stays neutral with regard to jurisdictional claims in published maps and institutional affiliations.

1. Introduction

In the last century, the world population reached a size three times greater than any previous value across the whole history of humanity. To cope with the rising request for nutrients, such as those provided by wheat and rice, current agricultural practices are based on the wide use of chemical fertilizer and pesticides. As a result, agrochemical multinationals have gradually acquired the control of global food production and modern agriculture is increasingly diverging from the traditional model [1]. Additionally, the extensive use of synthetic agrochemicals has generated heavy environmental pollution and serious risk for human and animal health due to their translocation along the food chain [1,2]. The massive use of pesticides has also led to a gradual loss of protection efficiency due to new resistances acquired by pests, with a continuous increase in pesticide dosage [2,3]. A sustainable and safe strategy to ensure crop production is to substitute agrochemicals with Plant Growth-Promoting Rhizobacteria (PGPR) as agents stimulating plant growth and health [3–5]. These beneficial microbes not only play an important role

in increasing soil fertility but also enhance the growth and vigor of the plants—PGPRs, by colonizing the roots, may enhance nutrient uptake by nitrogen fixation or P solubilization [4], reduce abiotic stresses by biofilm production [5] or regulate plant hormone production [4]. Emerging evidence has shown that rich microflora of the rhizosphere can reduce plant disease through several antagonistic mechanisms such as competition, the production of cell-wall-degrading enzymes, (e.g., chitinase, glucanase, and protease) [6], volatile compounds and siderophores [7], antibiosis or the induction of plants' systemic resistance [8]. Replacing agrochemicals with the application of PGPRs may have both economic and environmental impacts, including relevant benefits such as rising yields, reduction in or elimination of chemical residues, limited or no development of resistance by pests and pathogens, employment of agricultural raw materials, and a low risk to non-target organisms, including pollinators. For this reason, intensive research on this group of microorganisms has been taking over to develop new biofertilizers and biocontrol agents.

In this contest, *Bacillus* genera include several exo- and endophytic bacteria species and plant growth-promoting (PGP) features have been associated with different strains [9,10]. In addition to the benefits shared with other PGPR, such as solubilization of soil P, enhancement of nitrogen fixation, and siderophore production, *Bacillus* spp. are suitable as biofertilizers because: (i) their application has little, if any, effect on the composition of the soil microbial communities, being common members of the plant root microflora [11]; (ii) these bacteria may form endospores, which can survive at high temperatures and dehydration, making the formulation of a commercial product easier [12]; (iii) some *Bacillus* PGPR strains have also been reported to perform well under different environmental conditions [13]. As biocontrol agents, *Bacillus* spp. exhibit both direct and indirect mechanisms to suppress diseases caused by pathogens. These bacteria secrete a vast range of secondary metabolites, such as cell-wall-degrading enzymes, and antioxidants that assist directly the plant in its defense against pathogen attack [14]. As an indirect mechanism, *Bacillus* spp. are able to induce the acquired systemic resistance of the colonized plant [8].

This manuscript describes the screening of 22 *Bacillus* strains isolated from samples of the rhizosphere of *Juniperus sabina* [15] collected from the National Park of Ses Salines d'Eivissa, Formentera (Spain), focused on finding a PGPR strain with antagonistic activity against the phytopathogenic fungus *Macrophomina phaseolina*.

M. phaseolina (Tassi) Goid is responsible for charcoal root rot, the most common and widely spread root disease affecting more than 500 cultivated and wild plant species. The fungus is distributed worldwide and prevalently in arid areas with low rainfall and high temperature where it can survive for up to 15 years in the soil as a saprophyte [16]. *M. phaseolina* generally affects the fibrovascular system of the roots and basal internodes producing black sclerotia, which allow the fungus survival after the plants rotted [16].

Each year, this fungus induces heavy damages in agrarian plants with a high world market value, such as soy, sunflower, leguminous, and corn [16]. Soybean grains, in particular, are globally utilized not only as foods but also as substrates for feeds, fuels, and bio-based materials [17]. Thus, many efforts are made for the control of *M. phaseolina* to reduce or avoid the loss of agricultural yields and the consequent economic damage.

Additionally, PGPRs have been evaluated as biocontrol agents against *M. phaseolina* and strains belonging *to Pseudomonas* and *Bacillus* genera showed the best performance. In a study carried out by Simonetti et al. [18], two strains, namely *Pseudomonas fluorescens 9* and *Bacillus subtilis 54*, have been assayed for antifungal activity in combination with manganese phosphite or alone and shown to significantly reduced soybean disease severity induced by *M. phaseolina* compared to the untreated control.

Several studies are still in progress to identify the main antifungal metabolites produced by PGPRs and clarify their modes of action to achieve optimum disease control.

2. Results

2.1. Isolation and Screening of Plant Growth-Promoting Spore-Forming Rhizobacteria

Aerobic spore-forming bacteria were isolated from rhizosphere samples of *J. sabina* collected in Parque Natural de Ses Salines d'Eivissa, Formentera (Spain), as described in the Materials and Methods section. A preliminary characterization based on the bacterial morphology and growth properties has allowed the selection of 22 facultative anaerobic strains, mesophiles, which are able to grow at a different pH range (Table S1).

Analysis of the DNA sequence of the 16S RNA gene of the 22 strains allowed the identification of all of them as belonging to the *Bacillus* genus (Table S2). In order to confirm the different species obtained by BlastN analysis (Table S2), a phylogenetic analysis (Figure 1) was performed by comparing the 16S sequences with respective type strains (^{T}) available at the NCBI Taxonomy database. The analysis corroborated the different *Bacillus* species by >0.90 bootstrap values. All isolates belong to species commonly considered as PGPR for their ability to colonize roots [11,19] and produce antimicrobial compounds [14,19].

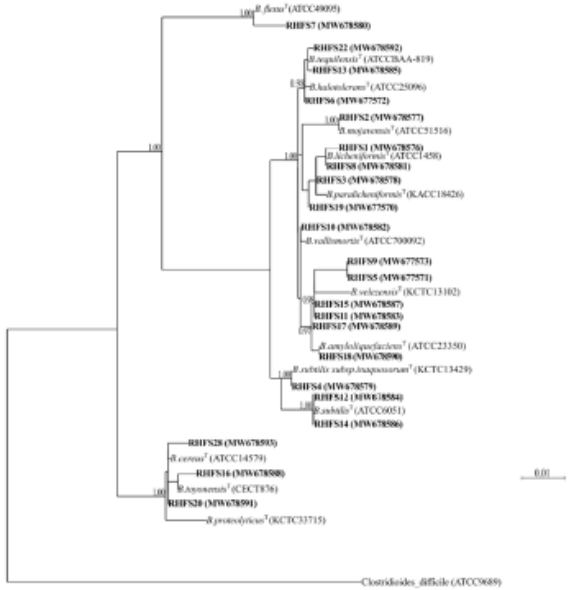

Figure 1. Phylogenetic tree of isolated rhizobacteria. The phylogenetic tree was constructed using the maximum-likelihood algorithm based on 16S rRNA gene sequences. The gene sequences of the isolated bacteria were aligned to the representative type strains (^{T}). The numbers in parentheses indicate the GenBank accession numbers. The percentage of replicate trees in which the associated taxa clustered together in the bootstrap test (1000 replicates) is shown next to the branches. The 16S rRNA sequence of *Clostridioides difficile* (ATCC9689) was used to assign an outgroup species.

The selected strains were analyzed for PGP traits by testing the presence of both fertilizing and biocontrol features. As summarized in Table 1, a high proportion was able to solubilize phosphate (Supplementary Figure S1), produce siderophores (Supplementary Figure S2) and indoleacetic acid, while only some of the strains were biosurfactant and biofilm producers and showed swarming motility.

Table 1. Summary of plant growth-promoting and biocontrol traits exhibited by 22 spore-forming bacteria isolates.

	Biofertilizer Activities					Biocontrol Activities						
Strains Code	Siderophores Production	PVK *	IAA *	Biofilm	Swarming	Protease Activity	Amylase Activity	Lipase Activity	Xylanase Activity	Cellulase Activity	Chitinase Activity	Catalase Activity
RHFS1	+	-	-	-	-	+++	+++	+	++	++	+	+++
RHFS2	-	++	-	+	+++	+++	+++	+	++	+++	++	-
RHFS3	-	+	+	-	–	+++	+++	++	+	+++	-	-
RHFS4	-	+	+	-	-	+++	+++	-	+++	+++	++	+++
RHFS5	+	-	+	-	-	+++	+++	-	+	+	++	++
RHFS6	-	+	++	-	-	+++	+++	-	+++	++	-	+++
RHFS7	-	-	++	-	-	+	-	+	+++	+++	++	+++
RHFS8	++	+	-	-	-	+++	+++	-	++	+	++	+++
RHFS9	+	-	-	+	+++	+++	+++	++	-	+++	++	++
RHFS10	+++	++	+	++	+++	+++	+++	++	+++	+++	++	+++
RHFS11	+	+	+	-	-	+++	+++	+	+++	-	++	++
RHFS12	-	+	+	+	-	-	+++	-	+++	+++	++	+
RHFS13	-	-	++	-	-	+++	-	-	++	-	++	++
RHFS14	-	++	++	-	-	+	+	-	+++	-	+	+++
RHFS15	+	+	+++	-	-	+++	+++	+	++	+++	++	-
RHFS16	+	+	+	+	-	++	++	-	+++	+++	-	-
RHFS17	+	+	+++	-	-	+++	++	-	+	+	++	+++
RHFS18	+++	++	++	+++	++	+++	+++	++	+++	+++	++	+++
RHFS19	++	++	+	+++	++	+++	+++	++	+++	+++	+	+++
RHFS20	+	-	+	-	-	+	++	-	++	++	++	+++
RHFS22	+	+	+	-	++	+++	-	-	+	++	++	-
RHFS28	-	-	-	-	-	+++	+++	-	++	++	++	++

+++: strong activity (formation halo ≥10 mm); ++: moderate activity (5 mm < halo < 10 mm); +: slight activity (halo < 5 mm); –: no activity; PVK *: Phosphate solubilization activity; IAA *: Indoleacetic acid.

Then, the potentiality as biocontrol agents of the 22 strains was tested analyzing their ability to secrete lytic enzymes (Supplementary Figure S3) [20]. As shown in Table 1, the number of protease and xylanase producers was the highest (over 90%) followed by amylase, chitinase and cellulase producers (over 80%), whereas less than 50% were lipase-producers (45%).

2.2. Antagonistic Activity of Spore-Forming Isolates against Fungal Plant Pathogen

The antagonistic activity of the 22 strains was examined against the phytopathogen *M. phaseolina* by dual-culture assay (Figure 2A).

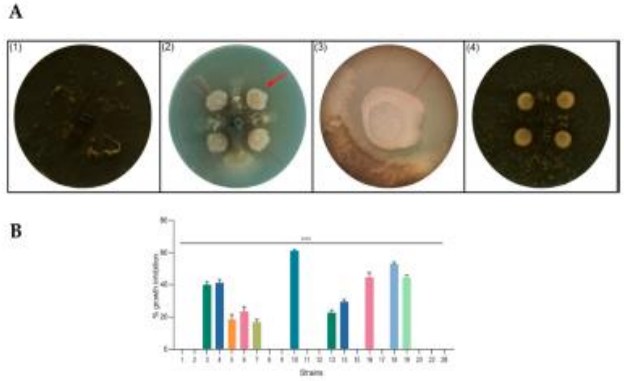

Figure 2. Antagonism assays in solid medium. (**A**) Representative photographs of dual-culture assay for in vitro inhibition of mycelial growth of *M. phaseolina* by isolated strains. (1) *M. phaseolina* (control plate); (2) example of active strain (RHFS10) against *M. phaseolina* growth; (3) images of interaction zone of RHFS10 strain and *M. phaseolina* acquired with a stereoscopic microscope (10× magnification); (4) example of inactive strain (RHFS28) against *M. phaseolina* growth; red arrow in panel 2 indicates the interaction zone magnified in panel 3. (**B**) Inhibition of fungal growth reported as the percentage reduction in the diameter of the fungal mycelia in the treated plate compared to that in the control plate. All experiments were performed in triplicate with three independent trials. Data are presented as means ± standard deviation ($n = 4$) compared to control *M. phaseolina* grown without bacteria. For comparative analysis of groups of data, one-way ANOVA was used and p values are presented in the figure: ****: extremely significant < 0.0001.

Based on the size of the inhibition zone in dual-culture tests, some strains were found to be highly efficient against the fungal pathogen while others had limited or no antimicrobial activity (Figure 2B). For a more detailed analysis, the produced inhibition halos were observed under a stereomicroscope, highlighting agar-diffusible antifungal molecule production by the most active strains (Figure 2A, panel 3; Supplementary Figure S4).

Of all analyzed isolates, RHFS10 and RHFS18 proved to higher potentiality than PGPR, since they possess traits beneficial for both plant growth, such as the ability to solubilize phosphorus or produce siderophores, and show antagonistic ability against phytopathogens. For these reasons, both strains were selected for further experiments. Strain RHFS28, able to produce lytic enzymes but not showing antifungal activity, was selected as a negative control for the next experiments.

To assess the effect of the cell-free culture supernatants (CFSs) of RHFS10 and RHFS18 on mycelial growth, the CFSs at 24, 48, 72 and 96 h were collected and tested against *M. phaseolina*. The commercial fungicide pentachloronitrobenzene (PCNB) dissolved in toluene was used as a positive control and toluene alone was used as a negative control of

the experiments (Figure 3A). The antifungal activity increased proportionally with the growth time reaching a maximum after 72 h, specifically for the RHFS18 strain (Figure 3B). Based on the efficiency of inhibition, measured by the percentage of mycelial growth reduction, strain RHFS10 was chosen for further investigation.

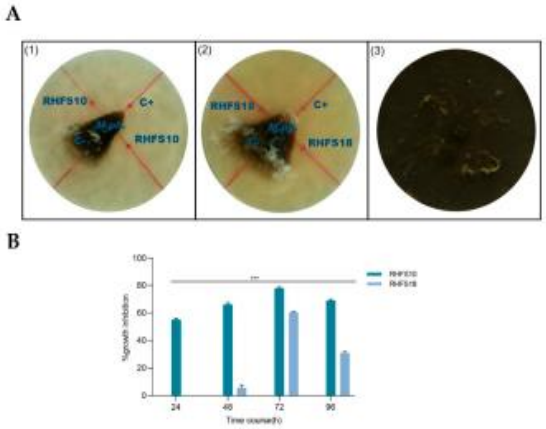

Figure 3. Antifungal activity of secreted metabolites by Plant Growth-Promoting Rhizobacteria (PGPR) strains. (**A**) Effects of the CSFs from RHFS10 (panel 1) and RHFS18 (panel 2) strains collected after 72 h of growth on the mycelial growth of *M. phaseolina* (panel 1). C+: Positive control, pentachloronitrobenzene; C−: Negative control, toluene. All experiments were performed in triplicate with three independent trials. (**B**) Antifungal activity of the Cell-Free Supernatants (CFSs) of the two strains RHFS10 and RHFS18 collected from 24 to 96 h of growth. Percentage of fungal growth inhibition was reported as the percentage reduction in the diameter of the fungal mycelia compared to control plate (panel 3). Data are presented as means ± standard deviation ($n = 3$). For comparative analysis of groups of data, one-way ANOVA was used and p values are presented in the figure: ***: extremely significant < 0.001.

2.3. *Characterization of Antifungal Metabolites*

The stability of the antifungal metabolites secreted by RHFS10 was tested by incubating the CFS collected after 72 h (72-CFSs) with different proteolytic enzymes or organic solvents and then tested for inhibition of mycelial growth.

As shown in Figure 4A, the 72-CFS still had notable activity after incubation with organic solvents but decreased under the action of proteinase K or pepsin.

Thermostability was verified incubating the 72-CFS at increasing temperatures for 1 or 3 h. The results showed that treatments at 65 and 75 °C do not affect the inhibitory effect against *M. phaseolina*, while at 85 °C a reduction in the antifungal activity was observed (Figure 4B).

Finally, metabolites of the 72-CFSs were extracted with ethyl acetate at pH 2.0 and pH 7.0 and the two obtained phases were separated and tested against *M. phaseolina*. The results showed that the antifungal activity was mainly associated with the aqueous phase at pH 7.0 (data not shown). This data indicated a protein nature of the bioactive molecules in agreement with the protease sensitivity recorded in the previous tests.

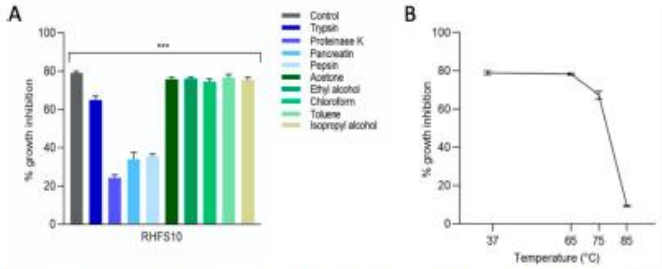

Figure 4. Stability of secreted antifungal metabolites. CFSs collected after 72 h (72-CFS) of RHFS10 was treated separately, with different enzymes and organic solvents (**A**) or incubated at increasing temperatures (37, 65, 75, and 85 °C) (**B**) and tested against *M. phaseolina*. All data represent the average of three separate experiments. ANOVA statistical analysis is extremely significant indicated, *** $p < 0.001$.

2.4. Purification of Antifungal Metabolites

To preliminarily identify the antifungal compounds released by the RHFS10 strain, 72-CFS was subjected to purification by two different steps. First, the 72-CFS was fractionated and the obtained fractions were tested against *M. phaseolina*. As shown in Figure 5A, the antifungal activity was observed in the fraction containing compounds with molecular weights between 10 and 50 kDa. In the second step of purification, the polypeptides present in 72-CFS were collected with ammonium sulfate, dialyzed to eliminate the polypeptides with a molecular weight lower than 10 kDa, and subjected to column chromatography. The three obtained fractions were tested against *M. phaseolina* and peaks 1 and 2 showed a wide zone of inhibition while no antagonistic activity was detected for the metabolites recovered in peak 3 (Figure 5B).

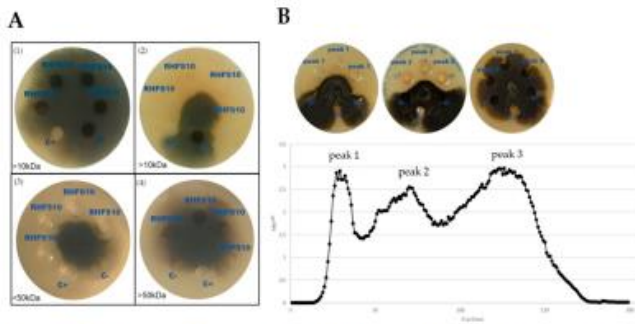

Figure 5. Antifungal activity of cell-free supernatant fractions of RHFS10. (**A**) 72-CFS was size-fractionated using 10, 30 kDa and, 50 kDa cutoff spin columns, and the obtained fractions were tested against *M. phaseolina*. The results obtained with fractions <10 (1), >10 (2), <50 (3) and >50 kDa (4) are reported. C+: Positive control, pentachloronitrobenzene; C−: negative control, toluene; RHFS10: 0.1 mL of fractionated 72-CFS. (**B**) Elution profile of 72-CFS by fractionation on Sephadex G-50 fine column chromatography. The antagonist activity of the three recovered peaks (1 mg/dot) is reported in the upper part of the panel. All data represent the average of three separate experiments. ANOVA statistical analysis is extremely significant indicated—$p < 0.001$.

2.4.1. Minimum Inhibitory Concentration

Minimum inhibitory concentration (MIC) of the antifungal compounds presents in peaks 1 and 2 was determined, incubating decreasing concentrations of peaks 1 and 2 (Figure 6(A1,A2)) with *M. phaseolina* plugs. The antifungal efficiency of the compounds present in the peaks was compared to the commercial fungicide PCNB (Figure 6(A4)). The results obtained after 5 days of incubation clearly showed higher antifungal activity of peaks 1 and 2 than the fungicide PCNB. In particular, the deduced MIC for both peaks was 50 µg/mL, 10 times less than that deduced for PCNB (0.5 mg/mL). We also compared the stability of the antifungal activity over time. In this regard, the bioactive compounds present in peaks 1 and 2 perfectly retained their fungal growth inhibition for up to 14 days, while PNCB's efficiency decreased after a week. Peak 3 confirmed its inactivity (Figure 6 (A3)).

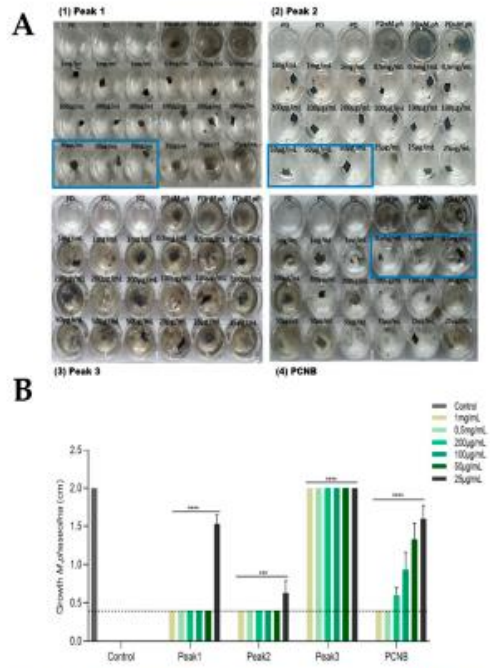

Figure 6. Minimum inhibitory concentrations of purified fractions of 72-CFS on fungal growth. (**A**) Minimum inhibitory concentration of the antifungal compound present in pick 1 (Panel 1), pick 2 (Panel 2) and pick 3 (Panel 3) of purified fractions of 72-CFS using a 24-well plate assay. The commercial fungicide pentachloronitrobenzene (PCNB) (Panel 4) was used as a reference. The tested concentrations are indicated. Fungal plugs incubated with only PD broth (PD + *M. phaseolina*) and the PD alone (PD) were used as a control. The blue lines represent the MICs of the tested samples. (**B**) Graphical representation of the MIC assay. The dotted line indicates the starting size (mm) of *M. phaseolina* plug (4 × 4 mm) at the beginning of the experiment. The results were obtained after 5 days of incubation at 28 °C. Data are presented as means ± standard deviation ($n = 3$ replication for each different concentration). ANOVA statistical analysis is extremely significant indicated—**** $p < 0.0001$ and *** $p < 0.001$.

2.4.2. Preliminary Identification of Bioactive Compounds

Finally, the three fractions were analyzed by liquid chromatography coupled with tandem mass spectrometry (LC–MS/MS). As shown in Table 2, several protease and lytic enzymes were identified in the two antifungal active peaks. Two different forms of subtilisin-like proteins were identified in peak 1, showing apparent molecular weights of 39 and 28 kDa and corresponding to the mature serine-protease and the proenzyme, respectively. Additionally, the glucuronoxylanase XynC was also detected. Both subtilisin-like protein forms were also present in peak 2, even if with a lower concentration, together with a B-glucanase, whereas peak 3 contains a metalloprotease and an alpha-amylase. As serine-proteases, beta-glucanase and glucoronoxylanase were demonstrated to act as antifungal agents [21,22], our results suggest that the activity of these secreted metabolites could be responsible, at least partially, for the antifungal action of RHPS10. To further corroborate this hypothesis, a mass spectrometry-based proteomic analysis on the previously described 72-CFSs of RHPS10 strain treated at increasing temperatures (cfr. 3.4) was performed. Again, the two forms of subtilisin and glucuronoxylanase XynC were identified in the samples retaining the antifungal activity. Interestingly, the two proteins were not detected in CFS from the negative control (RHPS28) when subjected to the same treatment. Although the genome of RHPS10 was in permanent draft stage (SAMN17389611), it allowed us to confirm the presence of all the purified protein genes, which when expressed could be involved in inhibiting fungal growth.

Table 2. The proteins identified on the three peaks are listed with their accession (AC) numbers and molecular weights.

Fractions	Mass (Da) [a]	Swiss Prot AC	Significant Sequences	Score	Description
Peak 1	47.924	XYNC_BACIU	18	1776	Glucuronoxylanase XynC OS = *Bacillus subtilis*
	39.483	SUBN_BACNA	5	1080	Subtilisin NAT OS = *Bacillus subtilis subsp. natto*
	27.42	SUBN_BACNA	5	865	Subtilisin NAT OS = *Bacillus subtilis subsp. natto*
	75.961	SACC_BACSU	1	795	Levanase OS = *Bacillus subtilis*
	38.141	PEL2_BACIU	3	566	Pectin lyase OS = *Bacillus subtilis*
Peak 2	27.365	GUB_BACAM	8	990	Beta-glucanase OS = *Bacillus amyloliquefaciens*
	39.483	SUBN_BACNA	5	800	Subtilisin NAT OS = *Bacillus subtilis subsp. natto*
	27.42	SUBN_BACNA	5	637	Subtilisin NAT OS = *Bacillus subtilis subsp. natto*
Peak 3	72.39	AMY_BACSU	1	41	Alpha-amylase OS = *Bacillus subtilis*
	34.106	MPR_BACSU	1	39	Extracellular metalloprotease OS = *Bacillus subtilis*

[a] Molecular mass of the Swiss Prot sequence in the absence of molecule processing.

3. Discussion

Fungal pathogens represent one of the most common causes of plant disease and are responsible for losing a third of crops annually [23], causing economic loss and impacting global poverty. Among phytopathogenic fungi, *M. phaseolina* (Tassi) Goid is one of the most virulent and dangerous plant pathogens. The fungus is responsible for charcoal rot disease and for the consequent significant yield losses in major crops such as maize, sorghum, soybean, and common beans each year. The harmfulness of the pathogen is due to its ability to produce phytotoxins, to survive for a long time in the soil, and to target any stage of plant growth affecting seeds, seedlings, and adult plants [24]. The persistence of *M. phaseolina* in the soil and in turn its capacity to trigger plant infection depends on its ability to compete with other microorganisms of the rhizosphere—for example, competing for organic sources or host root colonization. For this reason, a growing number of studies have been focusing on the isolation and characterization of PGPRs able to limit *M. phaseolina* growth. PGPRs can not only colonize the rhizosphere improving plant growth by enhancing nutrient uptake or regulating plant hormone production, but can suppress a broad spectrum of phytopathogens, producing different antagonistic compounds or competing for nutrients.

In this contest, the focus of our research was to identify promising Bacilli rhizobacteria acting as biofertilizers and biocontrol agents against *M. phaseolina*. *Bacillus* species are a major type of rhizobacteria able to be beneficial to plants and to perform the same role as chemical fertilizers [25] and pesticides [26]. As PGPR, *Bacillus* spp. act both by

direct and indirect mechanisms, secreting phytohormones, antioxidants, solubilizing soil P, enhancing nitrogen fixation, or producing cell-wall-degrading enzymes and siderophores that promote plant growth and suppress the pathogens [27].

Moreover, the ability of the *Bacillus* spp. the produce endospores makes them more suitable candidates for PGPR-based commercial products since the resistance features of the spores can ensure the persistence of the bacteria during industrial processing and after their spread in the environment [12].

To this aim, spore-forming bacteria were isolated from salt-pan rhizosphere (Formentera, Spain) of the nurse plant *J. sabina*. As a nurse plant, *J. sabina* ensures a beneficial organization of plant communities and maintenance of biodiversity, particularly in harsh environments [28]. Growing evidence highlights that nurse plants alter the composition of soil bacterial communities, selecting microbiota that are more effective at nutrient mineralization and involved in plant growth-promoting mechanisms. Among isolates, 22 spore-forming bacteria strains were identified at a species level and first screened for their plant growth-promoting traits. More than 50% of the selected strains have shown to solubilize insoluble phosphates, to produce siderophores and secrete IAA, the main plant auxin able to regulate growth and developmental processes. These findings confirm that the rhizosphere of nurse plants is a useful source of PGPRs. Then, the biocontrol activity against the fungus *M. phaseolina* has been tested by dual-culture assay.

Among the 22 isolates, strain RHPS10, identified as *B. vallismortis*, showed the best performance for plant growth-promoting applications both as biofertilizer and biocontrol agents. The fungal growth inhibition revealed in the cell-free supernatant assay suggested the secretion of antifungal extracellular metabolites not induced by direct contact with the fungus. These data were in agreement with the stereoscopic observation of coculture experiments. Additionally, the antagonist activity of RHPS10 was not influenced by the bacterial growth stage, suggesting a constitutive production of the antimicrobial compounds.

Stability experiments revealed a thermostability of the antifungal compounds up to 75 °C and resistance to various organic solvents. Instead, the sensitivity to protease treatment as well as the association of the antifungal activity with the aqueous phase during the extraction with an organic solvent suggests a proteinaceous nature of the metabolites.

Purification experiments have associated the antifungal activity with metabolites with molecular weights between 10 and 50 kDa, while LC–MS/MS analysis revealed the presence of proteases and hydrolytic enzymes in the active fractions. In particular a glucuronoxylanase of 45 kDa and a homologous of the serine protease Subtilisin NAT from *B. subtilis subsp. natto* that could be directly implicated in the fungal growth inhibition. Both proteins were absent in the inactive peak, confirming their involvement in the observed antifungal activity.

There are, indeed, several functions ascribed to the release of these compounds during the stationary phase of growth. It is well known that during this very phase of their life cycle, bacteria generally release hydrolytic enzymes mainly involved in the cell wall turnover and nutritional functions, which in many cases show antimicrobial and/or antibiofilm activity [29]. Moreover, it has been lately reported that subtilisin-like proteases and glucuronoxylanases can digest fungal cell wall structural proteins [30], supporting our preliminary results. Recently, it has been shown that *B. subtilis natto* can use several fungal materials as a carbon source for growth, pointing out the role of constitutively secreted protease as a nutrient scavenger as well as a potent tool for fungal biocontrol [31].

A further important result is the higher efficiency of the purified antifungal metabolites than the commercial fungicide PCNB, used as a positive control in antagonism assays. The minimum inhibitory concentration assessed for the bacterial bioactive compounds against *M. phaseolina* growth (50 µg/mL) was 10 times lower than the one estimated for the commercial fungicide PCNB (0.5 mg/mL). Interestingly, the bacterial metabolites also appeared to be more stable over time—they retained their antifungal activity for up to two weeks, while PCNB registered an efficiency reduction after 6 days only. Hence, the purified

bacterial bioactive metabolites might be employed in lower concentrations, reaching a higher long term efficiency compared to chemical fungicides.

Altogether, these results suggest a strong antifungal effect of the protein compounds produced by the RHFS10 strain and a promising prospect for agricultural applications. The bacterial bioactive proteins could represent a valid sustainable eco-friendly fungicide and have potential as a biocontrol agent as an alternative to chemical pesticides.

Future studies will focus on the effect of the *M. phaseolina* on the expression of antifungal metabolites produced by RHFS10, to verify if the fungus itself may enhance the production of the bioactive compounds already detected in this study or, perhaps, trigger the expression of new metabolites. Other studies also need to optimize their large scale production and to find their best formulation for their application in field.

4. Materials and Methods

4.1. Isolation of Bacteria

Samples of the rhizosphere of *Juniperus sabina* plants were collected from the National Park of Ses Salines d'Eivissa, Formentera (Spain). To isolate rhizospheric bacteria, 1 g of roots samples was washed three times with 2 mL sterile distilled water to remove impurities, transferred into 9 mL 1× PBS, and vortexed. The selection of spore-forming strains was promoted through a heat pretreatment at 80 °C to kill all vegetative cells. In total, 1 mL of the mixture was inoculated into 9 mL of LB (8 g/L NaCl, 10 g/L tryptone, 5 g/L yeast extract), serially diluted up to 10–6 and 0.1 mL of each dilution were spread on LB agar plates. Plates were incubated at 30 ± 1 °C for 2–3 days. Pure cultures were obtained by serial subculturing. Glycerol stocks of the isolates were prepared and stored at −80 °C.

4.2. Growth Conditions

Each bacterial isolate was characterized by visual inspection for colony color and morphology, such as colony shape, size, margin and appearance. The ability to grow in facultative anaerobic conditions was determined using the AnaeroGen sachets (Unipath Inc., Nepean, ON, Canada) placed in a sealed jar with bacteria streaked on LB agar plates and incubated at 37 °C for 3–4 days. To determine the optimum growth conditions, the bacterial isolates were grown in LB agar at different pH (2.0, 4.0, 6.0, 7.0, 8.0, 10.0, 12.0) [32] and temperature (4, 15, 25, 37, 50, 60 °C) ranges [33]. Plates were incubated until the appearance of bacterial colonies.

4.3. Isolates Identification by PCR Amplification of 16S rRNA

Exponentially growing cells were used to extract chromosomal DNA using the DNeasy PowerSoil kit (Qiagen, Hilden, Germany) according to the manufacturer's instructions. 16S rRNA gene was PCR amplified by using chromosomal DNA as a template and oligonucleotides forward 8F (5′-AGTTTGATCCTGGCTCAG-3′ annealing at position + 8/+ 28) and reverse 1517R (5′-ACGGCTACCTTGTTACGACT-3′ annealing at position + 1497/+ 1517). These two oligonucleotides were designed to amplify a 1500 bp DNA fragment and the reaction was carried out according to Grönemeyer et al. [34] in an Esco Swift™ MaxPro Thermal Cycler. The 1500 bp DNA amplified fragment was sequenced at the BioFab research sequencing facility and analyzed using Basic Local Alignment Search Tool (BLAST). Phylogenetic analyses were carried out using Seaview 4.4.0 software package (http://pbil.univ-lyon1.fr/software/seaview.html, accessed on 7 January 2020) on 16S ribosomal RNA genes aligned using the Muscle algorithm. All 16S rRNA sequences were deposited in the NCBI Sequence Read Archive and identified with the accession number as shown in Table S1.

Phylogenetic reconstruction for nucleotide alignment was carried out using the maximum likelihood algorithm (PhyLM). The gene sequences of the isolated bacteria were aligned to the representative type strains (T) belonging to the same species obtained from

BlastN analysis. The percentage of replicate trees in which the associated taxa clustered together in the bootstrap test (1000 replicates) is shown next to the branches.

4.4. In Vitro Screening for Plant Growth-Promoting (PGP) Traits

4.4.1. Phosphate Solubilization

The ability to solubilize inorganic phosphate was tested by growing the bacterial isolates on Pikovskaya agar (Oxoid Ltd., Hampshire, UK) dyed with bromophenol blue [35] for 10 days at 30 °C. The formation of more transparent zones around the bacterial colonies was indicative of inorganic phosphate solubilization on Pikovskaya agar.

4.4.2. Siderophore Production

To test siderophores production, 3 µL of overnight-grown culture in LB medium was spot-inoculated on iron-free S7 agar minimal medium. After 72 h of incubation at 28 °C, 10 mL of Chrome Azurol S (CAS) agar medium [36] was applied over agar plates containing cultivated microorganisms. Development of yellow-orange halo zone around bacterial spots was observed after 1 h of incubation.

4.4.3. Indole Acetic Acid Detection

To detect the IAA production, the bacteria were grown in LB broth for 72 h a 37 °C with shaking at 150 rpm. After, 2 mL of bacteria supernatant was mixed with 4 mL of Salkowski reagent (0.5 M $FeCl_3$ in 35% $HClO_4$ solution) and 2 drops of orthophosphoric acid, and was finally incubated for 30 min at 25 °C. The development of pink color indicates IAA production [37].

4.4.4. Biosurfactant Production

The bacterial strains were spot-inoculated on blood agar plates (BBL™ Trypticase™ Soy Agar (TSA II) with 5% Horse Blood) and after 72 h of incubation at 28 °C, the clear zone around the colonies indicates a positive result [38].

4.4.5. Swarming Motility

Bacterial isolates were analyzed for their swarming motility using LB with spot-inoculation on agar 0.7% and incubated at 37 °C overnight.

4.4.6. Biofilm Production

To evaluate the ability to produce biofilm, the isolates were separately grown in glass tubes in LB medium as described by Haney et al. (2018) [39]. Cultures were inoculated by adding 10 µL of an overnight culture of bacteria into 1 mL of sterile media, and the tubes were incubated statically at either 37 °C for 48 h.

4.5. Evaluation of Potential Biocontrol Features

4.5.1. Screening for Hydrolytic Enzymatic Activity

Twenty-two bacterial isolates were grown separately in 5 mL of LB broth a 37 °C overnight with shaking at 150 rpm. In total, 3 µL of each fresh bacterial culture was spot-inoculated on different assay plates to test hydrolytic enzyme activity. The protease activity was performed on Skimmed Milk Agar (SMA) [40] and the lipase activity on Tributyrene Agar medium [41]. After overnight at 37 °C, the formation of a clear halo around the colony was considered as positive production of these enzymes. To detect the amylase activity was used the method described by Sethi et al. (2013) [42] with Starch Agar plates. After the overnight incubation at 37 °C, the plates were flooded with iodine solution and the hydrolysis of starch was observed as a colorless zone with a violet background around grown colonies. For the detection of cellulase and xylanase activities, Xylanase Production Medium (XPM) agar plates were used with 0.5% xylan [43] (Megazyme) and a minimal medium with 0.5% carboxymethylcellulose (CMC) [44] as a sole carbon source. The plates were incubated at 37 °C for 3 days after which hydrolysis

zones were visualized by flooding the plates with 0.1% Congo Red for 15–20 min and then destained by washing twice with 1 M NaCl. Plates, where CMC and xylan were omitted, were used as nonsubstrate controls. Transparent hydrolytic zones around the colonies were considered positive. For the chitinase activity, the bacterial strains were spot-inoculated on colloidal chitin-containing medium plates [45]. After incubation at 25 ± 2 °C for 2–3 days, the clear zones around or within the colonies are considered positive evidence. The catalase activity was checked qualitatively as described by Geetha et al. (2014) [46]. Three percent H_2O_2 was added (3–4 drops) on the colonies grown on LB agar plates; effervescences of O_2 released from the bacterial colonies indicate the positivity of catalase activity.

All experiments were performed in triplicate.

4.5.2. Dual-Culture Assay

The isolated strains were examined in vitro for antifungal activity against pathogenic fungus *M. phaseolina* (Tassi) Goid (ATCC® 64334™). The fungus was obtained from infected soybean roots growing in Pergamino, Buenos Aires, Argentina, and it was maintained on Potato Dextrose Agar (PDA) in Petri dishes.

The in vitro antifungal bioassays were carried out based on the dual-culture method as previously described by Khamn et al. (2009) [47] with some modifications.

Fungal plugs of 6 × 6 mm diameter were placed at the center of PDA plates and 5 µL of bacteria strains overnight grown in LB broth was placed on the opposite four sides of the plates at 1.5 cm away from the fungal disc. Plates containing the fungal plugs without bacterial inoculation were used as control plates. All plates were incubated at 28 °C for five days. The percentage of inhibition of the fungal growth was calculated using the following formula:

$$\% = [(Rc - Ri)/Rc] \times 100$$

where Rc is the radial growth of the test pathogen in the control plates (mm), and Ri is the radial growth of the test pathogen in the test plates (mm). The experiment was repeated thrice. Bacterial strains that showed an inhibition of the growth of pathogenic fungus were observed by stereoscopic microscope 10× magnification.

4.5.3. Antifungal Assay of Cell-Free Supernatants (CFSs)

Bacteria were grown on LB at 28 ± 2 °C and aliquots of the suspensions, collected at 24 h intervals for the first 96 h. Cells were removed by centrifugation (7000× *g* for 30 min) and supernatants were filtered using 0.22 µm-pore-diameter membranes (Corning®) and concentrated 1:10. Then, 20 µL aliquots of sterilized supernatant samples were placed on the opposite four sides of the PDA plate at 1.5 cm from the fungal disc (6 × 6 mm diameter) of *M. phaseolina* [48]. As a positive control, fungicidal pentachloronitrobenzene ≥ 94% (PCNB) (Sigma-Aldrich, Saint-Louis, MO, USA) dissolved in toluene was used. Toluene alone was used as a negative control. Plates were prepared in triplicate, incubated at 28 °C for 5 days, and examined for zones of inhibition of grown colonies.

4.6. Extraction of Secondary Metabolites

The strains were grown in 300 mL of LB at 28 ± 2 °C and for 72 h. The broth cultures were then centrifuged at 9000× *g* for 30 min at 4 °C and filtered through a 0.22 µm syringe filter. The culture filtrate was extracted at pH7 and pH2 three times for each, mixed with an equal volume of EtOAc into the separating funnel, and shaken for complete extraction. The secondary compounds contained in the solvent phase were separated from the aqueous phase, dried with Na_2SO_4, and evaporated under reduced pressure to yield the crude extracts. The crude extracts were dissolved in 1 mL 2% methanol at a final concentration of 5 mg/mL, the aqueous phase was concentrated 1:10. All fractions were tested against *M. phaseolina* on PDA plates and incubated at 28 ± 2 °C for 5 days.

4.7. Stability of Antifungal Metabolites at Different Enzymes, Temperatures and Organic Solvent Conditions

In total, 100 µg/mL of enzymes (trypsin, proteinase K, pancreatin and pepsin) and 10% organic solvents (acetone, ethyl alcohol, chloroform, toluene and isopropyl alcohol) (see Figure 4) were added to 100 µL of culture supernatant. Enzyme-treated samples were incubated for 3 h at 37 °C (42 °C in the case of proteinase K) and the solvent-treated samples were incubated for 3 h at 25 °C and subsequently, 100 µL aliquots were tested for antifungal activity as described above. To assess the stability of the bioactive compounds at high temperatures, CSFs were incubated at 65, 75 and 80 °C for 1 or 3 h, and their activity toward *M. phaseolina* eventually tested.

4.8. Size-Fractionated Supernatants Tested for Antifungal Activity

RHFS10 strain was grown in 100 mL of LB broth for 72 h at 28 °C. The cultures were centrifuged at 7000× *g* for 30 min at 4 °C and the supernatants filter-sterilized with a 0.22 µm filter (Millipore, Bedford, MA, USA). The supernatants were size-fractionated (10, 30 and, 50 kDa cutoff spin column; Centricon, Millipore). Fractions were tested for antifungal activity and reported as a percentage of growth inhibition as described above.

4.9. LC–MS/MS Analyses

Protein extracts were electrophoretically separated on a 12.5% polyacrylamide gel, under denaturing conditions. Resulting lines were divided into 10 pieces, and each underwent trypsin in gel digestion procedure. NanoUPLC-hrMS/MS analyses of the resulting peptides mixtures were carried out on a Q-Exactive orbitrap mass spectrometer (Thermo Fisher Scientific, Waltham, MA, USA), coupled with a nanoUltimate300 UHPLC system (Thermo Fisher Scientific). Peptides separation was performed on a capillary EASY-Spray C18 column (0.075 × 100, 1.7 µm, Thermo Fisher Scientific) using aqueous 0.1% formic acid (A) and CH_3CN containing 0.1% formic acid (B) as mobile phases and a linear gradient from 3% to 30% of B in 60 min and a 300 nL min^{-1} flow rate. Mass spectra were acquired over an *m/z* range from 350 to 1500. To achieve protein identification, MS and MS/MS data underwent Mascot software (Matrix Science, London, UK) analysis using the nonredundant Data Bank UniProtKB/Swiss-Prot (Release 2020_03). Parameter sets were: trypsin cleavage; carbamidomethylation of cysteine as a fixed modification and methionine oxidation as a variable modification; a maximum of two missed cleavages; false discovery rate (FDR), calculated by searching the decoy database, ≤0.05. A comparison between the proteins found in the different samples allowed discriminating those specifically expressed by the strains showing promising antifungal activity.

4.10. Detection of Antifungal Metabolites

RHFS10 strain was grown in 2 L of LB broth at 28 °C for 72 h with shaking at 150 rpm. The cells were removed by centrifugation (9000× *g*, 30 min) and the supernatant fluid was filter-sterilized using 0.22 µm-pore-diameter membranes. The antifungal activity of the preparation was determined against *M. phaseolina* using the cell-free supernatant assay described above. The culture filtrate (1800 mL) was precipitated with ammonium sulfate (66% *w/v* saturation) and stored overnight at 4 °C with shaking. The precipitate was removed by centrifugation (12,000× *g*, 20 min, 4 °C), resuspended in PBS 1× buffer (0.01 mol L^{-1}, pH 6.5; 1/10 of the initial volume) and dialyzed against the same buffer for 48 h at 4 °C with several changes (dialysis tube, porosity 24, cutoff 12 kDa; Union Carbide Corporation, Danbury, CT, USA). The dialyzed precipitate was lyophilized, and the residue (483 mg) was dissolved in 6 mL ultrapure Milli-Q water and applied to a Sephadex G-50 fine column (Pharmacia, Uppsala, Sweden; 4.5–40 cm; flow rate 2.5 mL min^{-1}). The column fractions (3 mL each) were collected in homogeneous groups according to the chromatogram obtained by monitoring proteins concentration at 280 nm [49]. Fractions were lyophilized, tested for antifungal activity (1 mg/dot) against *M. phaseolina*, and analyzed by SDS-PAGE. The SDS-PAGE was performed with 20 µg of total proteins, fractionated on 12.5% SDS polyacrylamide gels and stained by Brilliant Blue Coomassie.

Protein concentration was determined with the Bradford assay (Bio-Rad Protein Assay, Hercules, CA, USA; cat no. 500-0006) with bovine serum albumin used as standard.

4.11. Minimum Inhibitory Concentrations

The MIC determination was performed in 24-well culture plates according to the method described by Agrillo et al. (2019) [50] with some modification. The wells were prepared in triplicate for each concentration. The retentates (peaks 1, 2, and 3) containing the antifungal compounds were diluted separately at different concentrations (1 mg/mL; 0.5 mg/mL; 200 µg/mL; 100 µg/mL; 50 µg/mL and 25 µg/mL) in a volume of 500 µL of ultrapure Milli-Q water and were inoculated with 500 µL of *M. phaseolina* plugs (4 × 4 mm) resuspended in 2 × PD broth. As a control, 500 µL of *M. phaseolina* plugs (4 × 4 mm) were resuspended in 2 × PD broth diluted with 500 µL of ultrapure Milli-Q water. The retentates were compared with the fungicidal PCNB ≥94% (Sigma-Aldrich) at the same different concentrations. The plates were incubated at 28 °C for 5 days and the MIC was taken as the lowest concentration of antifungal agent at which there was no visible growth of the fungus after incubation. Finally, the percentage of inhibition of the fungal growth was calculated using the formula described above.

4.12. Whole-Genome Sequencing

The most promising bacterial strain, RHFS10, which showed outstanding biocontrol performance, was selected for whole-genome sequencing to obtain future relevant genetic information. DNA extraction was performed using the method described above. Genome sequencing was performed by MicrobesNG (Birmingham, UK) with the genomic DNA library prepared using the Nextera XT library prep kit (Illumina) following the manufacturer's protocol. Libraries were sequenced on the Illumina HiSeq using a 250 bp paired-end protocol. Reads were adapter trimmed using Trimmomatic 0.30 with a sliding window quality cutoff of Q15 [51] and de novo genome assembly was carried out with SPAdes (version 3.7) via MicrobesNG (University of Birmingham, Birmingham, UK).

4.13. Statistical Analysis

All the statistical analyses were performed using GraphPad Prism 8 software. Data were expressed as mean ± SEM. Differences among groups were compared by ANOVA or t-test as indicated in figure legends. Differences were considered statistically significant at $p < 0.05$.

Supplementary Materials: The following are available online at https://www.mdpi.com/1422-0067/22/7/3324/s1: Table S1. Preliminary characterization of spore-forming bacteria isolated from the rhizosphere of *J. sabina* plants. Table S2. 16S rRNA gene-based molecular identity of isolated spore-forming bacteria, their accession numbers, and strain identification is reported. Figure S1. Potential plant growth-promoting traits of selected bacterial isolates. Figure S2. Potential plant growth-promoting traits of selected bacterial isolates. Figure S3. Hydrolytic activities of selected bacterial isolates. Figure S4. Preliminary dual-culture assay.

Author Contributions: Conceptualization, R.I.; methodology, S.C., C.P., A.C., and G.D.; validation, and formal analysis, S.C. and G.D.; investigation, S.C., M.M. and F.D.P.; data curation, S.C., A.E. and R.I.; writing—original draft preparation, R.I., S.C., and C.P.; supervision, R.I.; project administration, R.I.; funding acquisition, R.I. All authors have read and agreed to the published version of the manuscript.

Funding: This work was supported by POR Campania FSE 2014-2020 ASSE III–Ob. Sp. 14 Az. 10.5.2-Avviso Pubblico "Dottorati di Ricerca con Caratterizzazione Industriale"–D.D.n.155 del 17.05.2018 CUP E66C18000900002 CML OP_7741 18062AP000000001.

Institutional Review Board Statement: Not applicable.

Informed Consent Statement: Not applicable.

Data Availability Statement: Not applicable.

Acknowledgments: We thank Marcelo Anibal Carmona (Facultad de Agronomía, Cátedra de Fitopatología, Universidad de Buenos Aires, Buenos Aires, Argentina) to supply the strain of *Macrophomina phaseolina* used in this study.

Conflicts of Interest: The authors declare no conflict of interest.

References

1. Nicolopoulou-Stamati, P.; Maipas, S.; Kotampasi, C.; Stamatis, P.; Hens, L. Chemical Pesticides and Human Health: The Urgent Need for a New Concept in Agriculture. *Front. Public Health* **2006**, *4*, 148. [CrossRef]
2. Syed Ab Rahman, S.F.; Singh, E.; Pieterse, C.M.J.; Schenk, P.M. Emerging microbial biocontrol strategies for plant pathogens. *Plant Sci.* **2018**, *267*, 102–111. [CrossRef]
3. Cimmino, A.; Masi, M.; Evidente, M.; Superchi, S.; Evidente, A. Fungal phytotoxins with potential herbicidal activity: Chemical and biological characterization. *Nat. Prod. Rep.* **2015**, *32*, 1629–1653. [CrossRef]
4. Oleńska, E.; Małek, W.; Wójcik, M.; Swiecick, I.; Thijs, S.; Vangronsveld, J. Beneficial features of plant growth-promoting rhizobacteria for improving plant growth and health in challenging conditions: A methodical review. *Sci. Total Environ.* **2020**, *743*, 140682. [CrossRef] [PubMed]
5. Bhat, M.A.; Kumar, V.; Bhat, M.A.; Wani, I.A.; Dar, F.L.; Farooq, I.; Bhatti, F.; Koser, R.; Rahman, S.; Jan, A.T. Mechanistic Insights of the Interaction of Plant Growth-Promoting Rhizobacteria (PGPR) With Plant Roots Toward Enhancing Plant Productivity by Alleviating Salinity Stress. *Front. Microbiol.* **2020**, *11*, 1952. [CrossRef] [PubMed]
6. Pal, K.K.; McSpadden Gardener, B. Biological Control of Plant Pathogens. *Plant Health Instr.* **2006**, *36*, 37–45. [CrossRef]
7. Miljaković, D.; Marinković, J.; Balešević-Tubić, S. The Significance of *Bacillus spp.* in Disease Suppression and Growth Promotion of Field and Vegetable Crops. *Microorganisms* **2020**, *7*, 1037. [CrossRef]
8. Meena, M.; Swapnil, P.; Divyanshu, K.; Kumar, S.; Harish; Tripathi, Y.N.; Zehra, A.; Marwal, A.; Upadhyay, R.S. PGPR-mediated induction of systemic resistance and physiochemical alterations in plants against the pathogens: Current perspectives. *J. Basic Microbiol.* **2020**, *60*, 828–861. [CrossRef]
9. Gamez, R.; Montes, M.; Ramirez, S.; Schnell, S.; Rodriguez, F. Screening, plant growth promotion and root colonization pattern of two rhizobacteria (Pseudomonas *fluorescens* Ps006 and *Bacillus amyloliquefaciens* Bs006) on banana cv. Williams (Musa acuminata Colla). *Microbiol. Res.* **2019**, *220*, 12–20. [CrossRef]
10. Tamošiūnė, I.; Stanienė, G.; Haimi, P.; Stanys, V.; Rugienius, R.; Baniulis, D. Endophytic *Bacillus* and *Pseudomonas* spp. Modulate Apple Shoot Growth, Cellular Redox Balance, and Protein Expression Under in Vitro Conditions. *Front. Plant Sci.* **2018**, *9*, 889. [CrossRef]
11. Rabbee, M.F.; Ali, M.S.; Choi, J.; Hwang, B.S.; Jeong, S.C.; Baek, K.H. *Bacillus velezensis*: A Valuable Member of Bioactive Molecules within Plant Microbiomes. *Molecules* **2019**, *24*, 1046. [CrossRef] [PubMed]
12. Pesce, G.; Rusciano, G.; Sasso, A.; Isticato, R.; Sirec, T.; Ricca, E. Surface charge and hydrodynamic coefficient measurements of Bacillus subtilis spore by optical tweezers. *Colloids Surf. B* **2014**, *116*, 568–575. [CrossRef] [PubMed]
13. Gardner, B.B.M. Ecology of *Bacillus* and *Paenibacillus* spp. in Agricultural System. *Phytopathology* **2004**, *94*, 1252–1258. [CrossRef]
14. Raaijmakers, J.M.; De Bruijn, I.; Nybroe, O.; Ongena, M. Natural functions of lipopeptides from *Bacillus* and *Pseudomonas*: More than surfactants and antibiotics. *FEMS Microbiol. Rev.* **2010**, *34*, 1037–1062. [CrossRef] [PubMed]
15. Rodrigue-Echeverria, S. Influence of soil microbiota in nurse plant systems. *Funct. Ecol.* **2015**, *30*, 30–40. [CrossRef]
16. Kaur, S.; Dhillon, G.S.; Brar, S.K.; Vallad, G.E.; Chand, R.; Chauhan, V.B. Emerging phytopathogen *Macrophomina phaseolina*: Biology, economic importance and current diagnostic trends. *CR Microbiol.* **2012**, *38*, 136–151. [CrossRef]
17. Pagano, M.C.; Miransari, M. The importance of soybean production worldwide. *Soybean Prod.* **2016**, *1*, 1–26. [CrossRef]
18. Simonetti, E.; Viso, N.P.; Montecchia, M.; Zilli, C.; Balestrasse, K.; Carmona, M. Evaluation of native bacteria and manganese phosphite for alternative control of charcoal root rot of soybean. *Microbiol. Res.* **2015**, *180*, 40–48. [CrossRef]
19. Bacher, R.; Rokem, J.S.; Ilangumaran, G.; Lamont, J.; Praslickova, D.; Ricci, E.; Subramanian, S.; Smith, D.L. Plant Growth-Promoting Rhizobacteria: Context, Mechanisms of Action, and Road map to Commercialization of Biostimulants for Sustainable Agriculture. *Front. Plant Sci.* **2018**, *9*, 1473. [CrossRef]
20. Jadhav, H.; Shaikh, S.S.; Sayyed, R. Role of Hydrolytic Enzymes of Rhizoflora in Biocontrol of Fungal Phytopathogens: An Overview. *Rhizotrophs Plant Growth Promot. Bioremed.* **2017**, *978*, 183–203. [CrossRef]
21. Hong, T.-T.; Meng, M. Biochemical characterization and antifungal activity of an endo-1,3-beta-glucanase of *Paenibacillus sp.* isolated from garden soil. *Appl. Microbiol. Biotechnol.* **2003**, *61*, 472–478. [CrossRef]
22. Tariq, M.; Noman, M.; Ahmed, T.; Hameed, A.; Manzoor, N.; Zafar, M. Antagonistic features displayed by Plant Growth Promoting Rhizobacteria (PGPR): A Review. *J. Plant Sci. Phytopathol.* **2017**, *1*, 38–43. [CrossRef]
23. Fisher, M.C.; Henk, D.A.; Briggs, C.J.; Brownstein, J.S.; Madoff, L.C.; McCraw, S.L.; Gurr, S.L. Emerging fungal threats to animal, plant and ecosystem health. *Nature* **2012**, *48*, 186–194. [CrossRef] [PubMed]
24. Masi, M.; Sautua, F.; Zatout, R.; Castaldi, S.; Arrico, L.; Isticato, R.; Pecitelli, G.; Carmona, M.A.; Evidente, A. Phaseocyclopentenones A and B, Phytotoxic Penta-and Tetrasubstituted Cyclopentenones Produced by *Macrophomina phaseolina*, the Causal Agent of Charcoal Rot of Soybean in Argentina. *J. Nat. Prod.* **2021**, *84*, 459–465. [CrossRef] [PubMed]
25. Bhattacharyya, P.N.; Jha, D.K. Plant growth-promoting rhizobacteria (PGPR): Emergence in agriculture. *World J. Microbiol. Biotechnol.* **2012**, *28*, 1327–1350. [CrossRef] [PubMed]

26. Khan, N.; Martinez-Hidalgo, P.; Ice, T.A.; Maymon, M.; Humm, E.A.; Nejat, N.; Sanders, E.R.; Hirsch, A.M. Antifungal Activity of *Bacillus* Species Against *Fusarium* and Analysis of the Potential Mechanisms Used in Biocontrol. *Front. Microbiol.* **2018**, *320*, 175–189. [CrossRef] [PubMed]
27. Cazorla, F.M.; Romeo, D.; Pérez-García, A.; Lugtenberg, B.J.J.; De Vicente, A.; Bloemberg, G. Isolation and characterization of antagonistic *Bacillus subtilis* strains from the avocado rhizoplane displaying biocontrol activity. *J. Appl. Microbiol.* **2007**, *103*, 1950–1959. [CrossRef]
28. Taniguchi, T.; Usuki, H.; Kikuchi, J.; Hirobe, M.; Miki, N.; Fukuda, K.; Zhang, G.; Wang, L.; Yoshikawa, K.; Yamanaka, N. Colonization and community structure of root-associated microorganisms of Sabina vulgaris with soil depth in a semiarid desert ecosystem with shallow groundwater. *Mycorrhiza* **2012**, *22*, 419–428. [CrossRef]
29. Corvey, C.; Stein, T.; Düsterhus, S.; Karas, M.; Entian, K.-D. Activation of subtilin precursors by *Bacillus subtilis* extracellular serine proteases subtilisin (AprE), WprA, and Vpr. *Biochem. Biophys. Res. Commun.* **2003**, *304*, 48–54. [CrossRef]
30. Yan, L.; Qian, Y. Cloning and heterologous expression of SS10, a subtilisin-like protease displaying antifungal activity from *Trichoderma harzianum*. *FEMS Microbiol. Lett.* **2009**, *290*, 54–61. [CrossRef]
31. Schönbichler, A.; Díaz-Moreno, S.M.; Srivastava, V.; McKee, S.L. Exploring the Potential for Fungal Antagonism and Cell Wall Attack by *Bacillus subtilis natto*. *Front. Microbiol.* **2020**, *31*, 11–521. [CrossRef]
32. Cangiano, G.; Sirec, T.; Panarella, C.; Isticato, R.; Baccigalupi, L.; De Felice, M.; Ricca, E. The sps Gene Products Affect the Germination, Hydrophobicity, and Protein Adsorption of *Bacillus subtilis* Spores. *Appl. Environ. Microbiol.* **2014**, *80*, 7293–7302. [CrossRef] [PubMed]
33. Petrillo, C.; Castaldi, S.; Lanzilli, M.; Saggese, A.; Donadio, G.; Baccigalupi, L.; Ricca, E.; Isticato, R. The temperature of growth and sporulation modulates the efficiency of spore-display in *Bacillus subtilis*. *Microb. Cell Factories* **2020**, *19*, 185. [CrossRef] [PubMed]
34. Gronemeyer, J.L.; Burbano Roa, C.S.; Hurek, T.; Reinhold-Hurek, B. Isolation and characterization of root-associated bacteria from agricultural crops in the Kavango region of Namibia for Plant Growth Promoting Characteristics. *Plant Soil* **2012**, *71*, 566–571. [CrossRef]
35. Schoebitz, M.; Ceballos, C.; Ciampi, L. Effect of immobilized phosphate solubilizing bacteria on wheat growth and phosphate uptake. *J. Soil Sci. Plant Nutr.* **2013**, *12*, 1–10. [CrossRef]
36. Pérez-Miranda, S.; Cabirol, N.; George-Téllez, R.; Zamudio-Rivera, L.S.; Fernández, F.J. O-CAS, a fast and universal method for siderophore detection. *J. Microb. Methods* **2007**, *70*, 127–131. [CrossRef]
37. Damodaran, T.; Sah, V.; Nishra, V.K.; Jha, S.K.; Kannan, R. Isolation of salt tolerant endophytic and rhizospheric bacteria by natural selection and screening for promising plant growth-promoting rhizobacteria (PGPR) and growth vigour in tomato under sodic environment. *Afr. J. Microb. Res.* **2013**, *7*, 5082–5089. [CrossRef]
38. Sarwar, S.; Brader, G.; Corretto, E.; Aleti, G.; Abaidullah, M.; Sessitsch, A.; Hafeez, F.Y. Qualitative analysis of biosurfactants from bacillus species exhibiting antifungal activity. *PLoS ONE* **2018**, *13*, e0198107. [CrossRef]
39. Haney, E.F.; Brito-Sánchez, Y.; Trimble, M.J.; Mansour, S.C.; Cherkasov, A.; Hancock, R.E.W. Computer-aided discovery of peptides that Effect of phosphate solubilizing *Pseudomonas putida* on the growth of maize and its survival in the rhizosphere specifically attack bacterial biofilms. *Sci. Rep.* **2018**, *8*, 1871. [CrossRef]
40. Morris, L.S.; Evans, J.; Marchesi, R. A robust plate assay for detection of extracellular microbial protease activity in metagenomic screens and pure cultures. *J. Microbiol. Methods* **2012**, *91*, 144–146. [CrossRef]
41. Parsad, M.P.; Manjunath, K. Effect of media and process parameters in the enhancement of extracellular lipase production by bacterial isolates from industrial effluents. *Int. J. Microbiol. Res.* **2012**, *4*, 308–311. [CrossRef]
42. Sethi, S.; Alariya, S.S.; Gupta, S.; Gupta, L.B. Amylase activity of a starch degrading bacteria isolated from soil. *Int. J. Curr. Microbiol. Appl. Sci.* **2019**, *8*, 659–671. [CrossRef]
43. Meddeb-Mouelhi, F.; Moisan, J.K.; Beauregard, M. A comparison of plate assay methods for detecting extracellular cellulase and xylanase activity. *Enzym. Microb. Technol.* **2014**, *66*, 16–19. [CrossRef]
44. Hankin, L.; Anagnostakis, S. Solid media containing carboxy methyl cellulose to detect CM cellulase activity of microorganisms. *Microbiology* **1977**, *98*, 109–115. [CrossRef]
45. Kuddus, S.M.; Ahmad, R.I.Z. Isolation of novel chitinolytic bacteria and production optimization of extracellular chitinase. *J. Genet. Eng. Biotechnol.* **2013**, *11*, 39–46. [CrossRef]
46. Geetha, K.; Venkatesham, E.V.; Hindumathi, A.; Bhadraiah, B. Isolation, screening and characterization of plant growth promoting bacteria and their effect on *Vigna Radia* (L.) R. Wilczek. *Int. J. Curr. Microbiol. Appl. Sci.* **2014**, *3*, 799–809. [CrossRef]
47. Khamna, S.; Yokota, A.; Lumyong, S. Actinomycetes isolated from medicinal plant rhizospheric soils: Diversity and screening of antifungal compounds, indole-3-acetic acid and siderophore production. *World J. Microbiol. Biotechnol.* **2009**, *25*, 649–655. [CrossRef]
48. Kumar, P.; Dubey, R.C.; Maheshwari, D.K. *Bacillus* strains isolated from rhizosphere showed plant growth promoting and antagonistic activity against phytopathogens. *Microbiol. Res.* **2012**, *8*, 493–499. [CrossRef]
49. Lavermicocca, P.; Lonigro, S.L.; Evidente, A.; Andolfi, A. Bacteriocin production by *Pseudomonas syringae pv.ciccaronei* NCPPB2355. Isolation and partial characterization of the antimicrobial compound. *J. Appl. Microbiol.* **2001**, *86*, 257–265. [CrossRef]
50. Agrillo, B.; Mirino, S.; Tatè, R.; Gratino, L.; Gogliettino, M.; Cocca, E.; Tabli, N.; Nabti, E.; Palmieri, G. An alternative biocontrol agent of soil-borne phytopathogens: A new antifungal compound produced by a plant growth promoting bacterium isolated from North Algeria. *Microbiol. Res.* **2019**, *221*, 60–69. [CrossRef]
51. Bolger, A.M.; Lohse, M.; Usadel, B. Trimmomatic: A flexible trimmer for Illumina sequence data. *Bioinformatics* **2014**, *30*, 2114–2120. [CrossRef] [PubMed]

50. Agrillo, B.; Mirino, S.; Tatè, R.; Gratino, L.; Gogliettino, M.; Cocca, E.; Tabli, N.; Nabti, E.; Palmieri, G. An alternative biocontrol agent of soil-borne phytopathogens: A new antifungal compound produced by a plant growth promoting bacterium isolated from North Algeria. *Microbiol. Res.* **2019**, *221*, 60–69. [CrossRef]
51. Bolger, A.M.; Lohse, M.; Usadel, B. Trimmomatic: A flexible trimmer for Illumina sequence data. *Bioinformatics* **2014**, *30*, 2114–2120. [CrossRef] [PubMed]

CHAPTER VII: Genomic and Physiological Characterization of Bacilli Isolated From Salt-Pans With Plant Growth Promoting Features.

frontiers in Microbiology

ORIGINAL RESEARCH
published: 13 September 2021
doi: 10.3389/fmicb.2021.715678

Genomic and Physiological Characterization of Bacilli Isolated From Salt-Pans With Plant Growth Promoting Features

Claudia Petrillo[†], *Stefany Castaldi*[†], *Mariamichela Lanzilli*[2], *Matteo Selci*[1], *Angelina Cordone*[1], *Donato Giovannelli*[1,3,4,5,6] *and Rachele Isticato*[1,7]*

[1]Department of Biology, University of Naples Federico II, Complesso Universitario Monte S. Angelo, Naples, Italy, [2]Institute of Biomolecular Chemistry (ICB), CNR, Pozzuoli, Italy, [3]National Research Council – Institute of Marine Biological Resources and Biotechnologies (CNR-IRBIM), Ancona, Italy, [4]Department of Marine and Coastal Science, Rutgers University, New Brunswick, NJ, United States, [5]Department of Marine Chemistry & Geochemistry, Woods Hole Oceanographic Institution, Woods Hole, MA, United States, [6]Earth-Life Science Institute, Tokyo Institute of Technology, Tokyo, Japan, [7]Interuniversity Center for Studies on Bioinspired Agro-Environmental Technology (BAT Center), Portici, Italy

OPEN ACCESS

Edited by:
Sukhwan Yoon,
Korea Advanced Institute of Science and Technology, South Korea

Reviewed by:
Brent L. Nielsen,
Brigham Young University, United States
Woo Jun Sul,
Chung-Ang University, South Korea

***Correspondence:**
Rachele Isticato
isticato@unina.it

[†]These authors share first authorship

Specialty section:
This article was submitted to Microbiological Chemistry and Geomicrobiology, a section of the journal Frontiers in Microbiology

Received: 27 May 2021
Accepted: 10 August 2021
Published: 13 September 2021

Citation:
Petrillo C, Castaldi S, Lanzilli M, Selci M, Cordone A, Giovannelli D and Isticato R (2021) Genomic and Physiological Characterization of Bacilli Isolated From Salt-Pans With Plant Growth Promoting Features. Front. Microbiol. 12:715678. doi: 10.3389/fmicb.2021.715678

Massive application of chemical fertilizers and pesticides has been the main strategy used to cope with the rising crop demands in the last decades. The indiscriminate use of chemicals while providing a temporary solution to food demand has led to a decrease in crop productivity and an increase in the environmental impact of modern agriculture. A sustainable alternative to the use of agrochemicals is the use of microorganisms naturally capable of enhancing plant growth and protecting crops from pests known as Plant-Growth-Promoting Bacteria (PGPB). Aim of the present study was to isolate and characterize PGPB from salt-pans sand samples with activities associated to plant fitness increase. To survive high salinity, salt-tolerant microbes produce a broad range of compounds with heterogeneous biological activities that are potentially beneficial for plant growth. A total of 20 halophilic spore-forming bacteria have been screened *in vitro* for phyto-beneficial traits and compared with other two members of *Bacillus* genus recently isolated from the rhizosphere of the same collection site and characterized as potential biocontrol agents. Whole-genome analysis on seven selected strains confirmed the presence of numerous gene clusters with PGP and biocontrol functions and of novel secondary-metabolite biosynthetic genes, which could exert beneficial impacts on plant growth and protection. The predicted biocontrol potential was confirmed in dual culture assays against several phytopathogenic fungi and bacteria. Interestingly, the presence of predicted gene clusters with known biocontrol functions in some of the isolates was not predictive of the *in vitro* results, supporting the need of combining laboratory assays and genome mining in PGPB identification for future applications.

Keywords: spore-forming bacteria, biocontrol agents, halophiles, plant-growth-promoting bacteria, genome mining, Bacilli

INTRODUCTION

In the past decades, social concern about the environmental effects of the uncontrolled use of chemical pesticides, fertilizers, and herbicides in the agricultural field has risen considerably. The use of chemicals for the protection and enhancement of crops has led to several negative consequences: the formation of stable phytopathogenic variants, the reduction in the number of beneficial microorganisms, and the accumulation of toxic substances in soils and aquatic ecosystems (Reddy et al., 2009; Pertot et al., 2017). Given the increased global demand for crop production, researchers and industries are seeking new, more sustainable and greener approaches to pesticides and fertilizers (Glick et al., 2007). In this framework, the use of microorganisms known as Plant-Growth-Promoting Bacteria (PGPB) for crop production appears to be a promising alternative. PGPB improve crop fitness and yields both, through direct and indirect mechanisms. Direct mechanisms include the promotion of alternative nutrient uptake pathways, through the solubilization of phosphorus, the fixation of atmospheric nitrogen, the acquisition of iron by siderophores, and the production of growth hormones and molecules like vitamins, amino acids, and volatile compounds (Babalola, 2010). Indirect mechanisms instead, include the prevention or reduction of the damage induced by phytopathogens through the production of different classes of antimicrobial compounds such as hydrolytic enzymes that can lyse a portion of the cell wall of many pathogenic fungi (Jadhav et al., 2017).

The work presented here is part of a wide study aimed at identifying and selecting halophilic *Bacilli* with potential applications as biofertilizers or biocontrol agents. For this purpose, samples from the rhizosphere of the nurse plants *Juniperus sabina* and nearby soils were collected from salt-pans (Castaldi et al., 2021). Nurse plants, such as *J. sabina*, exert beneficial effects on their surrounding ecosystem, facilitating the growth and development of other plant species. This positive effect is in part due to the plant influence on the composition of soil microbial communities, generally selecting for microorganisms capable of mineralizing nutrients, enhancing soil fertility, and thus promoting plant growth and health (Hortal et al., 2013; Goberna et al., 2014; Rodríguez-Echeverría et al., 2016). For this reason, the nurse-plants rhizosphere and relative surrounding soil are a useful source of PGPB. In addition, bacteria growing in extreme environments, like salt-pans, have developed complex strategies to survive harsh conditions, which include the production of an array of diverse compounds, such as antioxidant pigments, lytic enzymes, and antimicrobial compounds, making them interesting biotechnological targets (Anwar et al., 2020). Among the PGPB, bacteria belonging to the *Bacillus* genus are of particular interest given their resistance to stressful environments and conditions due to their capacity of producing spores (Pesce et al., 2014), together with the ability to release a broad spectrum of secondary metabolites, the easy genetic manipulation, and the great ability to colonize plant surfaces (Kumar et al., 2011). In addition, the effectiveness of halo-tolerant *Bacillus* spp. to increase the growth of various crops under salt stress conditions has been widely reported (Shultana et al., 2020). Recently, we have identified and characterized PGPB *Bacillus* strains isolated from the rhizosphere of *J. sabina* (Castaldi et al., 2021). The two strains, named as *Bacillus* sp. RHFS10 and *Bacillus* sp. RHFS18, emerged for their promising PGP traits. These strains produce siderophores and solubilize phosphorus, enhancing plant nutrients uptake, and secrete indoleacetic acid (IAA), a phytohormone playing a key role in both root and shoot development. Additionally, both isolates showed a strong biocontrol activity, inhibiting the fungal phytopathogen *Macrophomina phaseolina* growth (Castaldi et al., 2021).

Here, we present the results of the screening of 20 halophilic *Bacilli* isolated from salt-pan sand samples. All the strains were characterized for PGP traits and five strains emerged for their high potentiality as biofertilizers and biocontrol agents. Comparative genomic analysis of the five sand strains and the previously characterized rhizospheric strains RHFS10 and RHFS18 revealed the presence of known genes involved in plant growth promotion and protection, sustaining, in part, the activities observed *in vitro*. Overall, this work suggests a strategy for the selection of potential PGP candidates belonging to *Bacillus* genus using combined *in silico* and *in vitro* approaches.

MATERIALS AND METHODS

Isolation of Bacteria

Bacillus strains used in this study were isolated from sand samples collected in the proximity of *J. sabina* plants growing in the salt-pans of Formentera (Spain). Sand samples were heat-treated at 80°C, for 15 min to kill vegetative cells and select for spore-forming bacteria, and 1 g of sample was suspended in 9 ml of TY broth (10 g/L tryptone, 5 g/L yeast extract, and 8 g/L NaCl) and 10-fold serial dilutions placed on TY plates (Cangiano et al., 2010). After 4–5 days of incubation at 30 ± 1°C, colonies were recovered and streaked on fresh TY plates, and pure cultures stored at −80°C into glycerol stocks (Giglio et al., 2011).

Phenotypic Characterization and Growth Conditions

The phenotypic variants of isolated strains were determined by visual inspection. The facultative anaerobic growth was determined using the AnaeroGen sachets (Unipath Inc., Nepean, Ontario, Canada) placed in a sealed jar with bacteria streaked on TY agar plates and incubated at 37°C for 3 days. To confirm the sporulation ability, the bacteria were grown in Difco sporulation medium (8 g/L Nutrient broth No. 4, 1 g/L KCl, 1 mM $MgSO_4$, 1 mM $Ca(NO_3)_2$, 10 μM $MnCl_2$, and 1 μM $FeSO_4$, Sigma-Aldrich, Germany) at 37°C for 30–48 h, and the presence of spores was checked by light microscopy. Salt, pH, and temperature tolerance were determined as follows: about 50 μl of culture of each isolate grown in TY broth for 6 h at 37°C (10^7 cells/ml) were transferred to individual tubes containing 5 ml of TY broth with different pH (2.0, 4.0, 6.0, 7.0, 8.0, 10.0, and 12.0) or NaCl concentration (0, 5, 10, 13, 15, and 18%) and left to grow at 37°C with agitation (Cangiano et al., 2014) . The temperature tolerance

of isolates was tested incubating the cultures at 37 (control), 4, 15, 25, 50, and 60°C. The growth (+) or no growth (–) in comparison with the controls after 24–48 h was recorded.

Plant Growth-Promoting Traits

Phosphate Solubilization

The phosphate solubilization activity was evaluated by spot inoculation of 3 µl of the freshly grown bacterial culture (10^7 cells/ml) onto Pikovaskya's agar medium (Pikovskaya, 1948). The plates were incubated at 28°C for 10 days. The formation of transparent zones around the bacterial colonies indicates a positive result (Schoebitz et al., 2013).

Siderophores Production

The siderophores production was determined by the Chrome Azurol S (CAS) assay as described by Pérez-Miranda et al. (2007). Three milliliter of freshly-grown bacterial cultures was spot-inoculated on CAS agar plates and incubated at 28°C. The formation of a yellow-orange halo zone around the bacterial colony was a positive indicator of siderophore production and the halo zone diameters were measured after 4 days of incubation.

Indoleacetic Acid Detection

The indoleacetic acid production was measured as described by Etesami et al. (2014), with some modifications. Briefly, each strain was cultured in 10 ml of TY broth at 37°C for 4 days with shaking at 150 rpm. Following growth, 1 ml of bacteria supernatant was mixed with 2 ml of Salkowski reagent (0.5 M $FeCl_3$ in 35% $HClO_4$ solution), and the solution was vortexed and incubated at room temperature for 30 min. The formation of pink color was considered a positive reaction (Damodaran et al., 2013). Quantitative estimation of IAA (µg/ml) was obtained by recording spectroscopic absorbance at 535 nm using a standard curve prepared separately with pure IAA (Sigma) in the range 0–100 µg/ml (Gordon and Weber, 1951). Sterile TY medium was used as control.

Biofilm Production and Swarming Motility

To detect the ability to produce biofilm, bacterial isolates were grown in 24-well culture plates in TY broth for 48 h without agitation at 37°C in according to O'Toole (2011). Then, the supernatant was discarded, adhered cells were rinsed three times with distilled water and 1 ml of a 0.1% crystal violet (CV) solution was added to stain the adhered biomass. Plates were incubated for 30 min at room temperature, washed carefully three times with distillated water and patted dry. Dye attached to the wells was extracted with 1 ml of 70% ethanol and quantified at an absorbance of 570 nm. Data were normalized by total growth estimated by OD600 nm, and the experiment was performed in triplicate.

Swarming motility was tested according to the method adopted by Adler (1966). TY agar 0.7% plates were spot inoculated with 3 µl of the freshly grown bacterial culture (10^7 cells/ml). After an overnight incubation at 37°C, the swarm diameters were measured.

Whole-Genome Sequencing of the Selected PGPB

DNA extraction was performed using the DNeasy PowerSoil kit (Qiagen, Hilden, Germany) according to the manufacturer's instructions. Genome sequencing was performed by MicrobesNG (Birmingham, United Kingdom) with the genomic DNA library prepared using the Nextera XT library prep kit (Illumina) following the manufacturer's protocol. Libraries were sequenced on the Illumina HiSeq using a 250 bp paired-end protocol. Reads were adapted and trimmed using Trimmomatic 0.30 with a sliding window quality cutoff of Q15 (Bolger et al., 2014) and the *de novo* genome assembly was carried out with SPAdes (version 3.7) *via* MicrobesNG. Genomes were annotated using Prokka (Seemann, 2014). Biosamples accession numbers for strains RHFB, RHF2, RHF6, RHF12, RHF15, RHS10, and RHFS18 are, respectively: SAMN17389615, SAMN17389609, SAMN17389610, SAMN17389612, SAMN17389613, SAMN17389611, and SAMN17389614. MIGS compliant details regarding each genome are available in the **Supplementary Table S1**.

Average Nucleotide Identity (ANI) values between the sequenced genomes and the closest bacterial species identified from the 16S rRNA phylogenetic analysis (see below) were obtained using the OrthoANI algorithm of EZBioCloud (Yoon et al., 2017). An ANI similarity of 95% was considered as a cut-off for species delineation.

Phylogenetic Analysis

The 16S rRNA genes were extracted from the sequenced genomes using Anvi'o v2.3.3 (Eren et al., 2021). and compared to 76 reference 16S rRNA genes from closely related strains identified using the Genome Taxonomy Database (GTDB)[1] taxonomy and retrieved from the NCBI database. All sequences were aligned using Seaview 4.4.0 software (Corrado et al., 2021), and the phylogenetic tree was constructed using the Maximum-likelihood algorithm with model GTR+I+G4. Statistical support was evaluated by the approximate likelihood-ratio test (aLRT) and is shown at the corresponding nodes of the tree. *Clostridium difficile* is used as an outgroup to root the tree.

Evaluation of Potential Biocontrol Activity

Isolated bacterial strains were tested *in vitro* for growth inhibitory activity against phytopathogenic fungi and bacteria are listed in **Table 1**. The phytopathogenic fungi are deposited in the fungal culture collection of the Plant Pathology Department of the University of Buenos Aires (FAUBA, Argentina) and were kindly supplied by Marcelo Anibal Carmona (Facultad de Agronomía, Cátedra de Fitopatología, Universidad de Buenos Aires, Buenos Aires, Argentina), except for *Stemphylium vesicarium*. All the fungi were stored on Potato Dextrose Agar (PDA) in Petri dishes. Dual-culture plate method was carried out to detect the antifungal activity in accordance with Xu and Kim (2014). Briefly, fungal plugs of 6 mm × 6 mm diameter were placed at the center of PDA plates and 5 µl of bacterial

[1]https://gtdb.ecogenomic.org

TABLE 1 | List of the phytopathogenic fungi and bacteria used in this study.

Pathogen type	Species	Strain	Provenience	Host plant
Fungi	*Macrophomina phaseolina*	2,012,013-1	Argentine	Soy
	Colletotrichum truncatum	17-5-5	Argentine	Soy
	Drechslera teres	FT	Argentine	Barley
	Cercospora nicotianae	Ck_2017_B35	Bolivia	Soy
	Stemphylium vesicarium		Italy	Pear
Bacteria	*Pseudomonas tolaasii*	2,192	-	Mushroom
	Pseudomonas syringae pv tabaci	ICMP 2706	-	Tobacco
	Pseudomonas syringae pv panici	ICMP 3965	-	Rice
	Pseudomonas caryophylli	NCPPB349	Italy	Carnations
	Pseudomonas syringae pv syringae	B475	-	Mango
	Pseudomonas syringae pv japonica	ICMP 6305	-	Wheat
	Pseudomonas syringae pv papulans	Psp26	-	Apple

strains grown overnight in TY broth were placed on the opposite four sides of the plates 1.5 cm away from the fungal disc. This method was repeated for each fungus. Controls consisted of plates containing the fungal plugs alone. All plates were incubated at 28°C for 5–7 days. The antagonism activity against bacterial phytopathogens was performed as described in Li et al. (2020) with some modifications. Bacterial pathogens were streaked on TY plates and incubated at 25°C overnight. Single colonies were suspended in TY broth and incubated at 25°C. Approximately 1×10^{-6} CFU/ml were mixed with melted 0.8% TY agar medium before pouring plates. After solidification, 5 µl of bacterial isolates solution ($OD_{600} = 1.0$) was spot inoculated onto the plates and incubated at 28°C for 48 h, before measuring the diameters of inhibition halos. All experiments were performed in triplicate.

Identification of Biosynthetic Gene Clusters

Obtained genomes were analyzed by antiSMASH 5.0 (Blin et al., 2019) and BAGEL 4 (van Heel et al., 2018) to identify biosynthetic gene clusters (BCGs) of potential antimicrobial compounds such as non-ribosomal peptide synthetases (NRPSs), polyketide synthases (PKSs), post-translationally modified peptides (RiPPs), hybrid lipopeptides (NRPS-PKS) and bacteriocins. Biosynthetic Gene Clusters that shared less than 70% amino acid identity against known clusters were regarded as novel.

RESULTS AND DISCUSSION

Isolation and Characterization of Spore-Forming Plant-Growth-Promoting Bacteria

Spore-forming bacteria were specifically isolated from sand samples collected from gaps among nurse plants, belonging to the genus *J. sabina*, in salt-pans as described in the Materials and Methods section. Based on morphological characteristics, a total of 20 isolates were selected and preliminarily characterized for growth properties (**Supplementary Table S2**). All the strains can be classified as facultative anaerobic, mesophiles and moderate halophiles, excluding RHF5 strain, which survives up to 60°C and strain RHFB unable to grow at temperature and salt concentration higher than 37°C and 5% NaCl, respectively (Ventosa et al., 1998; Schiraldi and De Rosa, 2016).

To identify potential PGPB, the 20 strains were evaluated *in vitro* for physiological traits associated with plant growth enhancement and biocontrol ability (**Table 2**). Strain performance was compared with those of two promising PGPB, RHFS10, and RHFS18 strains, belonging to the *Bacillus* genus and isolated from *J. sabina* rhizosphere of the same collection site (Castaldi et al., 2021) and proposed as biocontrol agents for their antagonistic activity against the phytopathogen *M. phaseolina*. Most of the new strains displayed root-colonization phenotypes since able to surface spread by swarming and to form biofilms (Amaya-Gómez et al., 2020), while only five were found either positive to both solubilization of phosphate, indoleacetic acid (IAA), and siderophore production. Strains RHF6, RHF15, and RHFB showed a better performance than when compared against the already characterized rhizobacteria strains RHFS10 and RHFS18, confirming that the microenvironments created under or nearby nurse shrubs are a promising source of PGPB (Rodríguez-Echeverría et al., 2016). All bacterial isolates were tested for *in vitro* activities of their extracellular hydrolytic enzymes (lipase, protease, amylase, xylanase, and cellulase) usually associated with biocontrol activity (Pal and McSpadden Gardener, 2006). As reported in **Table 2**, the highest hydrolytic activity was observed for RHF12, RHF15, and RHFB strains, comparable with that exerted by rhizosphere strains RHFS10 and RHFS18.

Based on these results reported in **Table 2**, seven strains were selected for whole-genome sequencing analysis. All selected strains were able to solubilize phosphate with efficiency higher than the other ones and to produce Biofilm, IAA, and siderophores. Further, strains RHF12, RHF15, RHFB, and RHFS18 emerged for their strong hydrolytic potential, often associated to biocontrol activity (Castaldi et al., 2021), while strain RHF6 showed the ability to growth up to 13% NaCl, showing the best salt tolerance (**Supplementary Table S2**).

Genome Sequencing and Phylogenetic Analysis

The obtained genomes had coverage of ~30×, with a variable number of contigs between 40 and 1,105 for RHF15 and

TABLE 2 | Summary of plant growth-promoting and biocontrol traits exhibited by 20 spore-forming bacteria isolates.

Strain	PGPB activities					Hydrolytic activities				
	Biofilm (OD_{570})	Swarming	PVK	IAA (μg/ml)	Siderophores	Lipase	Protease	Amylase	Xylanase	CMC
RHF1	–	++	++	–	+	–	++	++	+	++
RHF2	0.2	+	+	18	+	–	+	+	+	+
RHF3	–	–	–	–	–	+	++	++	+	–
RHF4	–	+	–	–	+	+	++	++	–	+
RHF5	0.2	–	–	2	–	–	+	++	–	–
RHF6	0.3	+	++	31	++	–	+	+	+	++
RHF7	0.4	–	–	–	–	–	+	+	–	–
RHF8	0.6	++	–	6	–	–	++	++	++	–
RHF9	–	–	+	3.2	–	–	++	++	–	–
RHF10	–	–	–	4	–	–	++	+	+	+
RHF11	0.2	+	–	–	–	–	+	+	+	–
RHF12	0.7	++	+	25	++	–	++	++	++	++
RHF13	–	++	++	3	+	+	–	++	+	++
RHF14	–	–	–	–	–	+	+	+	+	–
RHF15	0.6	++	++	23	++	+	++	++	++	++
RHF16	–	–	–	–	–	+	+	+	–	–
RHF17	0.5	++	+	–	+	+	+	+	++	+
RHFB	0.3	+	++	32	++	++	++	++	++	+
RHFE	–	–	–	–	–	+	+	+	–	–
RHFL	0.3	–	–	–	–	–	+	+	–	–
RHFS10[1]	0.3	++	+	12	++	++	++	++	++	++
RHFS18[1]	0.5	+	+	12	++	+	++	++	++	++

No activity (–), halo or colony diameter <5 mm (+), halo or colony diameter ≥5 mm (++), halo or colony diameter 10 mm (+++). Data are represented by means of at least three replicates ± SE at $p \leq 0.05$ using LDS. The strains selected for further studies are indicated in bold. PVK, Pikovskaya; IAA, indoleacetic acid; and CMC, carboxymethylcellulose.
[1]*Available from Castaldi et al. (2021).*

TABLE 3 | General features of the assembled genomes.

Analysis statistics	Strains						
	RHFB	RHF2	RHF6	RHF12	RHF15	RHFS10	RHFS18
Size (bp)	5,648,757	4,003,762	4,066,378	4,096,200	4,232,838	4,254,653	3,936,406
Number of contigs	158	52	156	280	40	46	1,105
Mean GC content (%)	40.57	43.74	46.3	44.01	43.39	43.95	46.14
CDS	5,413	3,988	3,901	3,997	4,282	4,182	3,87
N50	187,761	413,219	584,325	60,229	2,184,724	1,139,270	6,179
N75	82,022	306,766	292,476	34,071	1,049,735	348,257	3,118
L50	11	3	2	19	1	2	176
L75	21	6	4	42	2	4	397

RHFS18, respectively (**Table 3**). The genome of strain RHFS18 was particularly fragmented, and repeated sequencing of the same strain did not yield improved assembly suggesting that the results are not dependent on a low-quality sequencing library. The obtained genomes are approximately 4.0 Mbp long except for RHFB's genome, being the longest (5.6 Mbp) and the one with the highest number of predicted protein coding sequences compared to the others. Taxonomic identification of the strains was based on the phylogenetic analysis of the 16S rRNA sequence as well as the whole genome Average Nucleotide Identity. All the isolates were identified as members of the genus *Bacillus* (**Figure 1**) with six strains out of seven clustering into the same clade, and only strain RHFB falling in a different clade. The phylogenetic divergence observed for RHFB from the other strains agrees with the observed differences in physiological traits for this strain (**Supplementary Table S3**). Since most *Bacillus* species are phylogenetically close, 16S rRNA analysis is not always exhaustive to obtain an unambiguous assignment (Rooney et al., 2009). To overcome this issue and classify the strains at the species level, whole genome ANI was used (**Table 4**). Strain RHFB exhibited 96.95% ANI against the genome of the closest relative *Brevibacterium frigoritolerans* and was therefore identified as a *B. frigoritolerans* species. Strain RHF2 was identified as *Bacillus subtilis*, based on 99.96% ANI score. Strains RHF6 and RHFS18 were classified as members of the *Bacillus amyloliquefaciens* species, exhibiting 99.26 and 98.36% ANI, respectively. Strain RHF12 was identified as *Bacillus halotolerans*, based on 98.04% ANI score, while RHF15 was classified as *Bacillus gibsonii*, showing 99.6% ANI score. As shown in **Table 4**, RHFB, RHF12, and RHFS18 strains were

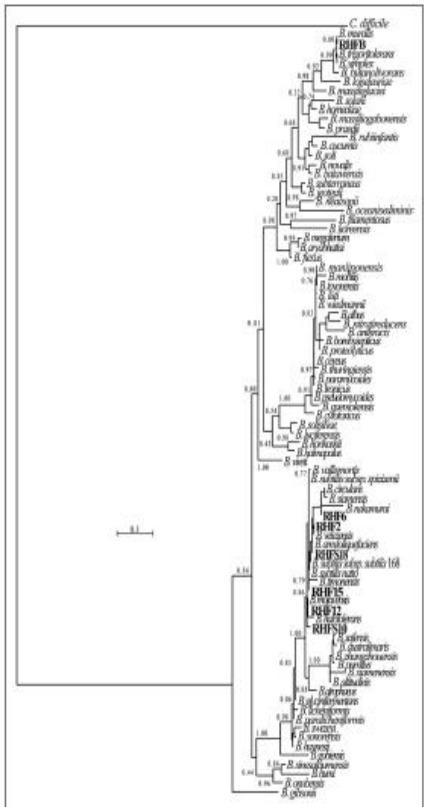

FIGURE 1 | Phylogenetic tree of the spore-forming bacteria isolated from salt-pans. The phylogenetic tree was constructed using the Maximum-likelihood algorithm with model GTR+I+G4, based on 16S rRNA gene sequences. The gene sequences of the isolated bacteria were aligned to reference bacteria belonging to the *Bacillaceae* family according to Genome Taxonomy Database (GTDB). Node support represents the approximate likelihood-ratio test (aLRT) and is shown at the corresponding node of the tree. *Clostridium difficile* is used as an outgroup.

TABLE 4 | Classification of the seven selected strains.

	16S rRNA similarity	ANI (best score)
RHFB	*B. trigoritolerans* (100%)	*B. trigoritolerans* (96.95%)
RHF2	*B. velezensis* (99.87%)	*B. subtilis* 168 (99.96%)
RHF6	*B. velezensis* (100%)	*B. amyloliquefaciens* (99.26%)
RHF12	*B. halotolerans* (98.51%)	*B. halotolerans* (98.04%)
RHF15	*B. subtilis* (100%)	*B. gibsonii* (99.6%)
RHFS10	*B. halotolerans* (97.5%)	*B. vallismortis* (93.48%)
RHFS18	*B. amyloliquefaciens* (100%)	*B. amyloliquefaciens* (98.36%)

The 16S rRNA similarity and ANI score against the closest relative identified from the phylogenetic analysis are reported for each isolate.

univocally matched with the same species, while for RHF2, RHF6, and RHF15 strains the two analyses returned different results. This mismatch between the two methods of classification is due to the poor discrimination between closely related species of the *Bacillus* genus due to their high morphological, biochemical, and genetic similarities (Celandroni et al., 2019). Since taxonomy annotations based on genetic markers, such as the 16S rRNA gene, can give variable results depending on the strain, ANI-based classification has been preferred in this study when showing ANI scores ≥95% (Jain et al., 2018). Based on this, RHF2, RHF6, and RHF15 were identified as *B. subtilis*, *B. amyloliquefaciens*, and *B. gibsonii*, respectively (**Table 4**). Only strain RHFS10 could not be classified at the species level due to the low ANI score (93.48%) when compared with the closest relative *Bacillus vallismortis* and it was classified as *Bacillus* sp. RHFS10 (**Table 3**). Further analysis will be required to fill this classification gap.

Environmental Adaptation to Halophilic Conditions

The phenotypic plasticity of the salt-pans isolates was investigated by comparing their growth parameters against the closest *Bacillus* species identified by the ANI analysis (**Table 4**). Temperature, pH, and salinity ranges required for growth were evaluated. These parameters are useful to identify distinct phenotypic strategies used by microorganisms to better adapt to environmental conditions (Agrawal, 2001). As expected, taxonomically closer strains showed small differences when compared with each other or with their representative species (red dashed lines in **Figure 2**). As already highlighted by the phylogenetic analysis, *B. frigoritolerans* RHFB strain presented a diverging phenotype, especially considering the lower salt tolerance compared to the other isolates. Interestingly, some strains, like *B. halotolerans* RHF12, *B. gibsonii* RHF15, and *Bacillus* sp. RHFS10, showed identical growth properties even though belonging to three different *Bacillus* species (**Figure 2**), while strains of the same species, like *B. amyloliquefaciens* RHF6 and RHFS18, exhibited different adaptations to NaCl concentration and pH range. Moreover, *B. amyloliquefaciens* RHF6 like *B. subtilis* RHF2 were able to grow at higher salt concentrations than their representative species, suggesting an adaptive phenotypic variation to the high salinity condition of salt-pans.

Analysis of Potential PGP and Biocontrol Traits

To confirm the *in vitro* PGP characterization of the isolates, a prediction of the genes (**Figure 3**) and proteins (**Table 5**) involved in biocontrol activity and plant growth promotion was performed. The analyses identified genes that can be attributed to the strains ability to improve nutrient availability, suppress pathogenic fungi, and resist oxidative stress and quorum sensing in all analyzed genomes. For instance, the genome of most of the seven strains included the pyrroloquinolone quinone synthase (*pqq*) and the dependent glucose dehydrogenase (*gdh*)

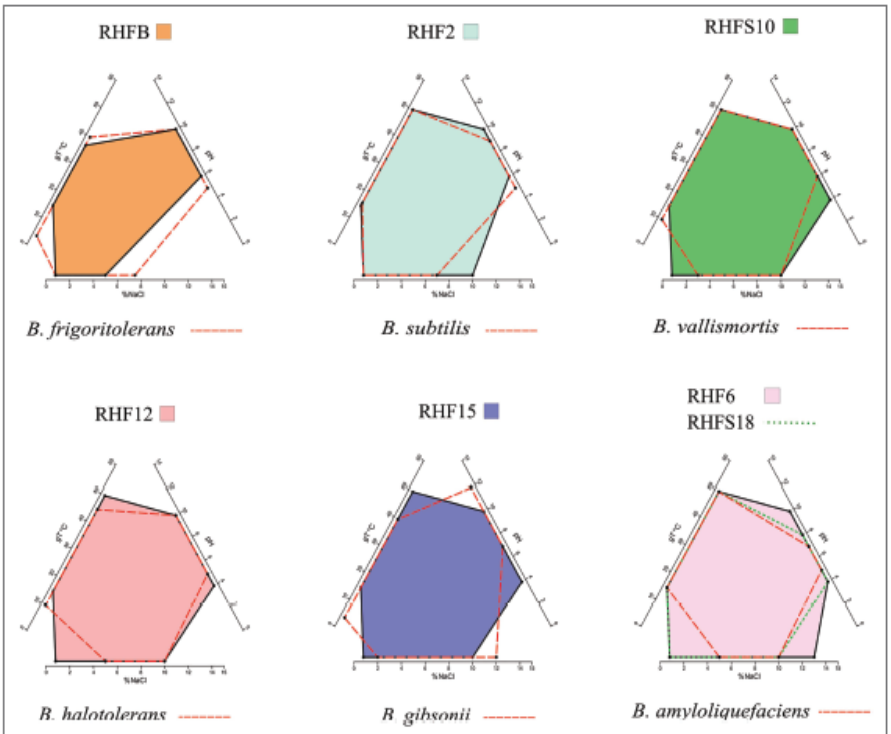

FIGURE 2 | Phenotypic plasticity of the salt-pan isolates. Multivariate polygons plots (Giovannelli et al., 2021, in preparation) showing the growth temperature (gT°C), pH, and salinity (% NaCl) boundaries observed for the seven isolates (polygons) and the range for the closest relative identified by ANI (red dashed lines). Each edge represents the range for the specific variables projected onto the axis. More information about polygons plot can be found at https://giovannellilab.github.io/polygonsplot/.

genes, involved in mineral phosphate solubilization as well as antifungal activities and systemic resistance induction. Interestingly, both isolates *B. amyloliquefaciens* RHF6 and RHFS18 did not carry the cofactor *pqq* gene cluster, suggesting that other mechanisms could co-exist (**Table 2**). IAA is one of the most common and effective plant-growth hormones. Besides plants, most rhizobacteria can produce and secrete IAA, increasing the growth and the yield of crops (Bunsangiam et al., 2019). All the strains produced Tryptophan-2-monooxygenase and Indole-3-acetamide hydrolase, able to convert Tryptophan in Indole-3-acetamide and then in IAA, respectively (Bunsangiam et al., 2019). The presence of other tryptophan synthases orthologs (subunits a and b) in all the analyzed genomes suggests alternative IAA biosynthesis pathways potentially involving different intermediates. This hypothesis is supported by the observation that *B. frigoritolerans* RHFB, one of the best IAA producers among the isolated PGPB, possessed the indole-3-pyruvate decarboxylase, a key enzyme of another Trp-dependent pathway for IAA production (Sitbon et al, 2000).

All the strains were predicted to be potentially able to fix nitrogen and produce nitric oxide, both useful features in agricultural practices (Ahmad et al., 2013), and to synthesize polyamines, as spermidine and putrescine, and the ACC deaminase, involved in lateral root development and plant growth enhancement under abiotic stress (Xie et al., 2014; Gupta and Pandey, 2019).

As expected, the genome of all the halophilic *Bacillus* strains contained multiple genes involved in antioxidant response, such as peroxidases, catalases, superoxide dismutase, and glutathione peroxidase (Hassan et al., 2020; **Figure 3**; **Table 5**). Other enzymes involved in abiotic stress responses were identified in the strains, as the osmoprotectants choline dehydrogenase, betaine-aldehyde dehydrogenase, and proline dehydrogenase (**Table 5**). The predicted production of osmotically active metabolites, as well as ROS scavenging enzymes, reflects the

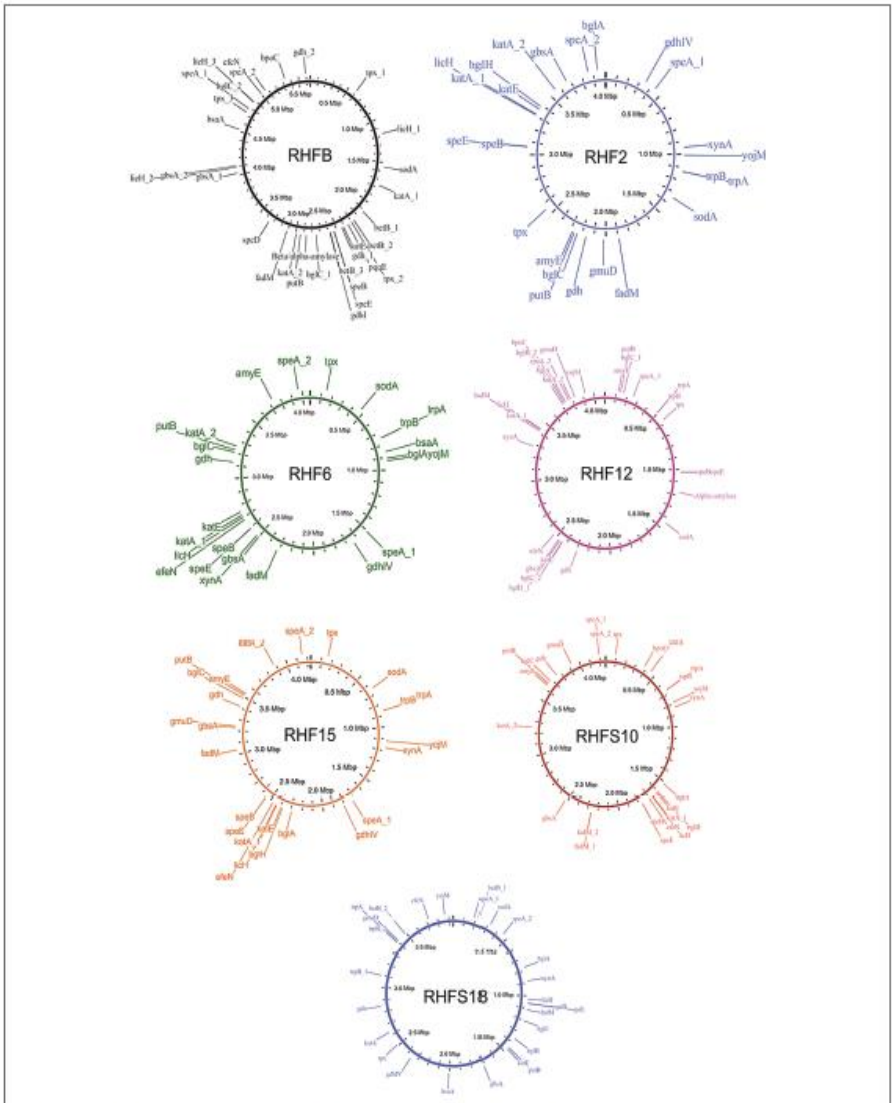

FIGURE 3 | Whole genome representations of the seven isolates showing the location of the identified PGP trait genes.

ability of the selected strains to survive in extreme environments, as salt-pans and to potentially alleviate abiotic stress in agricultural system.

Finally, all the isolates possessed in their genomes genes encoding for hydrolases involved in fungal cell-wall and starch degrading pathways, confirming the results obtained with the

TABLE 5 | Plant-Growth-Promoting traits-associated proteins identified in the proteome of the selected strains and their abundance.

PGP Trait	Protein	RHFB	RHF2	RHF6	RHF12	RHF15	RHFS10	RHFS18
Phosphate solubilization	Pyrroloquinoline quinone	1	1	0	1	1	1	0
	Glucose 1-dehydrogenase	2	2	2	2	2	2	2
Nitrogen fixing	Nitrogenases	6	6	4	6	6	6	2
Nitric oxide synthesis	Copper-containing nitrite reductase	1	2	1	3	2	2	1
IAA biosynthesis	Indole-3-pyruvate decarboxylase	1	0	0	0	0	0	0
	Tryptophan 2-monooxygenase	4	2	1	2	2	3	2
	Tryptophan synthase (subunit a and b)	6	7	6	7	7	5	7
	Tryptophan aminotransferase	0	0	0	0	0	0	0
	Tryptophan decarboxylase	0	0	0	0	0	0	0
	Indole-3-acetamide hydrolase	0	0	0	0	0	0	0
Putrescine and Spermidine-related production	Arginine decarboxylase	3	2	2	2	2	2	2
	Agmatine ureohydrolase	1	1	1	1	1	1	2
	Ornithine decarboxylase	0	0	0	0	0	0	0
	SAM decarboxylase	1	1	1	1	1	2	1
	Spermidine synthase	1	1	1	1	1	1	1
ACC deaminase activity	ACC deaminase	2	2	3	1	2	1	3
	D-cysteine desulfhydrase	1	0	1	0	0	0	1
Antioxidant activity	Peroxidases	9	10	4	9	9	8	4
	Catalases	10	12	11	11	12	11	8
	Superoxide dismutase	7	5	5	6	5	5	5
	Glutathione peroxidase	1	1	1	1	2	1	1
	Glutathione reductase	0	0	0	0	0	0	0
	Glutathione S-transferase	2	5	2	2	5	2	3
Abiotic stress	Choline dehydrogenase	0	1	1	2	2	1	1
	Betaine-aldehyde dehydrogenase	5	2	2	2	2	2	2
	Proline dehydrogenase	2	3	2	2	2	2	2
Cell wall and degrading	β-Glucosidase	1	3	2	5	3	3	3
	α-Glucosidase	3	4	4	3	4	4	2
	Endo-1,4-β-xylanase	5	7	7	4	5	7	9
	Glucoamylase	0	0	2	0	0	0	1
	α-Amylase	0	1	1	1	1	1	1
	Chitinase	1	0	0	0	0	1	1
	β-1,3-Glucanase	2	3	2	1	2	2	1
	Cellulase	0	3	2	3	3	4	2
	Protease	4	3	3	3	3	2	1

Only ≥40% similarity scores were considered. IAA, indole-3-acetic acid; ACC, 1-aminocyclopropane-1-carboxylate.

in vitro analysis, except for strain *B. frigoritolerans* RHFB whose genome did not carry α-amylase or cellulase genes.

Antimicrobial Activity Screening

To verify the antagonistic potential that emerged from the genome-mining, the isolates were dually cultured with fungal and bacterial plant pathogens (see **Table 1** for a list of the used phytopathogens). The results reveal that isolates inhibited plant pathogens growth on plates with different efficiency (**Figure 4**). Strains *B. subtilis* RHF2, *B. amyloliquefaciens* RHF6, and *Bacillus* sp. RHFS10 showed a broad inhibitory spectrum, being able to antagonize both phytopathogenic fungi and bacteria, while *B. halotolerans* RHF12 and *B. amyloliquefaciens* RHFS18 exhibited an antimicrobial activity limited to fungi. The highest antagonistic activity was observed for strain *Bacillus* sp. RHFS10, capable of inhibiting the growth of most of the test pathogens, confirming its biocontrol potential already observed by Castaldi et al. (2021). Unexpectedly, *B. frigoritolerans* RHFB exhibited no activity at all. Nevertheless, in the last decade, this species has been identified as a potential insect pathogenic bacterial species, with nematicidal

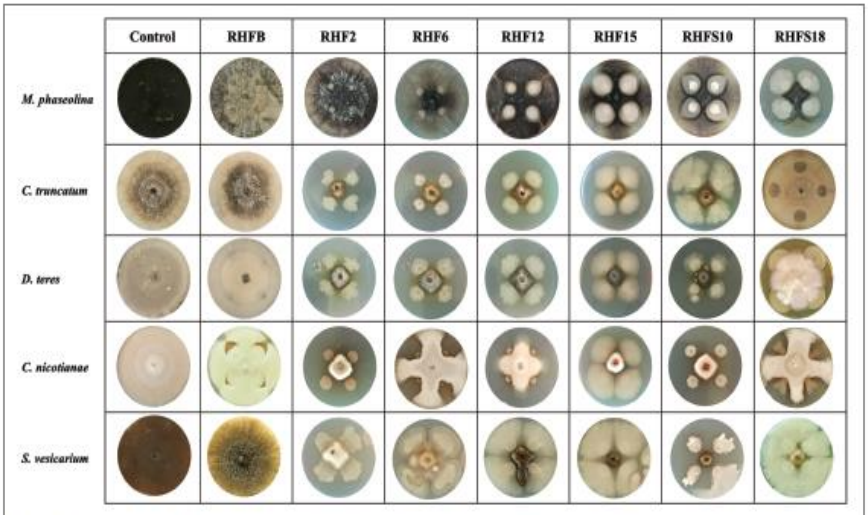

FIGURE 4 | Representative photographs of dual culture assay for *in vitro* mycelial growth inhibition of fungal phytopathogens.

activity (Selvakumar et al., 2011). The diversity observed in the antimicrobial activity against plant pathogens highlighted the phenotypic diversity of sand and rhizosphere isolated *Bacilli*, suggesting that in nature plant-associated bacteria may encounter different phytopathogens that may induce the acquisition of different antagonistic activity.

Genome Mining for Biosynthetic Gene Clusters

The biocontrol potential and the ability to enhance plant growth of PGPB are mostly attributed to their bioactive secondary metabolites. Proteins and metabolites released in the soil by PGPB, indeed, are implicated in root colonization, as well as in interactions with the plant immune response and the surrounding niche (Lugtenberg and Kamilova, 2009; Pieterse et al., 2014; Jamali et al., 2020). The strong antimicrobial activity of selected *Bacillus* strains is most likely due in part to the production of hydrolytic enzymes and siderophores observed in *in vitro* assays and confirmed by genome analysis (**Tables 2** and **5**). To better investigate this antagonistic activity, the biosynthetic potential of the halophilic PGPB was evaluated by using antiSMASH 6.0.0 to predict both characterized and unknown functioned secondary metabolites (**Figure 5**).

The bacterial isolates harbored BGCs coding for NRPSs, polyketide synthases (PKSs), post-translationally modified peptides (RiPPs), hybrid lipopeptides (NRPS-PKS; **Figure 5A**), and the majority of the BGCs are assigned to known products (**Figure 5B**; **Supplementary Table S4**). The unknown BGCs are type 3 polyketide synthase (T3PKS), RiPPs and terpenes (**Figure 5C**; **Supplementary Table S4**).

Novel Non-ribosomal Peptide Synthetases and Bacteriocins

NRPs are modular enzymes that synthesize secondary metabolites, some of which are known to be involved in plant disease control (Ongena and Jacques, 2008). Several bioactive compounds produced by *Bacillus* strains fit in this category, such as surfactin or fengycin (Keswani et al., 2020), both of them exhibiting antimicrobial activity potentially exploited for biocontrol in agriculture. We have identified one novel BGC belonging to the class of the NRPs from *B. amyloliquefaciens* RHF6 (**Figure 6**). This cluster of 66.3 Kb has six genes encoding 25 domains, which include six condensation (C) domains, seven adenylation (A) domains, one coenzyme A ligase (CAL) domain, two epimerization (E) domains, one thioesterase (TE) domain, one heterocyclization (Cy) domain and seven peptidyl carrier protein (PCP) domains. Among them, 24 domains are essential components of this cluster, and catalyze the incorporation of seven amino acids into the final product exhibiting the following sequence: D-Cys-Ser-Cys-Ala-Asn-D-Asn. This cluster shows no similarity to any known BGCs reported in the antiSMASH database (**Supplementary Table S4**). The single heterocyclization (C) domain in the first module of the BGC, could form a thiazoline ring from a residue of cystine (Cys). Interestingly, many antimicrobial drugs expose a thiazoline ring (Desai et al., 2016). This allows us to speculate on the potential antimicrobial activity of the compound produced by this novel BGC.

The seven genomes were also mined for potential novel bacteriocins BGCs using BAGEL4. Bacteriocins are ribosomally

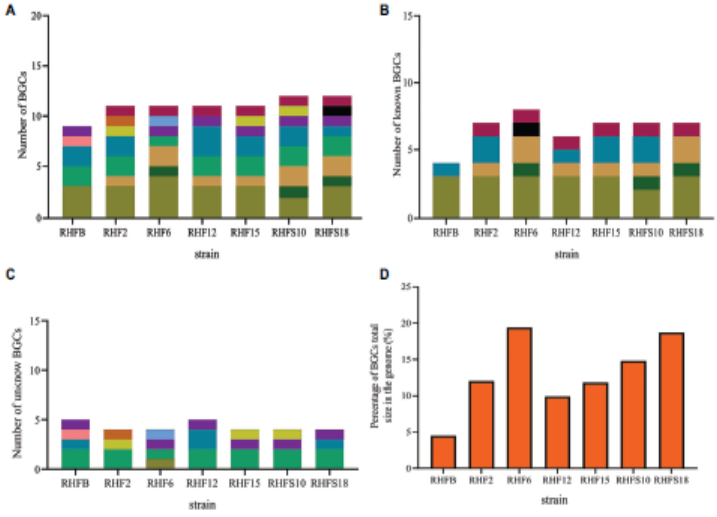

FIGURE 5 | Number of biosynthetic gene clusters harbored by the strains and the percentage contribution of Biosynthetic Gene Clusters (BGCs) to the total genome size. **(A)** Total number of BGCs; **(B)** number of reported BGCs in the genomes; **(C)** number of unknown BGCs. BGCs that have different numbers of genes or show less than 70% protein identity to the reported ones were regarded as novel; and **(D)** the percentage contribution of BGCs to the genomes.

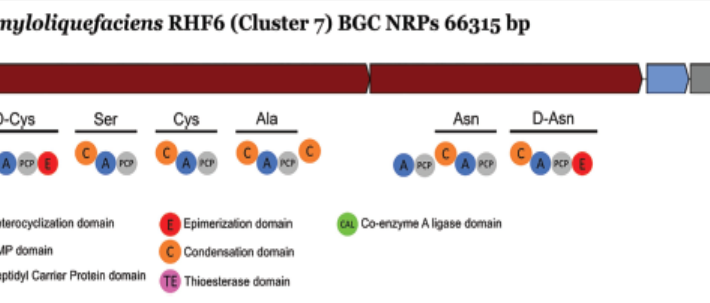

FIGURE 6 | Novel NRP Biosynthetic gene Clusters identified from the isolate *Bacillus amyloliquefaciens* RHF6.

synthesized antimicrobial peptides, generally active against bacteria closely related to producers (Cotter et al., 2013), and classified into three main classes: class I comprehends ribosomally produced and post-translationally modified peptides (RiPPs); class II unmodified peptides, and class III large antimicrobial peptides (Zhao and Kuipers, 2016). These molecules are directed against competitive microorganisms, and therefore generate a selective advantage for the producers. Generally, bacteriocins are highly specific against their target, although some might have a wider spectrum (Jack et al., 1995). The analysis made using BAGEL4, returned 15 regions of interest (in contrast with the antiSMASH analysis which revealed a higher number of bacteriocins, **Supplementary Table S4**), even though only six of them could be classified as novel bacteriocins, sharing ≤70% of similarity with known sequences from BAGEL4 database (**Figure 7**).

One orphan BGC of 27 genes is carried by both *B. amyloliquefaciens* RHF6 and RHFS18 strains (**Figures 7a.1,d.1**), although the core biosynthetic genes encode two different

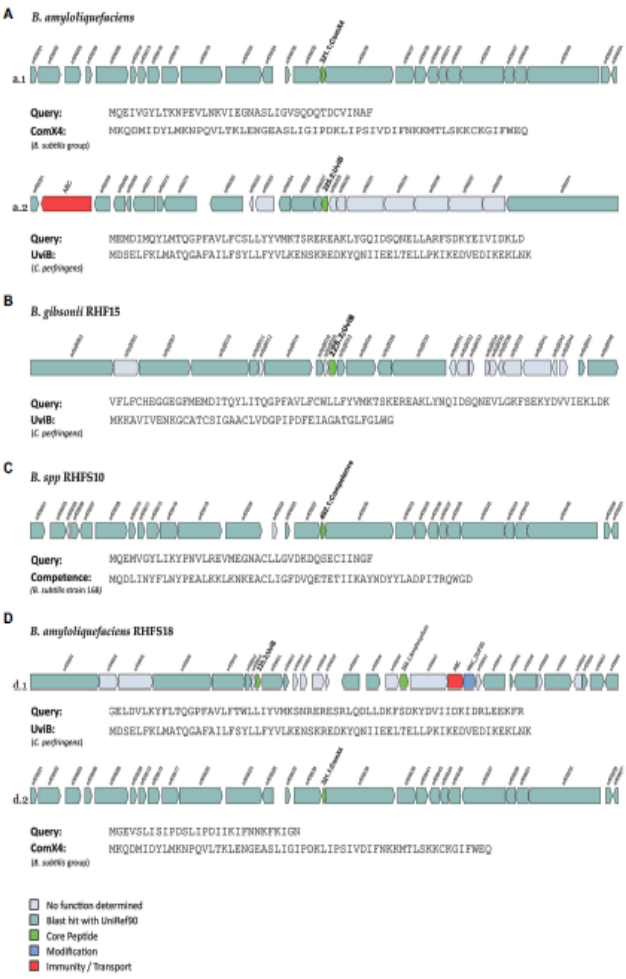

FIGURE 7 | Novel bacteriocins identified from the isolated Bacillus strains (**A:** B. amyloliquefaciens, **B:** B. gibsonii RHF15, **C:** B. spp. RHFS10 and, **D:** B. amyloliquefaciens RHFS18). The BGCs identified from BAGEL4 analysis are shown and compared to the most similar available in BAGEL4 database.

precursor peptides of 40 and 29 amino acids, respectively, sharing 41.03 and 57.14% of similarity with ComX4 from the *B. subtilis* group. In particular, ComX4 belongs to the ComX subclass of RiPPs according to the BAGEL4 database, and it is part of a major quorum-sensing system that regulates the development of genetic competence (Okada et al., 2005) and the production of surfactins (Caulier et al., 2019). *Bacillus amyloliquefaciens* RHF6 also harbors a BGC of 23 genes (**Figure 7A-a.2**), with the core biosynthetic gene encoding a 63-amino acids precursor peptide, showing a similarity of 36.51% compared to UviB, a class II bacteriocin first identified in the mobilizable plasmid pIP404, from *C. perfringens*, known to be bacteriocinogenic (Garnier and Cole, 1988). Interestingly, two different BGCs containing the same gene encoding for a

TABLE 6 | Antimicrobial activity of the seven selected strains against phytopathogenic fungi and bacteria.

Pathogen types	Species	RHFB	RHF2	RHF6	RHF12	RHF15	RHFS10	RHFS18
Fungi	*M. phaseolina*	–	–	–	+	++	+++	+++
	C. truncatum	–	–	+++	+++	+++	+++	+++
	D. teres	–	–	+++	+++	+++	+++	+++
	C. nicotianae	–	+++	++	++	+++	+++	++
	S. vesicarium	–	++	+++	++	+++	+++	–
Bacteria	*P. tolaasii*	–	–	+	–	–	+	–
	P. syringae pv tabaci	–	++	++	–	–	+	–
	P. syringae pv panici	–	++	++	–	–	+	–
	P. cariophilly	–	–	–	–	+	+	–
	P. syringae pv syringae	–	+	+	–	–	++	–
	P. syringae pv japonica	–	++	++	–	–	+	–
	P. syringae pv papulans	–	–	–	–	–	–	++

No inhibition (–), inhibitory zone <5 mm (+), inhibitory zone 5 mm (++), and inhibitory zone >5 mm (+++).

putative UviB-like bacteriocin, were found in strains *B. gibsonii* RHF15 (**Figure 7B**) and *B. amyloliquefaciens* RHFS18 (**7D-d.1**). Their precursor peptides share 42.1 and 33.4% similarity with UviB.

Finally, *Bacillus* sp. RHFS10 carries an orphan 28 genes BGC with a core biosynthetic gene encoding a 40-amino acids peptide sharing 35% of similarity with the competence pheromone of *B. subtilis 168*, a RiPP belonging to class I bacteriocins. *Bacillus* species are known to synthesize many well-studied bacteriocins, such as subtilin, ericin, paenibacillin, subtilosin, thuricin, and coagulin (Abriouel et al., 2011). Anyway, it is impossible to predict if the six compounds produced by strains *B. amyloliquefaciens* RHF6, and RHFS18, *B. gibsonii* RHF15 and *Bacillus* sp. RHFS10 actually have antimicrobial properties from genome sequence data only. Despite this, the antagonistic activity exerted by RHF6, RHF 15, RHFS10, and RHFS18 strains observed previously in *in vitro* assays (**Table 6**) could be associated with these potential compounds. This will need to be validated by further experiments.

CONCLUSION

In a historic moment in which the increasing population coupled with land degradation aggravates crop production, the use of plant growth promoting bacteria to ensure agricultural productivity has a huge impact on our society. These soil microorganisms enhance plant performance and represent an eco-friendly alternative to chemical fertilizers and pesticides (Hashem et al., 2019). When applied directly to the soil, PGPB enhance plant growth by different action mechanisms such as the production of different phytohormones, accelerating the mineralization of organic matter and improving the bioavailability of the nutrients, and protecting plants from pests' damages. The beneficial activity exerted by PGPB is in part mediated by a broad spectrum of secondary metabolites and enzymes. For example, polyamines, such as spermidine, play important physiological and protective roles in plants, resulting in an increase in biomass, altered root architecture, and elevated photosynthetic capacity. Until recently, these key metabolites were uncovered only by systematic investigation or by serendipity, often understating the PGPB potentiality during their screening. Many genes involved in PGB activity, in fact, could be silent under standard laboratory conditions, due to the absence of appropriate natural triggers or stress signals. More recently, the onset of the genomic era has facilitated the discovery of these ecologically important metabolites and novel strategies became available for PGPR characterization.

For example, genome mining allows to look over the whole genome of a PGPB strain and highlights genes encoding beneficial enzymes, involved in the enhancement of plant nutritional uptake or modulation of hormone levels, as well as for antimicrobial-encoding BGCs.

In this work, we have isolated soil halophilic *Bacilli* and performed their screening for PGP traits by using standard laboratory procedures and whole-genome analysis. *Bacilli* represent a significant fraction of the soil microbial community and some species are categorized as PGPB (Cazorla et al., 2007). They are also able to produce endospores, which besides enduring harsh environmental conditions fatal for other cell forms (Petrillo et al., 2020), permit easy formulation and storage of commercial PGPB-based products. In addition, salt-tolerant PGPB can easily withstand several abiotic stresses and ameliorate plant growth in degraded soil.

Seven *Bacillus* strains have been selected for *in vitro* PGP traits and identified at the species level by genome analysis. Based on genome mining, not only have we confirmed the beneficial activities PGP found by *in vitro* analysis, identifying the involved genes but also we have highlighted their strong potentiality by the discovery of novel biosynthesis gene clusters. Our results demonstrated that the genomic analyses, as genome mining, allow a full investigation of PGPB biosynthetic capacity for secondary metabolites and proteins and represent useful tools in the characterization of plant beneficial bacteria. Nevertheless, the divergences observed between the predicted biocontrol functions by found gene clusters and the results obtained by *in vitro* analysis, highlight the need of combining laboratory-assays and genome-mining in identification of new PGPB for future applications.

DATA AVAILABILITY STATEMENT

The datasets presented in this study can be found in online repositories. The names of the repository/repositories and accession number(s) can be found in the article/**Supplementary Material**.

AUTHOR CONTRIBUTIONS

RI: conceptualization, supervision, project administration, and funding acquisition. SC and CP: methodology. SC, CP, ML, and MS: validation and formal analysis. SC, CP, and DG: investigation. SC, CP, MS, AC, and RI: data curation. RI, SC, CP, and DG: writing original draft preparation. All authors have read and agreed to the published version of the manuscript.

ACKNOWLEDGMENTS

We thank Marcelo Anibal Carmona (Facultad de Agronomía, Cátedra de Fitopatología, Universidad de Buenos Aires, Buenos Aires, Argentina) for supplying the phytopathogenic fungi (*M. phaseolina*, *C. truncatum*, *C. nicotianae*, and *D. teres*) used in this study.

SUPPLEMENTARY MATERIAL

The Supplementary Material for this article can be found online at: https://www.frontiersin.org/articles/10.3389/fmicb.2021.715678/full#supplementary-material

REFERENCES

Abetouel, H., Franz, C. M. A. P., Ben Omar, N., and Gálvez, A. (2011). Diversity and applications of *Bacillus* bacteriocins. *FEMS Microbiol. Rev.* 35, 201–232. doi: 10.1111/j.1574-6976.2010.00244.x

Agrawal, A. A. (2001). Phenotypic plasticity in the interactions and evolution of species. *Science* 294, 321–326. doi: 10.1126/science.1060701

Ahmad, M., Zahir, Z. A., Khalid, M., Nazli, F., and Arshad, M. (2013). Efficacy of Rhizobium and *Pseudomonas* strains to improve physiology, ionic balance and quality of mung bean under salt-affected conditions on farmer's fields. *Plant Physiol. Biochem.* 63, 170–176. doi: 10.1016/j.plaphy.2012.11.024

Adler, J. (1966). Chemotaxis in Bacteria. *Science.* 153, 708–716. doi: 10.1126/science.153.3737.708

Amaya-Gómez, C. V., Porcel, M., Mesa-Garriga, L., and Gómez-Álvarez, M. I. (2020). A framework for the selection of plant growth-promoting rhizobacteria based on bacterial competence mechanisms. *Appl. Environ. Microbiol.* 86, e00760–e00820. doi: 10.1128/AEM.00760-20

Anwar, U. B., Zwar, I. P., and de Souza, A. O. (2020). "Chapter 12: Biomolecules produced by extremophiles microorganisms and recent discoveries," in *New and Future Developments in Microbial Biotechnology and Bioengineering*. ed. A. G. Rodrigues (Elsevier), 247–270.

Babalola, O. O. (2010). Beneficial bacteria of agricultural importance. *Biotechnol. Lett.* 32, 1559–1570. doi: 10.1007/s10529-010-0347-0

Blin, K., Shaw, S., Steinke, K., Villebro, R., Ziemert, N., Lee, S. Y., et al. (2019). antiSMASH 5.0: updates to the secondary metabolite genome mining pipeline. *Nucleic Acids Res.* 47, W81–W87. doi: 10.1093/nar/gkz310

Bolger, A. M., Lohse, M., and Usadel, B. (2014). Trimmomatic: a flexible trimmer for Illumina sequence data. *Bioinformatics* 30, 2114–2120. doi: 10.1093/bioinformatics/btu170

Bunsangtarn, S., Sakpuntoon, V., Srisuk, N., Ohashi, T., Fujiyama, K., and Limtong, S. (2019). Biosynthetic pathway of Indole-3-acetic acid in basidiomycetous yeast rhodosporidiobolus fluvialis. *Mycobiology* 47, 292–300. doi: 10.1080/12298093.2019.1638672

Cangiano, G., Mazzone, A., Baccigalupi, L., Isticato, R., Eichenberger, P., De Felice, M., et al. (2010). Direct and indirect control of late sporulation genes by GerR of *Bacillus subtilis*. *J. Bacteriol.* 192, 3406–3413. doi: 10.1128/JB.00329-10

Cangiano, G., Strec, T., Panarella, C., Isticato, R., Baccigalupi, L., De Felice, M., et al. (2014). The sps gene products affect the germination, hydrophobicity, and protein adsorption of *Bacillus subtilis* spores. *Appl. Environ. Microbiol.* 80, 7293–7302. doi: 10.1128/AEM.02893-14

Castaldi, S., Petrillo, C., Donadio, G., Piaz, F. D., Cimmino, A., Masi, M., et al. (2021). Plant growth promotion function of *Bacillus* sp. strains isolated from salt-pan rhizosphere and their biocontrol potential against macrophomina phaseolina. *Int. J. Mol. Sci.* 22:3324. doi: 10.3390/ijms22073324

Caulier, S., Nannan, C., Gillis, A., Licciardi, F., Bragard, C., and Mahillon, J. (2019). Overview of the antimicrobial compounds produced by members of the *Bacillus subtilis* group. *Front. Microbiol.* 10:302. doi: 10.3389/fmicb.2019.00302

Cazorla, F. M., Romero, D., Pérez-García, A., Lugtenberg, B. J. J., de Vicente, A., and Bloemberg, G. (2007). Isolation and characterization of antagonistic *Bacillus subtilis* strains from the avocado rhizoplane displaying biocontrol activity. *J. Appl. Microbiol.* 103, 1950–1959. doi: 10.1111/j.1365-2672.2007.03433.x

Celandroni, F., Vecchione, A., Cara, A., Mazzantini, D., Lupetti, A., and Ghelardi, E. (2019). Identification of *Bacillus* species: implication on the quality of probiotic formulations. *PLoS One* 14:e0217021. doi: 10.1371/journal.pone.0217021

Cotter, P. D., Ross, R. P., and Hill, C. (2013). Bacteriocins: a viable alternative to antibiotics? *Nat. Rev. Microbiol.* 11, 95–105. doi: 10.1038/nrmicro2937

Corrado, I., Petrillo, C., Isticato, R., Castillo, A., Corsaro, M. M., Sannia, G., et al. (2021). The power of two: An artificial microbial consortium for the conversion of inulin into Polyhydroxyalkanoates. *Int. J. Biol. Macromol.* 189, 494–502. doi: 10.1016/j.ijbiomac.2021.08.123

Damodaran, T., Sah, V., Rai, R. B., Sharma, D. K., Mishra, V. K., Jha, S. K., et al. (2013). Isolation of salt tolerant endophytic and rhizospheric bacteria by natural selection and screening for promising plant growth-promoting rhizobacteria (PGPR) and growth vigour in tomato under sodic environment. *Afr. J. Microbiol. Res.* 7, 5082–5089. doi: 10.5897/AJMR2013.6003

Desai, N. C., Makwana, A. H., and Rajpara, K. M. (2016). Synthesis and study of 1,3,5-triazine based thiazole derivatives as antimicrobial agents. *J. Saudi Chem. Soc.* 20, S334–S341. doi: 10.1016/j.jscs.2012.12.004

Eren, A. M., Kiefl, E., Shaiber, A., Veseli, I., Miller, S. E., Schechter, M. S., et al. (2021). Community-led, integrated, reproducible multi-omics with anvi'o. *Microbiol.* 6, 3–6. doi: 10.1038/s41564-020-00834-3

Etesami, H., Mirsyed Hosseini, H., Alikhani, H. A., and Mohammadi, L. (2014). Bacterial biosynthesis of 1-aminocyclopropane-1-carboxylate (ACC) deaminase and indole-3-acetic acid (IAA) as endophytic preferential selection traits by rice plant seedlings. *J. Plant Growth Regul.* 33, 654–670. doi: 10.1007/s00344-014-9415-3

Garnier, T., and Cole, S. T. (1988). Complete nucleotide sequence and genetic organization of the bacteriocinogenic plasmid, pIP404, from *Clostridium perfringens*. *Plasmid* 19, 134–150. doi: 10.1016/0147-619X(88)90052-2

Gigilo, R., Fani, R., Isticato, R., De Felice, M., Ricca, E., and Baccigalupi, L. (2011). Organization and evolution of the cotG and cotH genes of *Bacillus subtilis*. *J. Bacteriol.* 193, 6664–6673. doi: 10.1128/JB.06121-11

Glick, B. R., Cheng, Z., Czarny, J., and Duan, J. (2007). Promotion of plant growth by ACC deaminase-producing soil bacteria. *Eur. J. Plant Pathol.* 119, 329–339. doi: 10.1007/s10658-007-9162-4

Goberna, M., García, C., and Verdú, M. (2014). A role for biotic filtering in driving phylogenetic clustering in soil bacterial communities. *Glob. Ecol. Biogeogr.* 23, 1346–1355. doi: 10.1111/geb.12227

Gordon, S. A., and Weber, R. P. (1951). Colorimetric estimation of indoleacetic acid. *Plant Physiol.* 26, 192–195. doi: 10.1104/pp.26.1.192

Gupta, S., and Pandey, S. (2019). ACC deaminase producing bacteria with multifarious plant growth promoting traits alleviates salinity stress in french bean (*Phaseolus vulgaris*) plants. *Front. Microbiol.* 10:1506. doi: 10.3389/fmicb.2019.01506

Hashem, A., Tabassum, B., and Fathi Abd Allah, E. (2019). *Bacillus subtilis*: a plant-growth promoting rhizobacterium that also impacts biotic stress. *Saudi J. Biol. Sci.* 26, 1291–1297. doi: 10.1016/j.sjbs.2019.05.004

Hassan, A. H. A., Alkhalifah, D. H. M., Al Yousef, S. A., Beemster, G. T. S., Mousa, A. S. M., Hozzein, W. N., et al. (2020). Salinity stress enhances the antioxidant capacity of *Bacillus* and *Planococcus* species isolated from saline lake environment. *Front. Microbiol.* 11:561816. doi: 10.3389/fmicb.2020.561816

Hortal, J., Carrascal, L., Triantis, K., Thébault, E., and Meiri, S. (2013). Species richness can decrease with altitude but not with habitat diversity. *Proc. Natl. Acad. Sci. U. S. A.* 110, E2149–E2150. doi: 10.1073/pnas.1301663110

Jack, R. W., Tagg, J. R., and Ray, B. (1995). Bacteriocins of gram-positive bacteria. *Microbiol. Rev.* 59, 171–200. doi: 10.1128/mr.59.2.171-200.1995

Jadhav, H., Shaikh, S., and Sayyed, R. (2017). "Role of hydrolytic enzymes of rhizoflora in biocontrol of fungal phytopathogens: an overview," in *Rhizotrophs: Plant Growth Promotion to Bioremediation*. ed. S. Mehnaz (Singapore: Springer Singapore) 183–203.

Jain, C., Rodriguez-R, L. M., Phillippy, A. M., Konstantinidis, K. T., and Aluru, S. (2018). High throughput ANI analysis of 90K prokaryotic genomes reveals clear species boundaries. *Nat. Commun.* 9:5114. doi: 10.1038/s41467-018-07641-9

Jamali, H., Sharma, A., Roohi, and Srivastava, A. K. (2020). Biocontrol potential of *Bacillus subtilis* RH5 against sheath blight of rice caused by Rhizoctonia solani. *J. Basic Microbiol.* 60, 268–280. doi: 10.1002/jobm.201900347

Keswani, C., Singh, H. B., García-Estrada, C., Caradus, J., He, Y.-W., Mezaache-Aichour, S., et al. (2020). Antimicrobial secondary metabolites from agriculturally important bacteria as next-generation pesticides. *Appl. Microbiol. Biotechnol.* 104, 1013–1034. doi: 10.1007/s00253-019-10300-8

Kumar, A., Prakash, A., and Johri, B. (2011). "Bacillus as PGPR in crop ecosystem," in *Bacteria in Agrobiology: Crop Ecosystems* (Springer Berlin Heidelberg), 37–59.

Li, Z., Chakraborty, P., de Vries, R. H., Song, C., Zhao, X., Roelfes, G., et al. (2020). Characterization of two relacidines belonging to a novel class of circular lipopeptides that act against gram-negative bacterial pathogens. *Environ. Microbiol.* 22, 5125–5136. doi: 10.1111/1462-2920.15145

Lugtenberg, B., and Kamilova, F. (2009). Plant-growth-promoting rhizobacteria. *Annu. Rev. Microbiol.* 63, 541–556. doi: 10.1146/annurev.micro.62.081307.162918

O'Toole, G. A. (2011). Microtiter dish biofilm formation assay. *J. Vis. Exp.* 30:2437. doi: 10.3791/2437

Okada, M., Sato, I., Cho, S. J., Iwata, H., Nishio, T., Dubnau, D., et al. (2005). Structure of the *Bacillus subtilis* quorum-sensing peptide pheromone ComX. *Nat. Chem. Biol.* 1, 23–24. doi: 10.1038/nchembio709

Ongena, M., and Jacques, P. (2008). Bacillus lipopeptides: versatile weapons for plant disease biocontrol. *Trends Microbiol.* 16, 115–125. doi: 10.1016/j.tim.2007.12.009

Pal, K. K., and McSpadden Gardener, B. (2006). Biological control of plant pathogens. *Plant Health Instr.* 2, 1117-1142. doi: 10.1094/PHI-A-2006-1117-02

Pérez-Miranda, S., Cabirol, N., George-Téllez, R., Zamudio-Rivera, L. S., and Fernández, F. J. (2007). O-CAS, a fast and universal method for siderophore detection. *J. Microbiol. Methods* 70, 127–131. doi: 10.1016/j.mimet.2007.03.023

Pertot, I., Caffi, T., Rossi, V., Mugnai, L., Hoffmann, C., Grando, M. S., et al. (2017). A critical review of plant protection tools for reducing pesticide use on grapevine and new perspectives for the implementation of IPM in viticulture. *Crop Prot.* 97, 70–84. doi: 10.1016/j.cropro.2016.11.025

Pesce, G., Rusciano, G., Sasso, A., Isticato, R., Strec, T., and Ricca, E. (2014). Surface charge and hydrodynamic coefficient measurements of *Bacillus subtilis* spore by optical tweezers. *Colloids Surf. B Biointerfaces* 116, 568–575. doi: 10.1016/j.colsurfb.2014.01.039

Petrillo, C., Castaldi, S., Lanzilli, M., Saggese, A., Donadio, G., Baccigalupi, L., et al. (2020). The temperature of growth and sporulation modulates the efficiency of spore-display in *Bacillus subtilis*. *Microb. Cell Factories* 19:185. doi: 10.1186/s12934-020-01446-6

Pieterse, C. M. J., Zamioudis, C., Berendsen, R. L., Weller, D. M., Van Wees, S. C. M., and Bakker, P. A. H. M. (2014). Induced systemic resistance by beneficial microbes. *Annu. Rev. Phytopathol.* 52, 347–375. doi: 10.1146/annurev-phyto-082712-102340

Pikovskaya, R. I. (1948). Mobilization of phosphorus in soil in connection with the vital activity of some microbial species. *Mikrobiologiya* 17, 362–370.

Reddy, K. R. N., Reddy, C. S., and Muralidharan, K. (2009). Potential of botanical and biocontrol agents on growth and aflatoxin production by Aspergillus flavus infecting rice grains. *Food Control* 20, 173–178. doi: 10.1016/j.foodcont.2008.03.009

Rodríguez-Echeverría, S., Lozano, Y. M., and Bardgett, R. D. (2016). Influence of soil microbiota in nurse plant systems. *Funct. Ecol.* 30, 30–40. doi: 10.1111/1365-2435.12594

Rooney, A. P., Price, N. P. J., Ehrhardt, C., Swezey, J. L., and Bannan, J. D. (2009). Phylogeny and molecular taxonomy of the *Bacillus subtilis* species complex and description of *Bacillus subtilis* subsp. inaquosorum subsp. nov. *Int. J. Syst. Evol. Microbiol.* 59, 2429–2436. doi: 10.1099/ijs.0.009126-0

Schiraldi, C., and De Rosa, M. (2016). "Mesophilic organisms," in *Encyclopedia of Membranes*. eds. E. Drioli and L. Giorno (Berlin, Heidelberg: Springer Berlin Heidelberg), 1–2.

Schoebitz, M., Ceballos, C., and Ciampi, L. (2013). Effect of immobilized phosphate solubilizing bacteria on wheat growth and phosphate uptake. *J. Soil Sci. Plant Nutr.* 13, 1–10. doi: 10.4067/S0718-95162013005000001

Seemann, T. (2014). Prokka: rapid prokaryotic genome annotation. *Bioinformatics* 30, 2068–2069. doi: 10.1093/bioinformatics/btu153

Selvakumar, G., Sushil, S. N., Stanley, J., Mohan, M., Deol, A., Rai, D., et al. (2011). Brevibacterium frigoritolerans a novel entomopathogen of Anomala dimidiata and Holotrichia longipennis (Scarabaeidae: Coleoptera). *Biocontrol Sci. Tech.* 21, 821–827. doi: 10.1080/09583157.2011.586021

Shultana, R., Kee Zuan, A. T., Yusop, M. R., and Saud, H. M. (2020). Characterization of salt-tolerant plant growth-promoting rhizobacteria and the effect on growth and yield of saline-affected rice. *PLoS One* 15:e0238537. doi: 10.1371/journal.pone.0238537

Sitbon, F., Astot, C., Edlund, A., Crozier, A., and Sandberg, G. (2000). The relative importance of tryptophan-dependent and tryptophan-independent biosynthesis of indole-3-acetic acid in tobacco during vegetative growth. *Planta* 211, 715–721. doi: 10.1007/s004250000338

van Heel, A. J., de Jong, A., Song, C., Viel, J. H., Kok, J., and Kuipers, O. P. (2018). BAGEL4: a user-friendly web server to thoroughly mine RiPPs and bacteriocins. *Nucleic Acids Res.* 46, W278–W281. doi: 10.1093/nar/gky383

Ventosa, A., Nieto, J. J., and Oren, A. (1998). Biology of moderately halophilic aerobic bacteria. *Microbiol. Mol. Biol. Rev.* 62, 504–544. doi: 10.1128/MMBR.62.2.504-544.1998

Xie, S.-S., Wu, H.-J., Zang, H.-Y., Wu, L.-M., Zhu, Q.-Q., and Gao, X.-W. (2014). Plant growth promotion by spermidine-producing *Bacillus subtilis* OKB105. *Mol. Plant-Microbe Interact.* 27, 655–663. doi: 10.1094/MPMI-01-14-0010-R

Xu, S. J., and Kim, B. S. (2014). Biocontrol of fusarium crown and root rot and promotion of growth of tomato by paenibacillus strains isolated from soil. *Mycobiology* 42, 158–166. doi: 10.5941/MYCO.2014.42.2.158

Yoon, S.-H., Ha, S.-M., Lim, J., Kwon, S., and Chun, J. (2017). A large-scale evaluation of algorithms to calculate average nucleotide identity. *Antonie Van Leeuwenhoek* 110, 1281–1286. doi: 10.1007/s10482-017-0844-4

Zhao, X., and Kuipers, O. P. (2016). Identification and classification of known and putative antimicrobial compounds produced by a wide variety of Bacillales species. *BMC Genomics* 17:882. doi: 10.1186/s12864-016-3224-y

Conflict of Interest: The authors declare that the research was conducted in the absence of any commercial or financial relationships that could be construed as a potential conflict of interest.

CHAPTER IX: Heavy Metal-Tolerant PGPR strains and amelioration the growth of in wheat plants in Copper contamination soil.

During the period spent in the foreign laboratory at Helmholtz Center for Environmental Research - UFZ (Germany) under the direct supervision of Dr. Thomas Reitz, I have analyzed if the inoculation of some of 7 Bacilli, previously selected and studied in Petrillo and Castaldi et al. 2021, can be used as phytoremediation of heavy-metal-contaminated soils.

9.1 Introduction

Heavy metals (Zn, Zinc; Ni, Nikel; Co, Cobalt; Cu, Copper and, Cd, cadmium) have been widely distributed and a prominent apprehension for sustainable agriculture and human welfare (Rizwan et al., 2016). They have been discharged into the environment through anthropogenic activities such as fertilizers, industrial wastes, pesticides, mining, sewage etc. (Zhang et al., 2015). Many of these metals act as vital nutrients for plant growth under optimal concentrations but when they exceed their optimal limits, they tend to be toxic in nature (Gall et al., 2015). There is undoubtedly an urgent need to promote crop productivities by eliminating the metal toxicities from the food chain.
Among these, Cu is an essential micronutrient required in small amounts for normal plant activity. Currently, Cu pollution in agricultural soils, due to arbitrary use of pesticides, fungicides, industrial effluent, and wastewater irrigation, presents a major concern for sustainable agri-food production, especially in developing countries (Adrees et al., 2015). Plants, in general, are very sensitive to Cu toxicity, displaying metabolic disturbances and growth inhibition at Cu contents in the tissues only slightly higher than the normal levels. Excess Cu inhibits a large number of enzymes and interferes with several aspects of plant biochemistry, including photosynthesis, pigment synthesis, and membrane integrity. The most important effect is associated with the blocking of photosynthetic electron transport, leading to the production of radicals which start peroxidative chain reactions involving membrane lipids (Adrees et al., 2015).

Metal immobilizing and metal-resistant plant growth-promoting rhizobacteria (PGPR) have recently been studied to stimulate growth and reduce the bioavailability of heavy metals and their accumulation within plants (Wang et al., 2018). Metal resistant and growth-promoting bacteria provide resistance to plants in metal-polluted sites by the production of plant hormones such as indole-3-acetic acid (IAA), gibberellins etc. They also lead to the production of solubilizing phosphates, siderophores, and 1-aminocyclopropane-1 -carboxylate (ACC) - deaminase that promotes the plant growth and defense properties and reduces the translocation of heavy metals within the plant tissues (Chandra et al., 2018). The objective of the present study was to explore the role of 7 halophilic *Bacilli* (*Bacillus subtilis* RHF2, *Bacillus amyloliquefaciens* RHF6, *Bacillus halotolerans* RHF12, *Bacillus gibsonii* RHF15, *Bacillus frigoritolerans* RHFB, *Bacillus spp.* RHF10, and *Bacillus amyloliquefaciens* RHFS18) were previously characterized and identified as promising plant growth-promoting bacteria PGPBs in Petrillo and Castaldi et al. 2021, if they improve the wheat plant growth in Cu-contaminated soil with *in vivo* experiments.

9.2 Methods

9.2.1 Determination of Heavy Metal Tolerance

The heavy metal resistance of 7 *Bacilli* isolates was measured as described by Xiumei et al, 2014 with some modifications. Bacteria were grown in LB broth a 37 °C up to the exponential phase (~0.8 OD/mL). 150 µL of bacterial cultures (10^8 cells/mL) were inoculated into 15 mL of 0.7% LB agar and left to solidify in a Petri dish. $ZnSO_4$ x 7 H_2O, $CdCl_2$, $CuSO_4$ x 5 H_2O, $CoSO_4$ x 7 H_2O and $(NH_4)_2Ni(SO_4)_2$ x 6 H_2O were added to the medium with spot-inoculating 5 µL at different final concentrations (from 0.1mM to 50 mM). After incubation at 28°C for 3 days, the minimum inhibitory concentration (MIC) was defined as the lowest concentration of metal salt inhibiting bacterial growth.

9.2.2 Detection of the heavy metal resistance genes (HMRGs) in *Bacilli* strains

Genes involved in heavy metal resistance in 7 *Bacilli* genomes were identified by performing BLASTP searches against the BacMet

database (Pal et al., 2014), which contains genes with experimentally confirmed metal resistance functions.

9.2.3 *In vivo* assays: wheat Inoculation

To evaluate the efficacy of select *Bacilli* a pot experiment was conducted in greenhouse with growing conditions: at 23°C in photoperiodic conditions (16 h light and 8 h darkness) for 30 days.
The wheat seeds (common wheat (Weichweizen) variety "Quintus", unstained seeds (ungebeizt)) were surface sterilized by washing with 70% ethanol for 1 min followed by three washings with sterile distilled water. Thereafter, the seeds were treated with 1.5% sodium hypochlorite (NaOCl) solution for 5 min followed by six times of successive washings in sterile water to remove all traces of the disinfectant (Rudolph et al., 2015).
Three select bacteria for inoculation of the plants were grown separately in LB broth at 30 ± 2 °C overnight. The cultures were centrifuged at 5000 rpm for 10 min and the pellets were washed three times with sterile distilled water and resuspended in a final concentration of $1x10^7$ cfu/mL.
Then, the seeds were inoculated with three different strains and with a consortium of the three same select bacteria at room temperature overnight in a sterile hood. Seeds inoculated with sterile distilled water were used as a control.
Three wheat seeds equally spaced were sown in each plastic pot containing 1 kg soil (Albic Luvisol from Thyrow Research Station).
Before sowing the seeds, the soil was treated with 7mM of $CuSO_4$ x 5 H_2O and as control with 7mM of $MgSO_4$ dissolved in 2L of water and spray in soil.
The weight of each pot was marked and finally re-marked to check the water evaporation. The experiment was carried out with three replicates of each treatment in a completely randomized design (CRD). The plants were collected for further analysis at 30 days after sowing (DAS).

9.2.4 Growth Parameters

Wheat plants were carefully harvested from the soil at the end of the experiment. To remove the debris from the root surface, plant roots were cleaned with deionized water. Plant shoot length, root length and fresh were observed using a digital balance. All plant

parts were dried at 70 °C for the determination of the dry biomass until a constant weight was achieved.

9.2.5 Evaluation of Heavy metal tolerance index

Heavy metal tolerance index was calculated using method of Khanna et al., 2019. For this, dry weights of seedling samples were taken and tolerance index was calculated using the formula given below:

$$\%\text{Heavy metal tolerance index} = \frac{\text{Dry weight of Treated Plants}}{\text{Dry weights of Untreated plants (CN)}} x100$$

9.2.6 Statistical analysis

All the statistical analyses were performed using GraphPad Prism 8 software. Data were expressed as mean ± SEM. Differences among groups were compared by ANOVA or t-test as indicated in figure legends. Differences were considered statistically significant at $p < 0.05$.

9.3 Result and discussion

9.3.1 Heavy metal tolerance

The seven bacterial strains used in this study were isolated from the salt-pan sand and the rhizosphere of *Juniperus sabina* in the National Park of Ses Salines d'Eivissa, Formentera (Spain).
These bacteria were selected from the collection of 43 isolates, for their high potentiality as biofertilizers and biocontrol agents emerged with *in vitro* experiments and with genomic analysis (Petrillo and Castaldi et al., 2021). In this study, were further analyzed for heavy metal tolerance (Zn, Cd, Cu, Co, and Ni). Initial screening to detect the minimum inhibitory concentration (MIC) of five representative metals demonstrated that all bacteria are more resistant to Cu, Co and, Ni with mM between 10 and 15. Only the strain RHFS18 showed the highest (MIC) level against Cu, up to 18mM.
However, bacteria not shown the same tolerance for Zn and Cd with MIC between 0.1 and 5 mM (Table 1).

Table 1: Minimum inhibitory concentrations (MICs) of bacterial isolates against five heavy metals.

Strains	Zn (mM)	Cd (mM)	Cu (mM)	Co (mM)	Ni (mM)
B. subtilis RHF2	1	0.2	10	1	10
B. amyloliquefaciens RHF6	1	0.2	10	10	12
B. vallismortis RHFS10	5	0.2	12	10	10
B. halolerans RHF12	2	0.2	10	5	12
B. gibsonii RHF15	4	0.2	15	15	10
B. amyloliquefaciens RHFS18	3	0.1	18	12	10
B. frigoritolerans RHFB	3	0.1	10	12	12

Zn, zinc; Cd, cadmium; Cu, copper; Co, cobalt; Ni, nickel.

9.3.2 Genes and proteins involved in heavy metals tolerance

To confirm the *in vitro* characterization of the isolates, a prediction of the genes and proteins (Table 2) involved in heavy metal resistance activity was performed present in the proteome of selected bacteria. As expected, the genome of all selected *Bacilli* strains contained multiple genes involved in heavy metals resistance. Only in Ni and Co metals bacteria present lew resistance genes, except the strain RHFB. This suggests that the bacteria use other strategies to increase the resistance, such as chelation or the precipitation of toxic metals.

Table 2: Heavy metals associated proteins identified in the proteome of the selected strains.

Metals	Protein	RHFS2	RHF6	RHF12	RHF15	RHFB	RHFS10	RHFS18
	Copper-sensing transcriptional repressor *CsoR*	x	x	x	x	x	x	x
	Copper chaperone *CopZ*	x	x	x	x	x	x	x
Cu	Copper-exporting P-type ATPase	x	x	x	x	x	x	x
	Copper transport protein *YcnJ*	x	x	x	x	x	x	x
	Transcriptional activator protein *CopR*	x	-	x	x	x	x	x
	Copper homeostasis protein *CutC*	-	-	-	-	x	-	-
	Copper methylamine oxidase	-	-	-	-	x	-	-
	Nickel transport system permease protein *NikC*	-	-	-	-	x	x	-
Ni	Nickel transport system permease protein *NikB*	-	-	-	-	x	x	-
	Nickel-binding periplasmic protein	-	-	-	-	x	x	-
	Pyridinium-3,5-bisthiocarboxylic acid mononucleotide nickel insertion protein	-	-	-	-	x	-	-
	Zinc-type alcohol dehydrogenase-like protein SA1988	-	-	-	-	x	x	-
	zinc-specific metallo-regulatory protein	-	-	x	-		x	x
	Probable polyketide biosynthesis zinc-dependent hydrolase *PksB*	x	x	-	x	x	x	x
	Uncharacterized zinc protease Rv2782c	-	x	x	x	x	x	x
	Cadmium, cobalt and zinc/H(+)-K(+) antiporter	x	x	x	x	x	x	x
	Putative peptide zinc metalloprotease protein *YydH*	-	-	-	-	-	x	-
	Putative zinc protease *AlbF*	x	-	x	x	-	x	-
	Cadmium, zinc and cobalt-transporting ATPase	-	x	x	x	-	x	x
	Zinc-dependent sulfurtransferase *SufU*	-	x	x	x	-	x	-
	High-affinity zinc uptake system binding-protein *ZnuA*	x	x	x	x	x	x	x
Zn	High-affinity zinc uptake system ATP-binding protein *ZnuC*	x	x	x	x	x	x	x
	High-affinity zinc uptake system membrane protein *ZnuB*	x	x	x	x	x	x	x
	Zinc-dependent sulfurtransferase *SufU*	x		x	-	x	-	x
	Probable zinc-binding alcohol dehydrogenase Rv1895	x	x	x	x	x	x	x
	Periplasmic zinc-binding protein *TroA*	x	x	x	x	x	x	-
	Uncharacterized zinc-type alcohol dehydrogenase-like protein *YjmD*	x	x	x	x	x	-	x
	ATP-dependent zinc metalloprotease *FtsH*	x	x	x	x	x	x	-
	Zinc-transporting ATPase	x	x	x	x	-	-	x
	Zinc-specific metallo-regulatory protein	x	x	-	x	x	x	-
	Putative peptide zinc metalloprotease protein *YydH*	x	-	-	-		-	-
	Zinc transporter *ZitB*	-	-	-	-	x	-	-
	Zinc transporter *ZupT*	-	-	-	-	x	-	-
	Cadmium-transporting ATPase	-	-	-	-	-	x	-
	Cadmium, cobalt and zinc/H(+)-K(+) antiporter	x	x	x	x	x	x	x
Cd	Cadmium, zinc and cobalt-transporting ATPase	x	x	x	x	x	x	x
	Cadmium-induced protein *CadI*	x	-	-	x	-	-	-
	Cadmium resistance transcriptional regulatory protein *CadC*	-	-	-	-	-	-	-
	Cadmium, cobalt and zinc/H(+)-K(+) antiporter	x	x	x	x	x	x	x
	Cadmium, zinc and cobalt-transporting ATPase	x	x	x	x	-	x	x
	Cobalt/magnesium transport protein *CorA*	x	x	x	x	x	x	x
Co	Cobalt transport protein *CbiQ*	-	-	-	-	x	-	-
	Cobalt transport protein *CbiN*	-	-	-	-	x	-	-
	Cobalt transport protein *CbiM*	-	-	-	-	x	-	-
	Cobalt-factor III methyltransferase	-	-	-	-	x	-	-
	Cobalt-precorrin-6A reductase	-	-	-	-	x	-	-
	Cobalt-precorrin-8 methylmutase	-	-	-	-	x	-	-
	Cobalt-precorrin-5B C(1)-methyltransferase	-	-	-	-	x	-	-
	Cobalt-precorrin-2 C(20)-methyltransferase	-	-	-	-	x	-	-
	Cobalt-precorrin-4 C(11)-methyltransferase	-	-	-	-	x	-	-
	Cobalt-precorrin-5A hydrolase	-	-	-	-	x	-	-

The strains RHFS10, RHF15 and, RHFS18 were chosen for subsequently *in vivo* experiments to test their ability to improve the wheat plants grown in Cu-contaminated soil.

These bacteria have shown the best capability to tolerate Cu and other metals such as Zn and Co. Moreover, in precedent studies reported in Petrillo and Castaldi et al., 2021 and Castaldi et al., 2021, these bacteria have shown a strong biocontrol activity against different phytopathogenic fungi and promising biofertilizer activities.

9.3.3 Bacteria inoculation effects on wheat plant growth in Cu-contaminated soil

The wheat plant was used to estimate plant growth and biomass after 30 days of the experiment. The results showed that in stress and non-stress conditions, wheat plants inoculated with the select bacteria showed a one-fold higher plant development than the uninoculated controls. In control, the inoculation of three bacteria and the consortium of all bacteria increased the shoot length by about 50% (Figure 1-a), but in the root length, only the strain RHF15 has shown the best activity, enhancing the growth by 20% (Figure 1-b). In addition, fresh shoot weight and dry were enhanced by 60% (Figure 2 c-d) with bacteria inoculation. A different result was obtained into roots dry weight. All bacteria and the consortium have improved the weight by about 50% compared to the control but, with the inoculation of the RHFS10 strain are increased by 60%. As shown in figure 2, during the stress condition all parameters were drastically decreased compared to the control without heavy-metal stress (Figure 1 a-e). However, the inoculation of bacteria strains has increased the growth of plants by about 10% compared with control. Significantly, the inoculation of RHFS10 and RHFS15 strains resulted positive respect for the strain RHFS18 and consortium. These strains have improved plant growth by about 25 % in all parameters tested.

Figure 1: Effects of *B. vallismortis* RHFS10, *B. gibsonii* RHF15, *B. amyloliquefaciens* RHFS18 and consortium, in the shoot length (a) and root length (b), fresh shoot weight (c), and dry shoot weight (d) and root (e) of wheat plants in non-contaminated and contaminated soil with Cu. Nt: not treated with metal. Each value is the mean of replicates (n = 3). ± S.D (standard deviation) with a *p*-value ≤ 0.01.

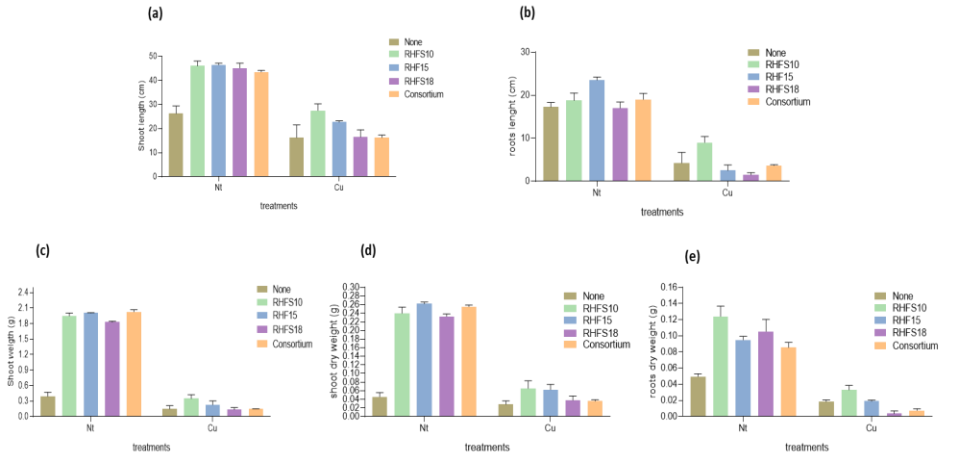

9.3.4 Heavy metal tolerance Index

Finally, the heavy metal tolerance index was observed to be lowered from 100% in control seedlings to 40% in 7 mM Cu stressed plants. An elevation in the tolerance index was recorded by 80% when Cd-stressed seedlings were amended with RHFS10 and RHF15 strain respectively and by 20% with inoculation by RHFS18 and consortium, respectively (Figure 2).

Figure 2: Heavy metal tolerance index in 30-days old wheat plant under Cu stress.

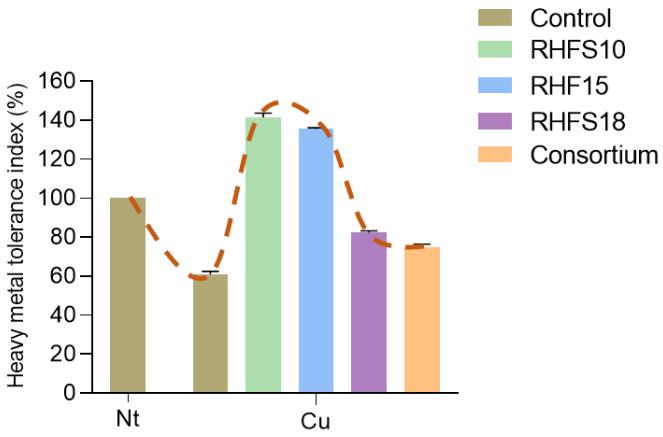

Data are presented as means of 3 replicates ± S.D (standard deviation) with a *p*-value ≤ 0.01. Nt: Untreated with Cu.

9.4 Conclusion

Crop production is a challenging issue to feed the increasing population due to biotic and abiotic stresses and uncertainty of climatic optima. Among abiotic stresses, Cu toxicity is also an important constraint limiting crop productivity worldwide. Cu is an essential element for plants at low levels, but in excess, it is phytotoxic at morphological, physiological, biochemical, and molecular levels. Cu interferes with various metabolic processes that are vital for plant growth and development.

Numerous studies reported the Cu induced growth inhibition, oxidative damage and antioxidant response in agricultural food crops such as wheat, rice, maize, sunflower and cucumber.

In this work, it's tested 7 halophilic Bacilli, previously characterized as a promising PGPB, in the tolerance at different concentrations of heavy metals. Three strains (RHFS10, RHF15 and, RHFS18) and a consortium of all three were selected for *in vivo* experiments in a wheat plants grown in Cu-contaminated soil.

These bacteria have shown an interesting biofertilizer activity in wheat plants grown without stress conditions. However, in soil Cu-contamination, preliminary studies suggest that the strain RHFS10 and RHF15 significantly increase the root and shoot length and weight of plants grown in stress conditions compared with the RHFS18 strain and the consortium. Certainly, further investigations are needed to confirm the data but, these results propose that the two PGPB can alter the toxicity of metals on the wheat plant and makes these strains excellent candidates for the enhanced restoration of contaminated soils through bacterial-assisted phytoremediation. The phytoremediation process is eco-friendly and could be used to reclaim the industrial soil from contaminants.

9.5 References

Muhammad R., Shafaqat A., Hina R., Jörg R., Daniel C. W. T., Erik M., Yong S O. & Wajid I. Phytomanagement of heavy metals in contaminated soils using sunflower: *A review, Critical Reviews in Env. Sci. and Techn.* , 2016, 18, 1498-1528. DOI: 10.1080/10643389.2016.1248199.

Zhaoyong Z., Li J., Zulpiya M., Ye Q. F. Sources identification and pollution evaluation of heavy metals in the surface sediments of

Bortala River, Northwest China. *Ecotoxicol. Environ. Saf*., 2016, 126, 94-101. DOI: 10.1016/j.ecoenv.2015.12.025.

Gall J. E., Boyd R. S., & Rajakaruna N. Transfer of heavy metals through terrestrial food webs: a review. *Environ. Monit. Assess.* 187, 201 (2015).

Adrees M, Ali S, Rizwan M, Zia-Ur-Rehman M, Ibrahim M, Abbas F, Farid M, Qayyum MF, Irshad MK. Mechanisms of silicon-mediated alleviation of heavy metal toxicity in plants: *A review. Ecotoxicol Environ Saf.* 2015, *119,* 186-97. DOI: 10.1016/j.ecoenv.2015.05.011.

Wang Q., Zhang W. J., He L. Y. & Sheng X. F. Increased biomass and quality and reduced heavy metal accumulation of edible tissues of vegetables in the presence of Cd-tolerant and immobilizing *Bacillus megaterium* H3. *Ecotoxicol. Environ.* 2018, 148, 269–274. DOI:10.1016/j.ecoenv.2017.10.036.

10.1371/journal.pone.0106618.

Chandra R., Kumar V., Tripathi S., Sharma P. Heavy metal phytoextraction potential of native weeds and grasses from endocrine-disrupting chemicals rich complex distillery sludge and their histological observations during in-situ phytoremediation. *Ecol. Eng.* 2018; 111, 143–156.

Petrillo C., Castaldi S., Lanzilli M., Selci M., Cordone A., Giovannelli D., Isticato R. Genomic and Physiological Characterization of Bacilli Isolated From Salt-Pans With Plant Growth Promoting Features. *Front Microbiol*. 2021, 13, 12-715678. DOI: 10.3389/fmicb.2021.715678.

Yu X., Li Y., Zhang C., Liu H., Liu J., Zheng W., Kang X., Leng X., Zhao K., Gu Y., Zhang X., Xiang Q., Chen Q. Culturable heavy metal-resistant and plant growth promoting bacteria in V-Ti magnetite mine tailing soil from Panzhihua, China. *PLoS One*. 2014, 4, 9-:e106618. DOI:

Pal C., Bengtsson-Palme J., Rensing C., Kristiansson E., Larsson D.G.J. BacMet: antibacterial biocide and metal resistance genes database. *Nucleic Acids Res*, 2014, *42,* 737–D743. DOI:10.1093/nar/gkt1252.

Rudolph N., Labuschagne, N., and Aveling T.A.S. The effect of plant growth promoting rhizobacteria on seed germination and seedling growth of maize. *Seed Sci. & Technol*, 2015, 43, 1-12. DOI: 10.15258/sst.2015.43.3.04.

Khanna K., Jamwal V.L., Gandhi S.G. Metal resistant PGPR lowered Cd uptake and expression of metal transporter genes with

improved growth and photosynthetic pigments in *Lycopersicon esculentum* under metal toxicity. *Sci Rep*, 2019, 9, 5855. DOI:10.1038/s41598-019-41899-3.

Castaldi S., Petrillo C., Donadio G., Piaz F.D., Cimmino A., Masi M., Evidente A., Isticato R. Plant Growth Promotion Function of *Bacillus* sp. Strains Isolated from Salt-Pan Rhizosphere and Their Biocontrol Potential against *Macrophomina phaseolina*. *Int J Mol Sci*., 2021, *24*, 3324. DOI: 10.3390/ijms22073324.

CHAPTER X: CONCLUSION

The increasing amount of chemical pollutants in soil via excessive use of synthetic chemical fertilizers and pesticides cause environmental damage with potential risks to human health.
To sustainable agriculture, crops produced need to be equipped with disease resistance, salt tolerance, heavy metal stress tolerance, and better nutritional value.
To fulfill the above-desired crop properties, one possibility is to use soil microorganisms such as bacteria, fungi, algae, etc., that increase the nutrient uptake capacity, water use efficiency, and crop protection (Armada et al., 2014).
The plant growth-promoting rhizobacteria (PGPR) are the most promising soil microorganisms. They can enhance health and plant growth without environmental contamination (Calvo et al., 2014).
Nowadays, different varieties of PGPR have been studied, and some of them have been commercialized, including the species *Pseudomonas, Bacillus,* and, *Azobacter* (Glick et al., 2012).
However, PGPR's successful utilization depends on its survival in soil, the compatibility with the crop on which it is inoculated, the interaction ability with indigenous microflora in soil, and environmental factors (Martinez-Viveros et al., 2010).
For these reasons, intensive research of new PGPRs has been taken over to develop new biofertilizers and biocontrol agents able to resist harsh environmental conditions.
This Ph.D. project has been structured along with two thematic areas, both based on this topic: isolation, identification, and characterization of secondary metabolites with antifungal activity to be used with biopesticides and search for new soil bacteria beneficial able to resist stressful environmental conditions to be used as bio-inoculants. The results obtained made it possible to improve the knowledge of the phytopathogenic fungus *M. phaseolina* with the isolation and chemical and biological characterization of two new penta- and tetrasubstituted cyclopentenones named phaseocyclopentenones A and B used to infect relevant agro-industrial crops.
Subsequently, bacteria with important biocontrol activity were identified against *M. phaseolina* and other phytopathogenic fungi and characterized for the molecules responsible for this activity.

These bacteria and their metabolites, such as phenazine and PCA, can reduce the incidence or severity of plant diseases instead of using chemical pesticides. Therefore, they could be proposed as natural antagonists to control different phytopathogenic fungi.
Future studies will focus on the characterization of these compounds to test them at different environmental conditions (T, pH) and observe their resistance via *in vitro* and *in vivo* experiments in plants infected by phytopathogens. Other studies will optimize their large-scale production and find the best formulation for their application in the field.
Concerning the second part of the Ph.D. thesis focused on isolating a new collection of halophilic Bacilli PGPRs, seven bacteria strains were selected emerged for their high potentiality as biofertilizers and biocontrol agents by experiments *in vitro* and *in vivo*. The combination of laboratory-assays studies with whole-genome studies proved useful helpful to finding gene clusters involved in PGPB activities.
The ability of these select bacteria to produce secondary metabolites against different phytopathogens and improve plant growth under different stress (salinity and heavy metals) provides a possibility to commercialize these bacteria or their microbial products.
Biostimulants involving halotolerant PGPRs and their metabolites are yet to take off and enter the market (Sunita et al., 2020). Hence, developing tailor-made bioformulations from these unique PGPRs and their metabolites can be crucial to combat salinity and other environmental stress and improve the yield of biotic and abiotic stress-affected agro-ecosystems leading to better productivity and sustainability agriculture. Future studies will focus on confirming their PGPR activities in the field and optimizing the best bioformulation.

Overview of the results obtained

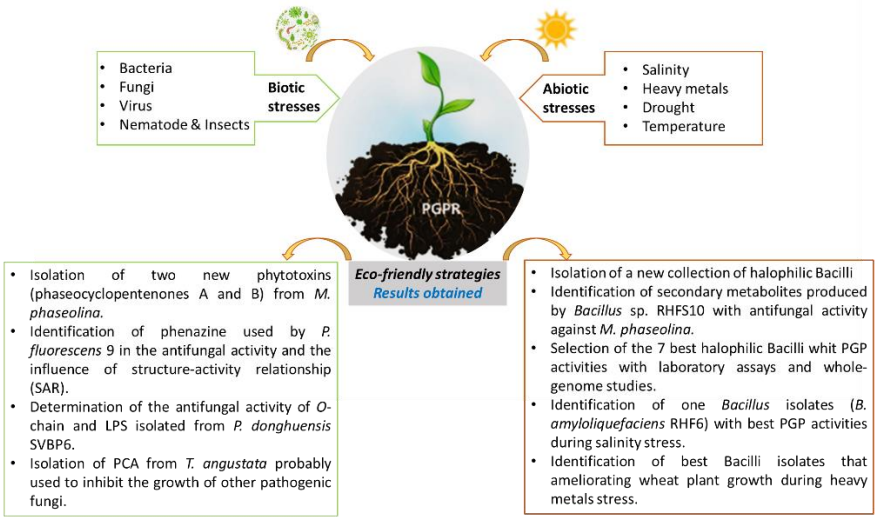

References

Armada E., Portela G., Roldan A., Azcon R. Combined use of beneficial soil microorganism and agrowaste residue to cope with plant water limitation under semiarid conditions. *Geoderma*. 2014, 232, 640–648.

Calvo P., Nelson L., & Kloepper J. W. Agricultural uses of plant biostimulants. *Plant Soil.* 2014, 383, 3–41.

Glick B.R. Plant growth-promoting bacteria: mechanisms and applications. *Scientifica* (Cairo). 2012, 96, 3401.

Martínez-Viveros O., Jorquera M. A., Crowley D. E., Gajardo G., and Mora M. L. Mechanisms and practical considerations involved in plant growth promotion by rhizobacteria. *J. Soil Sci. Plant Nutr.* 2010, 10, 293–319.

Sunita K, Mishra I, Mishra J, Prakash J, and Arora NK. Secondary Metabolites From Halotolerant Plant Growth Promoting Rhizobacteria for Ameliorating Salinity Stress in Plants. Front. Microbiol. 2020, 11, 567768.

APPENDIX I
SUPPLEMENTARY MATERIALS.

Chapter II: https://pubs.acs.org/doi/10.1021/acs.jnatprod.0c01287.
Chapter III: biomolecules-11-01728-s001.zip
Chapte IV: Download Word document
Chapter VI: ijms-22-03324-s001.pdf
Chapter VII: Data_Sheet_1.docx

APPENDIX II
LIST OF PUBBLICATIONS.

P1) Petrillo C, **Castaldi S**, Lanzilli M, Saggese A, Donadio G, Baccigalupi L, Ricca E, Isticato R. The temperature of growth and sporulation modulates the efficiency of spore-display in *Bacillus subtilis*. *Microb Cell Fact*. 2020, *19*, 185. DOI: 10.1186/s12934-020-01446-6.

Authors' contributions:
RI, ER, LB, conceived and designed the experiments; CP, **SC**, carried out most of the experimental work; ML, AS, GD contributed to some of the experiments; RI, ER, LB wrote and revised the manuscript. All authors read and approved the final manuscript.

P2) Masi M, Sautua F, Zatout R, **Castaldi S**, Arrico L, Isticato R, Pescitelli G, Carmona MA, Evidente A. Phaseocyclopentenones A and B, Phytotoxic Penta- and Tetrasubstituted Cyclopentenones Produced by *Macrophomina phaseolina*, the Causal Agent of Charcoal Rot of Soybean in Argentina. *J Nat Prod*. 2021, *84*, 459-465. DOI: 10.1021/acs.jnatprod.0c01287.

P3) Zdorovenko EL, Dmitrenok AS, Masi M, **Castaldi S**, Muzio FM, Isticato R, Valverde C, Knirel YA, Evidente A. Structural studies on the O-specific polysaccharide of the lipopolysaccharide from *Pseudomonas donghuensis* strain SVBP6, with antifungal activity against the phytopathogenic fungus *Macrophomina phaseolina*. *Int J Biol Macromol.* 2021, *182*, 2019-2023. DOI: 10.1016/j.ijbiomac.2021.05.187.

Authors' contributions:

Evelina L. Zdorovenko: Formal analysis, Writing - Original Draft Investigation, Visualization; Andrey S. Dmitrenok: Formal analysis; Investigation; Marco Masi: Investigation; **Stefany Castaldi**: Investigation; Federico M. Muzio: Investigation; Rachele Isticato: Writing - Review & Editing; Claudio Valverde: Writing - Review & Editing; Yuriy A. Knirel: Supervision, Writing - Review & Editing; Antonio Evidente: Project administration, Writing - Original Draft, Supervision.

P4) Castaldi S, Petrillo C, Donadio G, Piaz FD, Cimmino A, Masi M, Evidente A, Isticato R. Plant Growth Promotion Function of *Bacillus* sp. Strains Isolated from Salt-Pan Rhizosphere and Their Biocontrol Potential against *Macrophomina phaseolina*. *Int J Mol Sci.* 2021, *22*, 3324. DOI: 10.3390/ijms22073324.

Authors' contributions:
Conceptualization, R.I.; methodology, **S.C**., C.P., A.C., and G.D.; validation, and formal analysis, **S.C.** and G.D.; investigation, **S.C.**, M.M. and F.D.P.; data curation, **S.C.**, A.E. and R.I.; writing original draft preparation, R.I., **S.C.**, and C.P.; supervision, R.I.; project administration, R.I.; funding acquisition, R.I. All authors have read and agreed to the published version of the manuscript.

P5) Castaldi S[‡], Petrillo C[‡], Lanzilli M, Selci M, Cordone A, Giovannelli D and Isticato R. Genomic and Physiological Characterization of *Bacilli* Isolated From Salt-Pans With Plant Growth Promoting Features. *Front. Microbiol*. 2021, *12*, 715678. DOI: 10.3389/fmicb.2021.715678. [‡]: These authors share first authorship.

Authors' contributions:
RI: conceptualization, supervision, project administration, and funding acquisition. **SC** and CP: methodology. **SC**, CP, ML, and MS: validation and formal analysis. **SC**, CP, and DG: investigation. SC, CP, MS, AC, and RI: data curation. RI, **SC**, CP, and DG: writing original draft preparation. All authors have read and agreed to the published version of the manuscript.

P6) Cimmino A[‡], Bahmani Z, **Castaldi S**[‡], Masi M, Isticato R, Abdollahzadeh J, Amini J, Evidente A. Phenazine-1-Carboxylic Acid

(PCA), Produced for the First Time as an Antifungal Metabolite by *Truncatella angustata*, a Causal Agent of Grapevine Trunk Diseases (GTDs) in Iran. *J Agric Food Chem.* 2021, *69*, 12143-12147. DOI: 10.1021/acs.jafc.1c03877.

Authors' contributions:
ǂA.C. and ǂS.C. contributed equally to this work.

P7) Castaldi S*, Masi M, Sautua F, Cimmino A, Isticato R, Carmona M, Tuzi A, Evidente A. *Pseudomonas fluorescens* Showing Antifungal Activity against *Macrophomina phaseolina,* a Severe Pathogenic Fungus of Soybean, Produces Phenazine as the Main Active Metabolite. Biomolecules. 2021 Nov 19;11(11):1728. DOI: 10.3390/biom11111728. *: Corresponding author.

Authors' contributions:
Conceptualization, **S.C.**, M.M., F.S., M.C., and A.E.; methodology, **S.C.** and M.M.; writing—original draft preparation, **S.C.**, M.M., and A.E.; writing—review and editing, **S.C.**, M.M., F.S., A.C., R.I., M.C., A.T. and A.E. All authors have read and agreed to the published version of the manuscript.

APPENDIX III
COMMUNICATIONS.

A1) S. Castaldi, C. Petrillo, V. Totev Valkov, M. Chiurazzi, E. Ricca, R. Isticato *Application of Plant Growth Promoting Rhizobacteria (PGPR) for the improvement of agricultural productivity*. P53. GIM2019. Pisa. September 2019.

A2) C. Petrillo, I. Corrado, **S. Castaldi,** C. Pezzella, R. Isticato. *Identification of natural inulinase producing bacilli, for industrial applications*. P48. GIM2019. Pisa. September 2019.

Congresses organization

A1) Member of the organising committee of the II Industrial Biotechnology Congress: **BioID&A** (Biotechnology Identity and Application) held in Naples on October 28th, 2019.

APPENDIX IV
EXPERIENCES IN FOREIGN LABORATORIES.

A1) From January 13st 2020 to January 19st 2020, the research activity of Dr. Castaldi Stefany as ‘‘Invited Expert“ has been carried out at the “VTT Technical Research Centre of Finland Ltd (Espoo, Finland)”, thanks to IBISBA 1.0 project. The work was supervised by Dr. Tuulikki Seppänen-Laakso and Dr. Paula Jouhten.

27th September 2021

To Whom It May Concern,

This is to certify that Ms. Stefany Castaldi, a PhD student in biotechnology from University Federico II, Naples (Italy), has been in our research group as a Visiting Expert to participate in research activities of the TransNational Access (TNA) project "SporeDel: Optimization of the Spore-Display system for the mucosal delivery of drugs and antigens" within IBISBA 1.0 project, at VTT Technical Research Centre of Finland Ltd (Espoo, Finland) from 13-01-2020 to 19-01-2020, under direct supervision of Dr. Tuulikki Seppänen-Laakso.

Paula Jouhten

Paula Jouhten, Research Team Leader

A2) From July 1st 2021 to September 30st 2021, the research activity of Dr. Castaldi Stefany has been carried out at the "Helmholtz Center for Environmental Research – UFZ (Halle-Saale, Germany)" in the department of Soil Ecology. The work was supervised by Dr. Thomas Retiz.

UFZ HELMHOLTZ Centre for Environmental Research

Helmholtz Centre for Environmental Research – UFZ
Theodor-Lieser-Straße 4 · 06120 Halle (Saale) · Germany

To Whom it may concern,

Contact person:
Dr. Thomas Reitz
Scientist
Department Soil Ecology
Fon +49 345 558-5409
Thomas.Reitz@ufz.de

Halle/Saale, 30.09.2021

Confirmation of external stay in our department for Ms. Stefany Castaldi (Period: 01.06.2021 - 30.09.2021)

This is to certify that Ms. Stefany Castaldi, PhD student in biotechnology from University Federico II, Naples (Italy), has been in our research group at "Helmholtz Centre for Enviromental Research – UFZ" - Soil Ecology Department (Germany) from 1st July 2021 to 30st September 2021, under direct supervision of Dr. Thomas Reitz.

Sincerely

Dr. Thomas Reitz

Helmholtz-Zentrum für Umweltforschung GmbH - UFZ
Department Bodenökologie
Theodor-Lieser-Straße 4
D - 06120 Halle (Saale)

Helmholtz Centre for Environmental Research – UFZ

Company domicile: Leipzig

Permoserstr. 15, 04318 Leipzig, Germany
or
PF 500136, 04301 Leipzig, Germany
phone +49 341 235-0

info@ufz.de
www.ufz.de

Registration court: Leipzig district court
Commercial register No. B 4703

Chairman of the Supervisory Board:
MinDirig'in Oda Keppler

Scientific Director:
Prof. Dr. Georg Teutsch

Administrative Director:
Dr. Sabine König

Bank details:
HypoVereinsbank Leipzig
Sort code 860 200 86
Account No. 5080 186 136
Swift (BIC) code HYVEDEMM495
IBAN No. DE12860200865080186136
VAT No. DE 141 507 065
Tax No. 232/124/00416

EMAS

www.ufz.de

APPENDIX V
OTHERS PAPERS.

Petrillo *et al. Microb Cell Fact* (2020) 19:185
https://doi.org/10.1186/s12934-020-01446-6

Microbial Cell Factories

RESEARCH Open Access

The temperature of growth and sporulation modulates the efficiency of spore-display in *Bacillus subtilis*

Claudia Petrillo[1], Stefany Castaldi[1], Mariamichela Lanzilli[1,3], Anella Saggese[1], Giuliana Donadio[1,4], Loredana Baccigalupi[2], Ezio Ricca[1*] and Rachele Isticato[1]

Abstract

Background: Bacterial spores displaying heterologous antigens or enzymes have long been proposed as mucosal vaccines, functionalized probiotics or biocatalysts. Two main strategies have been developed to display heterologous molecules on the surface of *Bacillus subtilis* spores: (i) a recombinant approach, based on the construction of a gene fusion between a gene coding for a coat protein (carrier) and DNA coding for the protein to be displayed, and (ii) a non-recombinant approach, based on the spontaneous and stable adsorption of heterologous molecules on the spore surface. Both systems have advantages and drawbacks and the selection of one or the other depends on the protein to be displayed and on the final use of the activated spore. It has been recently shown that *B. subtilis* builds structurally and functionally different spores when grown at different temperatures; based on this finding *B. subtilis* spores prepared at 25, 37 or 42 °C were compared for their efficiency in displaying various model proteins by either the recombinant or the non-recombinant approach.

Results: Immune- and fluorescence-based assays were used to analyze the display of several model proteins on spores prepared at 25, 37 or 42 °C. Recombinant spores displayed different amounts of the same fusion protein in response to the temperature of spore production. In spores simultaneously displaying two fusion proteins, each of them was differentially displayed at the various temperatures. The display by the non-recombinant approach was only modestly affected by the temperature of spore production, with spores prepared at 37 or 42 °C slightly more efficient than 25 °C spores in adsorbing at least some of the model proteins tested.

Conclusion: Our results indicate that the temperature of spore production allows control of the display of heterologous proteins on spores and, therefore, that the spore-display strategy can be optimized for the specific final use of the activated spores by selecting the display approach, the carrier protein and the temperature of spore production.

Keywords: Display platform, Mucosal vaccines, *Bacillus subtilis*, Probiotics

Introduction

Endospores (spores) are quiescent cell forms produced by over 1000 bacterial species when the environmental conditions do not allow cell growth to continue [1]. In the spore form, these bacterial species can survive conditions, such as the prolonged absence of water and nutrients, the exposure to extremes of temperature and pH, to UV irradiations and to toxic chemicals, that would be lethal for other cell forms [2]. Although metabolically quiescent, the spore is able to sense the environment and respond to conditions that allow cell growth by germinating and generating a new vegetative cell [3]. Spore germination and resistance are in part due to the peculiar

*Correspondence: ericca@unina.it
[1] Department of Biology, Federico II University complesso universitario di Monte Sant' Angelo via Cinthia, 80126 Napoli, Italy
Full list of author information is available at the end of the article

structure of the spore, that has been studied in detail in *Bacillus subtilis*, the model system for spore formers [2, 4]. In *B. subtilis*, spores are formed by a partially dehydrated cytoplasm (core) surrounded by several protective layers: the thick peptidoglycan-like cortex, the multilayered, proteinaceous coat and the crust, the outermost layer formed of proteins and glycans [4]. In some species, including *B. anthracis*, *B. cereus* and *B. megaterium*, the outermost layer of the coat is the exosporium, a protective shell mainly made of glycoproteins [4].

The rigidity and compactness of the spore suggested the possibility of using this unusual cell as a platform to display heterologous proteins [5]. In a *proof-of-concept* work, the spore coat protein CotB of *B. subtilis* was used as a carrier to display the C fragment of the tetanus toxin (TTFC) of *Clostridium tetani* on the spore surface [5]. To this aim a genetic system was developed to generate gene fusions between the *cotB* gene and DNA coding for TTFC and to allow expression of the fusion during sporulation [5]. The mucosal administration of recombinant spores displaying TTFC was then shown protective against a challenge with the tetanus toxin and able to induce humoral and cellular immune responses [6, 7]. Over the years, the same approach has been used with other coat proteins as carriers and a variety of other heterologous proteins [8]. However, this display system has the drawback of generating recombinant spores, that in case of a field use could raise safety concerns [9]. To overcome this problem a non-recombinant display system based on the spontaneous and stable adsorption of heterologous proteins to bacterial spores has been also developed [10, 11]. Antigens and enzymes have been efficiently and stably adsorbed to spores [12, 13] and it has been proposed that the adsorption is due to the negative electric charge and the relative hydrophobicity of the spore surface [10, 14]. In addition, studies with *B. subtilis* and *B. megaterium* indicated that some proteins were able to infiltrate through "pores" of the outermost spore coat layers and localize in the inner coat of *B. subtilis* spores [15] or in the interspace between the exosporium and the outer coat in *B. megaterium* spores [16, 17].

The spore-display system by both the recombinant or non-recombinant approach, provides several advantages with respect to other display systems, such as a high stability even after a prolonged storage, the possibility of displaying large, multimeric proteins and the safety for a human use, demonstrated by the wide use of spores of some species as probiotics [18, 19]. Based on these, the activated spore has been proposed as a mucosal delivery system, as a vaccine vehicle, as a functionalized probiotic and as a platform to display enzymes [8, 20].

Both approaches are quite efficient, and it has been estimated that up to 3.0×10^3 heterologous molecules can be displayed by each recombinant spore of *B. subtilis* [8, 21]. The efficiency of the non-recombinant approach can be higher than that measured for the recombinant system and depends on the heterologous protein and the *Bacillus* species used [12, 15, 16, 20]. In spite of the efficiency of these systems, the possibility to increase and/or control the number of heterologous proteins presented on the spore is an important achievement for the full exploitation of this biotechnology tool. In the case of a use as a vaccine vehicle, for example, an increased efficiency of display results in a higher dose of antigen delivered or reduced amounts of spores needed for the immunization.

Based on a recent report showing that *B. subtilis* builds spores with different structure when grown at 25, 37 or 42 °C [22], we investigated whether the efficiency of spore-display by both recombinant and non-recombinant approaches could be modulated by modifying the temperature of spore production.

Results and discussion

Effects of the temperature on the recombinant display system

CotB, CotC and CotG are abundant coat proteins widely used as carriers to display heterologous proteins on the spore surface [8]. All three proteins have been recently found differentially represented in spores produced at 25, 37 or 42 °C, with CotB and CotG more abundant in spores prepared at 25 °C and CotC more abundant in 42 °C spores [22]. We used isogenic *B. subtilis* strains carrying DNA coding for the model antigen TTFC (*tetC*) fused to the gene coding for either CotB (*cotB*) [5] or CotC (*cotC*) [23] to evaluate the effect of the sporulation temperature on the fusion proteins. Spores of strains RH103 (*cotB::tetC*) and RH114 (*cotC::tetC*) were produced at 25, 37 and 42 °C and purified, as previously reported [22]. Surface proteins were extracted from RH103 and RH115 spores by the SDS-DTT or NaOH treatments, respectively and used for western blotting analysis with anti-CotB [5] or anti-CotC [23] antibodies.

As shown in Fig. 1, specific CotB-TTFC (upper panel) and CotC-TTFC (lower panel) signals were observed in all the samples but not in the negative controls, revealing that the temperature did not affect the self-assembly of the heterologous proteins around the spores. Moreover, we observed that the fusion protein CotB-TTFC was more represented in 25 °C spores than in 37 or 42 °C spores (upper panel), while the fusion CotC-TTFC showed the opposite trend (lower panel).

A flow cytometry approach was used to confirm and quantify the differences in the display of CotB-TTFC and CotC-TTFC at the various temperatures and evaluate their surface exposure. Spores of strains RH103

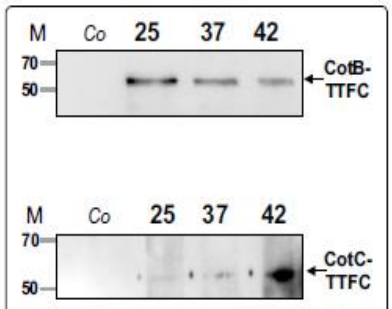

Fig. 1 Western blotting analysis of coat proteins. Purified spores of strains carrying the *cotB::tetC* (upper panel) or *cotC::tetC* (lower panel) were produced at the three temperatures and used to extract coat proteins by SDS-DTT (upper panel) or NaOH (lower panel) treatment as previously reported [22]. Proteins were reacted with anti-CotB (upper panel) or anti-CotC (lower panel) antibody. Control lanes (Co) were loaded with proteins extracted from spores of strains carrying either a *cotB* (upper panel) or a *cotC* (lower panel) null mutation

and RH114 were reacted with anti-TTFC [7] antibodies, then with fluorescently labeled secondary antibody and analyzed by flow cytometry as previously reported [24]. The threshold of positive events was set at 1×10^3 fluorescence intensity and the percentages of fluorescent events for each temperature are indicated in red in each panel. The flow cytometry analysis indicated that CotB-TTFC was displayed with the highest efficiency in spores prepared at 25 °C (86.9% positive events) and that such efficiency decreased in 37 and 42 °C spores (Fig. 2). The efficiency of display was opposite with CotC-TTFC with the highest levels observed with 42 °C spores (90.0% of positive events) and lower levels with 37 and 25 °C spores (Fig. 2). In addition, the fluorescent intensity peak for CotB-TTFC was tenfold higher at 25 °C than at 42 °C while for CotC-TTFC was tenfold higher at 42 °C than at 25 °C, suggesting that the sporulation temperature affected not only the amount of assembled heterologous proteins but also their surface display.

Results of Figs. 1, 2 indicated, respectively, the amounts of fusion proteins extracted and exposed on the spore surface but did not allow to exclude that other amounts of each fusion were actually present (but not extracted or not exposed) on spores produced at different temperatures. To address this issue, we used different isogenic strains of *B. subtilis* RH238, carrying the Green Fluorescent Protein (GFP) fused to CotC [23], and RH296,

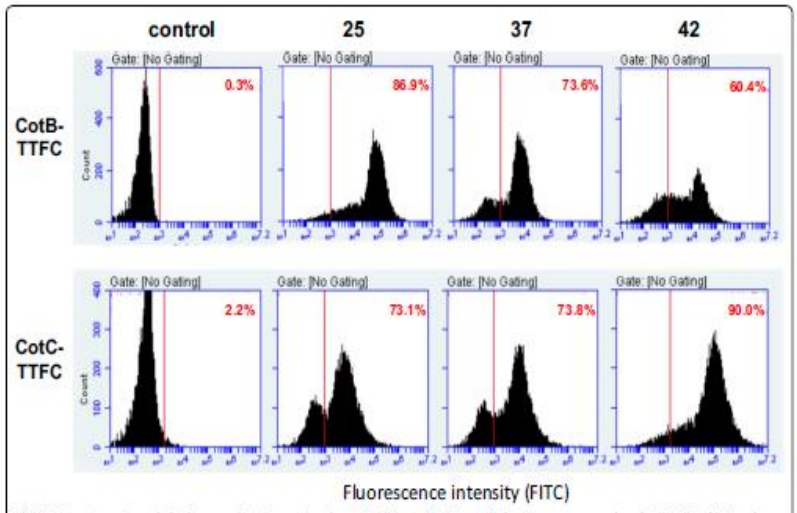

Fig. 2 Flow cytometry analysis of spores of strains carrying the *cotB::tetC* or *cotC::tetC* gene fusion. Spores were produced at 25, 37 or 42 °C and reacted with anti-TTFC antibody, then with FITC-conjugated secondary antibody. The analysis was then performed on the entire spore population (ungated). In each panel is indicated the percentage of positive events above the fluorescent intensity threshold of 1×10^3 (red line). As control experiment spores of an isogenic wild type strain (PY79) not containing any gene fusion were analyzed

carrying the Red Fluorescent Protein (RFP) fused to CotG [22]. A fluorescence microscopy analysis on spores prepared at 25, 37 or 42 °C and the quantification of the fluorescence signals performed by the ImageJ software, as previously reported [24], indicated that the CotG-based fusion was more abundant at 25 °C, less abundant at 37 °C and almost undetectable at 42 °C while the CotC-based fusion showed an opposite pattern (Fig. 3).

Results of Fig. 3, confirming results of Figs. 1,2, allow to conclude that the CotB- and CotG-based fusions are efficiently displayed when spores are produced at 25 °C, while CotC-based fusions are better displayed when spores are produced at 42 °C and, therefore, that is possible to modulate the amount and the surface exposure of fusion proteins displayed on the spore by changing the temperature of spore production on the base of the carrier protein used for the display.

Effects of the temperature on recombinant spores displaying two fusion proteins

An extension of the recombinant spore-display technology is the use of spores carrying more than one heterologous protein. By chromosomal DNA-mediated transformation [25], the gene fusion carried by strains RH238 (*cotC::gfp*) was moved into strain RH296 (*cotG::rfp*) obtaining strain RH406 that carried both fusions. As shown in Fig. 4, spores of strain RH406 presented both fluorescent proteins on their surfaces in similar amounts when spores were grown at 37 °C. When spores were produced at 25 °C the red fluorescent signal (CotG-RFP) was more abundant than the green one (CotC-GFP) that was instead predominant when spores were grown at 42 °C.

Results of Fig. 4 highlight an important improvement for the spore-display technology, showing that it is possible to produce spores that simultaneously display two heterologous proteins and to control which displayed protein has to be more abundantly represented by selecting the temperature of spore production.

Effects of the temperature on the non-recombinant display system

To evaluate the effects of the temperature on non-recombinant spore-display (adsorption) we used three model proteins: the pentapeptide HPHGH (herein PPT) of 0.77 kDa [26], the commercially available lysozyme

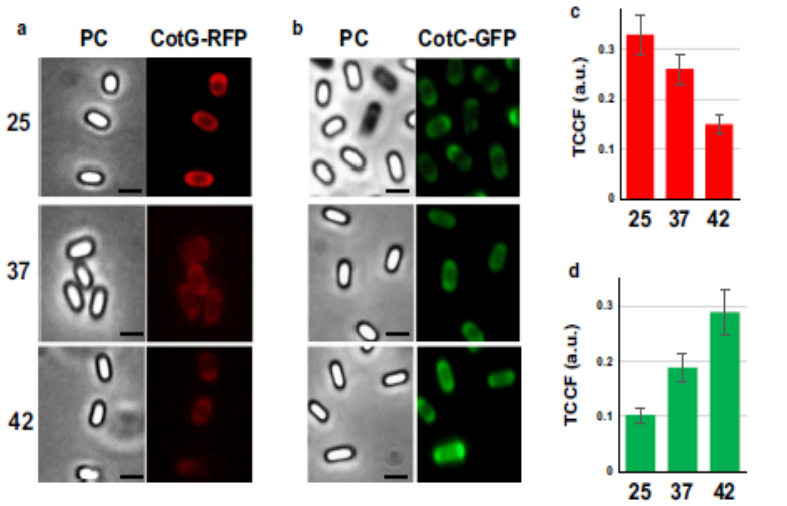

Fig. 3 Fluorescence microscopy analysis of spores displaying CotG-RFP or CotC-GFP. **a**–**c** Spores of strain RH296, carrying the *cotG::rfp* fusion (**a**) and of strain RH238, carrying the *cotC::gfp* fusion (**b**) were produced at 25, 37 or 42 °C and observed with a fluorescent microscope. The exposure time was the same for all samples with the same reporter gene. Phase contrast (PC), red-fluorescence (CotG-RFP) or green-fluorescence (CotC-GFP) microscopy images of representative spores are reported. Scale bar 1 µm. **b**–**d** Quantitative analysis of the fluorescence of more than 300 spores as in panels **a**–**c**, performed with the ImageJ software, as previously reported [22]. The Y-axis describes the Total corrected cellular fluorescence (TCCF) value

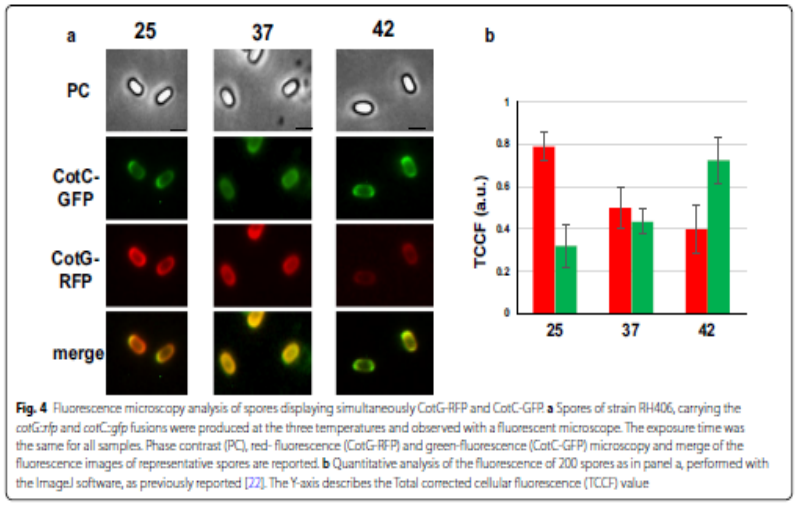

Fig. 4 Fluorescence microscopy analysis of spores displaying simultaneously CotG-RFP and CotC-GFP. **a** Spores of strain RH406, carrying the *cotG:rfp* and *cotC::gfp* fusions were produced at the three temperatures and observed with a fluorescent microscope. The exposure time was the same for all samples. Phase contrast (PC), red- fluorescence (CotG-RFP) and green-fluorescence (CotC-GFP) microscopy and merge of the fluorescence images of representative spores are reported. **b** Quantitative analysis of the fluorescence of 200 spores as in panel a, performed with the ImageJ software, as previously reported [22]. The Y-axis describes the Total corrected cellular fluorescence (TCCF) value

(herein LYS) of 14.4 kDa (Sigma) and the commercially available bovine serum albumin (herein BSA) of 66.4 kDa (New England-Biolabs). All three proteins were fluorescently labeled with rhodamine as previously described [26] and 10 mM of each model protein independently used for adsorption with 5.0×10^8 purified spores of the *B. subtilis* strains PY79 [27] produced at 25, 37 or 42 °C. The adsorption reactions were carried out for 1 h at 25 °C in 50 mM Sodium Citrate buffer, pH 4.0, as previously described [11]. Adsorbed spores were collected by centrifugation and analysed by fluorescence microscopy and flow cytofluorimetry, as previously described [24]. As shown in Fig. 5, all three proteins were adsorbed to the spores and the fluorescent signal distributed all around the spore surface. The relative fluorescence signals were analyzed by the ImageJ software (NIH), as previously reported [24]. Since the proteins were fluorescently tagged with rhodamine, an amine-specific label, the number of fluorophore molecules attached to each protein was different, impairing a comparison of fluorescence levels between different proteins. However, the analysis allowed to conclude that: (i) PPT adsorbed with similar efficiency to 37 °C and 42 °C and slightly less efficiently to 25 °C spores (37 = 42 > 25); ii) LYS had a pattern of adsorption similar to that described for PPT (37 = 42 > 25); and (iii) BSA adsorbed at similar levels to 25, 37 or 42 °C spores (25 = 37 = 42) (Fig. 5). Adsorbed spores were analyzed by flow cytometry and the percentage of positive-fluorescent events was obtained as described for Fig. 2. This quantitative analysis performed in duplicate on 100,000 spores/each, confirmed the fluorescence microscopy results of Fig. 5, indicating that PPT was absorbed much more efficiently at 37 or 42 °C, with respectively 75.95 and 77.80% positive events (p.e.) than at 25 °C (41.74% p. e.) (Fig. 6). A similar trend was observed with LYS, although the differences were smaller with 74.48, 82.15 and 90.44% p.e. at 25, 37 and 42 °C respectively, while no differences were observed with BSA with spores prepared at the three temperatures (Fig. 6).

Although the molecular mechanism of spore adsorption is not known in detail, it is likely that more factors are involved in the process. The negative electric charge and relative hydrophobicity of the spore surface have both been shown to influence the efficiency of adsorption [10, 14]. Since it has been previously reported that 25 °C spores are more hydrophobic than 37 and 42 °C spores [22], we hypothesized that the different relative hydrophobicity of spores could explain the reduced efficiency of adsorption of PPT and LYS to 25 °C spores. However, the GRAVY value, an estimation of protein hydrophobicity calculated by adding the hydropathy values of each amino acid residue of a protein and dividing by the number of residues in the protein [28], for PPT, LYS and BSA were −2.32, −0.15 and −0.45, respectively, with increasing positive values indicating an increasing hydrophobicity. Therefore, proteins with the least (PPT) and the highest (LYS) hydrophobicity value showed a similar

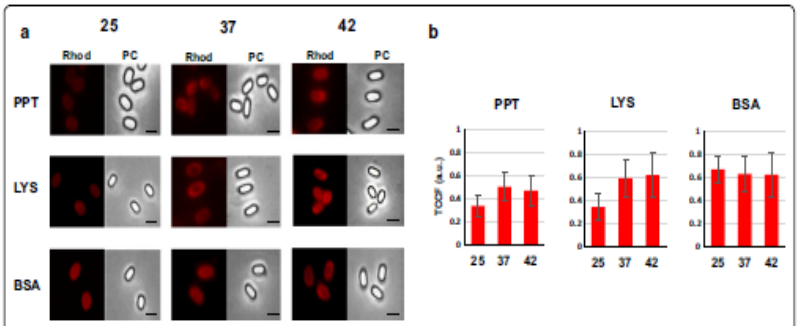

Fig. 5 Fluorescence microscopy of spores adsorbed with rhodamine-labeled PPT, LYS or BSA. **a** Fluorescence of PPT-Rd, LYS-Rd or BSA-Rd upon adsorption to wild type spores grown at 25, 37 or 42 °C. The same microscopy field was observed by phase contrast (PC) and fluorescence microscopy (Rhod). The exposure time was the same for all samples. **b** Quantitative analysis of the fluorescence of 300 spores as in panel a, performed with the ImageJ software, as previously reported [22]. The Y-axis describes the Total corrected cellular fluorescence (TCCF) value

adsorption pattern (Figs. 5,6), making it unlikely that the hydrophobicity is a major determinant of the efficiency of adsorption, in our experiments. Other physical and chemical parameters of the heterologous proteins, including probably the size and the isoelectric point, have to be considered as they may mediate the ability of proteins to cross the outermost spore layers [15–17], resulting in relevant for the efficiency of the process.

Localization of proteins adsorbed on 25, 37 or 42 °C spores

A previous report showed that RFP when adsorbed to spores is able to cross the crust and the outer coat, localizing at the inner coat level [15]. In that study, the RFP fluorescence signal was localized by comparison with the signal due to GFP fused to proteins known to be localized in various spore coat layers [15]. A similar approach was used to evaluate whether the temperature of spore production also affected the localization of the adsorbed proteins within the coat. Since the high red fluorescence signal produced by rhodamine-labeled PPT, LYS or BSA overlapped (and caused interference) with the region of detection for the GFP signal, the localization assays were performed adsorbing RFP to spores carrying the *cotC::gfp* fusion [15] and prepared at 25, 37 or 42 °C.

As previously reported [15], in 37 °C spores the red fluorescence signal of RFP was internal to the green signal of CotC-GFP (Fig. 7). While RFP localization did not change with 25 °C spores, it was slightly altered with 42 °C spores where the RFP signal was external with respect to the CotC-GFP signal (Fig. 7). The different localization of RFP is most likely due to the different coat structure of spore produced at the various temperatures and indicates that the lamellar and highly electron-dense outer coat (CotB-CotG rich) produced at low temperatures [22] is somehow a more permeable than the granular and thick coat (CotC rich) produced at 42 °C [22], at least with respect to RFP.

Conclusions

Main conclusion of this study is that the temperature of spore production affects the display of heterologous proteins on the spore surface:

- with the recombinant display the temperature modulates the amount and the surface exposure of the displayed proteins with CotB- and CotG-based fusions more efficient at low temperatures and CotC-based fusions are more efficient at high temperatures;
- when a recombinant spore carries two heterologous proteins each of them is differentially displayed at different temperatures on the base of the carrier used;
- with the non-recombinant display a modest effect is observed with small proteins (PPT and LYS) adsorbed more efficiently by 37 or 42 °C spores than by 25 °C spores;
- the localization of adsorbed RFP within the spore surface layers is modified by the temperature, indicating that spores produced at the low temperatures (CotB/CotG type coat) or at high temperature (CotC type coat) [22] have different adsorption properties.

Overall, this study indicates that the temperature of spore production is an essential parameter to be considered in the development of a spore-display system.

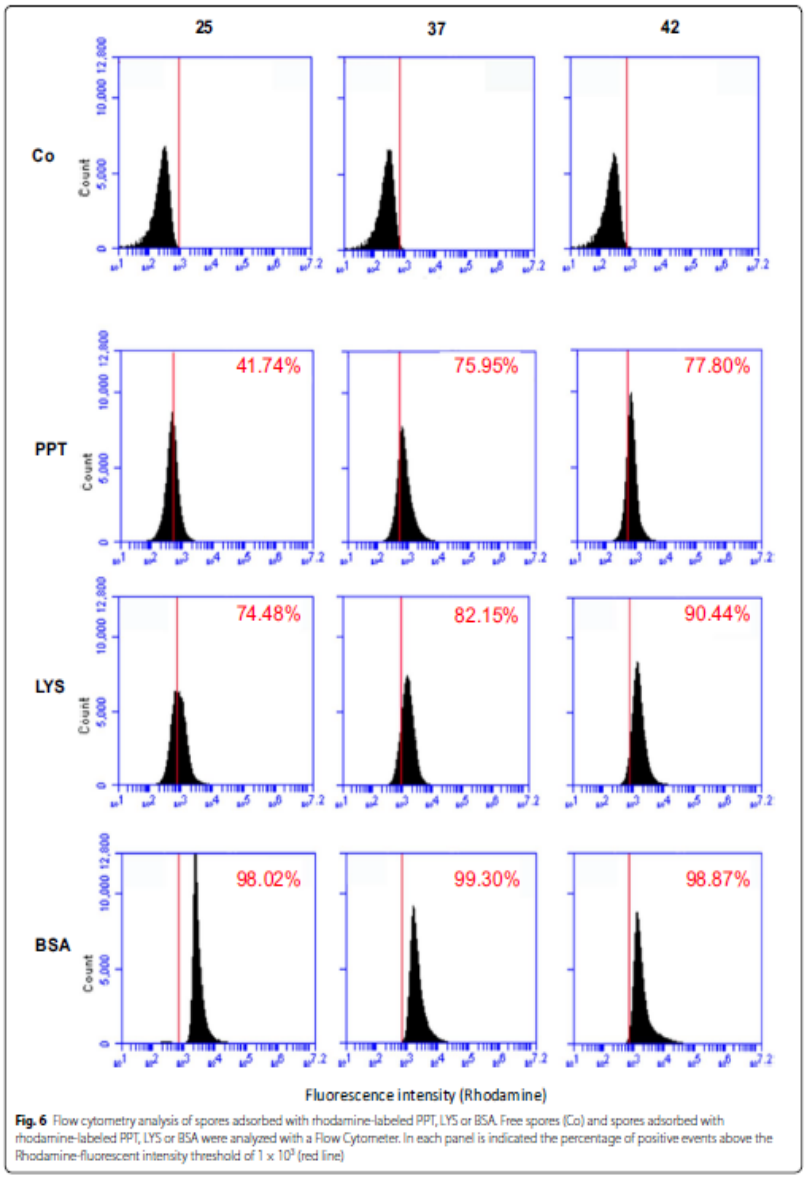

Fig. 6 Flow cytometry analysis of spores adsorbed with rhodamine-labeled PPT, LYS or BSA. Free spores (Co) and spores adsorbed with rhodamine-labeled PPT, LYS or BSA were analyzed with a Flow Cytometer. In each panel is indicated the percentage of positive events above the Rhodamine-fluorescent intensity threshold of 1×10^3 (red line)

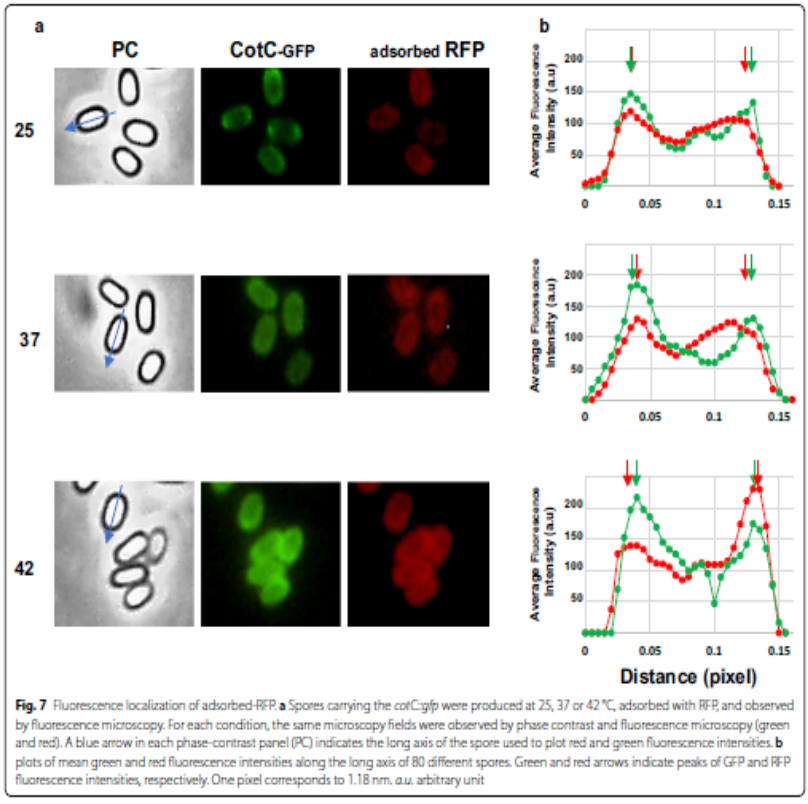

Fig. 7 Fluorescence localization of adsorbed-RFP. **a** Spores carrying the *cotC::gfp* were produced at 25, 37 or 42 °C, adsorbed with RFP, and observed by fluorescence microscopy. For each condition, the same microscopy fields were observed by phase contrast and fluorescence microscopy (green and red). A blue arrow in each phase-contrast panel (PC) indicates the long axis of the spore used to plot red and green fluorescence intensities. **b** plots of mean green and red fluorescence intensities along the long axis of 80 different spores. Green and red arrows indicate peaks of GFP and RFP fluorescence intensities, respectively. One pixel corresponds to 1.18 nm. *a.u.* arbitrary unit

Materials and methods

Spore production, extraction of coat proteins and western blot analysis

Sporulation at 25, 37 and 42 °C was induced by the exhaustion method in Difco Sporulation (DS) medium as recently reported [24, 29]. Mature spores were purified by cold-water washing using overnight incubation in H_2O at 4 °C to lyse residual sporangial cells. Spore purity (higher than 95%) was checked under optical microscope.

Spore coat proteins were extracted from a suspension of spores by SDS-DTT or NaOH treatment [30]. The concentration of extracted proteins was determined by using Bio-Rad DC protein assay kit (Bio-Rad), and 20 µg of total spore coat proteins were fractionated on 12.5% SDS polyacrylamide gels and staining by Brilliant Blue Coomassie or electro-transferred to nitrocellulose filters (Bio-Rad) for western blot analysis following standard procedures. CotC- and CotB- substrate specific antibodies were used at working dilutions 1:7000 for CotC-TTFC and CotB-TTFC detection [5, 21]. Then, a horseradish peroxidase-conjugated antirabbit secondary antibody was used (Santa Cruz). Western blot filters were visualized by the electro chemi luminescence method as specified by the manufacturer and processed to improve the contrast level using ChemidocXRS software (Bio-Rad).

The experiments have been repeated twice analyzing two distinct coat protein extractions.

Labeling with Rhodamine

2 mg/ml of pentapeptide HPHGH (PPT), commercially available lysozyme (LYS-Sigma), and bovine serum albumin (BSA-New England-Biolabs) were labeled with 50 µl of Rhodamine B isothiocyanate (Sigma) (1 mg/ml in DMSO) as specified by the manufacturer. The protocol is based on the reaction between the isothiocyanate group of Rhodamine and epsilon-NH_2 of Lysine residues of the protein to be labeled in order to obtain a fluorescent complex. Final molar Rhodamine/Proteins ratio was 0.06 and the labeling reactions were performed pH 8.5. The labeling was followed by dialysis in 1×PBS to remove the unbound fluorescent excess and lyophilization.

Binding reaction

10 mM of PPT-Rd, LYS-Rd, BSA-Rd were added to a suspension of 5.0×10^8 wild type spores, produced at different temperatures, in 50 mM sodium citrate pH 4.5 in a final volume of 200 µl. For the reaction with RFP, 1 µg of purified protein was added to the suspension of 1.0×10^8 spores produced at different temperatures, in 1.5 M PBS pH 4.0 in a final volume of 200 µl. After 1 h of incubation at 25 °C, the binding mixtures were washed and centrifuged (10 min at 13,000g) to fractionate adsorbed spores (pellet) from unbound protein (supernatant).

Flow cytometry

Recombinant spores expressing TTFC were analyzed by flow cytometry as previously described [31]. Briefly, 10^6 purified spores were incubated at room temperature for 30 min at room temperature in phosphate-buffered saline (PBS)-3% fetal bovine serum (FBS) prior to 1 h-incubation with anti-TTFC polyclonal antibodies diluted at 1:20 in 1×PBS–1%FBS. After three washes in 1×PBS, fluorescein isothiscyanate (FITC)-conjugated anti-rabbit immunoglobulin G (1:64; Sigma) was added and the mixture was incubated for 1 h at room temperature, followed by four washes in PBS.

For spores adsorbed with PPT-Rd, LYS-Rd and BSA-Rd, a total of 10^6 spores were resuspended in 0.5 ml of binding buffer and directly analyzed.

Flow cytometry analysis was performed by BD Accuri™ C6 Cytometer and BD Accuri™ C6 Software (BD Biosciences, Inc., Milan, Italy) collecting 100,000 events. Spore without the addition of primary and secondary antibodies or not adsorbed were used to measure the unspecific fluorescence, allowing to set the threshold of positive events at 1×10^3 fluorescence intensity. The experiments were repeated twice analyzing two independently prepared samples.

Fluorescence microscopy

10^5 adsorbed spores were resuspended in 50 µl of binding buffer and observed with an Olympus BX51 fluorescence microscope fitted with a 100× objective UPlanF1 and U-MNG or U-MWIBBP cube-filters to detect the red and green fluorescence emission respectively. The exposure times are in the range between 500 and 1000 ms. Captured images were processed with Image Analysis Software (Olympus) for minor adjustments of brightness, contrast and color balance and for creation of merge images. For RFP adsorbed spores, the fluorescence intensities and the distance between two fluorescent peaks were measured using unadjusted merged images with Image J processing software (version 1.48, NIH) as previously described [15]. To obtain the total corrected cellular fluorescence (TCCF), an outline was drawn around several fluorescent spores and area, integrated density and the mean fluorescence measured, along with several adjacent background readings. The TCCF was calculated by subtracting the area of selected cell × mean fluorescence of background readings to the integrated density.

Acknowledgements

Not applicable.

Authors' contributions

RI, ER, LB, conceived and designed the experiments; CP, SC, carried out most of the experimental work; ML, AS, GD contributed to some of the experiments; RI, ER, LB wrote and revised the manuscript. All authors read and approved the final manuscript.

Funding

No specific funds were receive to support this work.

Availability of data and materials

All data generated or analysed during this study are included in this published article and are available from the corresponding author on reasonable request.

Ethics approval and consent to participate

Not applicable.

Consent for publication

Not applicable.

Competing interests

The authors declare no competing interests.

Author details

[1] Department of Biology, Federico II University complesso universitario di Monte Sant' Angelo via Cinthia, 80126 Napoli, Italy. [2] Department of Molecular Medicine and Medical Biotechnology, Federico II University of Naples, Napoli, Italy. [3] Present Address: Institute of Biomolecular Chemistry, National Research Council of Italy, Pozzuoli (Naples), Italy. [4] Present Address: Department of Medicine, Surgery and Dentistry "Scuola Medica Salernitana", University of Salerno, Fisciano (SA), Italy.

Received: 31 July 2020 Accepted: 25 September 2020
Published online: 01 October 2020

References

1. Fritze D. Taxonomy and systematics of the aerobic endospore forming bacteria: Bacillus and related genera. In: Ricca E, Henriques AO, Cutting SM, editors. Bacterial Spore Formers. Norfolk: Horizon Bioscience; 2004. p. 17–34.
2. Driks A, Eichenberger P. The Spore Coat. Microbiol Spectr. 2016;4(2):817–29.
3. Setlow P. Germination of spores of *Bacillus* species: what we know and do not know. J Bacteriol. 2014;196:1297–305.
4. McKenney PT, Driks A, Eichenberger P. The *Bacillus subtilis* endospore: assembly and functions of the multilayered coat. Nat Rev Microbiol. 2013;11:33–44.
5. Isticato R, Cangiano G, Tran TH, Ciabattini A, Medaglini D, Oggioni MR, De Felice M, Pozzi G, Ricca E. Surface display of recombinant proteins on *Bacillus subtilis* spores. J Bacteriol. 2001;183:6294–301.
6. Duc LH, Huynh HA, Fairweather N, Ricca E, Cutting SM. Bacterial spores as vaccine vehicles. Infect Immun. 2003;71:2810–8.
7. Mauriello EMF, Cangiano G, Maurano F, Saggese V, De Felice M, Rossi M, Ricca E. Germination-Independent Induction of Cellular Immune Response by *Bacillus subtilis* Spores Displaying the C Fragment of the Tetanus Toxin. Vaccine. 2007;25:788–93.
8. Isticato R, Ricca E. Spore surface display. Microbiol Spectr. 2014. https://doi.org/10.1128/microbiolspec.TBS-0011-2012.
9. Detmer A, Glenting J. Live bacterial vaccines—a review and identification of potential hazards. Microb Cell Fact. 2006;5:23.
10. Huang JM, Hong HA, Van Tong H, Hoang TH, Brisson A, Cutting SM. Mucosal delivery of antigens using adsorption to bacterial spores. Vaccine. 2010;28:1021–30.
11. Sirec T, Strazzulli A, Isticato R, De Felice M, Moracci M, Ricca E. Adsorption of beta-galactosidase of *Alicyclobacillus acidocaldarius* on wild type and mutant spores of *Bacillus subtilis*. Microb Cell Fact. 2012;11:100.
12. Isticato R, Sirec T, Treppiccione L, Maurano F, De Felice M, Rossi M, Ricca E. Non-recombinant display of the B subunit of the heat labile toxin of *Escherichia coli* on wild type and mutant spores of Bacillus subtilis. Microb Cell Fact. 2013;12:98.
13. Mattossovich R, Iacono R, Cangiano G, Cobucci-Ponzano B, Isticato R, Moracci M, Ricca E. Conversion of xylan by recyclable spores of *Bacillus subtilis* displaying thermophilic enzymes. Microb Cell Fact. 2017;16(1):218.
14. Pesce G, Rusciano G, Sirec T, Isticato R, Sasso A, Ricca E. Surface charge and hydrodynamic coefficient measurements of *Bacillus subtilis* spore by optical tweezers. Colloids Surf, B. 2014;116:568–75.
15. Donadio G, Lanzilli M, Sirec T, Ricca E, Isticato R. Localization of a red fluorescence protein adsorbed on wild type and mutant spores of *Bacillus subtilis*. Microb Cell Fact. 2016;15:153.
16. Lanzilli M, Donadio G, Addevico R, Saggese A, Cangiano G, Baccigalupi L, Christie G, Ricca E, Isticato R. The exosporium of *Bacillus megaterium* QM B1551 is permeable to the Red Fluorescence Protein of the coral *Discosoma* sp. Front Microbiology. 2016;7:1572.
17. Lanzilli M, Donadio G, Fusco FA, Sarcinelli C, Limauro D, Ricca E, Isticato R. Display of the peroxiredoxin Bcp1 of *Sulfolobus solfataricus* on probiotic spores of *Bacillus megaterium*. N Biotechnol. 2018;46:38–44.
18. D'Arienzo R, Maurano F, Mazzarella G, Luongo D, Stefanile R, Ricca E, Rossi M. *Bacillus subtilis* spores reduce susceptibility to *Citrobacter rodentium*-mediated enteropathy in a mouse model. Res Microbiol. 2006;157:891–7.
19. Cutting SM. *Bacillus* probiotics. Food Microbiol. 2011;28:214–20.
20. Ricca E, Baccigalupi L, Cangiano G, De Felice M, Isticato R. Mucosal vaccine delivery by non-recombinant spores of *Bacillus subtilis*. Microb Cell Fact. 2014;13(1):115.
21. Mauriello EMF, Duc LH, Isticato R, Cangiano G, Hong HA, De Felice M, Ricca E, Cutting SM. Display of heterologous antigens on the *Bacillus subtilis* spore coat Using CotC as a fusion partner. Vaccine. 2004;22:1177–87.
22. Isticato R, Lanzilli M, Petrillo C, Donadio G, Baccigalupi L, Ricca E. *Bacillus subtilis* builds structurally and functionally different spores in response to the temperature of growth. Environ Microbiol. 2020;22(1):170–82.
23. Isticato R, Mase D, Mauriello EMF, De Felice M, Ricca E. Amino terminal fusion of heterologous proteins to CotC increases display efficiencies in the *Bacillus subtilis* spore system. Biotechniques. 2007;42:151–6.
24. Isticato R, Ricca E, Baccigalupi L. Spore adsorption as a nonrecombinant display system for enzymes and antigens. J Vis Exp. 2019;19:145.
25. Cutting S, Vander Horn PB. Genetic analysis In Molecular Biological Methods for *Bacillus*. Edited by Harwood C and Cutting S. Wiley, Chichester. 1990; pp. 27–74.
26. Donadio G, Di Martino R, Oliva R, Petraccone L, Del Vecchio P, Di Luccia B, Ricca E, Isticato R, Di Donato A, Notomista E. A new peptide-based fluorescent probe selective for zinc (II) and copper (II). J Mater Chem B. 2016;4:6979–88.
27. Youngman P, Perkins JB, Losick R. A novel method for the rapid cloning in *Escherichia coli* of *Bacillus subtilis* chromosomal DNA adjacent to Tn917 insertion. Mol Gen Genet. 1984;195:424–33.
28. Kyte J, Doolittle RF. A simple method for displaying the hydropathic character of a protein. J Mol Biol. 1982;157:105–32.
29. Crescenzo R, Mazzoli A, Cancelliere R, Bucci A, Naclerio G, Baccigalupi L, Cutting SM, Ricca E, Iossa S. Beneficial effects of carotenoid-producing cells of *Bacillus indicus* HU16 in a rat model of diet-induced metabolic syndrome. Beneficial Microbes. 2017;8:823–31.
30. Isticato R, Sirec T, Giglio R, Crispino A, Baccigalupi L, Rusciano G, Pesce P, Zito G, Sasso A, De Felice M, Ricca E. Flexibility of the programme of spore coat formation in Bacillus subtilis: bypass of CotE requirement by overproduction of CotH. PLoS ONE. 2013;8(9):e74949.
31. Santos FDS, Mazzoli A, Maia AR, Saggese A, Isticato R, Leite F, Iossa S, Ricca E, Baccigalupi L. A probiotic treatment increases the immune response induced by the nasal delivery of spore-adsorbed TTFC. Microb Cell Fact. 2020;19:42.

Publisher's Note